Durham E-Theses

The behaviour of an electron swarm in mixed oscillatory and undirectional electric fields

Vincent, J. H.

How to cite:

Use policy

THE BEHAVIOUR OF AN ELECTRON SWARM IN

MIXED OSCILLATORY AND UNIDIRECTIONAL

ELECTRIC FIELDS

by

J.H. VINCENT, B.Sc.

Being an account of the work carried out at the
University of Durham during the period from
September, 1962 to March, 1966.

Thesis submitted for the Degree of Doctor of Philosophy
in the University of Durham.

June 1966.

ACKNOWLEDGEMENTS

LIST OF PRINCIPLE SYMBOLS USED

α ...... Townsend's first ionization coefficient: the number of ionizing collisions made per electron per centimetre drifted.

ψ ...... Ionization rate per individual electron.

η ...... Ionizing efficiency (ionizations per volt).

μ ...... Electron mobility.

λ ...... Electron mean-free-path between collisions with gas molecules.

p ...... Gas pressure.

D ...... Diffusion coefficient for electrons.

u ...... Average electron energy (volts).

θ ...... $\dfrac{\mu E_{dc}}{2D}$

m ...... Mass of the electron.

M ...... Mass of the gas molecule.

uhf ...... Ultra-high-frequency.

dc ...... Unidirectional.

E_u ...... Applied uhf field in the gap.

E_{dc} ...... Applied dc field in the gap.

d ...... Gap width.

b ...... Radius of the holes in the emitting electrode.

L ...... Length of the holes in the emitting electrode.

PREFACE

This thesis describes experiments which have been performed at Durham to investigate the behaviour of electron swarms moving in a parallel plate gap under the influence of a unidirectional electric field on which is superimposed an ultra-high-frequency field of 48 Mc/second.

Electrons are emitted into the gap through holes in one of the plates and move across the gap under the influence of the dc field. The uhf field serves to increase the energy of the electrons in the gap, and if this energy is high enough ionization occurs.

Measurements have been made in several gases on the amplification of the stream of electrons crossing the gap, and of the uhf field required to cause electrical breakdown. Other measurements have been made in an attempt to determine the nature of electron flow through the holes in the emitting electrode.

From theoretical considerations of drift, diffusion and ionization, an expression is derived for amplification in the electron stream which is shown to be in reasonable agreement with the experimental results for the gases tested.

The latter half of this thesis deals with investigations into the effects of the generation of residual voltages in the gap by charging at the electrode surfaces under the influence of unidirectional current flow. A rigorous quantitative analysis of these effects has not yet been found, and therefore it has not been possible to take them into account in the

theoretical expression for amplification. However if the currents flowing in the gap are kept small, it is concluded that the effects of residual voltages are negligible, and therefore does not invalidate the comparison made between theory and experiments.

Acknowledgements.

List of principle symbols used.

Preface.

CHAPTER 1

INTRODUCTION

A gas in the normal state is almost a perfect insulator, but when a steadily increasing electrical stress is applied, a stage is reached when suddenly the gas becomes conducting. The field strength at which this occurs, the breakdown stress, E_s, was observed by early workers to be a function of the nature of the gas and the pressure. Later workers discovered that other variables affecting E_s were the electrode material, geometry, and the frequency of the applied field. Once the gas has become conducting, visible radiation is emitted, characteristic of the gas under stress.

Since the early days of the work, many attempts, notably by Townsend and his school, have been made to explain the mechanisms which lead up to breakdown. It was discovered that breakdown is not a sudden change from the non-conducting to the conducting state, but one which occurs over a finite period of time, i.e. the formative time. It is now known that ionization of the gas by the collision of free electrons with gas atoms or molecules is one of the chief factors contributing to breakdown, and this mechanism has been studied in detail by many workers. This thesis, describing work which is a continuation of that begun by Nicholls[1] (1960) and Long[2] (1962), is concerned primarily with those processes leading up to breakdown in several common gases under the influence of combined unidirectional and ultra-high-frequency electric fields. It is hoped that the present study will yield valuable information about the

nature of electron flow in such a system.

1. Processes leading to breakdown

1.1 The generation of electrons

Electrons moving in a gas suffer many collisions with gas molecules, and as a result they acquire a certain distribution of energies. (The Maxwillian distribution is a good approximation for the molecular gases, and the Druyvestyn distribution for the rare gases). If some of the electrons have sufficient energy, inelastic collisions with gas molecules can occur. Excitation occurs when some of the kinetic energy of the colliding electron is converted into the potential energy required to lift one of the atomic electrons into a higher energy level. Radiation is emitted when this electron decays back to its initial state. When the colliding electron has higher energy, enough may be transferred to ionize the atom or molecule. Thus a free electron is generated, and this, together with the original electron may ionize other atoms or molecules, in the same way, starting off the chain of events leading to an electron avalanche, and hence breakdown. (Townsend[4,6,7]).

1.2 Losses of electrons

In order to discuss breakdown, the electron loss processes must be taken into account. Electrons may be lost by drifting to one of the electrodes under the influence of the applied electric field, or by diffusion to the boundary of the system. These two processes are discussed and compared in detail in a later chapter of this thesis.

Electrons may be lost in the volume of the gas by recombining with

positive ions to form neutral atoms or molecules, or they may form

negative ions with neutral atoms or molecules. However in most of the

common gases studied, at least under normal laboratory conditions, these

two effects are negligible compared with drift and diffusion.

1.3 The criterion for breakdown

The criterion for breakdown is that for every electron in the gap

which is lost (one way or another), at least one new electron is generated.

Consider the balance between these processes for a given elementary

volume of the discharge. The equation of continuity, describing the rate

at which electrons enter or leave the volume by various processes is

given by Townsend[3] as

$$\nabla^2 (D.n) - \frac{\mu E_{dc}}{D} \cdot \frac{\partial n}{\partial z} + \psi n + x = \frac{\partial n}{\partial t} \qquad \dots \quad 1.1$$

where n is the electron density, D is the coefficient of diffusion (des-

cribed in greater detail in §2), μ is the electron mobility, and E_{dc} the

applied unidirectional electric field.

The rate of loss of electrons from the volume by diffusion is

represented by the term $\nabla^2 (D.n)$, the rate of loss by drift by $\frac{\mu E_{dc}}{D} \cdot \frac{\partial n}{\partial z}$.

The net rate at which electrons are generated within the volume is

represented by ψn, where ψ is the ionisation rate, taking into account

in this case all secondary electron generation processes, as well as

collision ionization. The rate at which electrons are supplied by some

external source is x.

Finally, $\frac{\partial n}{\partial t}$ represents the rate at which the electron density within

the volume changes with time. When the system is in a state of equilibrium,

-3-

this tends to zero.

If the overall loss rate exceeds the overall generation rate, electrons must be supplied from an external source in order to maintain the discharge, equilibrium being established between the current injected and that lost from the discharge.

However if the loss rate is less than the overall generation rate, equilibrium can now be achieved by the internal generation and loss processes, alone, so long as enough electrical energy is supplied to the system.

1.4 Breakdown in unidirectional fields

Electrons starting at the cathode are swept towards the anode in the applied dc field. When the voltage is high enough for multiplication to occur, an electron avalanche is formed, which is removed from the gas on reaching the anode. Losses of electrons by both diffusion and drift are considerable, and collision ionization in the gas is not sufficient alone to maintain the discharge. However the balance between the generation and loss processes required to keep the discharge running is preserved by the action of secondary electron generation effects, as described in §1.7.

Thus the discharge can be maintained without the help of an external source of electrons.

Important quantities used to describe breakdown in unidirectional fields are Ed and pd, where d is the electrode spacing, E the electric field, and p the pressure.

2
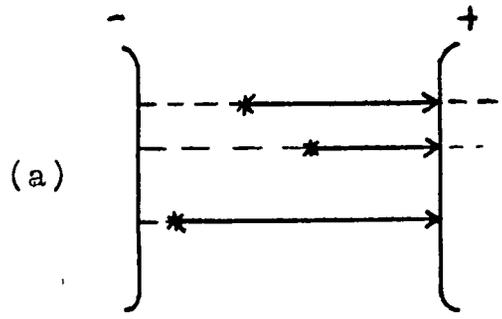
(a) — Unidirectional field.
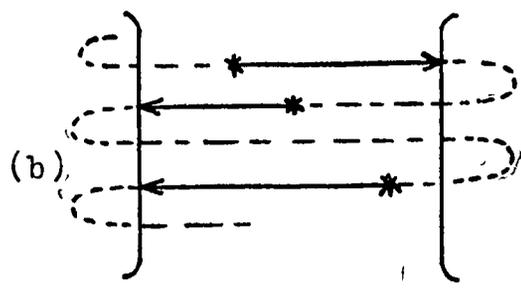
(b) — Low frequency alternating field.
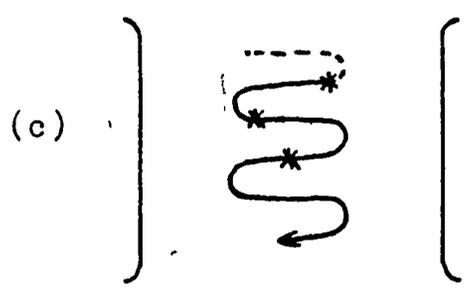
(c) — High frequency alternating field.
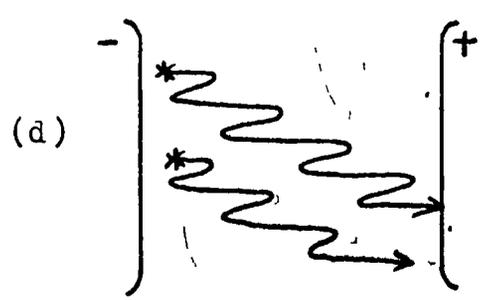
(d) — High frequency alternating field with d·c field superimposed.

Fig 1.1. The fate of electrons moving in a parallel plate gap under the influence of electric fields.

✱ denotes the appearance of an electron in the gap.

1.5 Breakdown in oscillatory fields

In unidirectional fields, as described above, the electron avalanche is swept straight to the anode and lost (see Fig. 1.1a). If the applied field is oscillatory, but the frequency is low, electrons are swept alternatively to each electrode in turn, with the same result (see Fig. 1.1b). At higher frequencies, however, the direction of motion of the electron swarm is reversed at the end of a half cycle before the swarm has reached the electrode, and is not lost as before (see Fig. 1.1c). Instead, the electrons oscillate to and fro in the gap, with no losses by drift except in the regions close to the electrodes (Schneider[31]). When multiplication occurs in the gas, the electron concentration builds up in the gap due to the many successive avalanches which occur in successive half cycles of the field. Breakdown is produced with applied fields much lower than in the unidirectional case, the ratio being about 1:2, (Gill and Donaldson[8]; Gutton and Gutton[9]). This is because losses of electrons are considerably reduced by the absence (almost) of drift. The predominant removal mechanism is now diffusion to the electrodes or to the walls of the vessel. Thus some high frequency discharges are known as 'diffusion-controlled' discharges. The same criterion for breakdown applies as in the unidirectional case, but becomes simplified in that diffusion is effectively the only active removal mechanism, except in the attaching or recombining gases.

The continuity equation now is

$$D.\nabla^2.n + \psi.n = 0 \qquad \qquad .... \quad 1.2$$
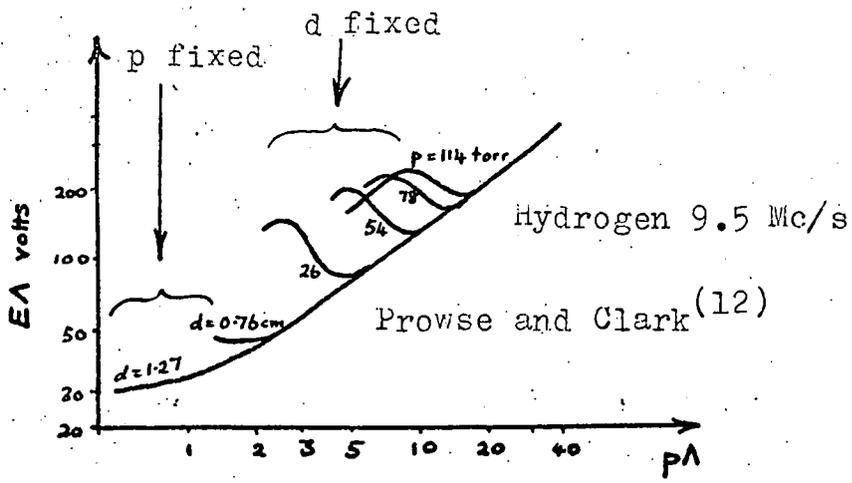
Fig 1.2. $E\Lambda$, $p\Lambda$ curves for Hydrogen(Branches occur
from the common curve when loss processes other
than diffusion start to appear).
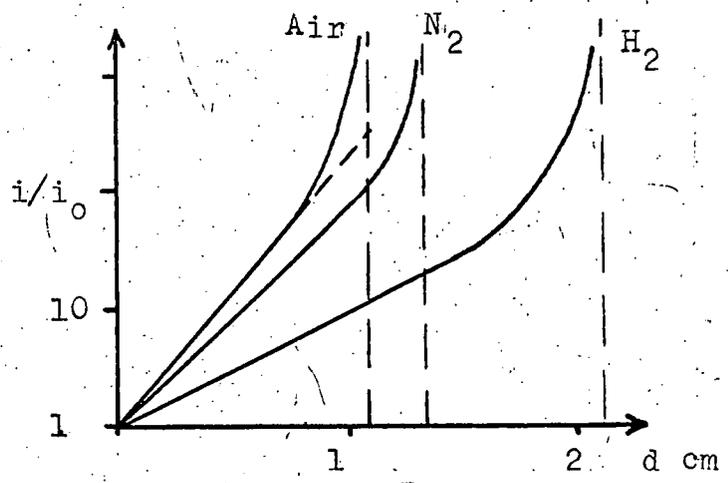
Fig 1.3. Typical curves of i/i_0 against gap width, d.

(Herlin and Brown[10]).

From the solution of this, the breakdown condition is given as $\psi = D/\Lambda^2$, where Λ, the diffusion length of the gap is a convenient quantity to define the gap geometry, and is an indication of the mean distance an electron must diffuse before it reaches a boundary. For a system where the electrodes consist of two parallel discs

$$\frac{1}{\Lambda^2} = \left(\frac{\pi}{d}\right)^2 + \left(\frac{2.405}{a}\right)^2 \qquad \ldots \ 1.3$$

where $\underline{d}$ and $\underline{a}$ are the gap width and electrode radius respectively. The first term represents electron losses axially, and the second term losses radially.

One of the results of this diffusion theory is that the breakdown stress will be constant for a given gas and pressure for various gap geometries, provided that Λ is constant also. Herlin and Brown[11] showed this to be true experimentally. Later, Prowse and Clark[12] showed that since D is a function of E_u/p, (where E_u is the rms value of the high frequency field), the curve of $p\Lambda$ against $E\Lambda$ for breakdown, (analogous to the Ed vs. pd curves in the unidirectional case) should be unique for any one gas, and they tested the theory successfully at a frequency of 9.5 Mcs/second. Thus the diffusion theory for pure high frequency discharges was shown to be valid. (See Fig. 1.2).

1.6 <u>Breakdown in combined unidirectional and uhf oscillatory fields</u>

Varnerin and Brown[13] have studied the case where a small unidirectional field, E_{dc}, is superimposed on the uhf field (see Fig. 1.1d). Providing that $E_{dc} \ll E_u$, it was shown that the diffusion theory still

holds if Λ is modified to Λ_m where

$$(1/\Lambda_m)^2 = (1/\Lambda)^2 + (E_{dc}/2.D/\mu)^2 \qquad \cdots \text{ 1.4}$$

This was obtained for the case where the only source of electrons is casual, but it may be extended to apply to case where the majority of electrons are concentrated at the centre of the gap, for example when the electron density distribution across the gap is approximately sinusoidal.

The uhf voltage required to break the gap down increases uniformly as the applied dc field is increased owing to the increase in electron losses by the introduction of drift.

1.7 Amplification of an injected stream of electrons

Consider a system in which electrons are emitted from a point on one electrode of a parallel-plate assembly into a gas stressed by a unidirectional field tending to sweep them towards the opposite electrode. Let i_o be the current emitted, and i the current collected at the anode.

Assuming that single-stage collision ionization is the only electron generation process occurring, Townsend[4,6,7] derived the expression

$$i/i_o = e^{\int_o^d \alpha . dx} \qquad \cdots \text{ 1.5}$$

where   is Townsend's first ionization coefficient, being the number of ionizing collisions made by each electron in each centimetre that it drifts through the gas, and depending on the electron energy distribution, and hence on α/p. If ψ is the ionization rate, then $\psi = W\alpha$, where W is the velocity that the electron drifts through the gas.

If collision ionization were the only electron generation process occurring in the gas, the curve of $\log i/i_o$ against d would be a straight

line. Townsend's experimental results show this to be true for small gap widths, but for longer gaps, the curve departs upwards from linearity, amplification taking values larger than those predicted by the simple theory (see Fig. 1.3). Townsend first interpreted this departure from the theory in terms of a secondary process in which positive ions generated by collision ionization, (i.e. the α-process), themselves collide with gas molecules and produce ion pairs (i.e. the β-process). However it was later established that collision ionization of the gas by positive ions under normal breakdown conditions is not energetically possible. A more likely theory of secondary electron generation was suggested, in which positive ions and photons generated in the gap by the α and excitation processes strike the cathode and release electrons from the surface. The expression for i/i_0 was modified to take this into account, thus

$$i/i_0 = e^{\alpha d}/\left(1 - \frac{w}{\alpha} \cdot e^{(\alpha d - 1)}\right). \qquad \ldots \ldots \; 1.6$$

where $\underline{w}$ is the number of secondary electrons produced at the cathode per electron on the gap.

The breakdown condition is satisfied when

$$1 = \frac{w}{\alpha} \cdot e^{(\alpha d - 1)} \; , \; \text{from Eq. 1.6.}$$

This is Townsend's criterion for breakdown in unidirectional fields.

Townsend's theory does not take into account the effects of diffusion. In recent work, Lucas[14], has calculated an expression for amplification in the presence of diffusion. Later chapters in this thesis describe measurements of amplification when the injected electron stream is subjected to combined high frequency and unidirectional fields. Here,

diffusion may be expected to become even more important, and much of this thesis is devoted to problems connected with this possibility.

1.8 Choice of suitable ionization coefficients for uhf conditions

When a unidirectional electric field is applied to the gap, the electron flow in the gap below breakdown is predominantly drift controlled. When ionization occurs, Townsend's first ionization coefficient, α, is commonly used, being the number of ionizing collisions an electron makes in one centimetre that it has <u>drifted</u>. In the case where a uhf field is applied, electron flow is predominantly diffusion controlled, and Herlin and Brown[10] suggested that ψ/D is a suitable ionization coefficient, being proportional to the number of ionizing collisions an electron makes in <u>diffusing</u> a unit distance.

At breakdown, ψ/D may be easily obtained from the breakdown condition, $\Lambda^2 = D/\psi$, but the task is not so easy below breakdown. Attempts to obtain ψ by Nicholls[1] from measurements of ionization currents flowing in combined dc and uhf fields were not entirely successful because at that time the nature of electron flow in the gap was not fully understood for these conditions. (See Chapter 2).

2. Diffusion of electrons in a gas

In view of the importance of electron diffusion in the present study, some of the important aspects are discussed here in the introduction.

$$D(\partial n/\partial x) \qquad\qquad D(\partial n/\partial x) - D(\partial^2 n/\partial x^2)\delta x$$
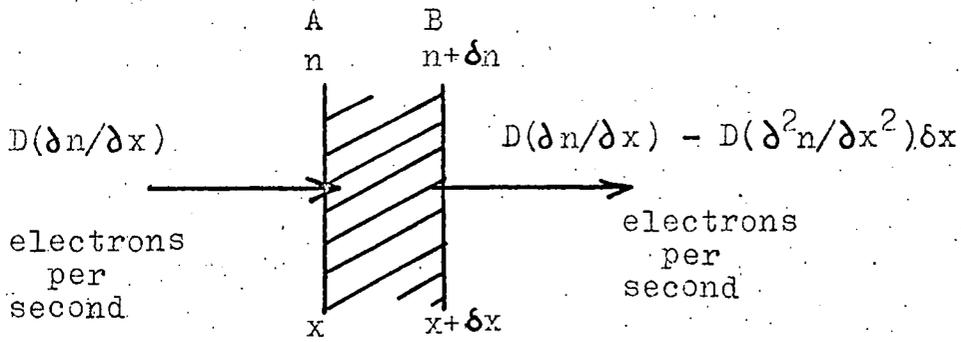
Fig 1.4. Electron flow by diffusion through an elementary slice of gas in the absence of an electric field.
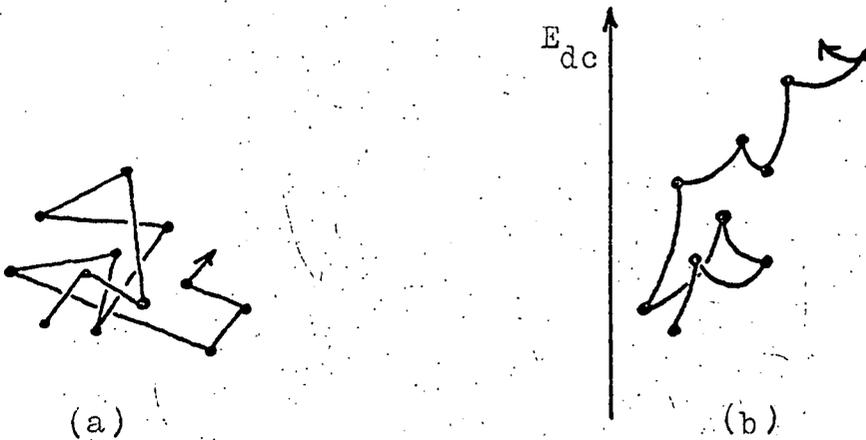
Fig 1.5. (a) Diffusion in the absence of a field.
(b) Diffusion in the presence of a field.

• Gas molecules.
→ The path of an electron.

2.1 Basic diffusion relations

Electrons in a gas are constantly colliding with molecules of the gas, and thus come into thermal equilibrium with the gas. In time, any concentration of electrons will move such that, provided there are regions of weaker concentrations of them, the initial concentration is decreased. This motion tends to bring about a uniform density of electrons in the body of the gas. Once this has been achieved, the diffusion process still continues, but not with the net effect that the electron density distribution in the system does not alter further, a steady state having been reached.

Fick's Law describes the behaviour of such a system when no external fields are applied. Consider a plane drawn in a gas along a direction where the electron density is constant. Let the electron density at this point be $\underline{n}$, and the concentration gradient at this plane be $\partial n / \partial x$. Then Fick's Law states that the electron flow crossing unit area of the plane per second is $D. \partial n / \partial x$, where D, the electron diffusion coefficient is given by

$$D = \lambda \bar{c}/3 \qquad \qquad \dots \quad 1.7$$

where λ is the mean free path between collisions that an electron makes with gas molecules, and $\bar{c}$ is the average random velocity of electrons, assuming a Maxwellian distribution.

Now consider two such planes, A and B, (see Fig. 1.4), of unit area, separated by a small distance δx. If at time t, the electron concentration is $\underline{n}$ at plane A, then at B, it will be $n - (\partial n / \partial x)\delta x$.

From Fick's Law, the number of electrons flowing into A in a small time interval δt will be $D(\delta n/\delta x)\delta t$, and the outflow from B will be

$$D(\delta n/\delta x)\delta t - D(\delta^2 n/\delta x^2)\delta x. \delta t.$$

Then the volume contained by A and B gains a net total of $D(\delta^2 n/\delta x^2)\delta x$ electrons per second.

Thus the rate of change of electron concentration is given by

$$\delta n/\delta t = D. \delta^2 n/\delta x^2 \qquad\qquad \cdots\cdots 1.8$$

In three dimensions this becomes, $\delta n/\delta t = D.\nabla^2 n.$ $\cdots\cdots$ 1.9

This is the equation of continuity for electron flow in and out of the region (dx, dy, dz) for the case when no external electric field is applied. (When an electric field is applied terms must be added to this expression to account for drift, ionization, and other effects which might affect the flow of electrons. (see Eq. 1.1).

It is of considerable interest to compare the above relation with the expression for heat flow in a conducting medium.

i.e. $k \delta^2 \phi/\delta x^2 = \delta\phi/\delta t$, in the one dimensional case $\cdots\cdots$ 1.10

where $\delta\phi/\delta t$, the rate of change of temperature in the element (dx, dy, dz), is directly analogous to $\delta n/\delta t$, the rate of change of electron density in Eq. 1.8, and $\delta^2 \phi/\delta x^2$ is similarly directly analogous to $\delta^2 n/\delta x^2$ and where $k = K/\sigma s$, K being the coefficient of thermal conductivity, σ the density of the material and s the specific heat of the material.

Both D and k have units of $cm^2/second$, and k has come to be known as the 'temperature diffusivity'.

It is sometimes very useful to be able to think of a diffusion problem in terms of the directly analogous problem in thermal conductivity. The solutions of Eqs. 1.8 and 1.10 are identical in form.

2.2 Particle distribution in space and time under diffusion

Einstein[15,16] considered the spatial and temporal distribution of particles moving independently of each other with chaotic heat motions. Consider that when $t=0$ there are N_o particles at the origin, $x=0$.

The number that are located at time, t, between x and $x+dx$ is given by

$$N_x = (N_o/(4\pi Dt)^{1/2}) . e^{-x^2/4Dt} . dx \qquad \dots \quad 1.11$$

This expression has the form of the Gaussian error curve, from which it has been shown that the displacement of the average particle is $(4Dt/\pi)^{1/2}$ in one dimension, $(8Dt/\pi)^{1/2}$ in two and $(12Dt/\pi)^{1/2}$ in three.

These forms have very useful applications in making rough calculations of particle displacements in diffusion problems, and comes into practice in later chapters of this thesis.

2.3 Ratio of the diffusion coefficient and the mobility

From Eq. 1.7, $D = \lambda \bar{c}/3$. Similarly the mobility is given by

$$\mu = \lambda e/m\bar{c} \qquad \dots \quad 1.12$$

From these two relations

$$D/\mu = \bar{c}^2 m/3e = \frac{2}{3e}(m\bar{c}^2/2) = 2u_{ave}/3 \qquad \dots \quad 1.13$$

where u_{ave} is the average electron energy, and is a function of E/p. The numerical quantity, 2/3, occurs when a Maxwellian distribution is assumed for the velocity of the electrons.

2.4 Ambipolar diffusion

In many studies, the forces between charged particles can be ignored. However when there are sufficient amounts of charges of both sign present, and one type is diffusing more rapidly than the other, the charge separation thus produced may set up a considerable space charge field locally. Such a field can alter the diffusion coefficients of the carriers of both signs. The effect of this electric field is to retard the diffusive motions of the electrons, and to enhance that of the positive ions, such that the flow rates of both types of carrier tend to become equal. In the present experiment, however, where the studies are confined to the region below breakdown, densities of electrons and positive ions are so small that ambipolar diffusion may be neglected.

2.5 Back diffusion

Back diffusion is an important process occurring when electrons or ions are emitted from a source on the surface of an electrode into a region containing a gas. The emitted carriers suffer collisions with gas molecules, the result being that some may return to the emitting electrode. The effect was first observed during early experiments in which electrons were released from a cathode by shining on ultra-violet light. If i_o is the current collected at the anode when the system is evacuated (thus making it possible to assume that i_o is the current actually emitted from the emitting electrode surface), and i is the current reaching the anode in the presence of a gas, it was observed for a given voltage on the gap, and in the absence of ionization, that i/i_o was less than unity, decreas-

ing further as the pressure was increased. This pressure dependence suggested that the effect may be due to diffusion and theories based on the concept of back diffusion were forwarded in an attempt to explain the results.

One of these theories was that of J. J. Thomson[16,17] in which he suggested that the process is one in which the electrons are effectively 'reflected' back to the emitting electrode by the gas, and depends on the electr.. having finite initial energy as they come into the gap. His theoretical expression for i/i_o gives reasonable agreement with the experimental results in hydrogen and nitrogen, but fails in the case of the atomic gases. (Theobald[18]).

A sophisticated theory for the diffusion of electrons moving out into the gap from a point on the cathode under the influence of a uni-directional field was developed by L. G. H. Huxley[19], in which an expression for the electron density distribution in the gap was obtained from the solution of the steady state continuity equation for electrons moving in the gas by a mixture of drift and diffusion. The theory was applied successfully over the surface of the anode to explain Townsend's measurements on the spread of a stream of electrons crossing the gap. Long[2] has attempted to extend the theory into the region close to the emitting electrode, for the calculation of back diffusion currents in the special case of combined dc and uhf fields in the gap. (See Chapter 2).

The applicability to the present experiment of Thomson's theory of back diffusion, and Long's extension of the Huxley theory are discussed

at length in Chapter   of this thesis.

2.6 Diffusion limited lifetime in uhf discharges

In pure uhf discharges, the diffusion limited lifetime, given by $t_d = \Lambda^2/D$,[10] represents the average time during which an electron will remain in the gap before it is lost by diffusion.

When a small dc field is superimposed on the uhf field, and $E_{dc} \ll E_u$, Λ^2 in the above expression is replaced by Λ_m^2 [13] (see Eq. 1.4), to take account of the decrease in the lifetime of the electron by the introduction of drift.

2.7 Drift and diffusion

In the absence of an electric field electrons in a gas diffuse freely as described in §2.1, and there is no drift. Electrons traverse straight paths between successive collisions with gas molecules (Townsend[5]) (see Fig. 1.5a). In the presence of a field, drift and diffusion occur simultaneously. The motion of the electrons between collisions is now perturbed so that they try to move in the field direction instead of the direction with which they initially move away from the collision. The resultant effect is that the paths between collisions become curved towards the direction of the applied field, and there is a net advance in the field direction. (See Fig. 1.5b).

The relative importances of diffusion and drift, particularly in combined dc and uhf fields, are discussed in detail in a later chapter of this thesis.

3. Phenomena associated with the electrode surfaces

Since the earliest days of gas discharge physics, problems have been encountered associated with the state of cleanliness of the electrode surfaces.

J.J. Thomson[20] in his experiments in which he passed a beam of cathode rays at right angles through an electric field placed between two parallel plates, observed that the deflection of the beam by the field decreased steadily with time as the beam was continuously applied. He concluded that ions and electrons from the beam diffused to the plates, causing charging, and thus reducing the effective field between the plates.

In unidirectional discharges, there has been observed a marked difference in breakdown potential for clean and dirty electrodes, (Llewellyn-Jones and Davies[21]). But in uhf discharges, where the electrodes play a far less important part in the discharge, there is no marked difference. (Llewellyn-Jones and Morgan[22]).

In the case of combined dc and uhf fields, the surfaces become important again. Experiments by Long[2] have lead to the conclusion that during a discharge in combined fields, the plates become charged up such that the effective unidirectional voltage on the gap is reduced. It was suggested that this charging process was made possible by the presence of insulating layers on the electrodes and that such layers could be the result of the action of discharges on molecules of grease present in the system during the experiment.

Detailed work has been performed on the nature of the contamination

experienced in ultra-high vacuum plant. (Holland, Laurenson and Priest-land[23]; Christy[24]). It was shown that certain silicone oils commonly used in diffusion pumps produced vapours, which under electron bombardment, polymerize to form permanent insulating deposits. Of the two common silicone oils used in diffusion pumps, grade 705 was observed to produce less than half the contamination than was produced by grade 704 under similar conditions.

Oxidation of the electrode surfaces is another possible source of the formation of insulating surface layers. However, Llewellyn-Jones[21] showed that in the case of aluminium electrodes, the oxide could be effectively removed by bombarding the surface with hydrogen ions.

In this thesis, more studies into surface phenomena and their associated effects (with regard to the present experiment) are described, firstly by studying the time dependence of the current flowing across the gap in the absence of the uhf field, and then by measuring the residual voltage produced in the gap, using the ellipsoid voltmeter[25].

Emitting Electrode

Collecting Electrode

E_u

P_1

P_2

V_1

V_2

i_1

i_2

Filament

Backing Plate

G_1 i_1 G_2 i_2
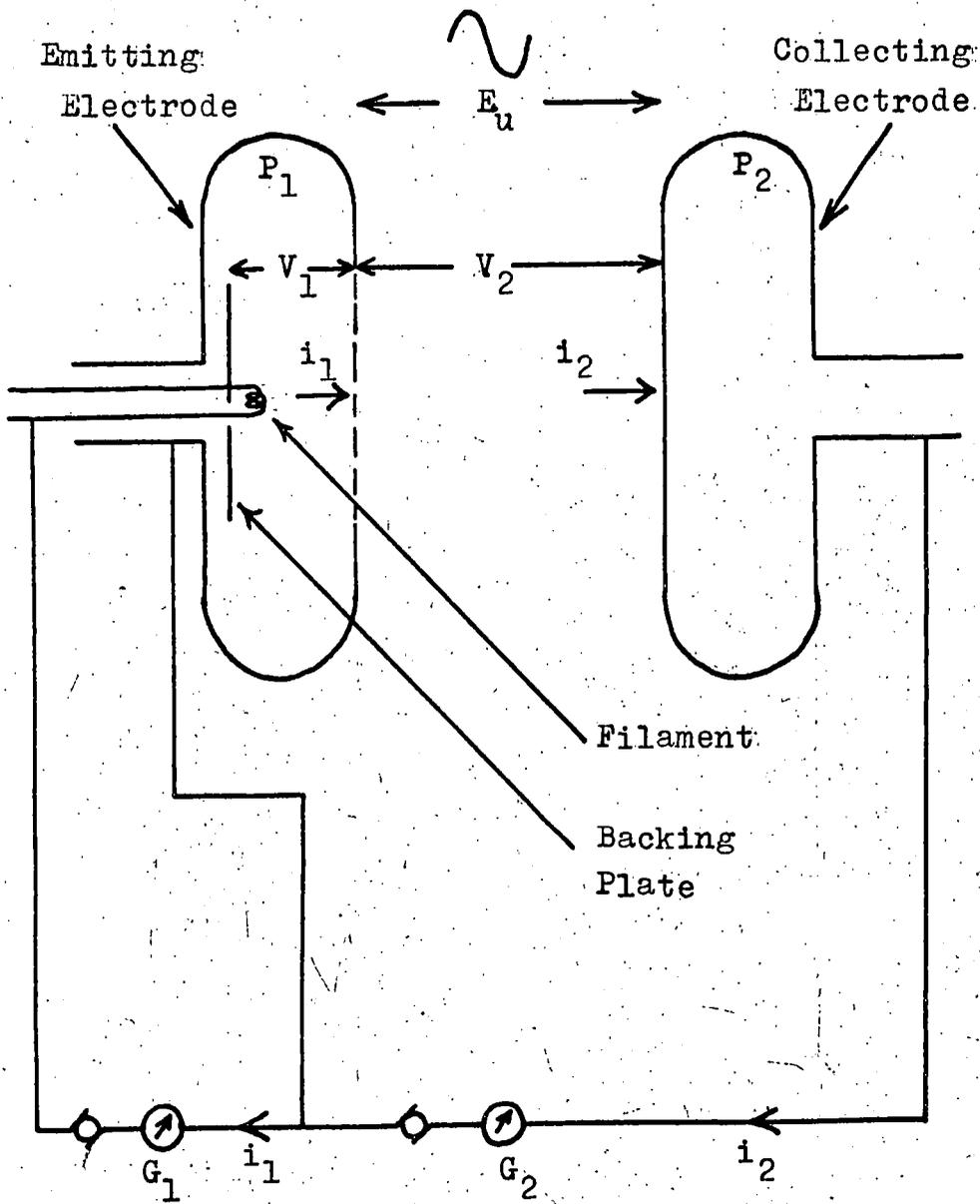
Fig 2.1. Diagram of electrode assembly, indicating the voltages applied and directions of current flow.

CHAPTER 2

THE PROBLEM

1. Basic practical aspects

The aim of the experiment is to provide information about the behaviour of a swarm of electrons introduced into a gas stressed by known parallel unidirectional and ultra-high-frequency electric fields. This is done using an apparatus similar to that used by Townsend in his experiments for the measurement of the ionization coefficient, . (See Chapter 1, §1.7). Electrons generated thermionically are admitted into the gap of a parallel plate electrode assembly through holes in one of the plates, P_1. (See Fig. 2.1). Once the electrons are in the gap their energy is enhanced by the uhf field, E_u, while they are caused to drift across the gap to the opposite electrode, P_2, by the unidirectional field, E_{dc}. The chief measurable quantity is the flux of electrons to the collecting electrode, and this is affected by the processes of drift, diffusion and ionization which occur in the gas as functions of the nature of the gas, its pressure, the dimensions of the gap and the magnitudes of the applied electric fields.

The voltages applied are

a) V_1, the dc voltage between the filament and P_1, required to sweep electrons from the filament towards the back of the holes through which the electrons emerge into the gap.

b) V_2, (E_{dc}), the dc voltage applied across the gap to sweep the electrons from P_1 to P_2.

c) E_u, the uhf field applied to the gap to increase the energy of electrons in the gap.

The currents measured are

a) The current, i_1, from the filament which reaches the back of the emitting electrode, P_1. Of this only a small fraction of the electrons arriving stand a chance of getting through the holes and into the gap. The actual current which is introduced into the gap this way depends on the gas pressure, the temperature of the filament, and on V_1.

b) i_2, the current collected by the collecting electrode, P_2.

2. Definition of amplification

Amplification is defined in the present experiment as the ratio of the current collected by the collecting electrode, P_2, with the uhf field on, (i_2), to that collected with the uhf field off, (i_{20}), the dc field being kept constant.

Amplification, $A = i_2/i_{20}$ 2.1

Throughout this thesis, the curves relating A with the applied uhf field, E_u, for a given value of gas pressure and applied dc field, E_{dc}, are referred to as AMPLIFICATION CURVES.

3. Previous work

Investigations using the type of apparatus just described have
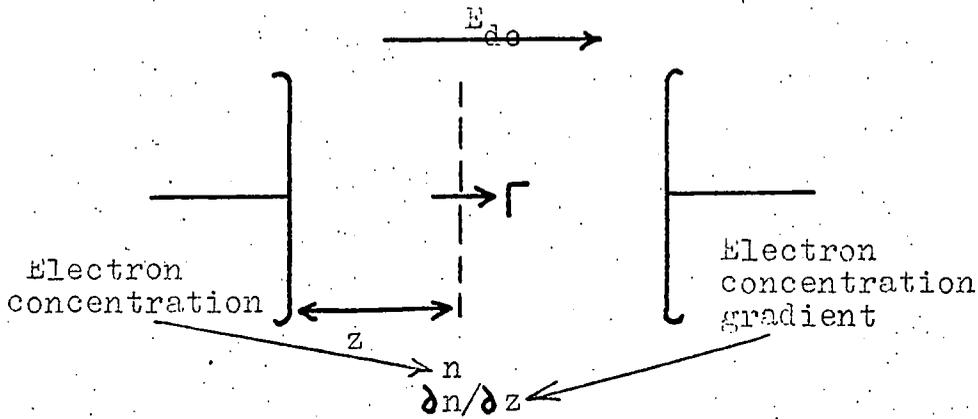
Fig 2.3. Diagram for current density equation
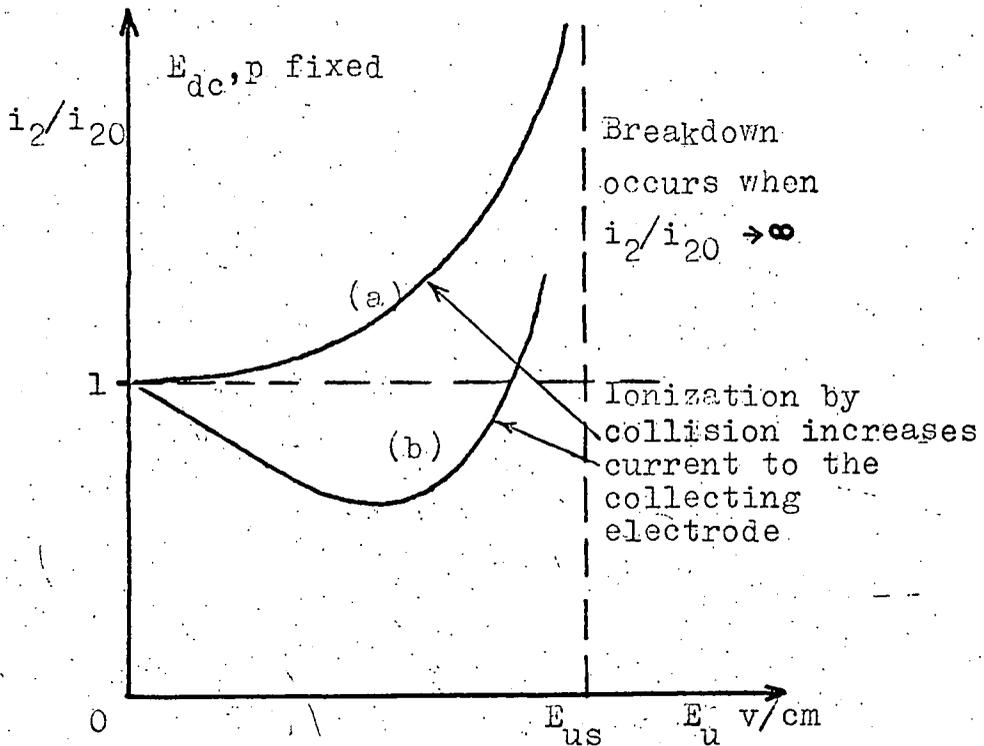
Fig.2.2. (a) Expected shape of amplification
curve.
(b) Actual shape of amplification
curve.

previously been made at Durham by Nicholls[1] and later by Long[2].
Measurements of amplification were obtained and curves plotted of A
against the uhf field, E_u, keeping E_{dc} and pressure constant for a
given curve. It was originally expected that the curve would start at
$A = 1$ when E_u was zero, then increase with E_u, getting gradually steeper
and eventually approaching infinity as ionization by collision increases
the current flowing to the collecting electrode. (See Fig. 2.2a). It
was hoped from such a curve to calculate values for the pre-breakdown
high-frequency ionization coefficient in the manner similar to Townsend
for avalanches in dc fields only. (Ch. 1, §1.7). However it is not
possible to do this satisfactorily because the experimental amplification
curves do not follow the simple form described above. Instead, the
curves show an initial decrease in amplification at lower values of E_u,
eventually increasing and rising above unity only when ionization gets
well established at higher values of E_u (see Fig. 2.2b). For higher
values of E_{dc} this dip is reduced in size, and vice-versa for smaller
values of E_{dc}. Before accurate values of the ionization coefficient can
be obtained from these curves, the dip must be accounted for. It has
been at least partially explained in terms of electrons diffusing back
to the emitting electrode. The possibility that electrons are swept back
to the emitting electrode by drift in the appropriate cycles of the uhf
field was considered by Nicholls, but no satisfactory conclusions could
be drawn. There follows a brief summary of the early theoretical work
performed in attempts to explain the shape of the amplification curves.

3.1 The work of Nicholls[1,26] (1960)

Consider the case of one-dimensional electron flow in the gap under the influence of the combined dc and uhf electric fields when no ionization occurs.

The equation for the current density vector in electrons per second flowing through unit area is given by

$$\Gamma = n \mu E_{dc} - D \partial n/\partial z \qquad \dots \quad 2.2$$

where n is the number of electrons per cc. at a distance z from the emitting electrode. (See Fig. 2.3). The first term in this expression is the contribution due to the electron mobility, μ, and the second term is due to the concentration gradient of electrons in the gap.

When there is no ionization, and no electrons are lost by diffusing radially out of the gap, $\partial \Gamma/\partial z = 0$. Therefore, $\Gamma = C$, a constant. Then Eq. 2.2 becomes $n \mu E_{dc} - D \partial n/\partial z = C$ and the solution for n is

$$n = n_0(e^{\mu E_{dc} z/D} - e^{\mu E_{dc} d/D})/(1 - e^{\mu E_{dc} d/D}) \qquad \dots \quad 2.3$$

inserting the boundary conditions that $z = 0$ when $n = n_0$ and $z = d$ when $n = 0$. (Putting $E_{dc} = 0$ in this equation gives $n = n_0(1-z/d)$, the equation when diffusion is the only loss process occurring).

Substituting for n in Eq. 2.2 gives

$$\Gamma = \mu E_{dc} n_0/(1 - e^{-\mu E_{dc} d/D})$$

$$\rightarrow \mu E_{dc} n_0 \qquad \dots \quad 2.4$$

because $e^{-\mu E_{dc} d/D}$ is negligible under the conditions of the experiment. If Γ is the current density across the gas to electrode boundary, it
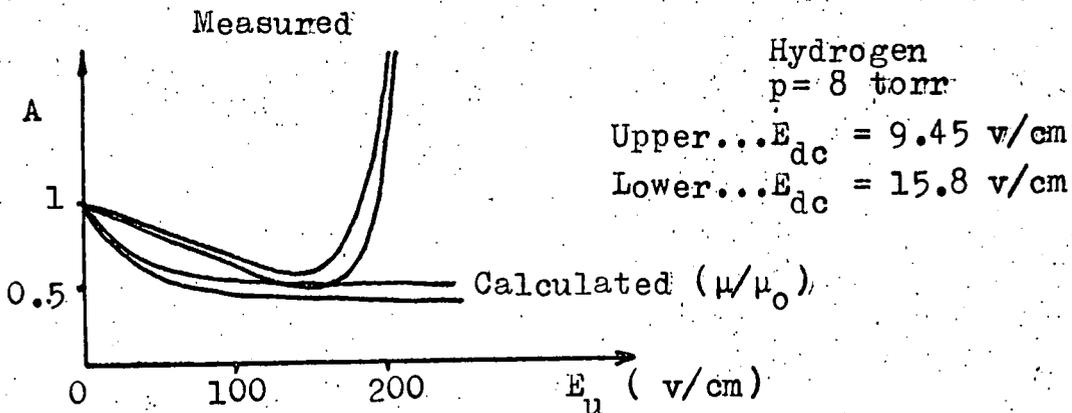
FIG 2.4. Comparison between experimental and calculated amplification curves.(Nicholls).
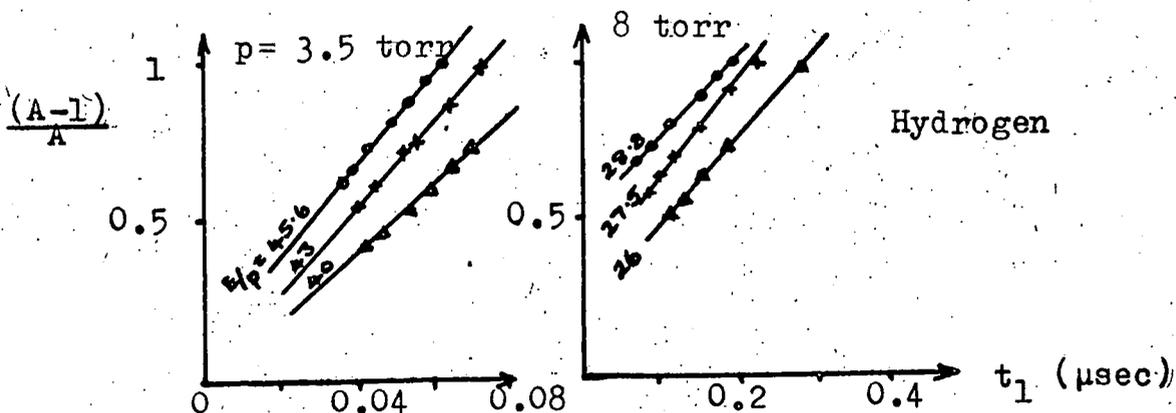
FIG 2.5. (A-1)/A as a function of electron lifetime, t_1 (Nicholls).
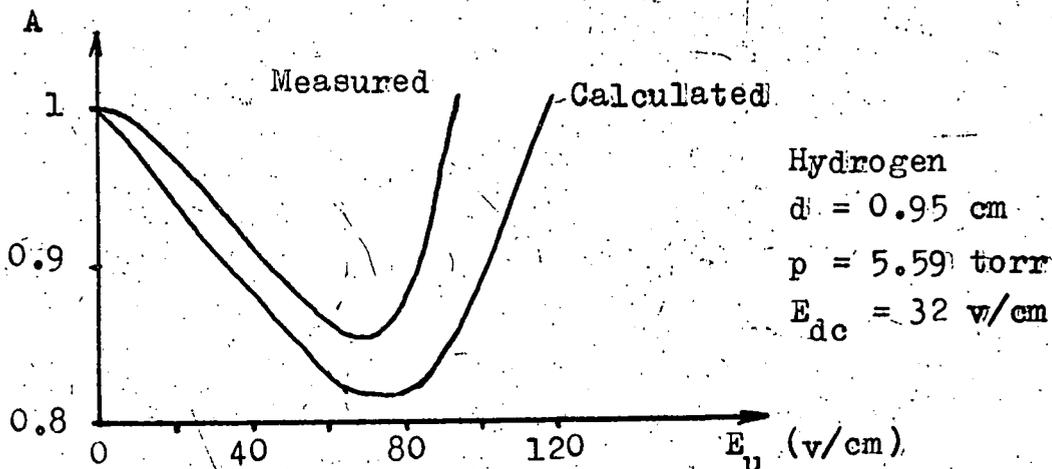
FIG 2.6. Comparison between experimental and calculated amplification curves.(Long)

must be proportional to the current flowing through the galvanometer, G_2. (i.e. i_2). Then let Γ_o be the current density flowing to the collected electrode when the uhf field is applied, but with no ionization.

Then, in the absence of radial diffusion, amplification

$$A = i_2/i_{20} = \Gamma_u/\Gamma_o = \mu_u/\mu_o \qquad \text{.... 2.5}$$

where the subscripts for μ apply to the same conditions that were defined for Γ.

Values for the mobility μ in hydrogen were obtained from Crompton and Sutton[27], and Nicholls plotted theoretical curves relating i_2/i_{20} to the uhf field when no ionization occurs. Theoretical and experimental curves for a typical set of conditions are compared in Fig. 2.4. Agreement between the two is fair.

This theory suggests that the dip observed in the amplification curves is associated with the drop in mobility of the electrons as their random energy is enhanced by the uhf field. The theory does not take into account the behaviour of the electrons as they emerge into the gap, nor of diffusion of electrons radially.

3.1.2 Calculation of the ionization coefficient, Ψ, hence α.

The lifetime of the electron in the gap in the combined fields is controlled by drift as well as diffusion, instead of by diffusion alone as in the pure uhf case. The new diffusion and drift limited lifetime is given by $t_d = \Lambda_d^2/D$, where $1/\Lambda_d^2 = 1/\Lambda^2 + (E_{dc}/2(D/\mu))^2$ (Varnerin and Brown[13]).

Nicholls developed a theory to take account of the fact that in the presence of the dc field the electron may be in the gap for a time shorter than the time during which, on the average, it will generate one new electron.

Let t_b be the electron lifetime in a pure uhf discharge. Then one new electron will be generated by an electron in that time.

Then, $$\psi t_b = 1. \qquad \qquad \dots \quad 2.6$$

The lifetime of the electron in the gap is now reduced to t_d by applying a small dc field, keeping E_u, (and hence ψ, provided that the dc field is small enough), constant.

A number of electrons, N, entering the gap at time $t = 0$ will on the average leave at time t_d. Since each electron will produce on average one new one in time t_b, the number produced by N initial electrons in time t_d is Nt_d/t_b.

Then the total progeny of one electron initially entering the gap is

$$1 + (t_d/t_b) + (t_d/t_b)^2 + \dots \quad \text{etc.}$$

Let N_0 electrons enter the gap at the start of every time interval of length t_d. Then at any instant there will be $N_g = N_0(1+(t_d/t_b)+ \dots)$ electrons in the gap.

i.e. $$N_g = N_0 (1 - t_d/t_b)^{-1}. \qquad \qquad \dots \quad 2.7$$

If all these are swept to the collecting electrode, (ignoring losses by back diffusion)

$$N_g/N_0 = A, \text{ amplification.}$$

From Eq. 2.6,

$$\psi t_d = (A-1)/A \qquad \qquad \dots \quad 2.8$$

From the theoretical curves for amplification (Fig. 2.4) it is seen that the effective current in the absence of collision ionization levels off to a steady value at about the minimum in the dip of the experimental curves. Thus it is possible to effectively remove the back diffusion component from the experimental curve to give a curve in which amplification is always greater than unity. These modified values of A were used in the calculation of   from the above expression.

Typical curves of $(A-1)/A$ against t_d are shown in Fig. 2.5. The method of Varnerin and Brown[13] was used to calculate t_d. (Prowse and Nicholls[26] also deduced values of t_d from their own measurements of breakdown stress in the combined fields, and these were found to be in good agreement with those of Varnerin and Brown).

These curves are straight lines of slope ψ. From $\psi = W\alpha$, where W is the electron drift velocity corresponding to the mean value of the uhf field, values of α/p were calculated, giving moderate agreement with those obtained by Brown[28]. Perfect agreement could not be expected, because the theory does not take into account those electrons, generated in the gap by collision ionization, which diffuse back to the emitting electrode.

3.2 The work of Long[2,29] (1962)

Consider a gas in which a steady state has been attained between ionization and electron drift.

The equation of continuity for a bounded region within the gas may be written as

$$\nabla^2 n - 2\theta \, \partial n / \partial z + \frac{\Psi n}{D} = 0 \qquad \dots \quad 2.9$$

where $2\theta = \mu E_{dc} / D$.

Any variation of the uhf field will alter $/D$, and also μ in this equation. The experimentally measureable quantity is the current flowing to the collecting electrode, and the current density, , is related to the electron density, n, by the equation

$$\Gamma = n \, \mu \, E_{dc} - D. \nabla \, n \qquad \dots \quad 2.10$$

which is the same as Eq. 2.2, except that now diffusion is considered in three dimensions. The holes in the surface of the emitting electrode are essentially point sources of electrons. Long assumed that the case where the emitting electrode contains many holes (about 50 in his experimental case) is in fact the same problem as the case where there is only one hole, and conducted his theoretical analysis accordingly. The problem of a single point source on an infinite conducting plane emitting electrons out into a gas has been treated by Huxley[19].

The substitution $U = n \, e^{-\theta z}$ reduces Eq. 2.9 to

$$\nabla^2 U + (\Psi/D - \theta^2). U = 0 \qquad \dots \quad 2.11$$

Let the point source be at the origin of coordinates, and let a typical point in the inter-electrode space be defined by (x,y,z), where z is directed along the direction of the applied field, and also by r and ρ, where r is the distance from the origin, and ρ is the projection of r on the emitting electrode. Then the electron density, n, at such a point is given by

$$n = Be^{\theta z} \left\{ \frac{z}{r} \frac{d}{dr} \left(\frac{e^{-\ell r}}{r}\right) + \left(\frac{z-2d}{r_1}\right) \frac{d}{dr_1} \left(\frac{e^{-\ell r_1}}{r_1}\right) \right.$$
$$\left. + \frac{(z+2d)}{r_2} \cdot \frac{d}{dr_2} \left(\frac{e^{-\ell r_2}}{r_2}\right) + \ldots\ldots \right\} \qquad \ldots \quad 2.12$$

where $r^2 = \rho^2 + z^2$; $r_1^2 = \rho^2 + (z-2d)^2$; $r_2^2 = \rho^2 + (z+2d)^2$; etc....

$\rho^2 = x^2 + y^2$. Also $\ell^2 = (\theta^2 - \frac{\psi}{D})$

The constant B is proportional to the strength of the source. Solutions of this form can only be obtained if ($\psi/D - \theta^2$) is negative. If positive the solution is of the sinusoidal form.

Long found it convenient to subdivide the various electron currents flowing in the gap, thus;

a) i_e, the total current emitted from the source, which in this case is the hole in the emitting electrode, P_1.

b) i_B, the current flowing to P_1 by back diffusion.

c) i_2, the current flowing to the collecting electrode, P_2.

d) the current due to electrons generated in the gap by collision ionization.

e) the current due to the radial flow of electrons out of the gap, which is negligible here.

there is no ionization, $i_2 + i_B = i_e$, but when ionization occurs, $i_2 + i_B$ is greater than i_e because i_2 and i_B both contain electrons which are created by ionization in the gap. Then, $i_2 + i_B = i_e + \psi \int_V n \cdot dV$, where dV is an elementary volume in the gap, and V is the whole effective volume of the gap.

The gap transmission coefficient, T_g, is a convenient quantity to describe the current reaching P_2 in terms of the current emitted.

$$T_G = i_2/i_e = i_2/(i_2 + i_B - \psi \int_V n.\,dV). \qquad \dots \quad 2.13$$

Over the conducting surfaces, $n = 0$ (Herlin and Brown[10]), and the current density is given by $\Gamma = -D\,\partial n/\partial z$. The expression for n (Eq. 2.12) is inserted into this relation and the current density flowing to each electrode, Γ_2 and Γ_B, is calculated by inserting the appropriate boundary conditions, i.e. $z = 0$ at P_1, and $z = d$ at P_2. The currents i_2 and i_B are obtained by integrating the current density over the surface of the corresponding electrode.

For i_2, Γ_2 is integrated between the limits $\underline{a}$ and zero, and for i_B, Γ_B is integrated between the limits $\underline{a}$ and $\underline{b}$, where $\underline{a}$ is the overall electrode radius, and $\underline{b}$ is the radius of the hole in the emitting electrode.

It can be shown that

$$n.\,dV = \frac{2\pi\psi B}{(\theta - \ell)} \quad e^{(\theta - \ell)d} - 1 \qquad \dots \quad 2.14$$

Now substituting for i_2, i_B, and $\psi \int_V n.\,dV$ we get

$$T_g^{-1} = 1 + \frac{d}{2}(\theta + \ell)(-1 + e^{-(\theta - \ell)d}) + \frac{d}{2b}e^{-\ell b}e^{-(\theta - \ell)d} \quad \dots \quad 2.15$$

This expression is normalised to become unity when the uhf field is zero. Then $\theta = \theta_1 = E_{dc}/2(D/\mu)_{dc}$ where $(D/\mu)_{dc}$ corresponds to the energy supplied to the electrons by the dc field alone.

Hence, $\qquad T_{gn} = (1 + \frac{d}{2b}e^{-\theta_1 b})T_g.$ $\qquad \dots \quad 2.16$

Now, $T_g = i_2/i_c$, thus $T_{gn} = \dfrac{i_2/i_e}{i_{20}/i_{e0}}$

If it is assumed that the number of electrons emerging into the gap

does not depend on the uhf field, $i_e = i_{eo}$.

Then, $T_{gn} = i_2/i_{20}$ = Amplification, A. 2.17

In order to make theoretical calculations of A from Eqs. 2.15, 2.16 and

2.17, values of μ/D were used based on the measurements of Varnerin and

Brown[13] in hydrogen. Values of ψ/D for hydrogen were obtained from

measurements of the ionizing efficiency by Leiby[30] and Clark[12].

It is of interest to consider the case where ionization is negligible.

Then $\theta = \ell$.

Then, $T_{gn} \rightarrow e^{-b(\theta_1 - \theta)}$ 2.18

under the experimental conditions chosen.

Agreement between theory and experiment for the amplification

curves was good over the limited range of conditions tested. (See Fig. 2.6).

4. Influence of the previous work on the present study

In his theory for the shape of the amplification curves, Nicholls

does not take into account the size of the holes through which the

electrons emerge into the gap. The radius of the hole does appear in

the expression derived by Long, but features unexpectedly predominantly.

This can be seen most clearly by inspecting the expression for amplifica-

tion in the absence of ionization. (Eq. 2.18).

Both theories agree moderately well with experiment, with Long's

theory based on Huxley's work comparing slightly better than Nicholls'

in the limited ranges of experimental conditions tested. However, neither

agreement is sufficiently close to render the theories conclusive. The

present experiment sets out in the first place to test both theories over a wider range of conditions in the gap, and for other gases as well as hydrogen.

Despite the agreement obtained by Long with experiment, the importance of $\underline{b}$ is slightly surprising. Eq. 2.18 indicates that as $\underline{b}$ is decreased, the fraction of electrons which are lost by back diffusion also decreases. On the other hand, it might be expected that back diffusion would increase as $\underline{b}$ is decreased, in view of the greater area now exposed to the back diffusing electrons. Experiments where $\underline{b}$ is varied are described in Chapter 6, to show whether, in fact, there is any dependence of the amplification curves on the hole size.

Nicholls' calculation of the ionization coefficient were not altogether satisfactory because the dip in the amplification curves was not fully explained. An attempt is made later in this thesis to produce a more precise theory for the dip. In studies such as this, it is important to know which are the controlling mechanisms for the loss of electrons from the gap, and a theoretical study is carried out on the relative predominances of drift and diffusion under various sets of conditions in a later chapter.

CHAPTER 3

THE APPARATUS

The apparatus used in the present experiment is essentially the same as that used firstly by Nicholls, and then by Long. Certain modifications have been made, however, in order to improve the versatility of measurement, if required.

Preliminary calculations on the relative importances of drift and diffusion (see Chapter 7) indicate that at long gap widths, for given values of E_u and E_{dc}, drift is more prominent than at short gap widths. (During the early planning of the present experiment, it was thought that conditions in the gap for which drift was the controlling electron loss mechanism would considerably reduce the effects of back diffusion, and thus make it easier to explain the shape of the amplification curves. Later in this thesis it will be shown that this view is, in fact, an over-simplification of what actually happens.) The requirement that we should be able to work with longer gap widths meant that larger electrodes had to be designed, which in turn involved modifications in the uhf power supply.

Also, bearing in mind the problems of surface phenomena encountered by the previous workers, a grease-free vacuum system was designed in an attempt to remove at least some of the causes of these.
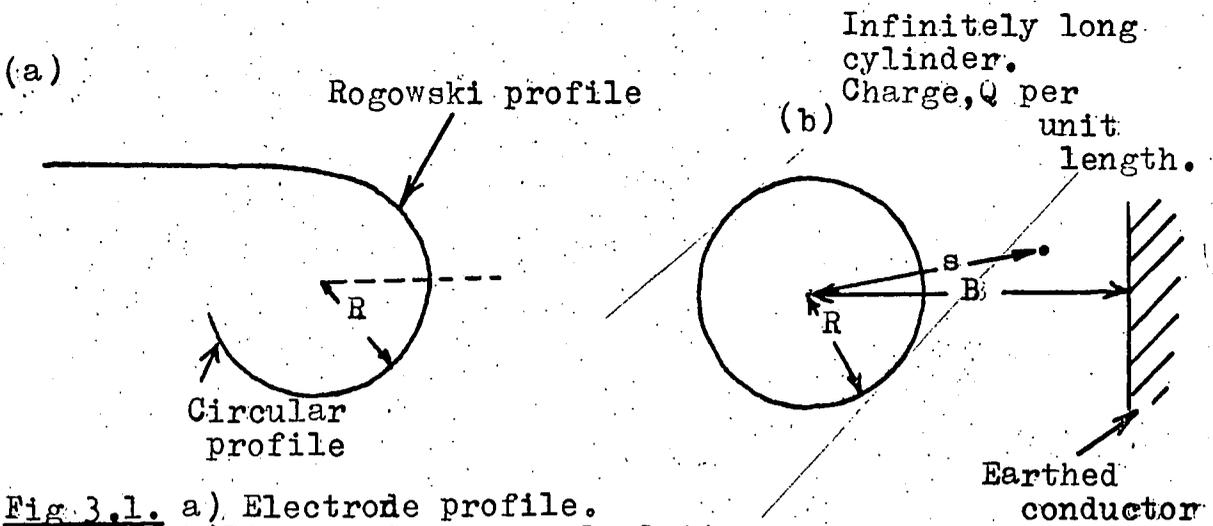
Fig 3.1. a) Electrode profile.
b) Diagram for the calculation
of the field near an infinitely
long conducting cylinder.
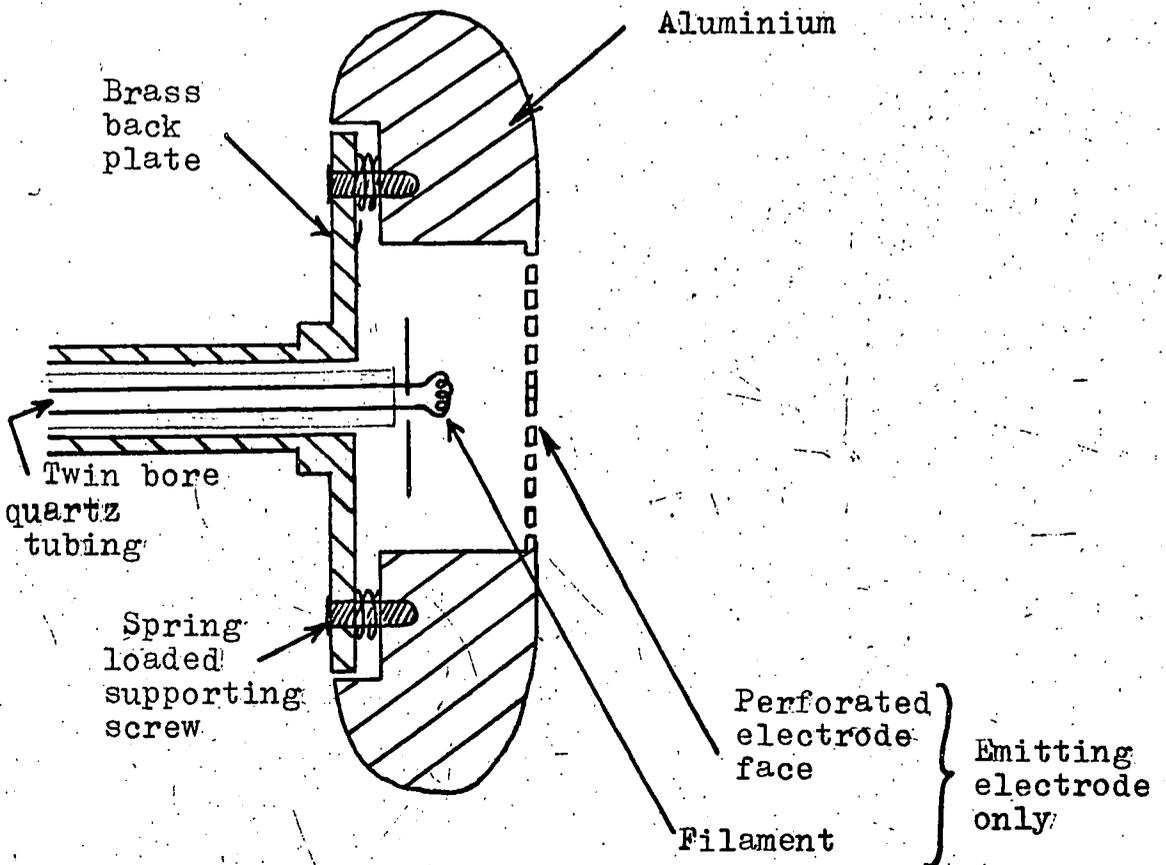
Fig 3.2. Electrode assembly.(Approximately to scale).

1. The electrodes

1.1 The design of the electrodes

In the design of a new electrode system, the necessary experimental requirements must be satisfied. The field in the gap must be uniform, and it must be greater there than at any other point around either electrode. This ensures that breakdown, when it occurs, is at the region where the field is uniform (i.e. along the axis of the gap), and not at the edges of the electrodes. A useful criterion for obtaining a reasonably good uniform field in the gap is that the electrode radius, a, should be equal to or greater than the electrode spacing, i.e. $a \geq d$. To prevent breakdown at the edges of the electrodes, the electrodes must be properly profiled. Bearing this in mind, the design was based on the 120° Rogowski profile[32], corresponding to a maximum gap width of 3 cms, (which is the largest value decided on for the present experiment), with a flat face of radius $a = 3$ cm. From the point of view of the design of the new test cell, it was found necessary to round off the back of each electrode more sharply than given by the Rogowski profile. For this, a circular section of radius R was chosen. (See Fig. 3.1a). The problem now is to calculate the maximum field around the edge of the electrode and to ensure in the final design that this is always less than the field in the uniform field region of the gap. The following is a very crude calculation, but serves as a useful approximate guide to the determination of a suitable value for R.

It can be assumed that the field near the Rogowski part of the profile will not give rise to any problems of unwanted sparking, but at this stage no such assumption can be made about the field near the back edge of the electrode. Precise calculation of this field presents a very complicated problem in electrostatics. However some idea of the magnitude of the field in this region may be obtained from considering the field near an infinite conducting cylinder of radius $\underline{R}$. (See Fig. 3.1b).

For this cylinder, the field strength at a point P, distance s from the axis of the cylinder is given by

$$E_p = Q/s \qquad \qquad \dots \quad 3.1$$

where Q is a constant depending on the charge per unit length of the cylinder.

And at the surface of the cylinder where the field is a maximum,

$$E_{max} = Q/R \qquad \qquad \dots \quad 3.2$$

Now consider that there is an earthed conductor a distance $\underline{B}$ from the axis of the cylinder. Then the potential difference between the cylinder and the earthed conductor is given by

$$V_R - V_B = \frac{Q}{s} \cdot ds \qquad \qquad \dots \quad 3.3$$

$$= Q \cdot \ln(B/R)$$

where V_R is the potential at the surface of the cylinder, and V_B is the potential on the earthed conductor. $(V_B = 0)$.

Then in Eq. 3.3, substituting from Eq. 3.2 for Q,

$$E_{max} = \frac{V_R - V_B}{R.\ln(B/R)} \qquad \dots\quad 3.4$$

This calculation is performed for an infinitely long cylinder. If anything, the field near the back of the actual electrode will be greater than this owing to the additional curvature involved. Therefore we may crudely deduce that for the electrode

$$E_{max} > V_R/R.\ln(B/R) \qquad \dots\quad 3.5$$

Now consider the gap system, with the opposite electrode earthed (potential V_B).

Then with a uniform field in the gap, $E_{gap} = V_R - V_B/d$ $\qquad \dots\quad 3.6$

For breakdown to occur only at the gap centre, along the axis common to both electrodes

$$E_{gap} > E_{max}$$

Then,

$$\frac{V_R - V_B}{d} > \frac{V_R - V_B}{R.\ln(B/R)}$$

Thus, $\qquad \ln(B/R) > d/R$

Or, $\qquad B > R\, e^{d/R} \qquad\qquad\qquad \dots\quad 3.7$

The maximum gap width envisaged in the present experiment is 3 cm. Then, in Eq. 3.7 try $d = d_{max} = 3$ cm, and $R = d_{max}/2 = 1.5$ cm. Therefore, from Eq. 3.7 B > 11 cm. This inequality holds for all values of d less than 3 cm, provided that the value of $R = d_{max}/2 = 1.5$ cm. is used.

Using this value of R, sparking will not occur at the edge of either electrode provided that all earthed conductors are further away

than 9.5 cm. from the edge.

Dummy electrodes, made of wood and covered with aluminium foil, were used in electrolytic tank tests to check the validity of the results obtained from the above calculations. The results of these tests did not go so far as to verify the theory because the tank tests were not sufficiently accurate, but they did not show any sharp deviation from the conclusions drawn from the theory.

It was concluded that the proposed design with $R = 1.5$ cm is a suitable one provided that gap widths above 3 cm are not used, and that all external earthed conductors are placed more than 9.5 cm away from the edge of either electrode.

1.2 Construction of the electrodes

In the previous work of Nicholls[1] and Long[2] the electrodes used were made of brass. The new electrodes were constructed of 99.9% pure aluminium, hollow as shown in Fig. 3.2, with brass back plates. The electrodes were turned roughly to the required shape in the lathe and the final accurate profiles were obtained by projecting the shadow of each electrode onto a master curve, filing and polishing the electrode until the shadow and the master curve coincided. The inside faces of the electrodes were milled until the thickness over the plane region was about .1 cm. Holes of diameter .0344 cm were drilled in the flat face of the emitting electrode, countersunk on the inside so that each hole is effectively a tube of length equal to diameter. To reduce the likelihood of positive ions from the gap passing through these holes

and striking the filament, causing unwanted secondary emission of electrons, as well as damage to the filament itself, no holes were drilled at the centre of the face in a region of radius about .2 cm.

The electrode shells are attached to the back plates by four screws which are spring loaded to enable fine adjustment of the orientation of the faces.

The internal electrodes (i.e. the filament and the cathode plate inside the emitting electrode) are supported by .4 cm diameter twin bore quartz tubing through which the various connections are fed.

(After preliminary measurements of amplification had been obtained using these electrodes, the faces were gold-plated (by evaporation) in order to eliminate the possibility of effects due to oxide layers. Unless otherwise stated, all the results quoted in this thesis were obtained using the gold-plated electrodes).

2. <u>The gap assembly and test cell</u>

The test cell was designed with the following requirements in mind:-

a) The cell must be large enough to house the electrodes in such a way that no earthed conductors are closer than 9.5 cm from the edges of them.

b) The electrodes must be easily demountable, many times if necessary.

c) The system as a whole must have high vacuum properties and be

Pyrex Test Cell

PTFE
insulator

P_1 P_2

UHF indicating
meter

Viton
'O'-rings

Brass Bellows

Tuning
condenser

Asbestos
backing ring

Glass/metal
seal

$\lambda/4$ Transmission
line

Mica condenser
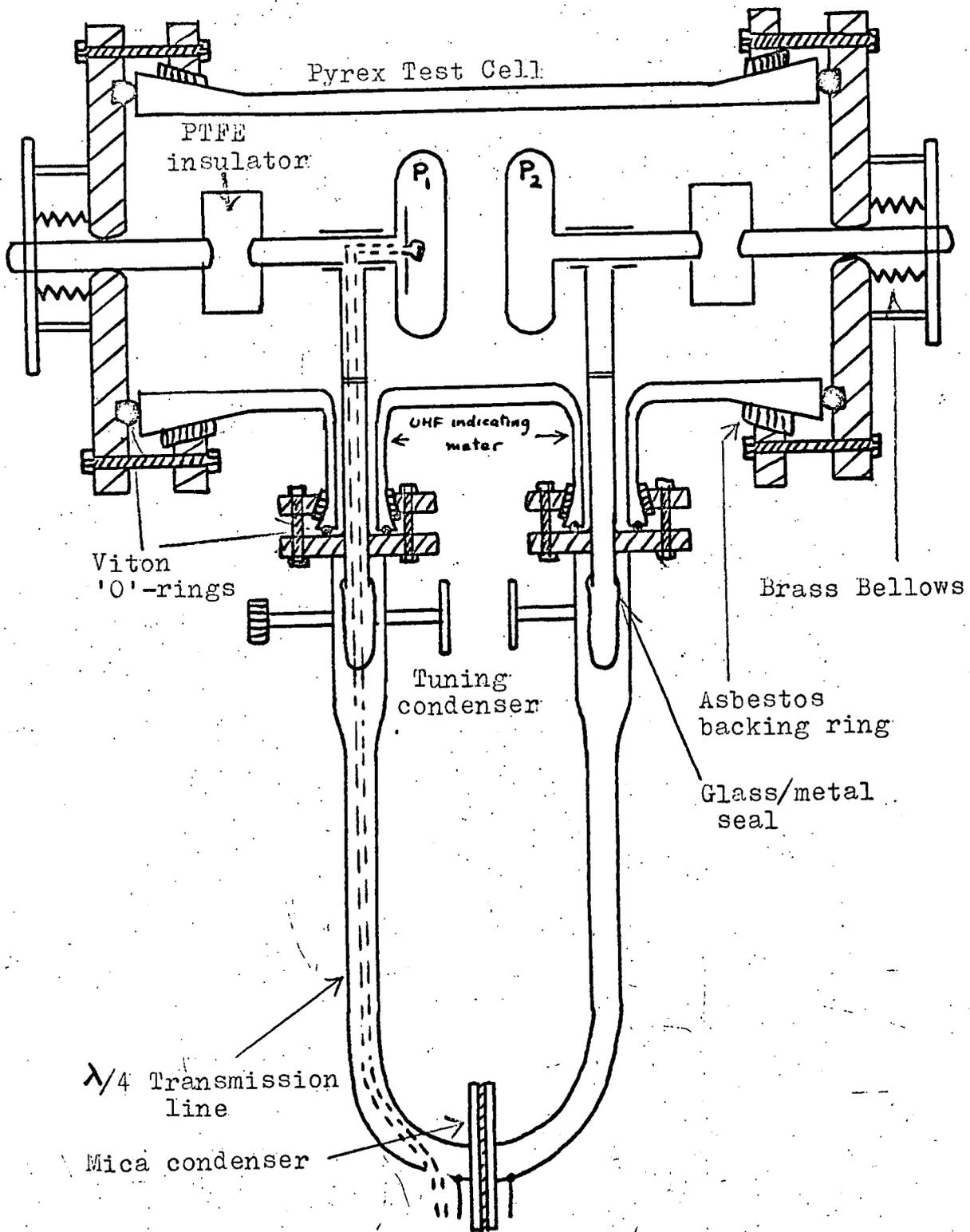
Fig 3.3. The tuned test assembly.

grease-free.

d) The inter-electrode spacing must be easily variable.

e) Access must be made for the elements of the transmission line carrying the uhf power to the gap, and also for the leads to the various current measuring circuits and the filament power supply.

f) The voltage in the gap is measured using a metal bead suspended[25] in the gap by a quartz fibre, so the axis of the gap must be in the horizontal plane. Provision must be made for raising or lowering the bead out of or into the gap as required. This instrument is discussed in detail in §5.1 of this chapter.

The Pyrex glass test cell was built to the required specifications by Quick-fit Visible Flow Ltd. All the demountable vacuum seals make use of 'viton' O-rings, compressed between the ground glass ends of the cell and the steel end plates. (See Fig. 3.3). Viton was chosen in preference to more conventional rubbers on account of its better vacuum and outgassing properties over a wider range of temperatures. It is possible to bake such seals up to temperatures of $200^{\circ}C$ if required.

The electrodes are insulated from the earthed end plates of the cell by PTFE insulating plugs, and are situated at the open end of a $\lambda/4$ parallel wire transmission line, each electrode stem being connected to its appropriate branch of the line by means of sliding T-junction, which enables gap width variation to be made. (See Fig. 3.3). The gap width is variable by means of adjustable bellows in each end plate, and can thus be controlled from outside.

-36-

Glass pipeline

Cold trap

Copper foil

Oil diffusion pump

Pirani gauge

Metal valve (Mullard VMT-18P)

Oil manometer

TEST CELL

Penning gauge

Bellows gauge

GAS

ROTARY BACKING PUMP
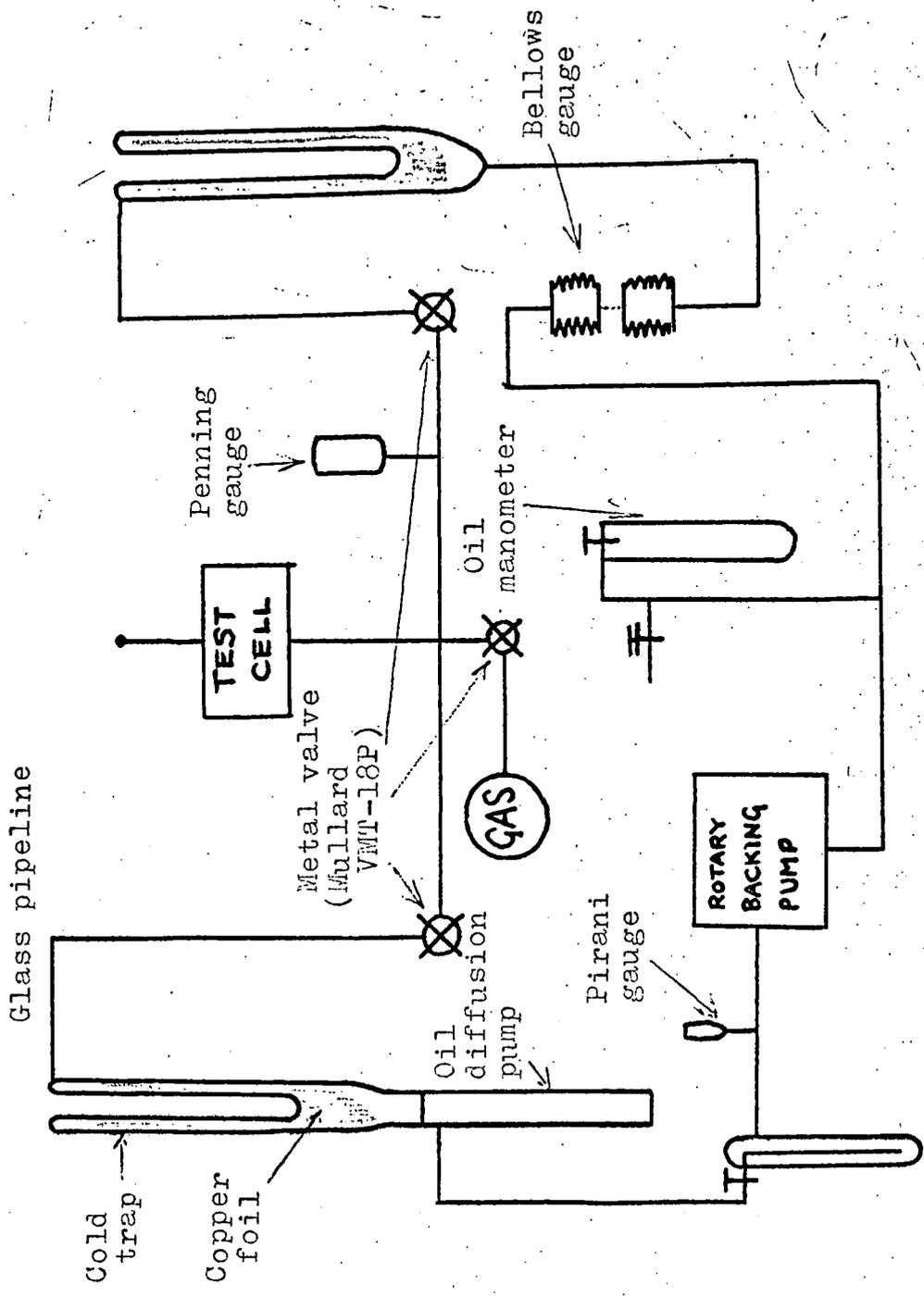
Fig 3.4. The vacuum system.

The steel end plates are mounted on adjustable steel rails which enable the electrodes to be lined up along a common horizontal axis.

3. The vacuum system

Long[2] concluded that many of the difficulties experienced in measuring the gap current were due to the formation of insulating films on the electrode surfaces, and that such films directly resulted from running a discharge in the presence of vapours given off by silicone greases and oils. The experiments of Laurensen, Holland and Priestland[23] confirm this view.

In the present experiment, it is desirable to eliminate silicone vapours as far as possible. As a first step, the silicone grade 704 oil in the diffusion pump was replaced by silicone grade 705[23]. Immediately on top of the diffusion pump was placed a glass cold trap packed with copper foil. (See Fig. 3.4). Silicone molecules or any other organic impurities back streaming from the pump and striking the copper surface are absorbed, thus not reaching the test region of the system. Efficiency of this trap increases with the area of copper exposed to the vacuum. A similar trap was placed close to the bellows pressure gauge.

The pipeline was constructed of 2 cm diameter Pyrex tubing, and grease-free metal stop-cocks (Mullard VMT-18P) were incorporated, keeping the distances of the various parts of the system from the pumps as small as possible to keep the overall pumping efficiency of the system high.

Pressure is measured in three ranges as follows:-

a). In the range 0.5 torr to atmospheric pressure, pressure is measured

using the differential bellows gauge[1,2,33]. (See Fig. 3.4). The pressure in the test system is compared with that in an auxiliary system (in which the pressure is measured accurately using an oil mano-meter) by measuring the deflection of the bellows. The deflection of the bellows is amplified by an optical lever system, and is easily calibrated as indicated above. From the calibration, a sensitivity was obtained of 0.0525 torr/mm. on the scale of the optical lever.

It can be shown that the bellows gauge sensitivity is independent of the initial tension of the bellows when in the null position (i.e. equal pressures in both test and auxiliary systems), and also that the pressure in the test system, as measured by the gauge, is a linear function of bellows displacement from the null position. (See Appendix 1).

b) In the range 10^{-2} to 1 torr, pressure is measured by an Edwards Pirani gauge.

c) In the range 10^{-6} to 10^{-2} torr, pressure is measured using an Edwards Penning gauge.

The glass is outgassed by heating tape, with which the pipeline is lagged, and the metal taps by built-in 240 volt mains heaters. Thus temperatures up to 200°C are easily obtained. It is not possible to outgas the test cell at this temperature because of the soft-soldered electrical connections present inside the electrodes. However the cell can be safely outgassed at 100°C, and this was done by the application of steam jackets.

Spectroscopically pure (See Appendix 2) gas samples contained in 1 litre glass flasks are obtained from British Oxygen Co. Ltd. Gas can be admitted to the system as slowly as required through a single metal stop-cock. Before an experiment is performed, the test system is pumped out and outgassed until a pressure (with the pumps still running) approaching 10^{-5} torr is obtained. A rate of rise in pressure of not greater than 5×10^{-7} torr/second is tolerable for the purposes of the present experiment.

The system is flushed several times with gas before the actual sample to be tested is admitted.

4. The ultra-high-frequency apparatus

4.1 Electron ambit considerations

Previous similar experiments by Nicholls, and by Long were performed using high frequency apparatus that resonated at 106 Mc/second. The electrode assembly is effectively a terminating capacitance at the open end of a quarter-wave parallel-wire transmission line, and tuning to the frequency of the oscillator supplying the power is achieved by another variable condenser in parallel with the main gap. With the design of the larger electrodes to cope with the longer gap widths envisaged in the present experiment, tuning to a resonant frequency of 106 Mc/sec becomes impracticable as a result of the increased load on the end of the line. By decreasing the resonant frequency of the system, it is possible to design a new line which will carry the electrodes and
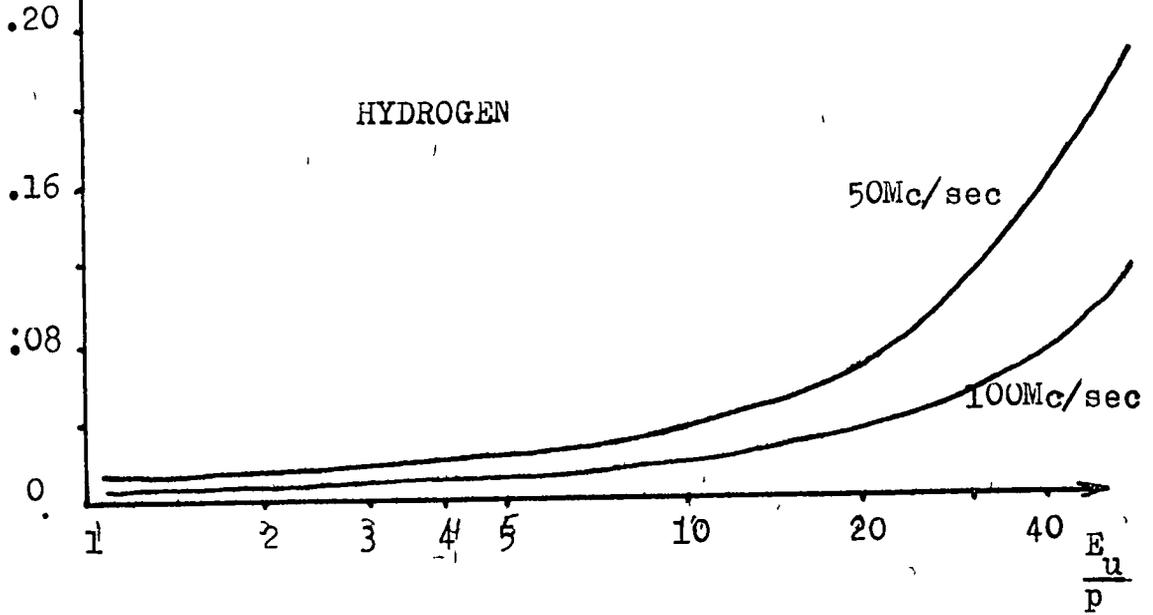
Fig 3.6. Variation of electron ambit with E/p.
(Calculated from Townsend drift velocity data[5].)
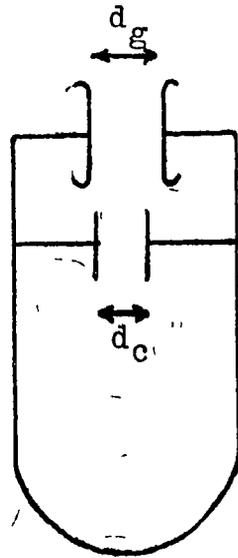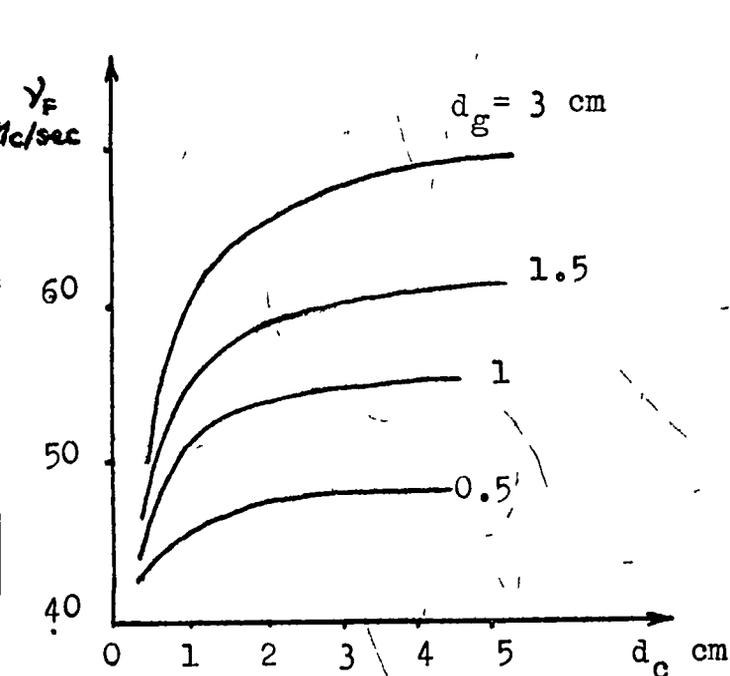
Fig 3.7. Resonant frequency of the test assembly as
a function of the separation of the tuning plates.

a suitably large tuning condenser, yet leave a conveniently long loop at the closed end for the reception of uhf power from the oscillator. Consider the possibility of operating at a new frequency of about 50 Mc/second.

At this stage it is necessary to consider the electron ambit in the gap at this new frequency (i.e. the distance moved in one half cycle of the applied uhf field). Fig. 3.6 shows roughly how the electron ambit (calculated from Townsend[5] drift velocity data) varies with E/p at frequencies of 50 and 100 Mc/second in hydrogen. It can be seen for both frequencies that below $E/p = 50$ v/cm.torr, and for gaps longer than 0.5 cm, the electron ambit can be regarded as small compared to the gap width. Therefore at a frequency of 50 Mc/sec, as at 100 Mc/sec, electron removal is mainly by diffusion and so the diffusion theory of breakdown applies for pure oscillatory fields. The limits for such conditions are when a) the frequency is so low that the electron ambit is comparable with the inter-electrode spacing and b) when the frequency is so high as to be comparable with the collision frequency of electrons with gas molecules. Between these limits there is little variation in the breakdown field with frequency[8,34]. Therefore it is reasonable to assume that the results obtained at about 50 Mc/sec can be directly compared with the corresponding results of Nicholls and Long working at 106 Mc/sec, and that little difference will be expected.

4.2 Design and construction of the tuned gap assembly

In order to keep the resonant frequency of the gap assembly constant when the electrode spacing is varied, a tuning condenser in parallel

with the gap is adjusted to keep the total capacitance on the end of the line constant.

Let the capacitance of the test gap be C_g, and of the tuning condenser, C_c.

Let the respective gap widths be d_g and d_c, and plate radii a_g and a_c.

The permittivity of free space is approximately equal to that of air. Then $\epsilon_0 = \epsilon_{air}$, approximately.

The total capacitance at the end of the line, $C = C_g + C_c$. Therefore, $C = \epsilon_0 \cdot 4\pi(r_g^2/d_g + a_c^2/d_c)$.

And if $a_g = a_c$,

$$1/d_g + 1/d_c = G, \text{ a constant} \qquad \dots \quad 3.8$$

The tuning of this system gets increasingly sensitive as d_c is decreased. At small values of d_c, very small deflections of d_c from the resonance position may cause very large fluctuations in the voltage across the test gap. The smallest comfortable value of d_c is typically about .5 cm, below which tuning is too critical to be satisfactory. Impose the conditions that when $d_{g.max} = 3$ cm, make $d_{c.min} = .5$ cm. Then when $d_{g.min} = 0.5$ cm, $d_{c.max} = 3$ cm. Therefore for the resonant frequency corresponding to the constant total capacitance, C, tuning may be comfortably achieved over the whole range of d_g required.

A line was built consisting of two limbs of 0.95 cm diameter copper tubing, 15 cm apart, the closed end split by a mica condenser to insulate the electrodes from one another during the application of the dc field,

and overall length about 40 cms. (See Fig. 3.3).

In an experiment to investigate the resonance properties of the system, a signal from a variable frequency generator was fed into the line from a loop loosely coupled to the closed end of the line. The voltage between the electrodes (which is a maximum for the line) was indicated by means of a rectifying bridge capacitively coupled to the branches of the line close to that end. The resonant frequency of the system was thus measured for various conditions of d_g and d_c. The family of curves in which the resonant frequency of the system is plotted against d_c for various values of d_g (See Fig. 3.7) is an indication of the tuning capabilities of the test system. From these curves, it is clear that the line constructed to the above specifications can be conveniently tuned over all the required experimental conditions at frequencies around 50 Mc/second.

4.3 The uhf oscillator

An existing free-running, tuned anode-tuned grid oscillator was rebuilt to oscillate at the new required frequency. Two power tetrodes, (Mullard QY3-65) are employed, and the anode voltage is supplied from a 1000 volt power pack, being smoothly variable by means of a Variac transformer at the in-put of the power pack.

The lengths of the tuned elements (tuned quarter-wave, parallel-wire transmission lines, constructed from copper tubing 0.95 cm in diameter and with limbs 7.5 cm apart) were adjusted until the device oscillated at a frequency close to 50 Mc/second. Once this was achieved,
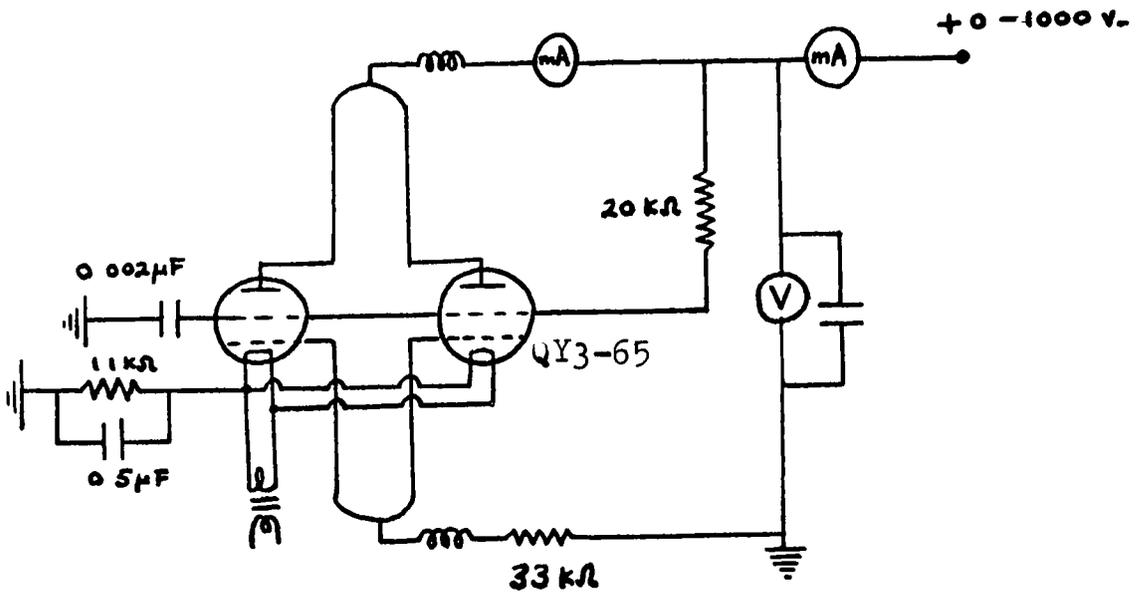
Fig 3.8.a. Diagram of the uhf oscillator circuit.
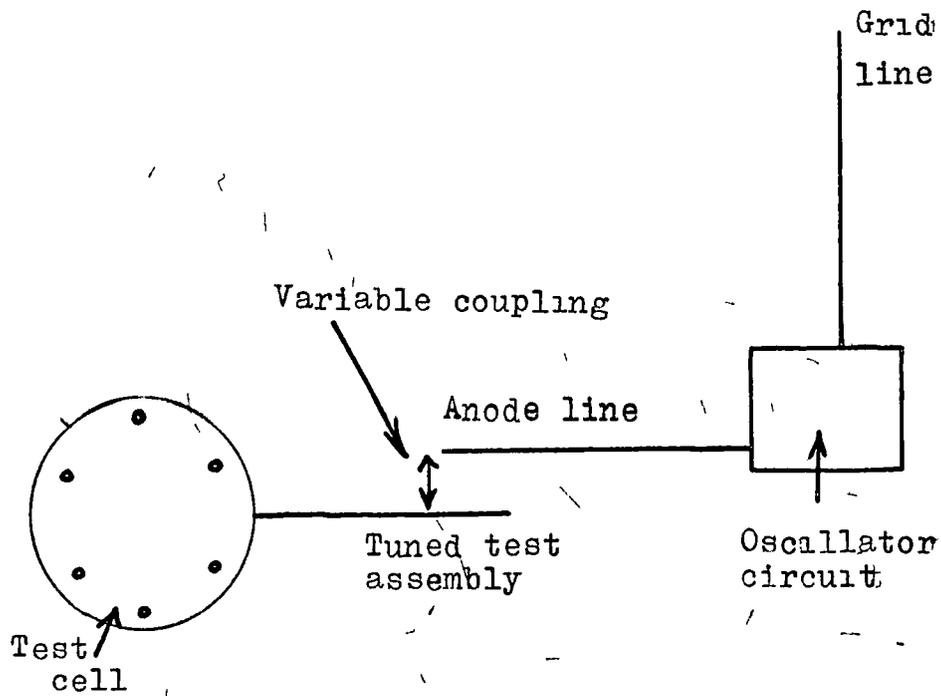
Fig 3.8.b. Geometrical arrangement of the tuned elements.
(Side view).

subsequent fine tuning was obtained by fine control of the length of the grid line, using a 'trombone'-type slide.

The complete oscillator circuit is shown in Fig. 3.8a. It is housed in a sliding rack so that the whole assembly may be raised or lowered in order to vary the coupling between the oscillator and the test load. The oscillator is screened by aluminium sheeting, and the two power tetrodes are air cooled by an electric fan.

Over-coupling between the tuned elements occurs if they are placed too close together resulting in 'double-humping' or frequency jumping. To avoid this, the lines are set up at right angles to each other. (See Fig. 3.8b).

The frequency of the oscillator was measured using a set of Lecher wires to which the oscillator is loosely coupled, and found to be 48 Mc/second.

5. Voltage measurement at ultra-high-frequencies

In principle, the method of measuring the voltage in the gap is the same as that developed by Nicholls[1], but certain modifications have been made in which the apparatus has been simplified to some extent. It is not possible to connect a direct reading voltmeter between the electrodes because the current flowing through the voltmeter would de-tune the test assembly. Therefore it is not possible to measure the voltage between the electrodes directly. To overcome this, an indicat-ing meter loosely coupled to the open end of the line is calibrated in

terms of the gap voltage by means of a suitable step-over instrument.

5.1 The ellipsoid voltmeter

The ellipsoid voltmeter was developed by Thornton and Thompson[25] for the absolute measurement of high electric fields. A small metallic ellipsoid suspended in the gap between two plane electrodes by a near-torsion-free insulating fibre oscillates about its axis of suspension with a frequency which is a function of the electric field in the gap (having initially been set into oscillation by external means).

The working formula for the instrument is

$$E^2 = k(n^2 - n_o^2) \qquad \qquad .... \quad 3.9$$

where n is the frequency of torsional oscillations of the ellipsoid in the presence of an electric field, E, and n_o is the frequency in the absence of the field. The constant, k, depends on the mass and dimensions of the ellipsoid.

Thornton and Thompson showed that the torque acting on the ellipsoid is proportional to the square of the applied field, and that the instrument therefore gives true root mean square values. Measurements are independent of frequency of applied fields, and therefore the device may be calibrated for the application of known dc fields (i.e. k measured), and then used in turn to calibrate a suitable indicating meter for the measurement of uhf fields. The ellipsoid voltmeter used thus is a 'step-over' instrument between the known dc field, and the unknown uhf field, the working quantity being the frequency of oscillation of the ellipsoid.

Modification of Eq. 3.9 gives

$$E^2 = k(n + n_0)(n - n_0)$$

$$= 2kn_0(n - n_0) \text{ approximately for small applied}$$

voltages.

Let $(n - n_0) = \mathcal{N}$, say.

Then, $E^2 = 2kn_0\mathcal{N}$.

Differentiating this, we get the sensitivity

$$d\mathcal{N}/dE = (1/kn_0).E. \qquad \qquad \dots \quad 3.10$$

The ellipsoid voltmeter is very sensitive if small changes in field produce large changes in the difference $(n - n_0)$. Thus it is seen from Eq. 3.10 that the system for a given k and n_0 gets increasingly sensitive as the level of E is increased. Alternatively, for a given field and ellipsoid dimensions, the system may be made more sensitive by decreasing the product kn_0, either by using a fibre of smaller stiffness, and/or by using a less dense metal for the construction of the ellipsoid.

In the present experiment the ellipsoid takes the form of a Woodsmetal disc of diameter about 0.5 cm, and is suspended from a fine quartz fibre. At some point on the fibre is attached a small piece of fine iron wire about 0.2 cm long. The disc is set into oscillation initially by deflecting this wire with a weak magnet.

It was necessary to design a grease-free apparatus for moving the ellipsoid in and out of the gap. For this purpose the fibre is suspended from a brass/iron plug which is capable of sliding vertically in the
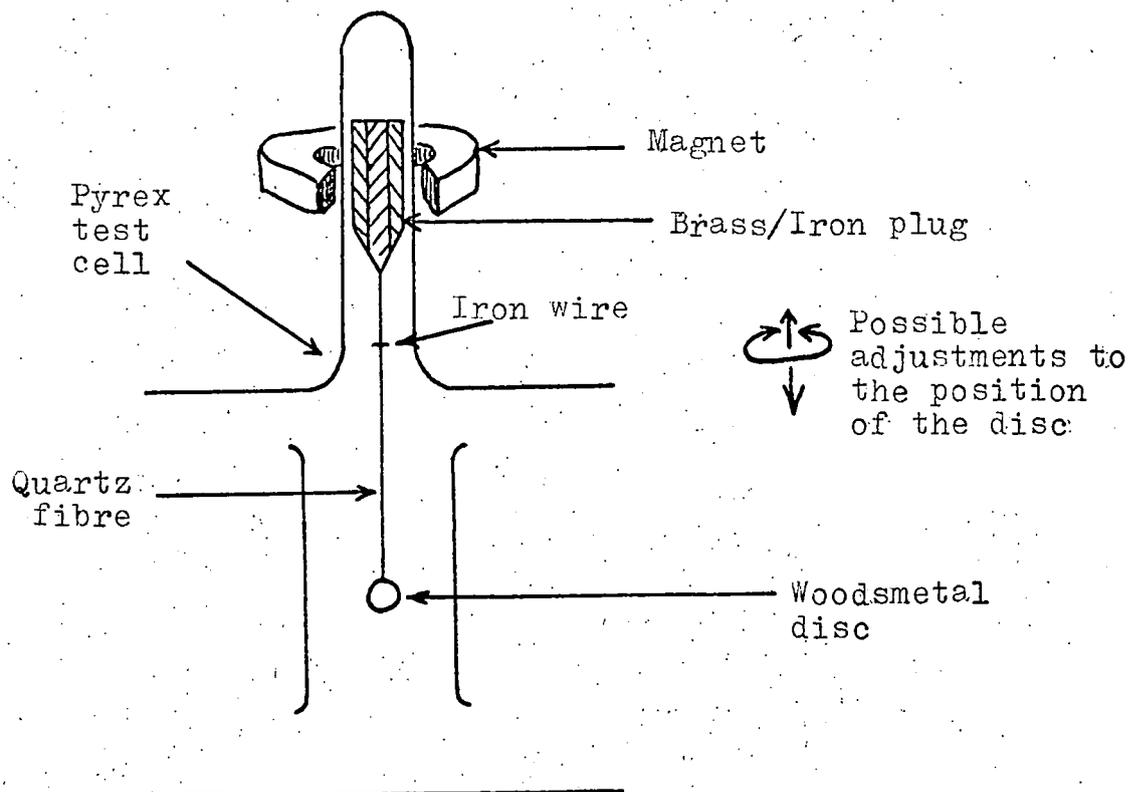
Fig 3.9. General arrangement of the ellipsoid
voltmeter system.
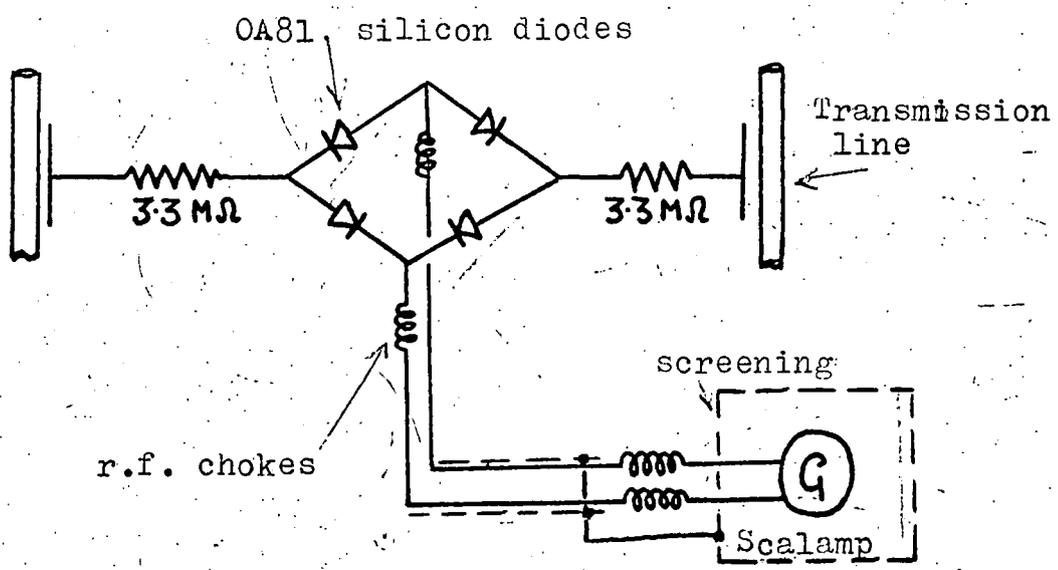
Fig 3.10. The uhf indicating circuit.

glass tube immediately above the gap. Thus the whole assembly may be moved in the vertical plane (for raising or lowering the bead), or may be rotated in the horizontal plane (for varying the orientation of the ellipsoid in the gap) by means of an external magnet. (See Fig.3.9).

The ellipsoid voltmeter was originally incorporated into this apparatus as an aid to the measurement of the uhf field. However, another important application has been devised for the measurement of small residual voltages left in the gap after running a discharge. This application is described in greater detail later in this thesis.

5.2 The uhf indicating circuit

The indicating meter takes the form of a full-wave diode rectifier whose terminals are loosely coupled capacitatively across the test line as close the gap as possible. (See Fig. 3.10).

The circuitry makes use of OA81 silicon diodes, and is designed such that the current flowing through the recitifer is small, and the resistance of the circuit high, thus keeping the additional load on the line to a minimum, as well as protecting the diodes. The current flowing through the rectifier is measured using a sensitive Scalamp galvanometer, suitably screened and earthed. High-frequency 'pick-up' is further reduced by a system of radio-frequency chokes.

5.3 Calibration of the uhf indicating meter

The curves relating $E_{dc(calibration)}$ and ϕ (the deflection of the uhf indicating meter when the uhf field is applied) with $(n_o^2 - n_o^2)^{1/2}$ are straight lines.

i.e. $E_{dc(calibration)} = h(n^2 - n_o^2)^{1/2}$

$\phi = g(n^2 - n_o^2)^{1/2}$ g, h constants.

Then assuming that the ellipsoid voltmeter is not frequency dependent, $E_{dc(calibration)}$ is equivalent to the rms uhf field, E_u, for a given value of n.

Then, $E_u = (h/g) \cdot \phi$ 3.11

5.4 Accuracy of uhf measurements

The accuracy with which the uhf indicating meter may be calibrated in terms of the uhf voltage in the gap depends on the accuracy with which the frequency of oscillation of the ellipsoid can be determined. The following standard experimental procedure is adopted.

The ellipsoid is set oscillating in the gap. The clock is started when the ellipsoid passes through the equilibrium position (observed from above as it passes the cross-wire of the viewing telescope). The clock is stopped when the bead passes through the same point a certain whole number of swings later, and n is calculated from the total time and the total number of swings completed. The readings were standardised as far as possible during a given calibration by always timing over the same number of swings. Also, care was taken to ensure that the amplitude of the swings was the same at the start of each timing operation.

Due to the errors introduced mainly in the starting and the stopping of the clock, it is not possible with the ellipsoid to detect changes in voltage of less than about 20 volts. However, a satisfactory calibration

-47-

Pick-off unit   Difference amplifier   Potential for charging batteries
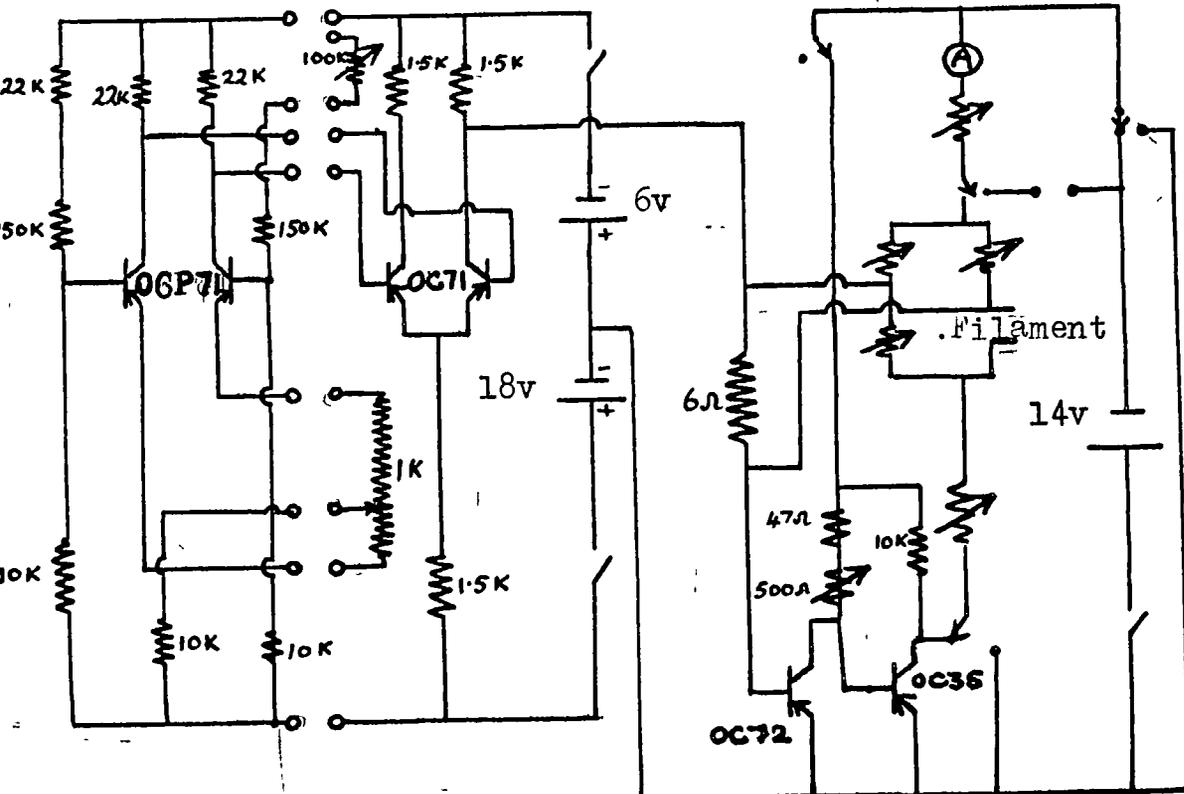
Fig 3.11. Circuit for the stabilization of $i_{1(2)}$, the current leaving the filament. (Long)
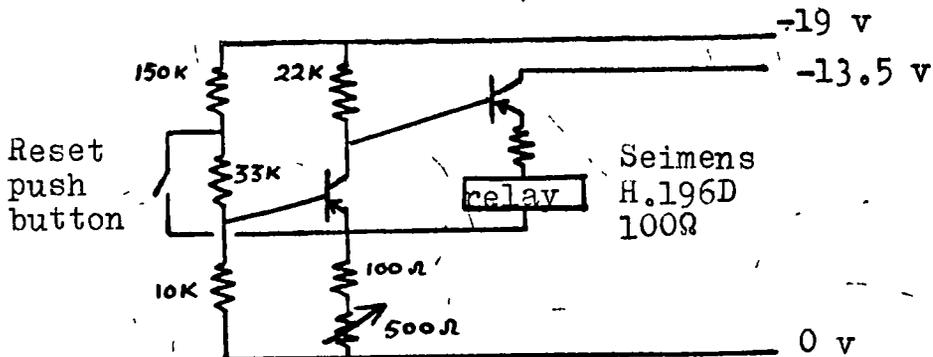
Fig 3.12. Circuit for the protection of galvanometer, G_2, from high currents flowing in the gap.

of the uhf indicating meter may be obtained by plotting many points on the curves of $E_{dc(calibration)}$ and ϕ versus $(n^2 - n_o^2)^{1/2}$, and using a suitable statistical analysis to calculate the best straight lines. From the calibrations obtained, it is possible to measure the gap voltage to within an accuracy of $\pm 2\%$ over the range required.

6. The current supply and measurement system

The current supply and the measurement system is described in detail by Long[2]. Certain slight modifications only have been made.

It is necessary, in order to obtain satisfactory values of the gap current, to stabilize the current emitted into the gap, and it is assumed for the present that this can be done by stabilizing the current, i_1, flowing from the filament to the inside of the emitting electrode. A transistorized bi-stable circuit of the type designed by Wolfendale[35] was modified by Long[2], employing phototransistors to make it sensitive to impinging light. (See Fig. 3.11). The system is arranged so that when i_1 reaches the required value, the spot of galvanometer G_1 impinges on two balanced phototransistors placed close together on the scale. These feed currents into a difference amplifier which depend on the exact position of the spot, and hence on i_1. The amplified difference signal is applied to the base of a high power transistor placed in series with the filament supplying the electrons, and causes the current flowing through the filament, hence its temperature, to be varied automatically according to the position of the spot.

Filament supply

r.f. rejection system

V_1

V_2

L_1

L_2

G_1

G_1
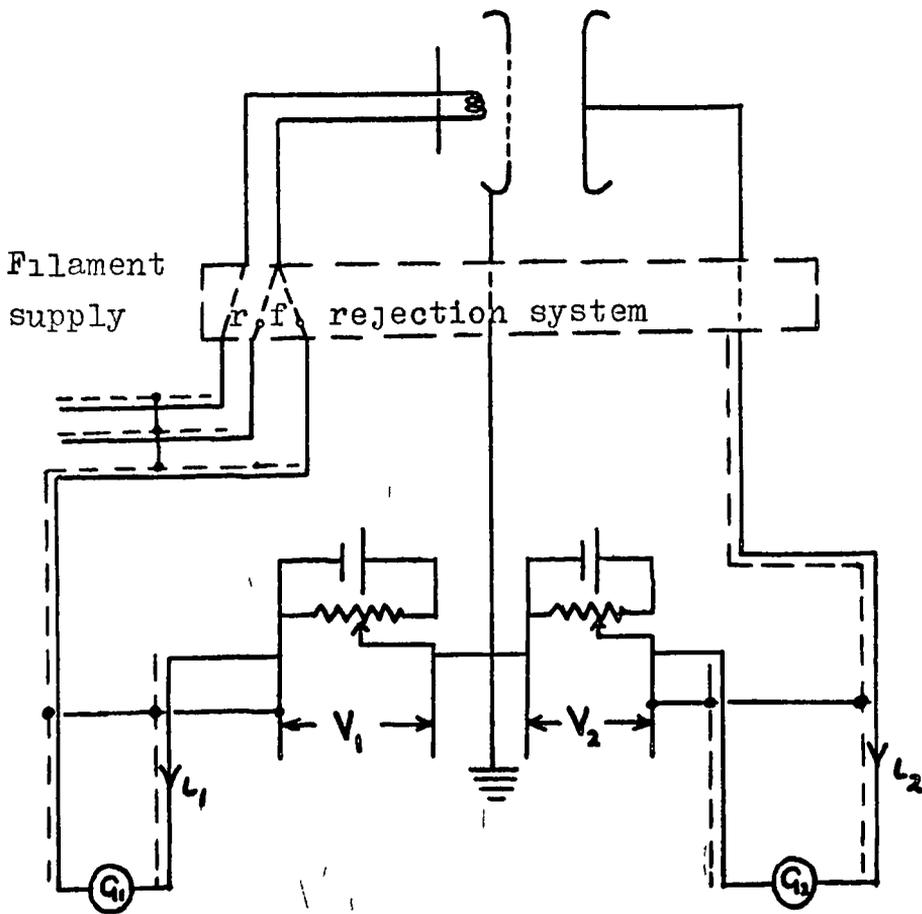
Fig 3.13. The current measurement and voltage supply system.

Thus by suitable arrangement of the circuit the spot can be 'locked' onto the phototransistors, and a high degree of stabilization of i_1 can be obtained below about 10^{-6} amperes. Above this, small fluctuations in i_1 begin to occur as the filament is now running at a higher level but these are not large enough to become superimposed on the gap current, i_2.

The galvanometer, G_2, used to measure the gap current, i_2, is protected from the high current flowing at breakdown by a similar type of circuit. (See Fig. 3.12). When the galvanometer deflection reaches a certain value the spot energizes the base of a phototransistor which triggers a circuit operating a relay, which in turn short circuits the galvanometer.

The current measurement and dc voltage supply system are shown in Fig. 3.12. Voltages V_1 and V_2 are supplied by dry batteries, and varied by means of potentiometers. Currents i_1 and i_2 are measured by galvanometers G_1 and G_2. G_1 has a maximum sensitivity of 7.5×10^{-8} amps/cm, and G_2 a maximum sensitivity of 5×10^{-10} amps/cm.

Careful screening of all leads is arranged to reduce high-frequency 'pick-up' to a minimum.

EXPERIMENTAL MEASUREMENTS OF AMPLIFICATION

Curves showing the variation of amplification with the applied uhf field had previously been obtained in hydrogen by Nicholls[1] and Long[2], both in non-grease-free vacuum systems. The following paragraphs describe new measurements of amplification made in a grease-free vacuum system, using larger electrodes and larger gap widths, and covering a comprehensive range of E_{dc} and pressures in hydrogen, nitrogen, helium and neon.

1. Method of measuring amplifications

Gas was admitted slowly into the test cell and the pressure measured using the bellows gauge. The filament temperature was monitored automatically so that the current, i_1, flowing to the back of the emitting electrode when the voltage, V_1, was applied was kept constant. (See Chapter 3). The stabilization process was assumed to be operating satisfactorily when the current, i_{20}, flowing to the collecting electrode in the presence of E_{dc} and with E_u zero, maintained a steady value. When i_{20} had stabilized sufficiently, the uhf field was applied, and i_2 measured. Stepwise increments of E_u were applied, and i_2 measured at each step, until the system was close to breaking down. As a check on the reproducability of the results, the readings were repeated with E_u decreased again in steps. Actual breakdown was avoided after it was observed in the early sets of measurements that a given amplification

A

(a)

p= 1 torr   2   3   4

1

NITROGEN

$d= 2.9$ cm

$E_{dc} = 1.89$ v/cm

O   50   100 E_u v/cm

A

1

(b)

1   2   3   4

NITROGEN

$d' = 2.9$ cm

$E_{dc} = 1.89$ v/cm

O   50   100 E_u v/cm
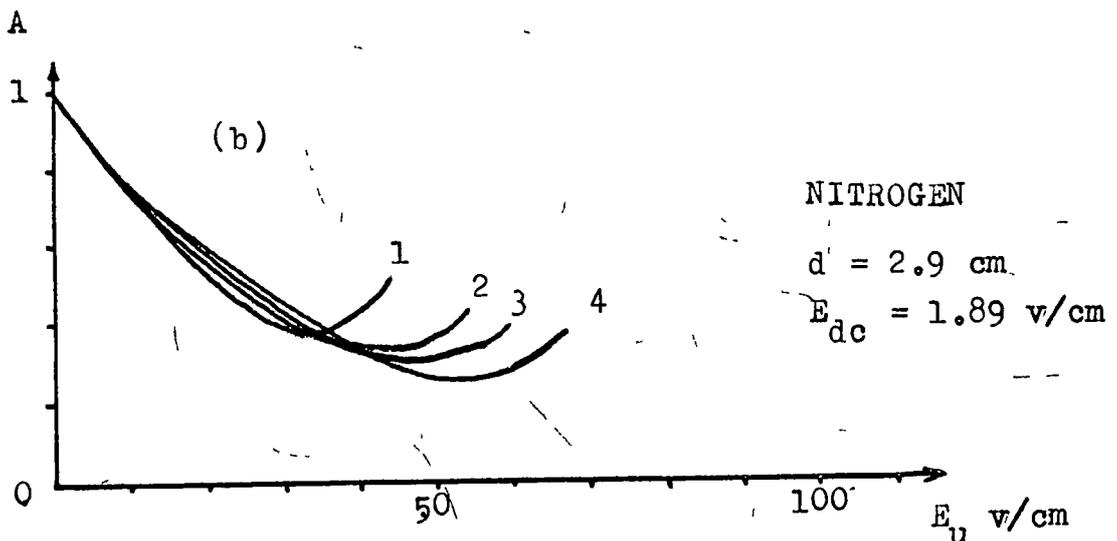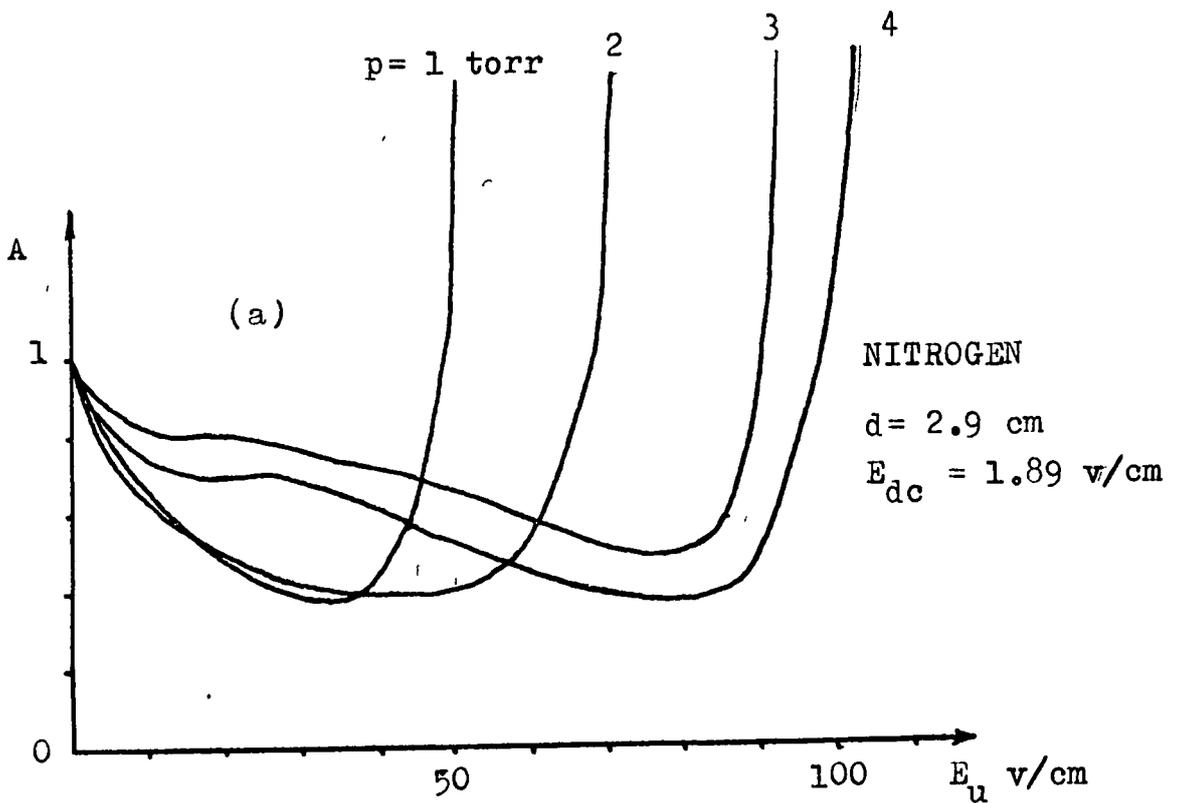
Fig 4.1. The effects on the amplification curves of
charging at the electrode surfaces.

(a) Breakdown allowed.

(b) Breakdown avoided.

curve could not always be exactly reproduced immediately after a breakdown had occurred. This may be explained in terms of charging at the electrode surfaces, and is discussed in greater detail in a later chapter. As an example of the effects of passing a high current in the gap, Fig. 4.1 compares two families of amplification curves obtained in nitrogen, one in which breakdown was allowed to occur at the end of each run, and the other in which breakdown was carefully avoided. The systematic behaviour of the curves, as the pressure is varied, is marked when high currents are avoided in the gap, but becomes considerably disrupted when breakdown is allowed to occur.

It has not been possible during the present work to obtain a value for i_{20} which is absolutely steady. (See Chapter 9). To account for the drifts in i_{20}, a check on its value was made for every two or three readings of i_2, the frequency depending on the magnitude of the drifts. (See Preface).

Nicholls[1] showed that the shape of the amplification curves does not depend appreciably on the voltage, V_1, between the filament and the emitting electrode. A value is chosen, therefore, which is low enough to avoid breakdown between the filament and the emitting electrode, (such a breakdown would render the stabilization of i_1 impossible), yet high enough to provide a sufficient flux of electrons into the gap through the holes in the emitting electrode.

Amplification, $A = i_2/i_{20}$, is plotted as a function of E_u for various values of E_{dc} and pressure.

-51-

2. Limitations on the range of experimental conditions

Restrictions on the range of experimental conditions that can be tested are imposed by the limited capabilities of the apparatus used. For instance, at pressures higher than about 8 torr (varying slightly from gas to gas) insufficient flux of electrons is given off from the filament to provide a measurable current in the gap. At higher pressures, the flux of electrons can be increased sufficiently by increasing the filament temperature, but this has the effect of reducing the sensitivity of the stabilization of i_1. The maximum stable voltage that can be generated at the gap using the present oscillator is about 400 volts, so at gaps around 3 cm, the highest available field strength is of the order of 130 v/cm.

With these limitations in mind, the measurements were confined to the pressure range 0 to 8 torr in all the gases tested.

3. Notes on the quantities to be measured

In the calculation of A, it is not necessary to obtain i_2 or i_{20} in absolute units, since A is the ratio of these two quantities. However, the galvanometers G_1 and G_2 were calibrated so that the currents i_1, i_2 and i_{20} can be obtained in amperes if required.

Currents i_2 and i_{20} are measured in the units of cm of galvanometer deflection, and may be measured accurately to the nearest 0.05 cm. If the current flowing in the gap is such that it gives a G_2 deflection of 1 cm, accuracy to within 5% can be obtained in the reading of i_2. For most of

A.

HYDROGEN
$d = 2.8$ cm
$p = 0.48$ torr

$E_{dc} = 25 \rightarrow 35$ v/cm

20.82

17.35

13.88

10.41

6.94

$E_{dc} = 3.47$ v/cm

1.5

1

.5

4   8   12   16   20   24 E_u v/cm

Fig 4.2. Amplification in Hydrogen.(Pressure fixed).

HYDROGEN
d = 2.8 cm
p = 1.04 torr

E_{dc} = 50 → 70 v/cm

E_{ac} = 3.47 v/cm

6.94

10.41

13.88

17.35

20.82

27.76

34.70

41.64

A

1.5

1.0

0.5
0   4   8   12   16   20   24   28   32 E_u v/cm
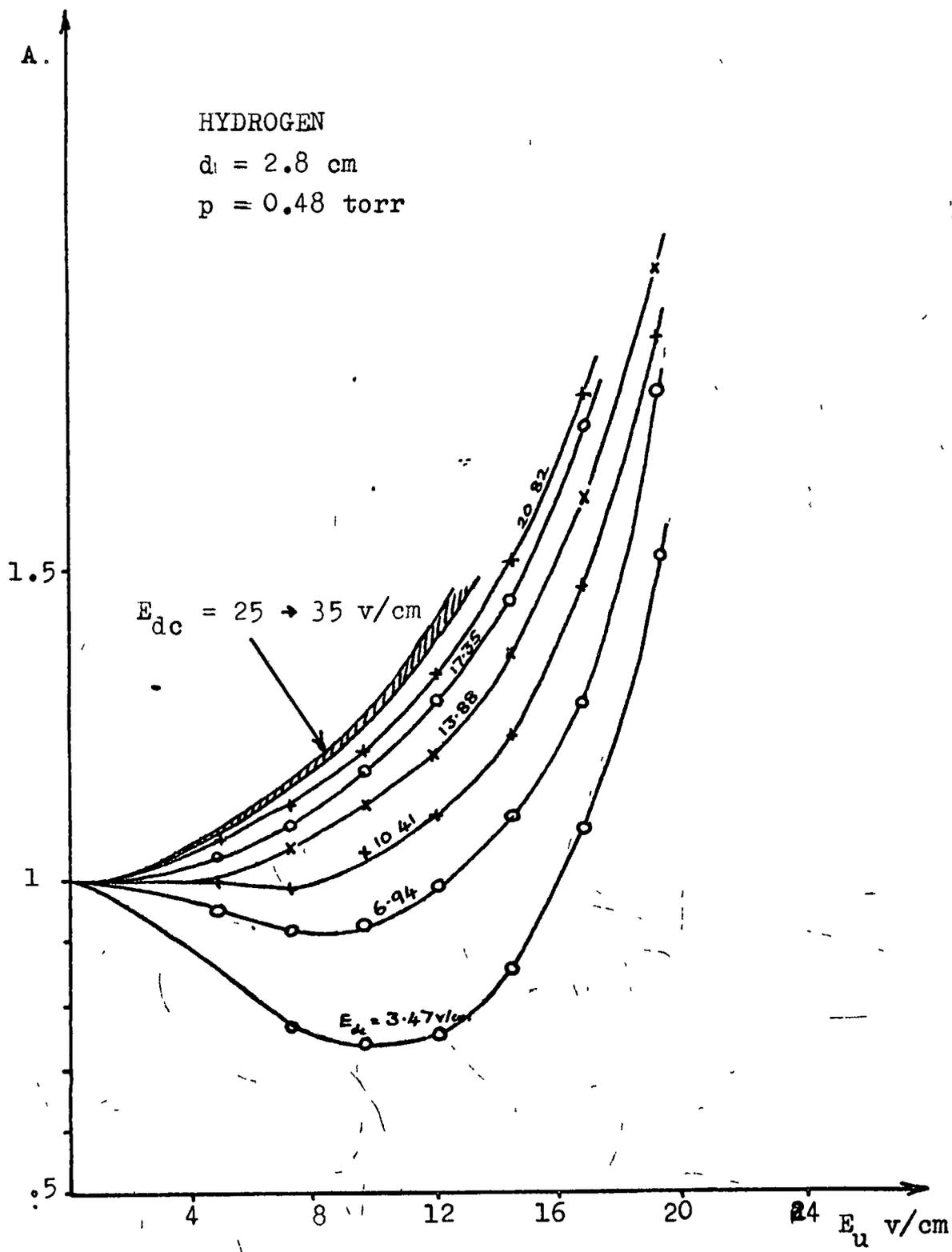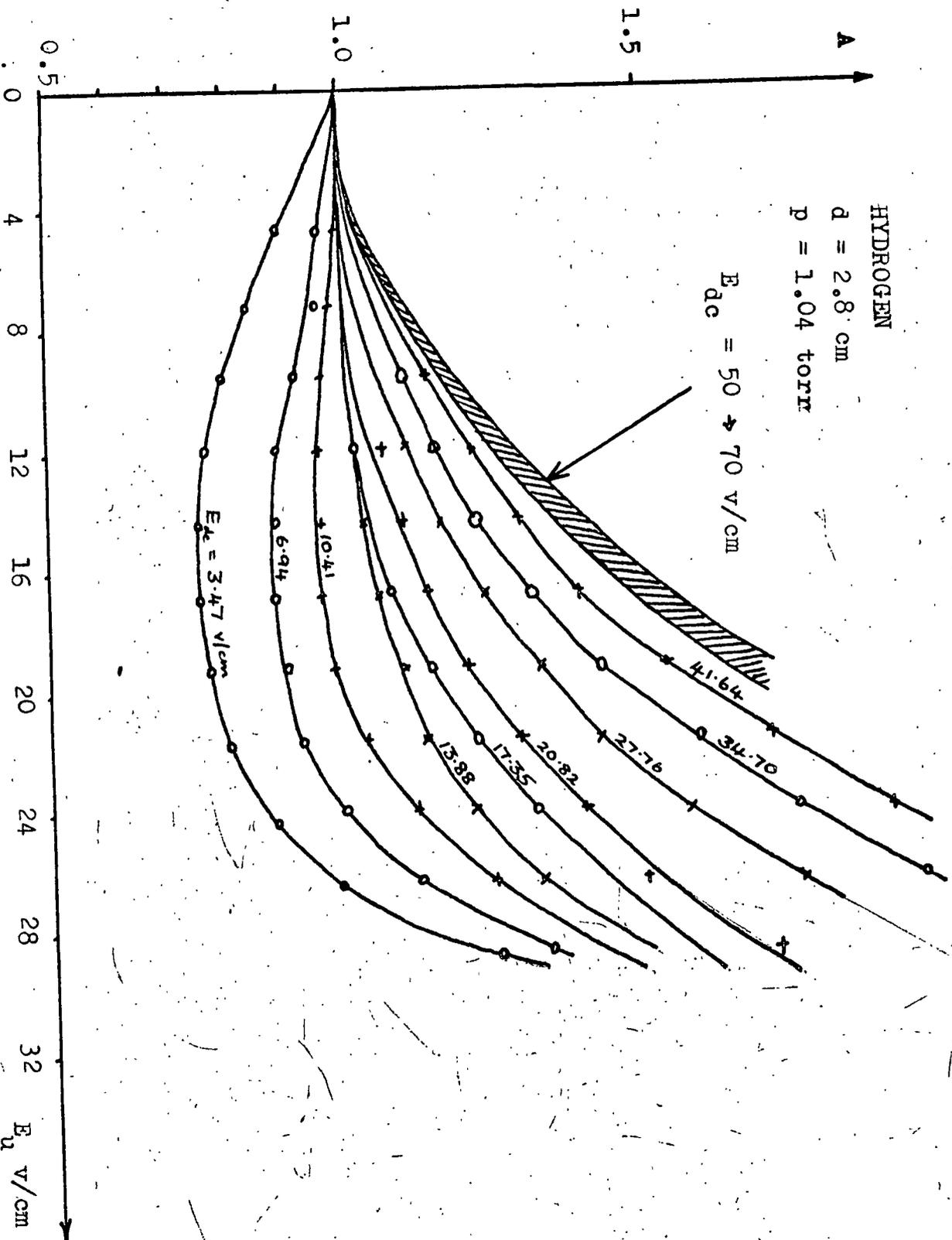
Fig 4.3. Amplification in Hydrogen.(Pressure fixed).

Fig 4.4. Amplification in Hydrogen.(E_{dc} fixed).

HYDROGEN
d = 2.64 cm
E_{dc} = 1.89 v/cm

p = 1 torr

E_u v/cm

Fig 4.5. Amplification in Hydrogen.(E_{dc} fixed).

HYDROGEN

d= 2.64 cm   p= 1 torr

E_{dc} = 7.56 v/cm

E_u v/cm

Fig 4.6. Amplification in Hydrogen.(E_{dc} fixed).

p= 1 torr

HYDROGEN

d = 2.64 cm

E_{dc} = 18.9 v/cm
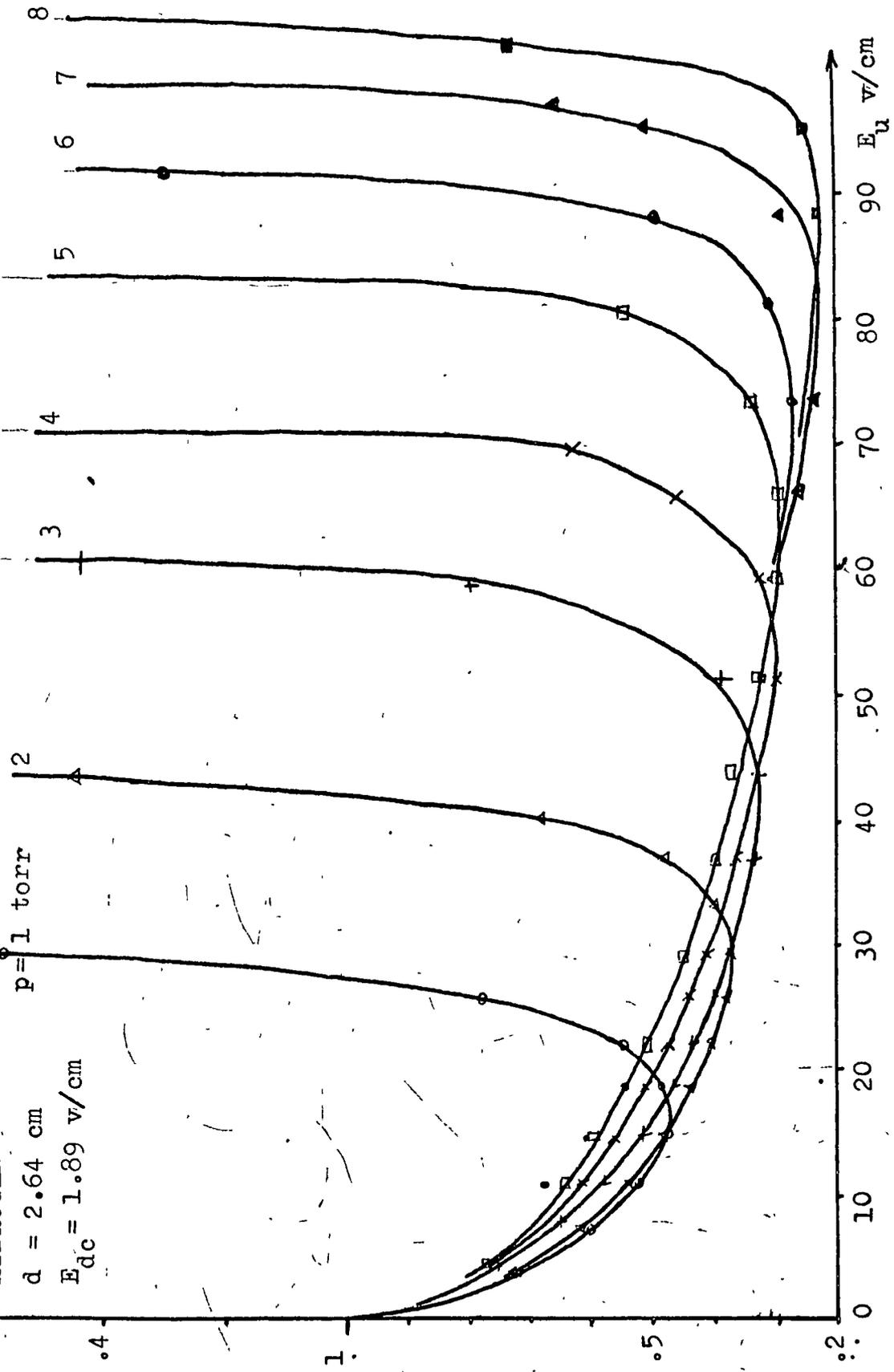
the experimental results quoted below, accuracy is considerably greater than this.

Typically in the pressure range used, i_1 is of the order 2 x 10^7 amps, and i_{20} is of the order of 10^{-9} amps.

The accuracy of the uhf field measurements varies from about $\pm 5\%$ at 10 v/cm to about $\pm 1\%$ at 100 v/cm. The accuracy of measurement of the applied field, E_{dc}, varies from about $\pm 5\%$ at 2 v/cm to about $\pm 1\%$ at 20 v/cm.

4. Experimental measurements of amplification

During the following measurements of amplification, breakdown was carefully avoided, for reasons already discussed. Therefore no measurements of the breakdown field are given. However, since the breakdown conditions are of importance in interpreting the amplification curves, measurements of breakdown stress were made independently of the amplification curves, and are presented in Chapter 5.

4.1 Amplification in hydrogen

Preliminary measurements of amplification in hydrogen enabled the dip in the amplification curves observed by the previous workers to be quickly re-established.

Extensive sets of amplification curves were obtained for hydrogen in the pressure range 0.5 to 8 torr, with values of E_{dc} ranging from 0.7 to 70 v/cm. The experiments were performed at gap widths around 3 cm. (See Figs. 4.2, 4.3, 4.4, 4.5 and 4.6).

Fig 4.7. Amplification in Nitrogen.(E_{dc} fixed).
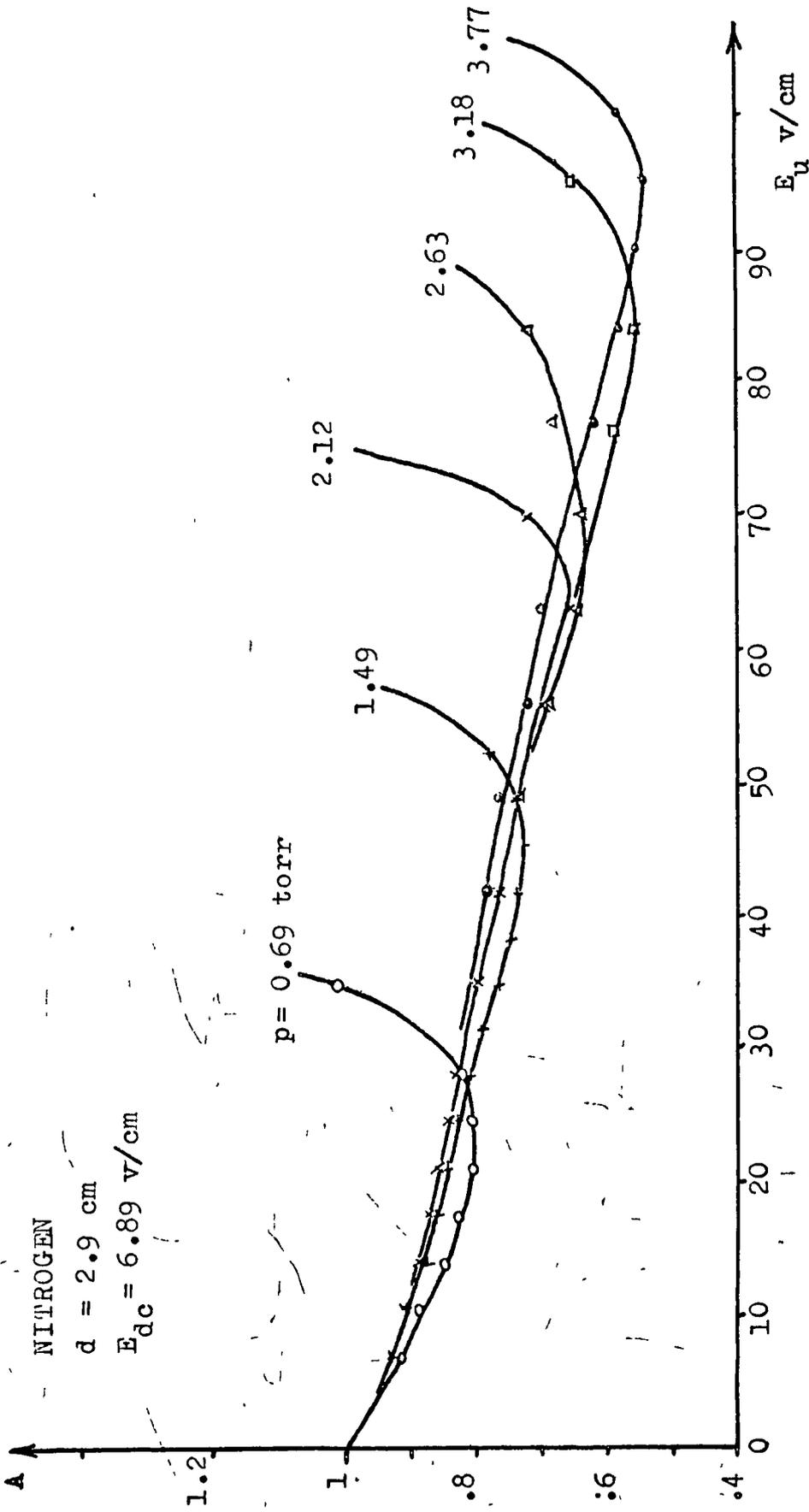
NITROGEN

d = 2.9 cm

E_{dc} = 6.89 v/cm

p = 0.69 torr

Fig 4.8. Amplification in Nitrogen. (E_{dc} fixed).

NITROGEN

d = 2.9 cm

E_{dc} = 10.34 v/cm

p = 0.5 torr

Fig 4.9.Amplification in Helium
(E_{dc} fixed).

HELIUM
d = 2.64 cm
E_{dc} = 1.89 v/cm

p= 1 torr
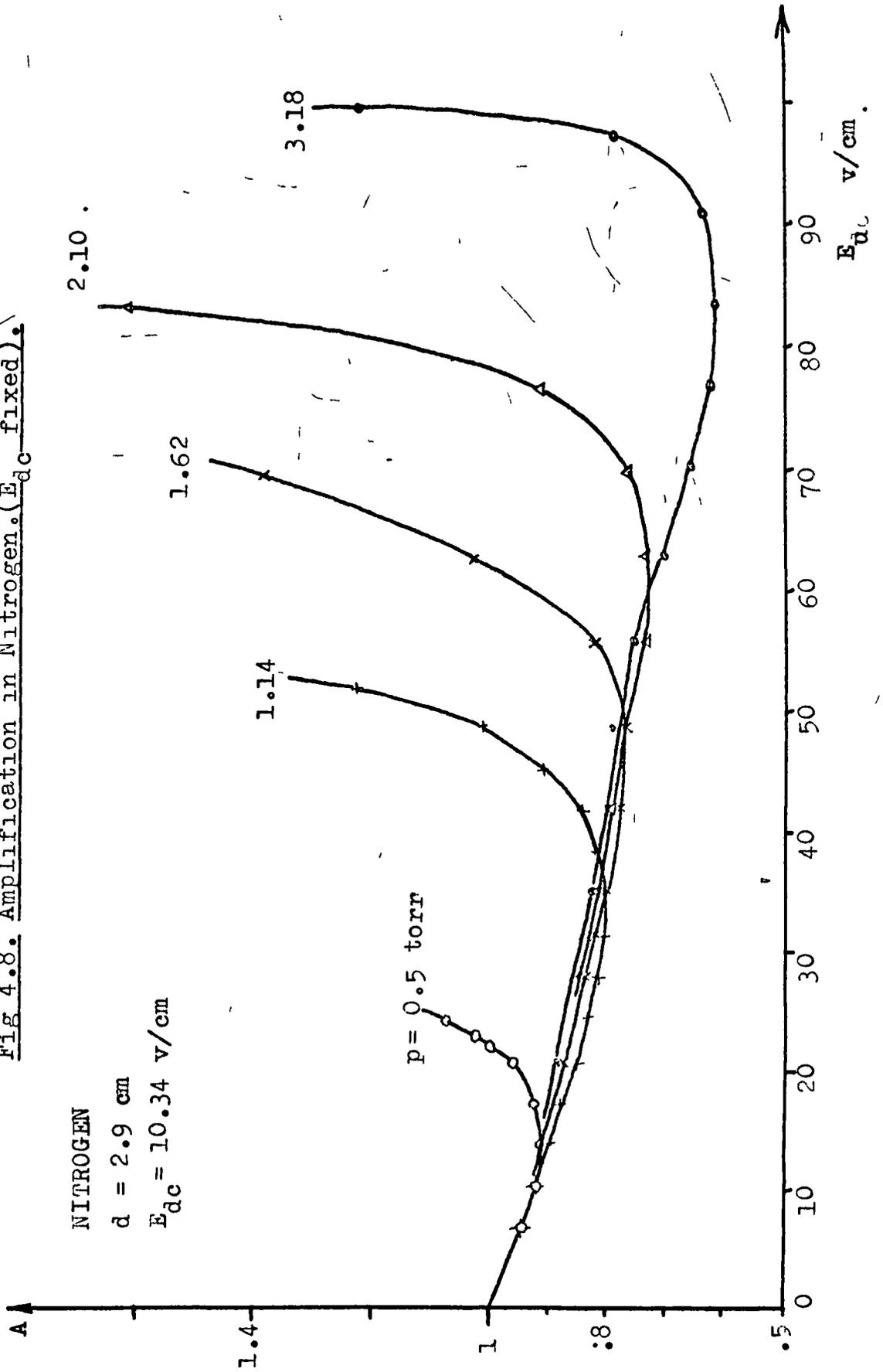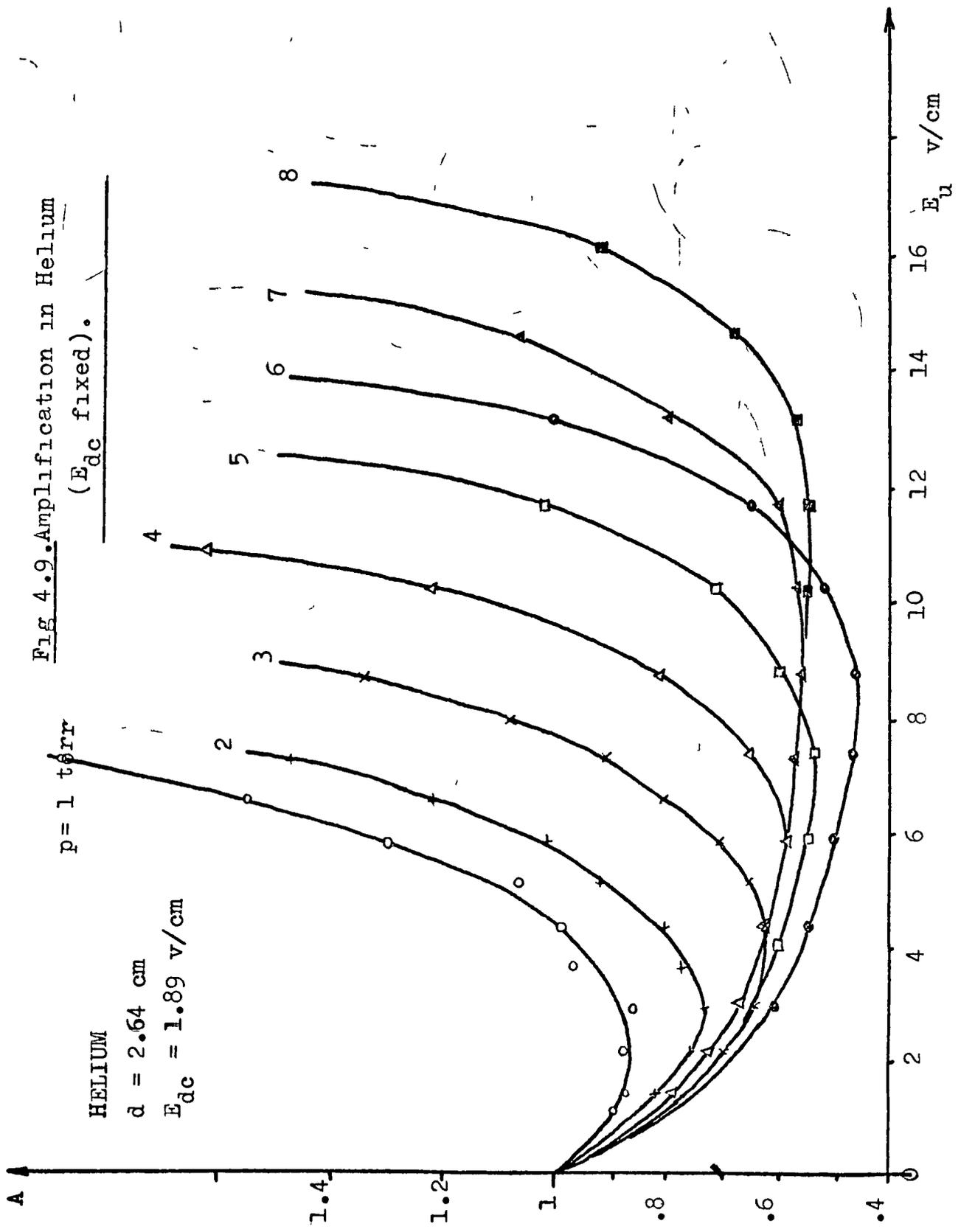
Fig 4.10. Amplification in Helium (E_{dc} fixed).

HELIUM

d = 2.64 cm

E_{dc} = 7.56 v/cm

p = 1 torr

E_u v/cm
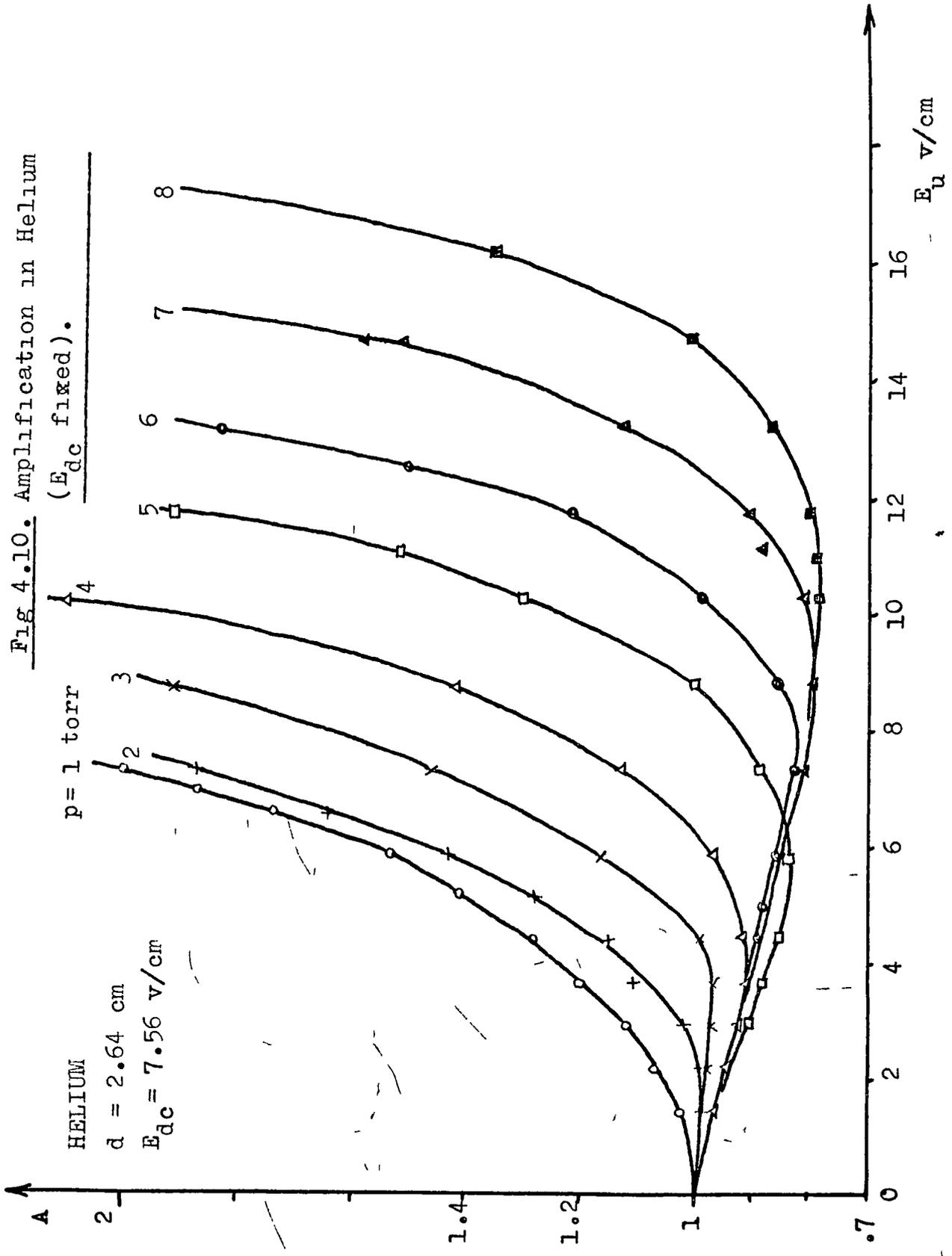
Fig 4 11 Amplification in Helium
(E_dc fixed)

$p = 2$ torr

HELIUM
$d = 2\ 64$ cm
$E_{dc} = 18\ 9$ v/cm

A

E_u v/cm
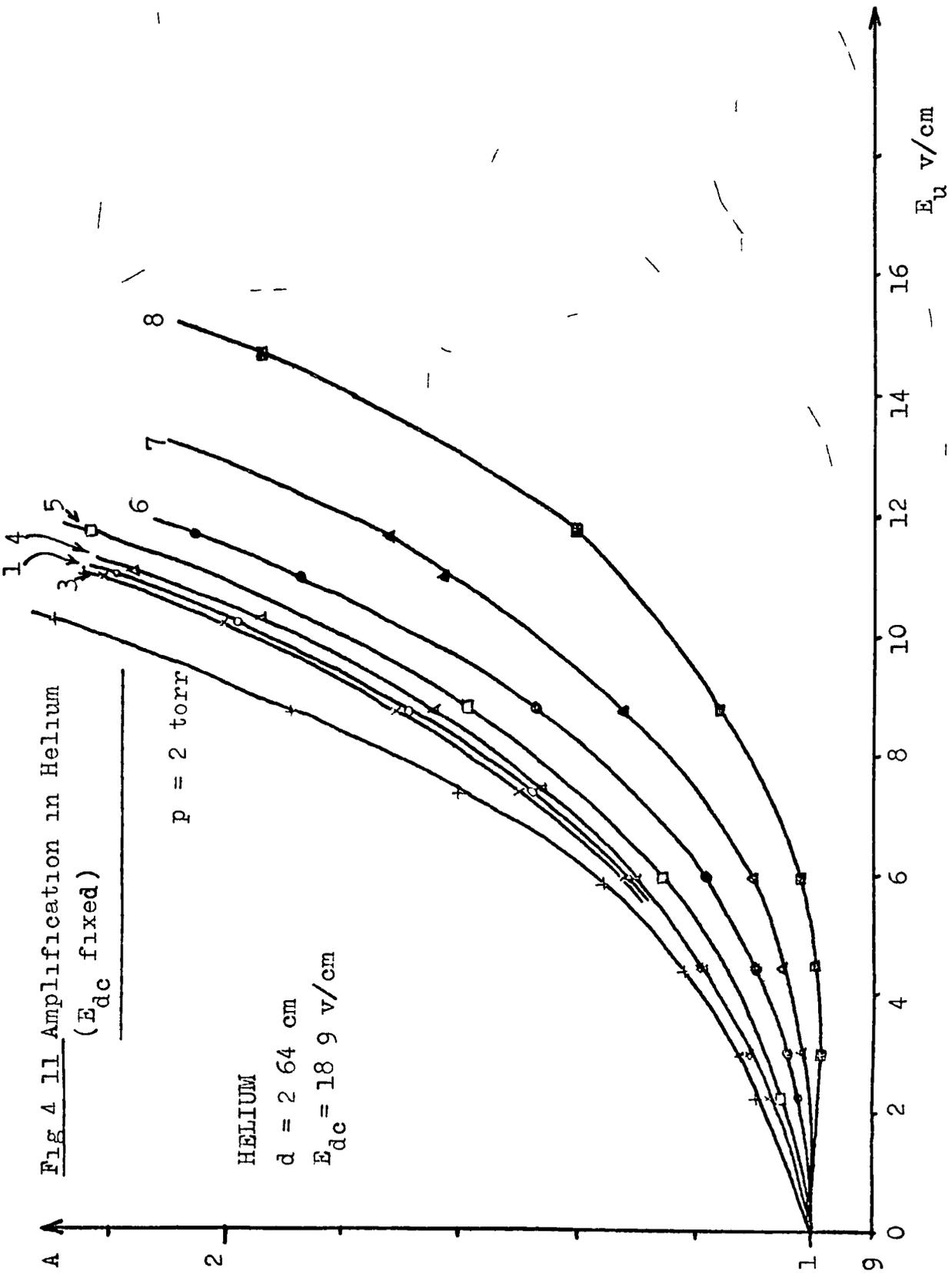
The general shape of the curves is described in Chapter 2, §3. The onset of ionization at higher values of E is clearly defined by the corresponding increase in amplification. This rise, which is continuous up until breakdown, is steep at low values of E_{dc}, but becomes less steep for larger values of E_{dc}. The size of the dip decreases with increasing E_{dc}, and eventually E_{dc} may be increased to the stage where the dip is removed altogether. At still higher values of E_{dc} and low E_u, amplification is not so strongly dependent on E_{dc}, and the curves for successive high values of E_{dc} become indistinguishable. (See Figs. 4.2 and 4.3).

Families of aplification curves, plotted with E_{dc} fixed, and varying the pressure from curve to curve, (See Figs. 4.4, 4.5 and 4.6), show that below the onset of ionization amplification exhibits only a slow pressure dependence, and such that for a given value of E_u, an increase in pressure produces a small corresponding increase in amplification.

4.2 <u>Amplification in nitrogen</u>

Amplification curves were obtained for nitrogen in the same way as for hydrogen, for pressures ranging from 0.5 to 4 torr, for $E_{dc} = 6.89$ and 10.34 v/cm and for gap widths around 3 cm, (See Figs. 4.7 and 4.8). The curves exhibit the same general characteristics as for hydrogen.

4.3 <u>Amplification in helium</u>

Amplification curves were obtained for helium in the pressure range 1 to 8 torr, with E_{dc} ranging from 1.89 to 18.9 v/cm, and gap widths around 3 cm. (See Figs. 4.9, 4.10 and 4.11). The curves exhibit similar
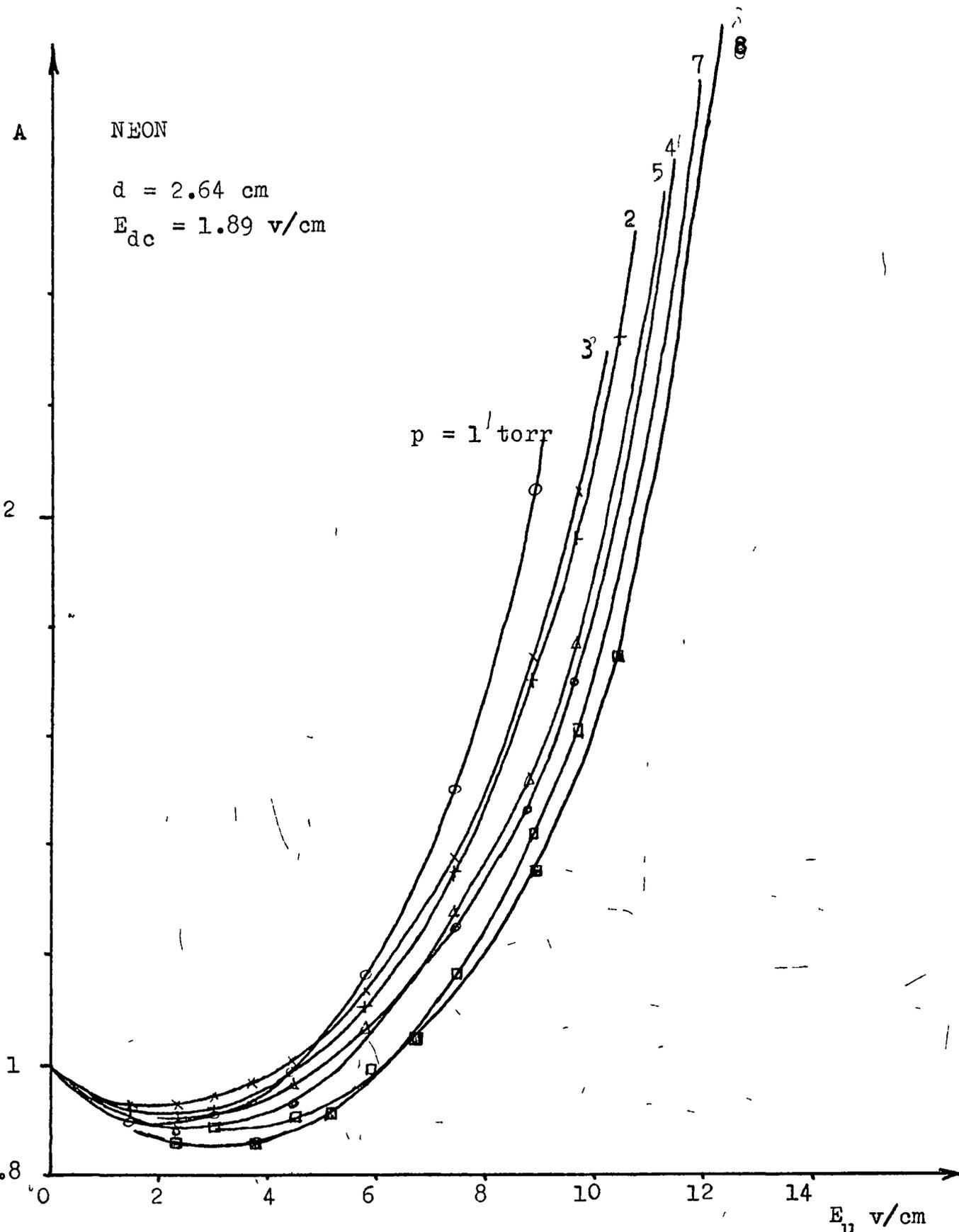
Fig 4.12. Amplification in Neon.(E_{dc} fixed).
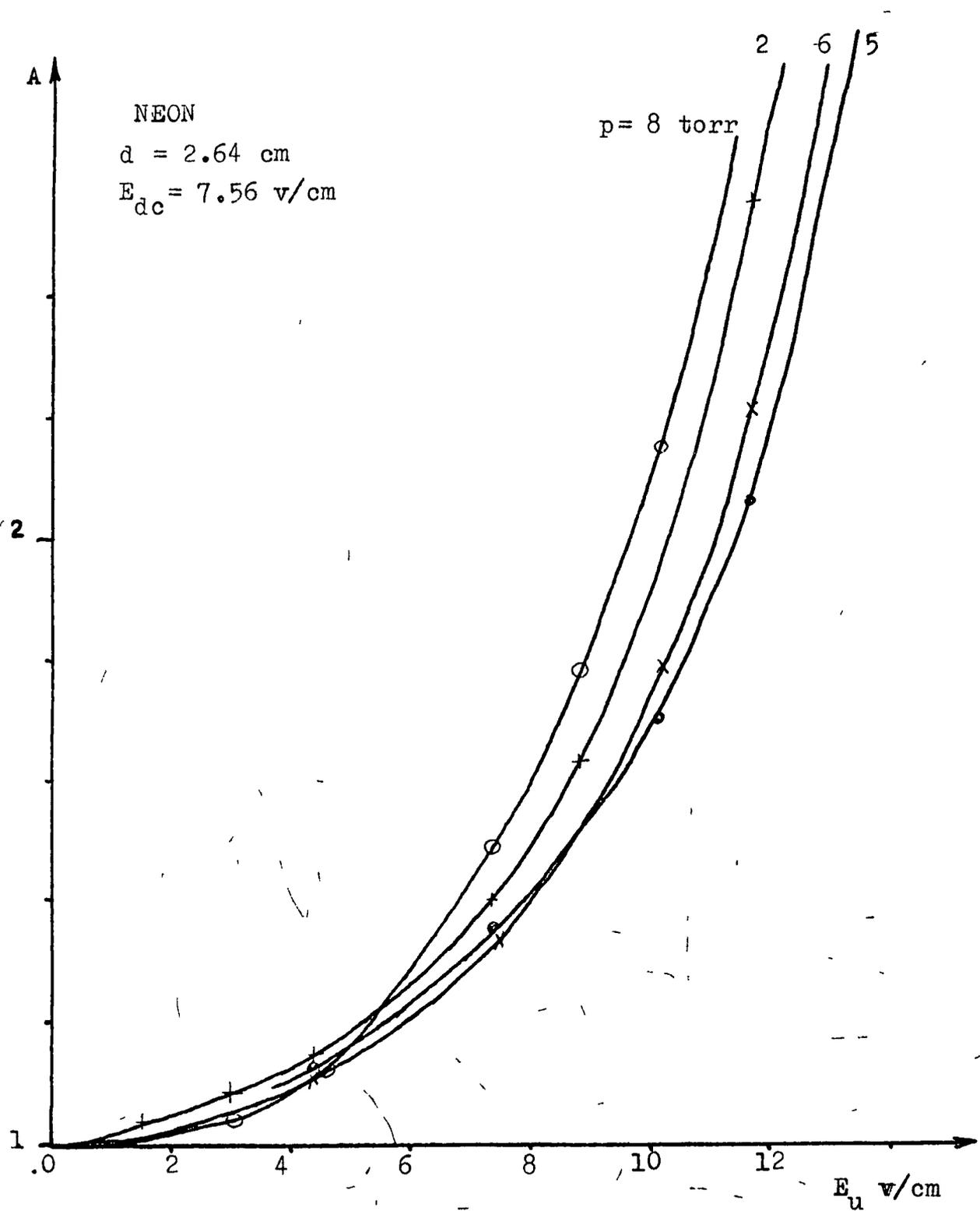
Fig 4.13. Amplification in Neon. (E_{dc} fixed).
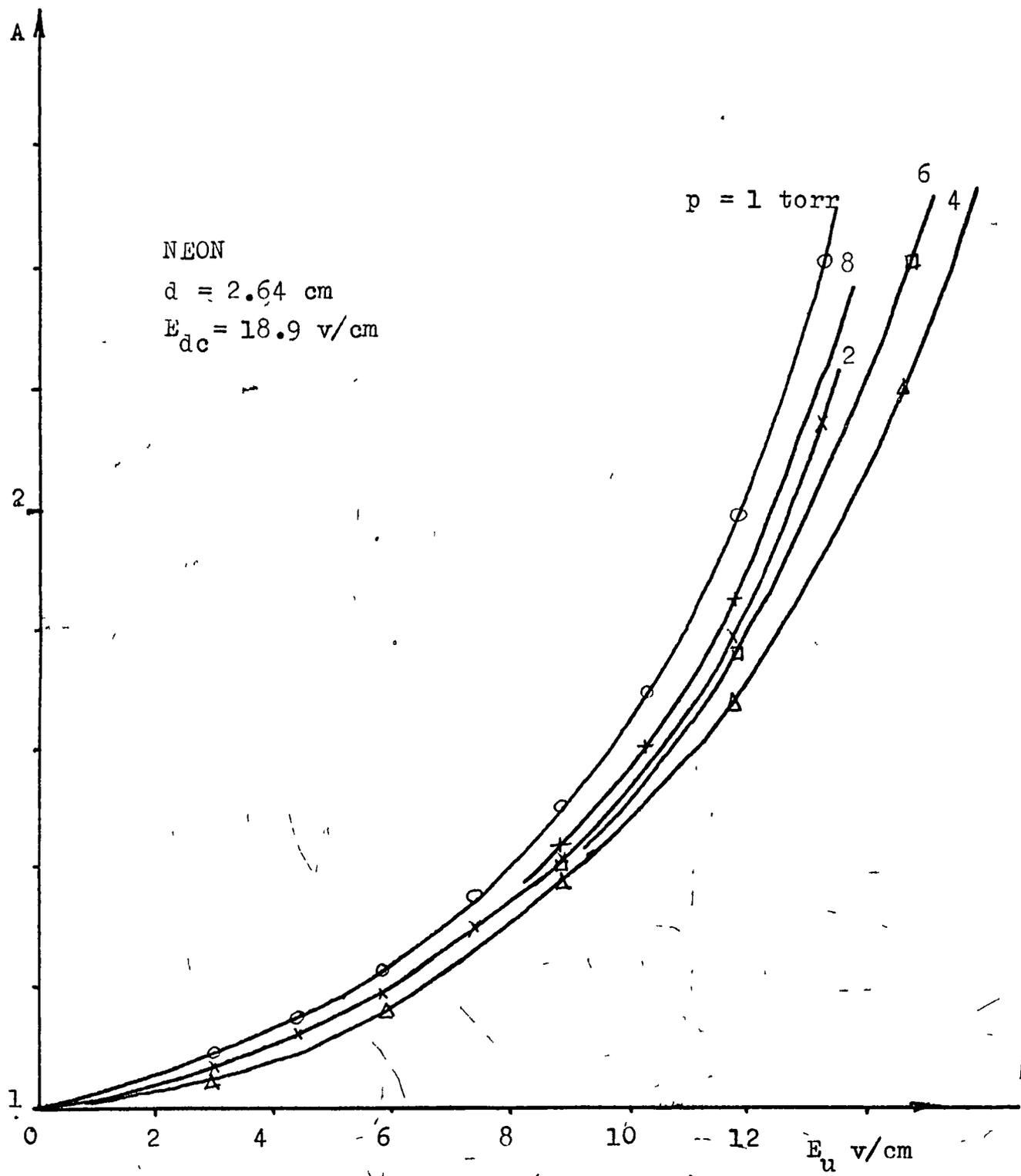
Fig 4.14: Amplification in Neon.(E_{dc} fixed).

characteristics to those for hydrogen and nitrogen, except that the scale of E_u is very much reduced.

4.4 Amplification in neon

Amplification curves were obtained for neon in the pressure range 1 to 8 torr, with E_{dc} ranging from 1.89 to 18.9 v/cm, and gap widths around 3 cm. (See Figs. 4.12, 4.13, and 4.14). The dip in the amplification curve is only apparent at very low values of E_{dc}, and is removed completely throughout the above pressure range when values of E_{dc} greater than about 7 v/cm are applied. The pressure dependence of amplification is considerably more marked than in the cases of hydrogen, nitrogen and helium.

5. General Discussion

The shape of the amplification curves at low values of E_u is affected mainly by the relative importances of drift and diffusion of electrons in the gap. At higher uhf fields, the electron flow considerations become complicated by the introduction of ionization. A later chapter of this thesis sets out to examine theoretically the relationship between drift and diffusion for various conditions in the gap. At this stage it suffices to describe briefly the main factors influencing the shape of the amplification curves.

When a pure uhf field is applied, the main electron loss is by diffusion. As E_{dc} is then superimposed, and gradually increased, the rate of loss of electrons by drift increases, and diffusion becomes less

important in relation to drift. As drift becomes more and more effective, the dip in the amplification curve becomes smaller. At some stage, as E_{dc} is increased, drift may be expected to take over from diffusion as the dominant electron removal mechanism. Eventually, E_{dc} may be increased to a value high enough to completely remove the dip.

It has been suggested[1,2] that the dip may be caused by the loss of electrons by back diffusion, which increases as the energy of the electrons is increased. (See Chapter 2). It is tempting to state therefore that the removal of the dip indicates the elimination of back diffusion as an effective loss process. However, this may not be the case. For instance, if E_{dc} is high enough on its own to produce multiplication in the injected electron stream, then as E_u is increased from zero, the ionization rate will start to increase immediately. If the ionization rate initially increases faster with E_u than the rate of electron loss by back diffusion, the dip will be removed while back diffusion is still going on.

It is of interest to compare the amplification curves obtained for the various gases. For elastic collisions between electrons and gas atoms or molecules, the fraction of the electron energy which is lost per collision is inversely proportional to the mass of the atom or molecule struck. Therefore we would expect for a given E/p that the random energy of the electrons is less in a light gas than in a heavy gas and hence the diffusion coefficient to be less. This is an oversimplification, however, and is complicated by the occurrence of inelastic

collisions. At low E/p, the fractional energy loss of an electron per collision, taking inelastic collisions into account, has been shown[3,5] to increase for gases in the order Ne, He, N_2, H_2. Therefore the diffusion coefficient should increase in the opposite sense, and if the dip in the amplification curve _is_ due to back diffusion, it might be expected to be greater in the order H_2, N_2, He, Ne. This crude picture does not agree with the experimental results, and it is not possible to conclude with any certainty at this stage that back diffusion _is_ the mechanism causing the dip.

Later in this thesis more rigorous attempts are made to find a theory which satisfactorily explains the shape of the amplification curves.

CHAPTER 5

ELECTRICAL BREAKDOWN OF GASES AT ULTRA-HIGH-FREQUENCIES

In this study of the events leading up to breakdown in a gas under
the influence of combined uhf and dc electric fields, it is desirable,
for completion of the picture, to obtain measurements of the uhf break-
down field corresponding to the conditions of gap width, gas pressure
and E_{dc} encountered in the amplification curves. (See Chapter 4).
From these measurements at breakdown, the aim is to obtain values of
the uhf ionization coefficient for gases in the same experimental environ-
ment in which the amplification curves were obtained. These values will
be employed later in this thesis in the interpretation of the shape
of the amplification curves. (See Chapter 8).

1. Method of measuring the breakdown field

All the measurements to be described in this chapter were performed
with no artificial source of electrons. The initiation of the discharge
thus depends on the appearance in the gap of a casual electron. With
this in mind, the following procedure was adopted.

Gas was admitted into the system to the required pressure, and
E_{dc} and the gap width were set to the required values. The uhf field
was increased slowly in small increments until an instantaneous break-
down occurred. The uhf field was removed, and the system left to recover
for a few minutes. The uhf field was again applied, and raised to a
value just below that at which the first breakdown occurred. This field
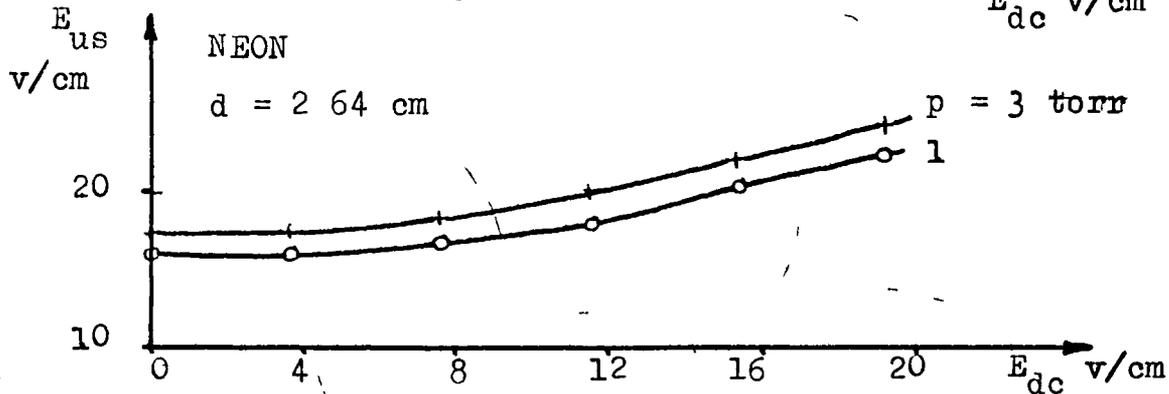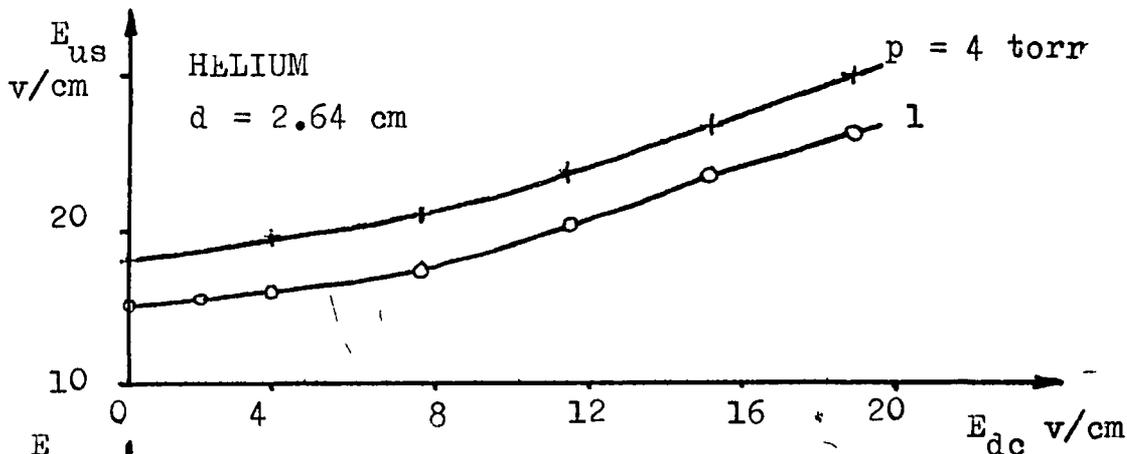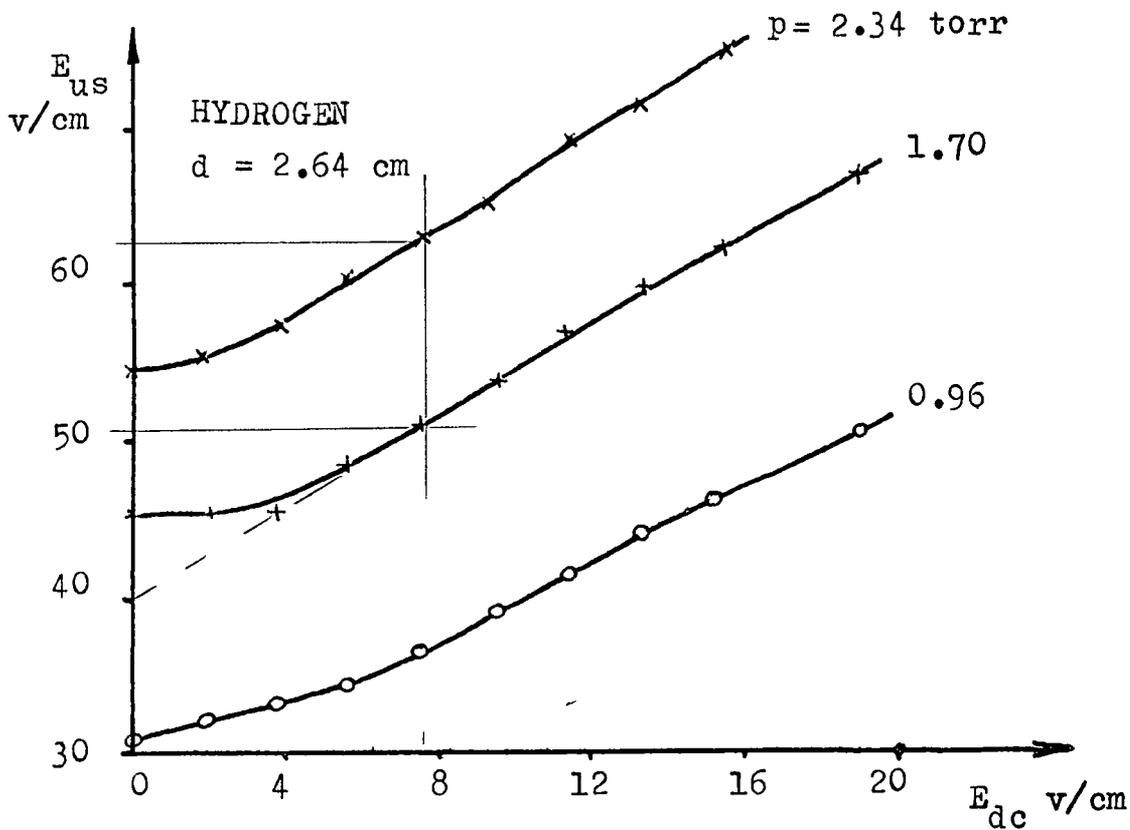
Fig 5.1 Uhf breakdown stress as a function of E_{dc}

was maintained for a few minutes to allow enough time for a casual electron to appear, and if no breakdown occurred during this time, the field was further increased to that which caused the instantaneous breakdown previously. If breakdown again occurs instantaneously, the value just below this was taken for the breakdown field.

Measurements of the breakdown field were performed in hydrogen, nitrogen, helium and neon.

2. Variation of the uhf breakdown field with a superimposed dc field

Typical results showing the variation of the uhf breakdown field, E_{us} (r.m.s. v/cm), with a superimposed dc field, E_{dc}, are presented in Fig. 5.1. The general shape of the curves is the same for all the gases tested. At low values of E_{dc}, E_{us} increases slowly at first, then more rapidly as E_{dc} is increased further, becoming an almost linear function of E_{dc}, of which the slope, for a given gas, appears to be independent of pressure. This increase in the uhf breakdown stress may be explained qualitatively as follows. As E_{dc} is increased, losses of electrons by drift are enhanced, and the lifetime of the average electron in the gap is decreased. In order to preserve the balance between the loss and generation processes, required for breakdown, the ionization rate, hence the uhf field, must be increased.

In this particular set of measurements, the results must be treated with caution. Each time a discharge is struck in the gap the presence of the applied dc field causes a large unidirectional current to flow
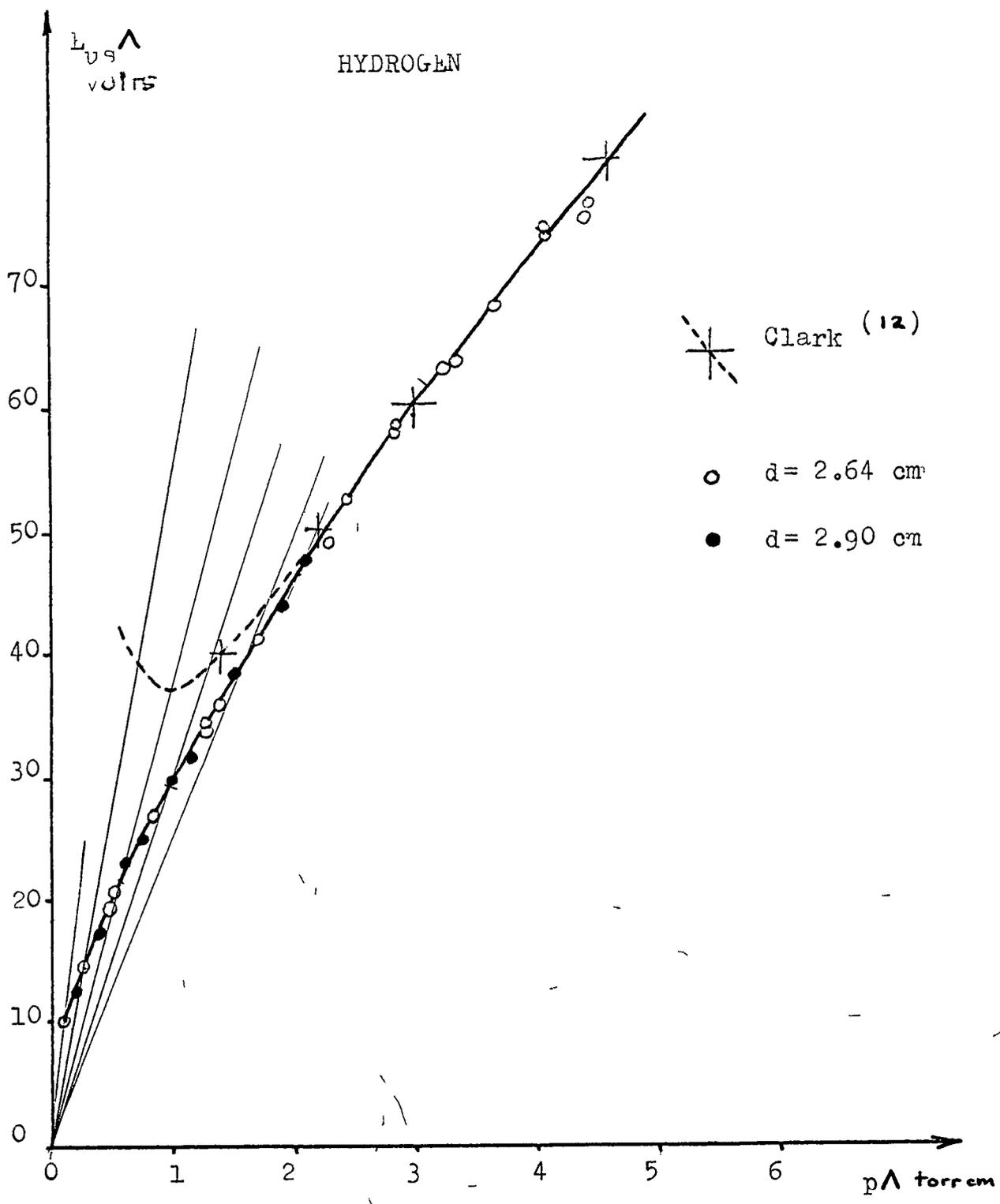
Fig 5.2 Pure uhf breakdown in Hydrogen

in the gap, thus producing considerable charging at the electrode surfaces. (See Chapter 9). Thus the effective value of E_{dc} in the gap at any time is strongly dependent on the discharge that occurred while the previous point on the curve was being obtained. In view of the uncertainty thus introduced, these measurements were not pursued in detail.

3. Measurements of breakdown field at pure uhf

Measurements of breakdown stress were performed for gases stressed by pure uhf fields, and curves were plotted showing the variation of $E_{us}\Lambda$ with $p\Lambda$, where Λ is the diffusion length of the gap. Experiments of this type have already been performed in detail at Durham by Clark[12,37]. Here that work is extended to cover the range of experimental conditions relevant to the present amplification measurements. For a given curve the procedure adopted was to keep Λ constant, and to measure the breakdown field for a range of pressures.

> (Note:- A later chapter describes measurements which show that there is no net charging in the gap during a pure uhf discharge. Therefore the measurements of breakdown stress at pure uhf are likely to be considerable more reliable than those made in the presence of a dc field.)

3.1 Breakdown in hydrogen

Measurements of breakdown stress were obtained in hydrogen in the pressure range 0 to 8 torr, with gap widths of 2.64 and 2.90 cm. (See Fig. 5.2).

It is seen that for the whole range of pressure used, the curve
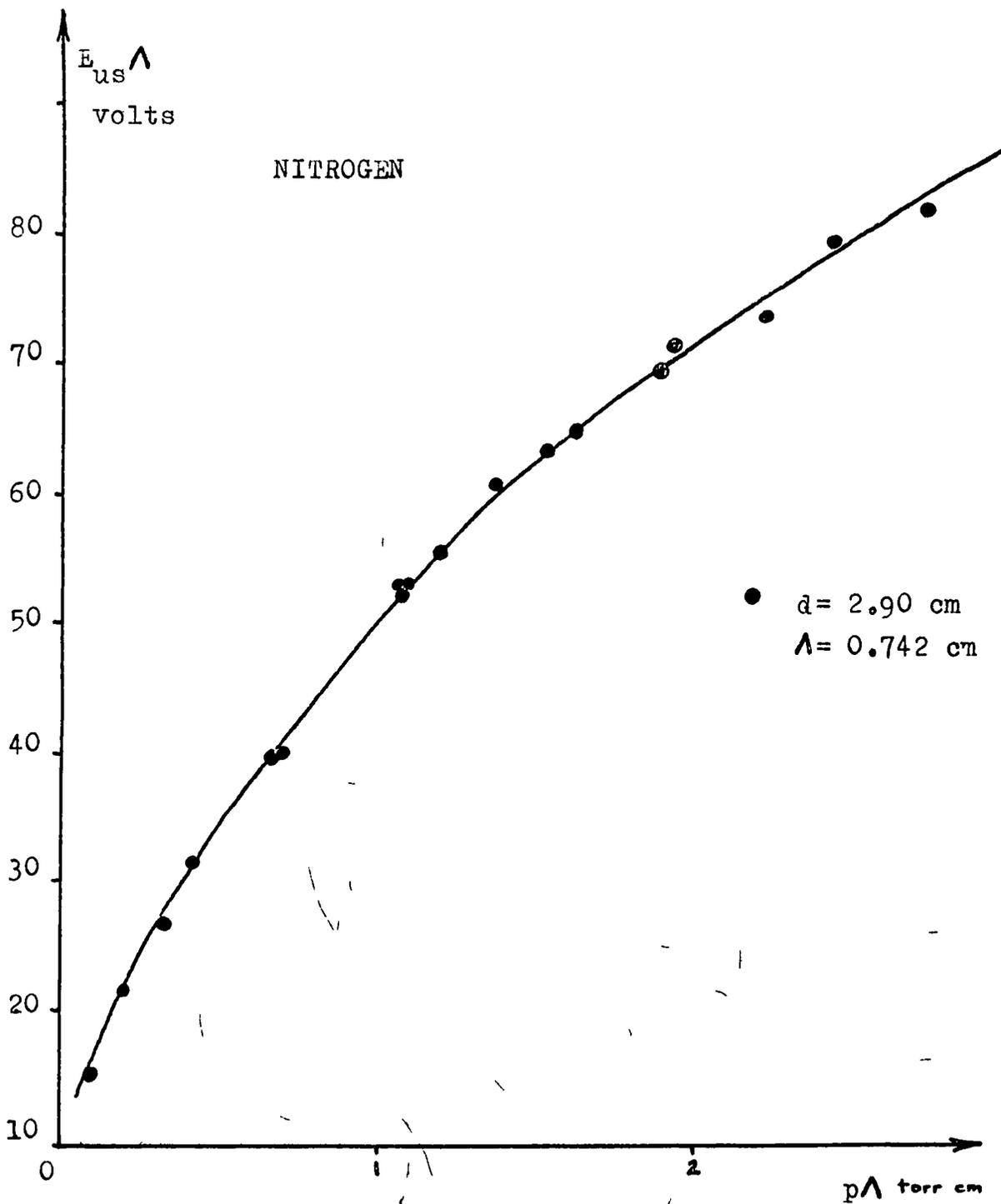
Fig 5.3. Pure uhf breakdown in Nitrogen.
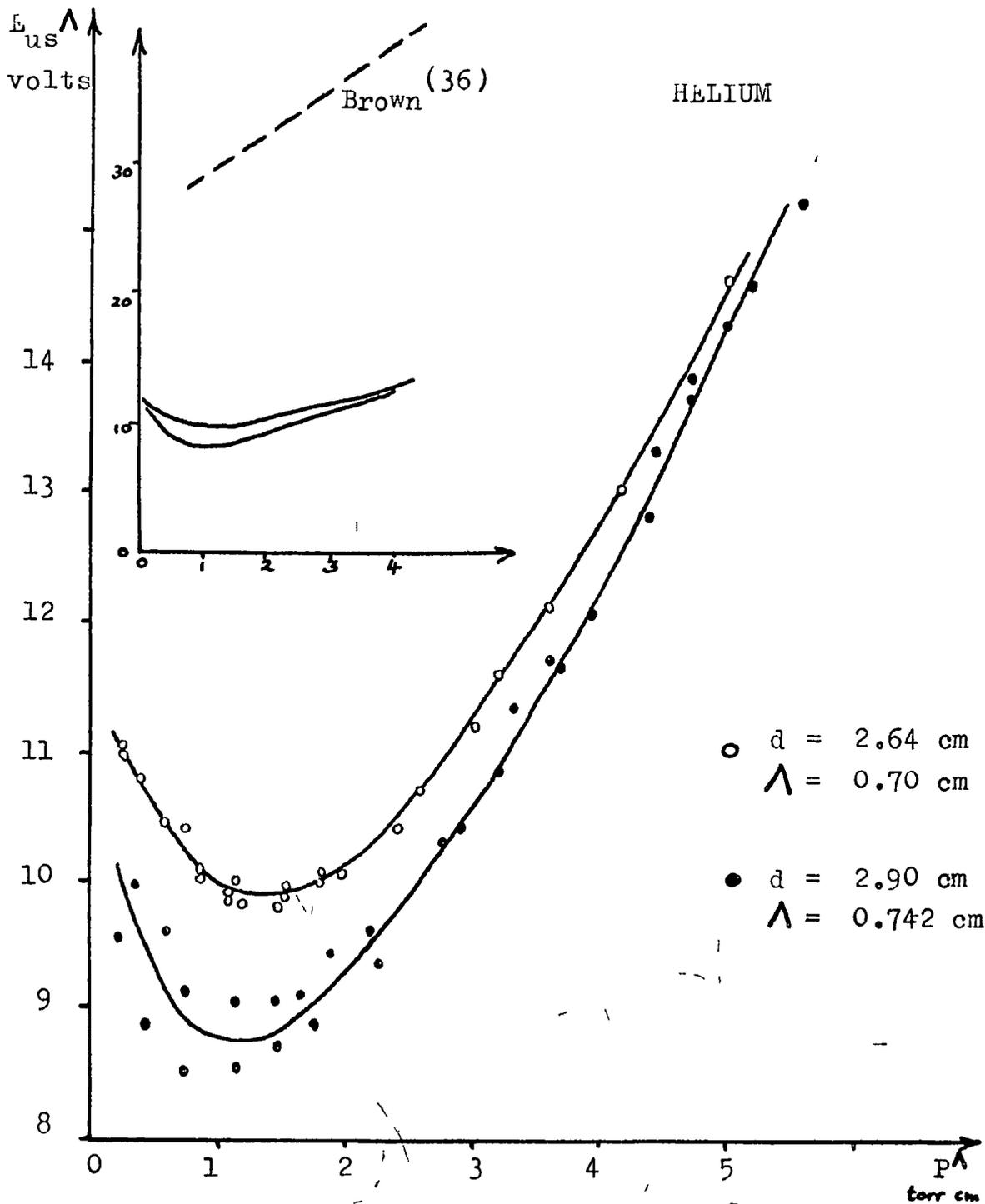
Fig 5.4. Pure uhf breakdown in Helium.
(Inset Comparison with Brown's Results[36])

of $E_{us}\Lambda$ against $p\Lambda$ is unique for both gap widths. At the high pressure end of the curve, E_{us} decreases uniformly with pressure, agreeing extremely well with Clark's measurements over this region. In the low pressure region, Clark's curves, obtained for smaller gap widths and a frequency of 9.5 Mc/sec, branch upwards, while the present curve continues the downward trend. The reasons for this discrepancy between Clark's and the present measurements are discussed in §3.5 of this chapter.

3.2 Breakdown in nitrogen

Measurements of breakdown stress were obtained in nitrogen in the pressure range 0 to 4 torr, with a gap width of 2.90 cm. (See Fig. 5.3). Over the full range of pressure used, E_{us} decreases uniformly with pressure. Clark's measurements in nitrogen were obtained for conditions of pressure and gap width that differ so greatly from these that no fair comparison can be drawn with the present results.

3.3 Breakdown in helium

Measurements of breakdown stress were obtained in helium in the pressure range 0 to 8 torr, with gap widths of 2.64 and 2.90 cm. (See Fig. 5.4). The breakdown field decreases uniformly with pressure down to p about 1 torr.cm, below which it rises sharply again. Over the whole of the above pressure range as far as can be ascertained from the very limited range of gap widths used, the curve appears to be dependent on the gap width. Clark performed no breakdown measurements in helium. However, compared with the results of Brown[36] it is seen that the present values of the breakdown field are considerably lower.
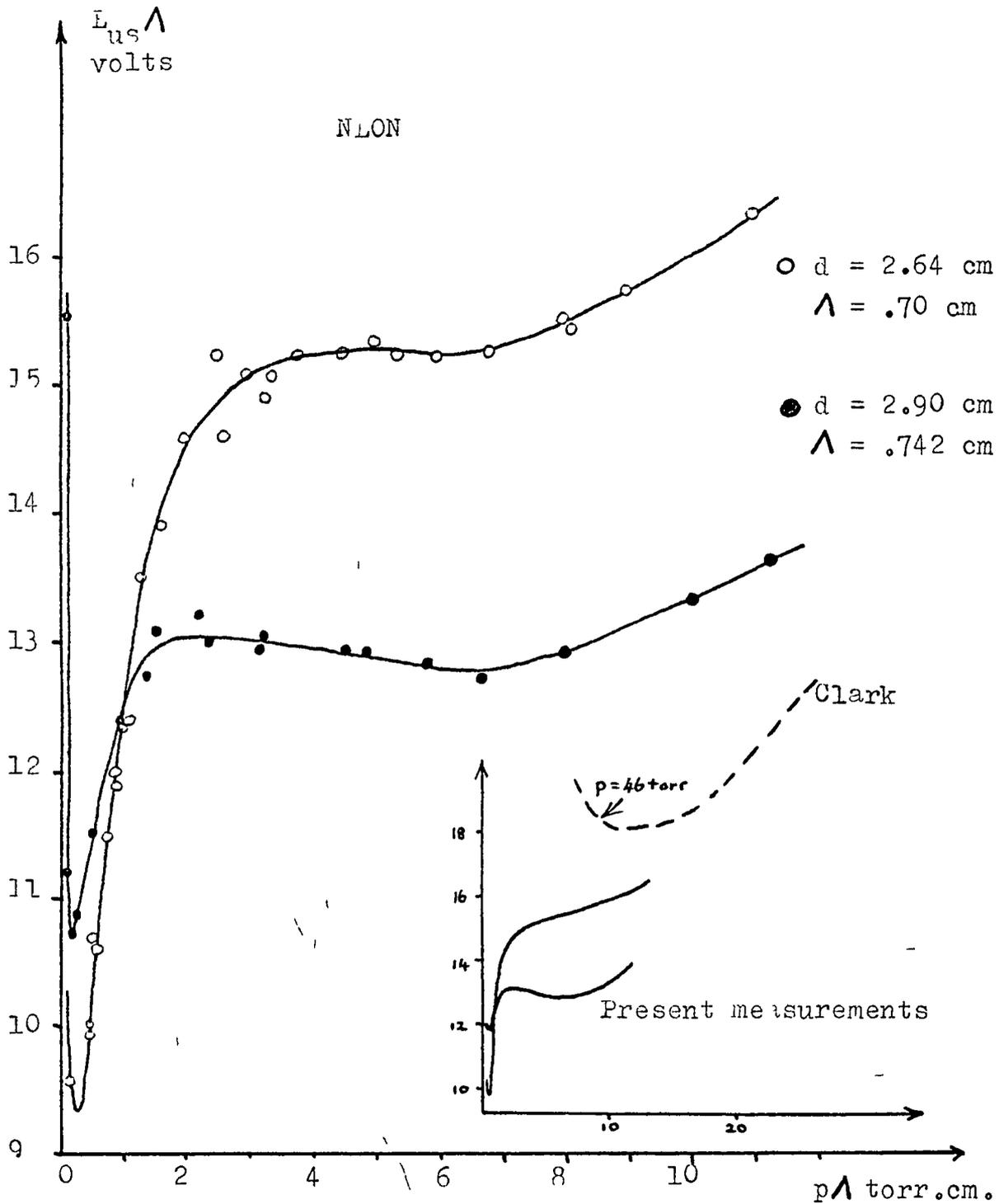
Fig 5.5 Pure uhf breakdown in Neon
(Inset Comparison with Clark's results.[12])

3.4 Breakdown in neon

Measurements of breakdown stress were obtained in neon in the pressure range 0 to 15 torr, with gap widths of 2.64 and 2.90 cm. (See Fig. 5.5). At the higher end of this pressure range, E_{us} decreases uniformly with pressure, but as the pressure is decreased, goes through a minimum at $p\Lambda$ about 6 torr.cm, then rising again slightly before dropping sharply to reveal another minimum at $p\Lambda$ about 0.2 torr.cm, after which it rises sharply again. As in helium, the curve appears to be quite strongly dependent on the gap width.

Clark's measurements in neon do not extend to such low values of p , so, again, no fair comparison can be made with the present results.

3.5 The diffusion theory of breakdown

The shape of the E_{us} , p curves has been studied in detail by many workers. Prowse and Clark[12] showed that provided the only electron removal mechanism is diffusion, and the only electron generation process is single-stage collision ionization (α), the curve should be unique for a given gas, independent of the dimensions of the gap. Therefore the diffusion theory of breakdown at ultra-high-frequencies[10] should apply.

At breakdown, $\quad \psi / D = 1/\Lambda^2 \quad\quad\quad\quad$ 5.1

It is convenient to consider the ionization coefficient η , the number of ionizing collisions that an electron makes in falling through a potential of one volt.

Then, $\quad -\eta = \alpha / E$

$$= \frac{\psi}{\mu E} \cdot \frac{1}{E} \cdot$$

$$= \frac{\Psi}{D} \frac{D}{\mu} \cdot \frac{1}{E^2} \qquad \qquad \dots \quad 5.2$$

And at breakdown in uhf fields, making use of Eq. 5.1 in Eq. 5.2

$$\eta = \frac{1}{\Lambda^2} \frac{1}{E_{us}^2} \frac{D}{\mu} \qquad \qquad \dots \quad 5.3$$

Then providing that diffusion is the controlling electron removal mechanism, η may be obtained as a function of E/p from the $E_{us}\Lambda$, $p\Lambda$ curves, using established data of other workers for D/μ.

The diffusion theory of uhf breakdown holds provided that

a) the electron ambit in the gap in one half cycle of the uhf field is small compared to the gap width,

b) the electron mean-free-path is small compared to the diffusion length, Λ, of the gap,

c) the collision frequency for impacts between electrons and gas molecules is large compared to the frequency of the applied uhf field, and

d) the wavelength of the applied uhf field is large compared to the diffusion length of the gap.

If any of these conditions are not satisfied, the breakdown curve will deviate from the uniqueness postulated by Prowse and Clark. The value of $p\Lambda$ at which this deviation occurs is strongly dependent on the gap dimensions, and the frequency and magnitude of the applied field. This is illustrated in Fig. 5.2 for hydrogen where Clark's curves are seen to deviate from the unique curve at higher values of $p\Lambda$ than in the present experiment.
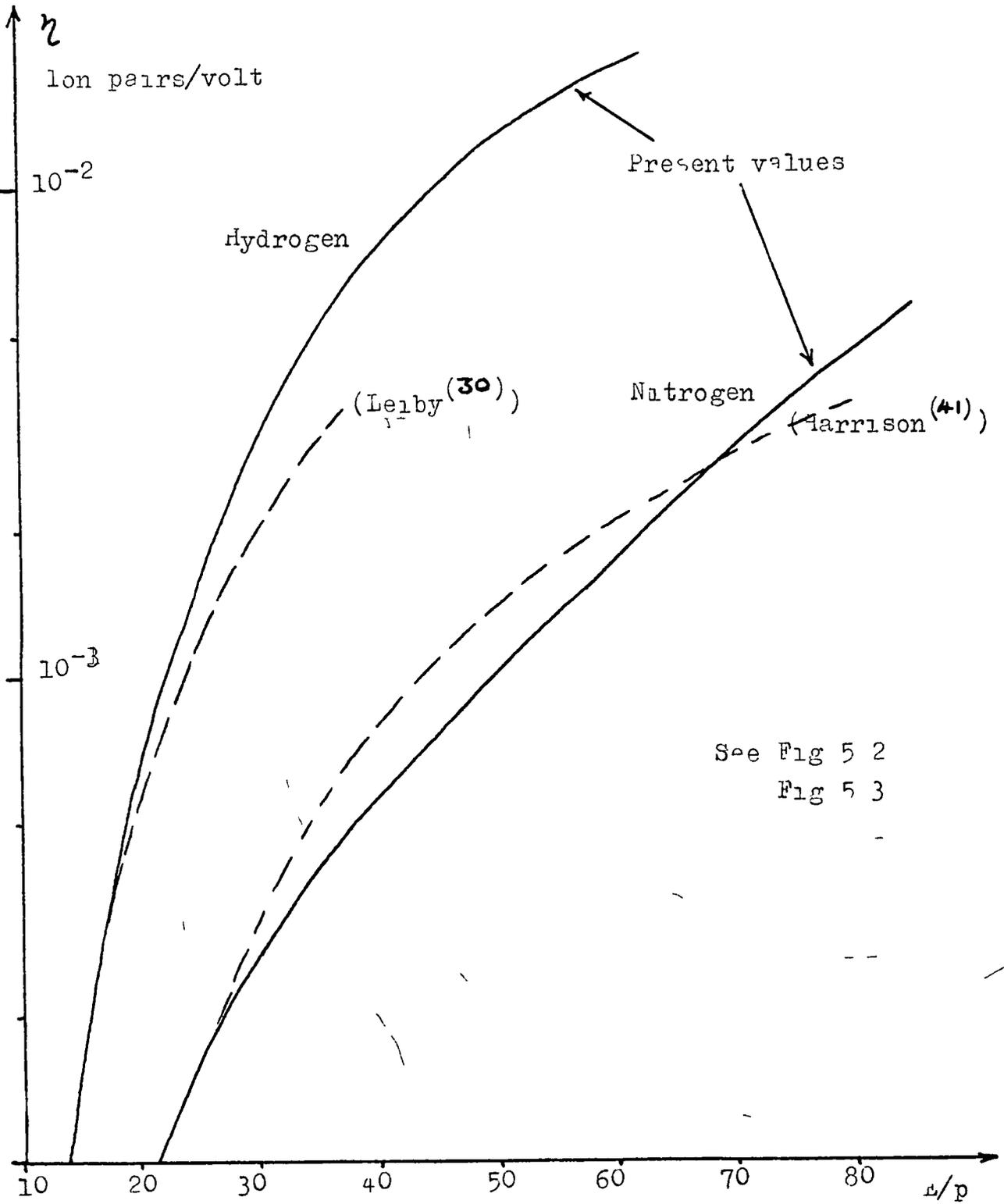
Fig 5 6 Values of η for Hydrogen and Nitrogen from
uhf breakdown measurements

TABLE 5.1

TABLE SHOWING THE RANGE OF CONDITIONS OVER WHICH THE DIFFUSION THEORY

OF BREAKDOWN SHOULD APPLY

Gas	Hydrogen	Nitrogen	Helium	Neon
Electron Ambit Limit	$E/p < 50$	$E/p < 50$	$E/p < 30$	$E/p < 20$
Mean-free-path limit	$p < 0.020$	$p < 0.050$	$p < 0.060$	$p < 0.12$
Collision frequency limit	$p < 0.052$	$p < 0.052$	$p < 0.104$	$p < 0.074$
Uniform field limit	Wavelength of oscillation of field, 625 cms, is far greater than , so diffusion theory applies.			

Electron ambits calculated from Townsend drift velocity data[5].

Collision frequency data from Brode[39].

Random velocity data from Townsend data[5].

The conditions in the present experiments over which the diffusion theory of breakdown should apply are set out for hydrogen, nitrogen, helium and neon in Table 5.1.

3.6 Application of the diffusion theory of breakdown in hydrogen and nitrogen

For the limited range of gap widths tested in hydrogen and nitrogen Figs. 5.2 and 5.3 indicate quite clearly that the $E_{us}\Lambda$, $p\Lambda$ curves are unique for each gas, and not dependent on the gap width. Therefore the diffusion theory should apply safely over most of the conditions tested, and this is confirmed by the conditions stated in Table 5.1.

Therefore using Eq. 5.3, the ionization coefficient η is calculated as a function of E/p from the measurements of breakdown stress. (See Fig. 5.6). Values of D/μ for hydrogen are obtained from the data of Varnerin and Brown[13], and for nitrogen from the data of Deas and Emeleus[40].

The values of η thus obtained for hydrogen agree satisfactorily with those obtained by Leiby[30], Prowse and Clark[12] and Varnerin and Brown[13] and the values for nitrogen agree similarly with those obtained by Harrison[41].

3.7 Application of the diffusion theory of breakdown to helium and neon

The minimum in the breakdown curve for helium, and that in the neon curve at the higher value of $p\Lambda$, do not appear to coincide with any of the limits to the diffusion theory mentioned so far. However the minimum in the neon curve at the lower value of $p\Lambda$ is very close to both the mean-free-path and the collision frequency limit.

From the limited amount of data obtained for breakdown in helium
and neon, it is clear that the breakdown curve is _not_ unique, but _is_
dependent on the gap width, although we see from Table 5.1 that diffusion
ought to be the controlling electron removal mechanism over all the
conditions tested except at very low pressures. This leads to the con-
clusion that over the range of the present measurements, the diffusion
theory postulated by Prowse and Clark apparently fails. This suggested
departure from the breakdown theory appears only under the present
conditions of long gap widths and low pressures. The theory was tested
successfully by Prowse and Clark for shorter gap widths and higher
pressures. A possible mechanism that would invalidate the theory would
be the emergence of an electron generation process other than single-
stage collision ionization, dependent on the dimensions of the gap.
One possible mechanism may be closely linked with the abundance of
metastable atoms formed in helium and neon. At high pressures, a
metastable atom has a high probability of colliding with an atom of
impurity in the gas, and may, if the metastable energy of the impinging
atom is slightly higher than the ionization potential of the struck im-
purity, give up its metastable energy to ionize the impurity atom. (Pen-
ning effect). In this case, the net effect is simply to enhance the value
of the single-stage collision ionization coefficient, and does not
basically alter the theoretical argument of Prowse and Clark. But at lower
pressures, the probability that the metastable atom will collide with
a suitable impurity is reduced, and it may instead diffuse to the
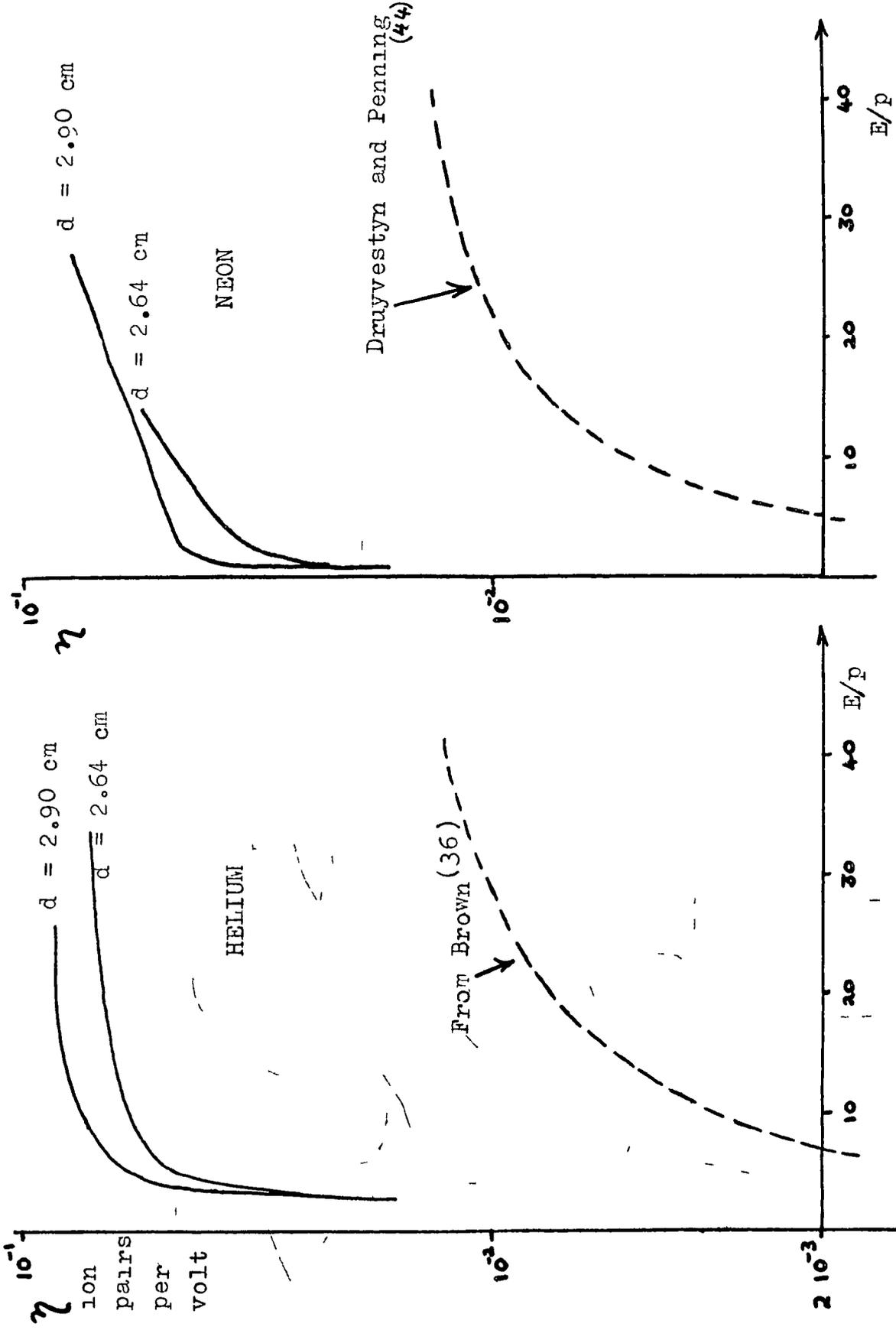
Fig 5.7. Values of η for Helium and Neon from uhf breakdown measurements.

electrodes where it might readily give up its energy to assist the release of electrons from the surface of the metal. This effect will be dependent on the gap dimensions, as well as the pressure and the impurity content of the gas under test.

If it _is_ an additional electron generation process which is causing the departure from the theory in the present experiments, then so long as diffusion is still the controlling electron loss process, the diffusion theory of breakdown may be applied. The ionization coefficient, η , is then calculated for helium and neon from Eq. 5.3, and plotted as a function of E/p. (See Fig. 5.7). Values of D/μ for helium are obtained from the data of Reder and Brown[42], and for neon from the data of Mierdel[43]. It is seen that the calculated values of η are more than an order of magnitude greater than any of the standard data published for pure helium and neon, (Helium[44,45]; Neon[44,36]), and this is consistent with the view that an additional electron generation process is occurring as well as single-stage collision ionization. η is then a measure of the total multiplication of electrons in the gap, taking into account all generation processes.

If, on the other hand there is a loss procedure occurring other than diffusion, the diffusion theory of breakdown does not apply. In this case, the ionization coefficients calculated in the manner described above are fictitious, and may not be used with confidence later.

3.8 Comments

The values of the ionization coefficient in hydrogen and nitrogen obtained by the above method are reasonably satisfactory, and there is

no apparent reason why these should not be used later in helping to explain the shape of the amplification curves in those gases.

The values obtained for helium and neon must, however, be viewed with caution since it is not certain that the application of the diffusion theory of breakdown is valid in the range of conditions tested. This needs to be investigated further. Breakdown measurements are required over a wide range of gap widths and gas pressures, (and taking special care to obtain high gas purity), embracing all the conditions ranging from those used by Clark to those used in the present experiments, in order to establish firmly the failure of the theory of Prowse and Clark, and, (if successful), under what conditions this occurs. A possible mechanism has been suggested to account for the departure from the theory, but in view of the limited amount of data obtained, this cannot be supported quantitatively at this stage.

Pure Aluminium

Brass

← L → 2b

Enlarged view
of emitting hole

Demountable
centre plug
containing the
emitting hole

(Approximately to scale)
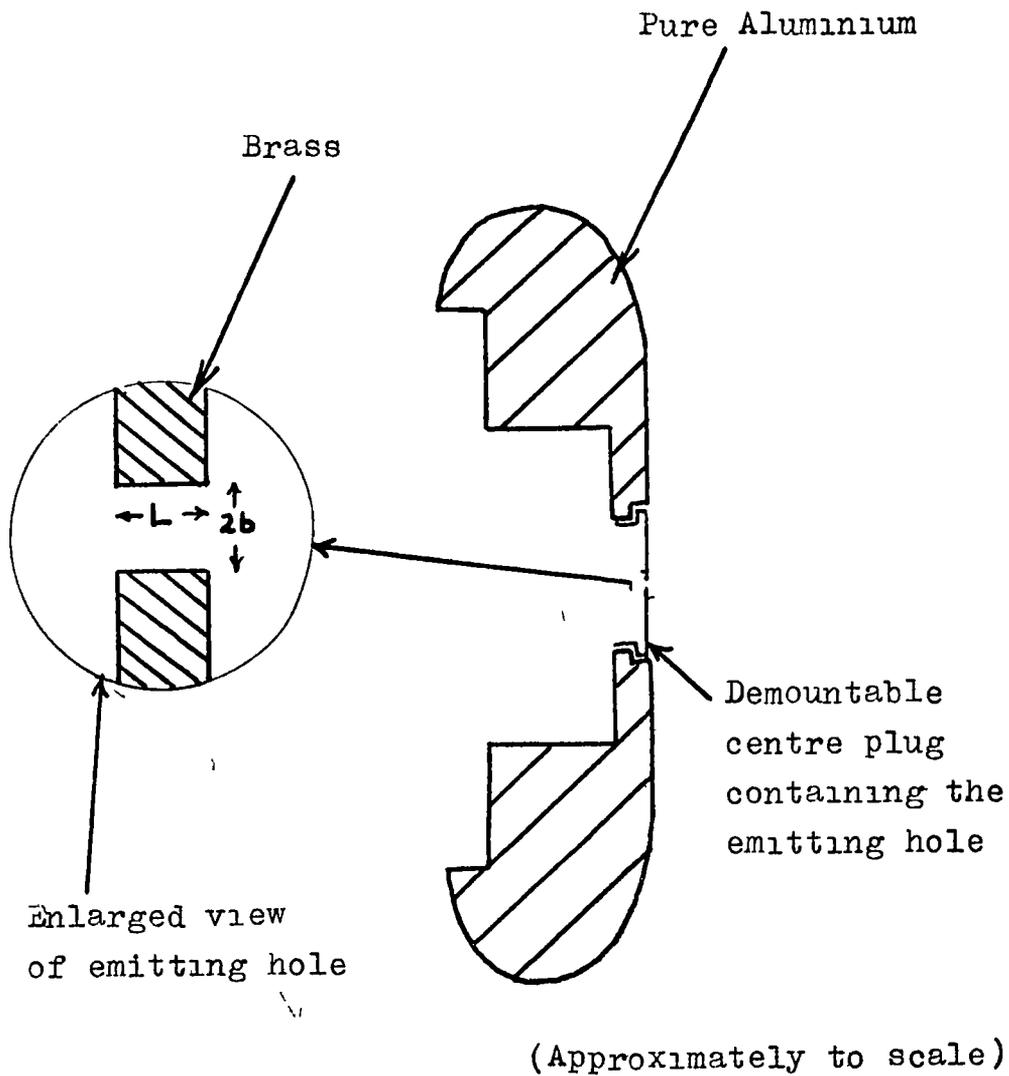
Fig 6.1. Modified emitting electrode for experiments
where it is required to vary the size of
the emitting hole.

CHAPTER 6

EXPERIMENTS TO INVESTIGATE THE NATURE OF ELECTRON FLOW WITHIN THE HOLES

IN THE EMITTING ELECTRODE

It is seen from Chapter 2 that the theory developed by Long[2]
to account for the shape of the amplification curves is heavily depend-
ent on the radius of the holes in the emitting electrode through which
the electrons emerge into the gap. This chapter describes experiments
which were performed to test this particular aspect of the theory, and
also to investigate the nature of the flow of electrons down these holes.
All the measurements were performed in hydrogen.

1. Modifications to the apparatus

A new emitting electrode was constructed of pure aluminium, as
close as possible to the dimensions of the one used for the other experi-
ments described in this thesis. (See Fig. 6.1). A large central hole
of diameter about 2.5 cm was drilled in the flat face, and a number of
short brass plugs were constructed to slide into this hole, and fit flush
with the face of the electrode. Each plug consists of a short brass
cylinder, closed at one end. The closed end is pierced centrally with
a small circular hole, which, with the plug in position, constitutes
a single emitting hole in the electrode face.

2. Measurements of amplification for holes of various sizes

The diameter and length of the emitting hole were measured using

	b cms	L cms
o	0 0340	0.1035
●	0.1035	0.1035
+	0 0265	0 0264
×	0.1043	0.0264
△	0 0265	0 0520
□	0 0875	0.0520

HYDROGEN
$d = 2\ 59$ cm
$p = 2$ torr
$E_{dc} = 7\ 72$ v/cm
$V_1 = 75$ volts
$i_1 = 4\ 10^{-6}$ amps

E_u v/cm
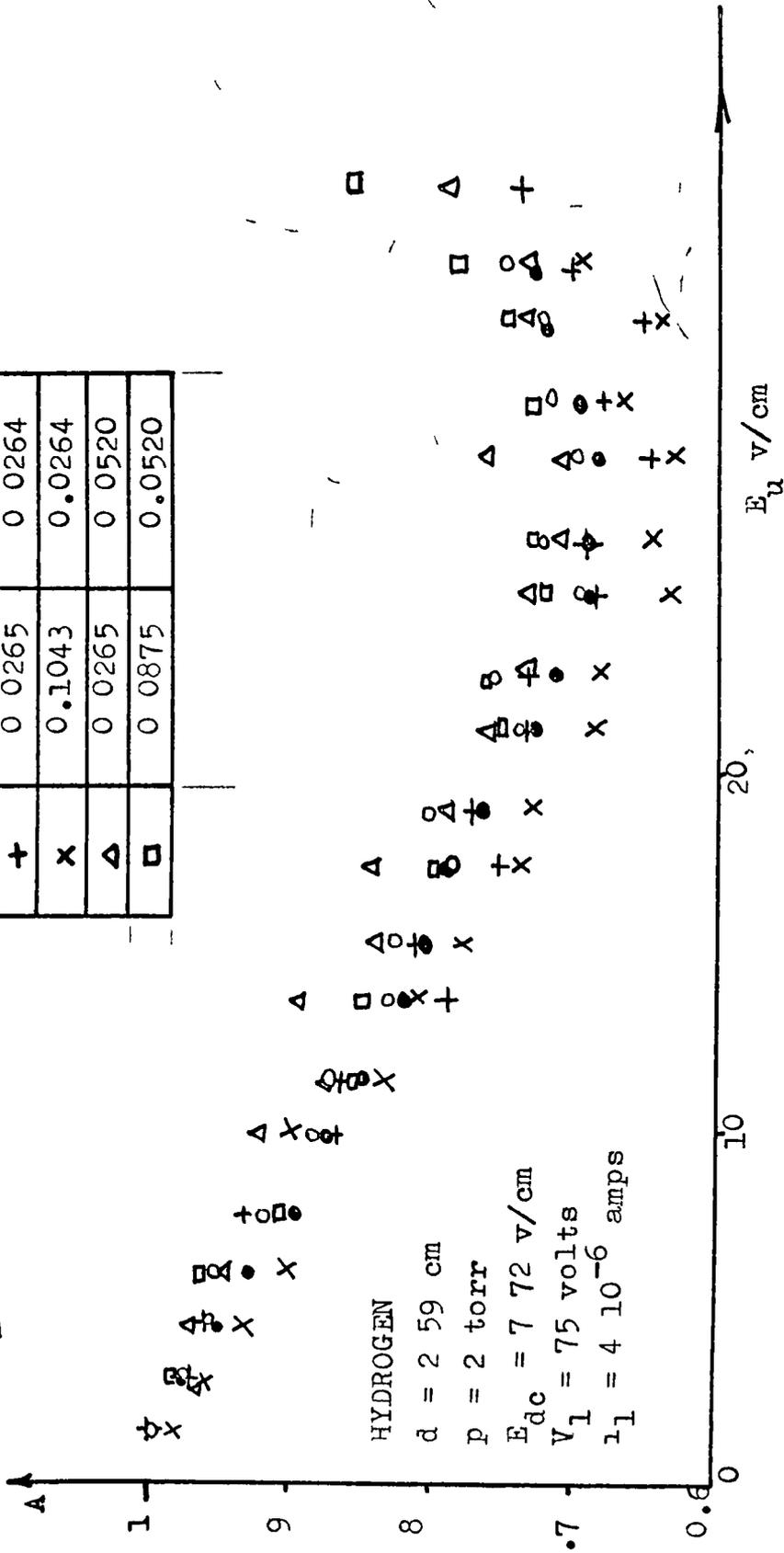
Fig 6 2 Amplification curves for various emitting hole dimensions

a travelling microscope and micrometer gauge respectively. With this plug in position, amplification curves were obtained in the usual way. (See Chapter 4). The measurements in this instance were confined to hydrogen in the region below the onset of collision ionization. When sufficient curves had thus been obtained, the emitting electrode was removed from the system, the emitting hole was enlarged and the dimensions of the hole were re-measured. The experiment just described was repeated for this new hole size. Measurements were performed for hole radii b, ranging from .017 to .104 cm.

This whole procedure was repeated for hole lengths, L, ranging from .025 to .104 cm. Care was taken to ensure that from experiment to experiment, the only quantities that were allowed to vary were the dimensions of the hole. All other quantities were maintained the same throughout all the runs. i.e. $d = 2.59$ cm, $E_{dc} = 7.72$ v/cm, p = 1 and 2 torr, $V_1 = 75$ volts, and $i_1 = 4.10^{-6}$ amps.

The results of this investigation are presented in Fig. 6.2. From these, it is not possible to detect a systematic variation in the shape of the amplification curve with variations in the hole dimensions. What small variations are observed may well be accounted for in terms of the error introduced by the charging up of the electrode surfaces under the influence of the gap current. (See Chapter 9). Although these results were obtained with only one hole in the emitting electrode, there is no apparent reason why the same effect should not be observed when there is more than one, as in the main bulk of the amplification measurements

Upper graph labels:

HYDROGEN
p = 1 torr
d = 2.59 cm
E_{dc} = 7.72 v/cm
V_1 = 75 volts
i_1 = 4.10^{-6} amps

y-axis: i_{20} cm galvo defl^n.

x-axis: b cm, marked 0.1

	L	
O	0.0264	cm
+	0.0520	
X	0.1035	

Handwritten (top right):
0   78
08 50
06 28
03 07

Lower graph labels:

HYDROGEN
p = 2 torr
d = 2.59 cm
E_{dc} = 7.72 v/cm
V_1 = 75 volts
i_1 = 4.10^{-6} amps.

y-axis: i_{20}

x-axis: b cm, marked 0.1

Handwritten (right):
0 38
08 24
06 14
3 4
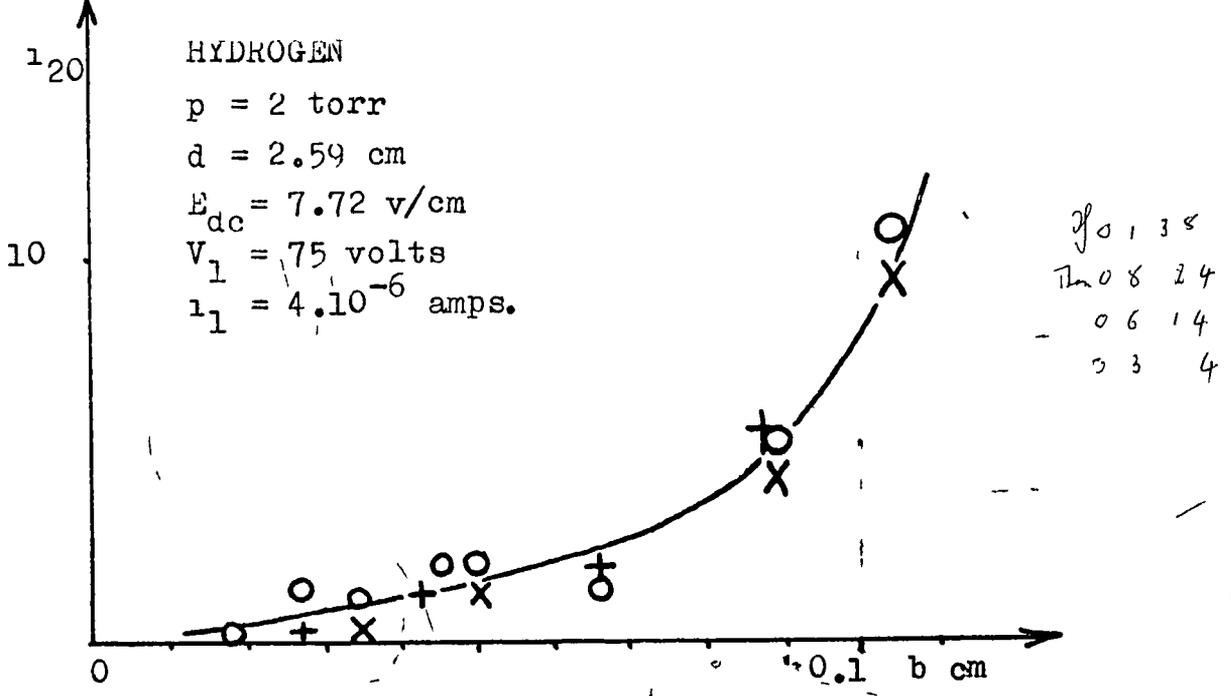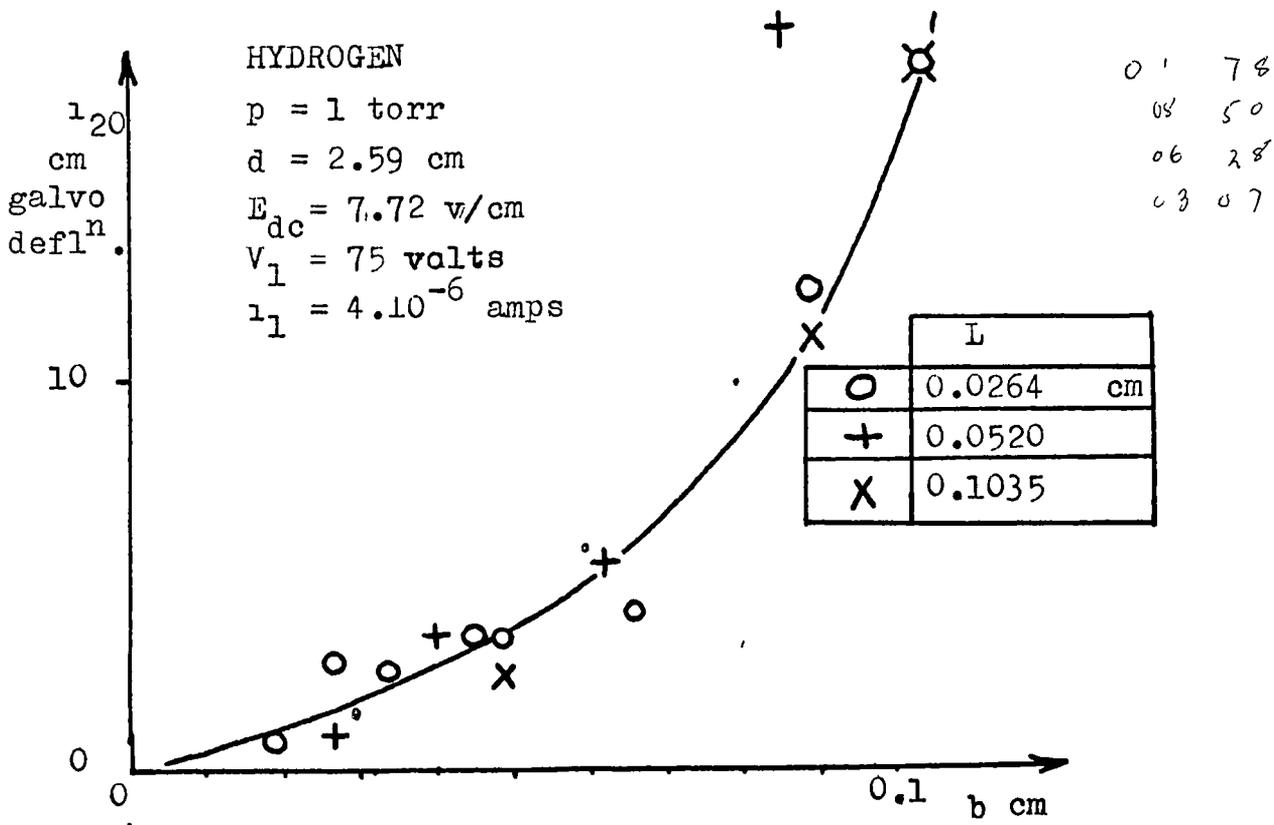
Fig 6.3. Variation of i_{20} as a function of the dimensions of the emitting hole.

described in Chapter 4.

The results of this experiment therefore lead to the firm conclusion that Long's theory for the shape of the amplification curves in hydrogen[2, 29] considerably overestimates the importance of the size of the emitting holes.

3. **The effect of the hole dimensions on the magnitude of the current entering the gap**

The current flowing to the collecting electrode in the absence of a uhf field, i_{20}, is plotted as a function of the hole radius, b, for a range of values of the hole length, L, keeping E_{dc}, i_1, V_1, d and the gas pressure constant. (See Fig. 6.3). The quantity that we would like to know as a function of the hole dimensions is the actual current emerging from the emitting electrode, i_e, but it is reasonable to assume under the above conditions that i_e is proportional to i_{20}.

i.e. $$ i_e = \Lambda\ i_{20} $$

where   is constant in this case, depending only on d, E_{dc}, the gas pressure, and the nature of the gas.

It is seen from the curves that i_{20}, hence i_e, increases approximately *is not distinguishable from square* as the square of the hole radius, b, although the accuracy of the results, owing to the slow drifts observed in i_{20} (See Chapter 9), is not sufficient to allow this to be determined exactly.

It is reasonable to expect that, if electrons are lost to the wall of the hole, the current emerging into the gap should decrease as the

length of the hole is increased. However, the curves show that the current flowing to the collecting electrode, hence i_e, does not vary appreciably with L over any of the range of b and L used. Therefore it must be concluded that electrons are <u>not</u> lost to the hole wall on their passage through the hole. This unexpected result has prompted the following discussion into the nature of electron flow through a hole in the emitting electrode.

3.1 <u>Drift and diffusion of electrons within the emitting hole</u>

Electrons from the filament move towards the back of the emitting electrode by drift and diffusion, controlled by the voltage V_1. Those electrons entering the hole may still be under the influence of V_1, owing to the penetration of V_1 into the hole. This effect is steadily reduced as the electrons move further into the hole. For a very short hole the electrons are still influenced by V_1 when they emerge out of the far side, by which time they are also under the influence of the dc field in the gap, and although some may be lost by radial diffusion to the wall of the hole, the majority will be swept out into the gap. However for longer holes, the field penetration from either side may not be as great in comparison, and there may be a region within the hole which is field free. In this region, the electrons are influenced by diffusion alone. The chances now that an electron will cross this field-free region now depends on the relation between the length and the radius of the region.

Due to the field penetration into the hole, a radial component of field may be expected within the hole, but this effectively disappears

with the axial field. Therefore the radius of the field-free region is approximately equal to the physical radius of the hole.

Within this field-free region, we may estimate the relative probabilities that a) the electrons will diffuse to the wall of the hole, or that b) the electrons will diffuse to the ends of the region. Those that diffuse to the far end of the hole, will come under the influence of the field in the gap, and this is the component that we are interested in here, since these are the electrons which actually get into the gap.

Diffusion in a cylindrical cavity is described by the diffusion length, Λ, given by

$$1/\Lambda^2 = (\pi/d)^2 + (2.405/r)^2 \qquad \text{.... 6.1}$$

where the first term on the right hand side corresponds to diffusion laterally, and the second term to diffusion radially out of a cylindrical container[10].

In this case we are concerned with a container of radius b and length L_o, where L_o is the length of the field-free region inside the hole. The chance that an electron will be lost by diffusion to the wall of the hole, compared to the chance that it will diffuse to the far end of the hole is given by σ, where

$$\sigma = \frac{(2.405/b)^2}{(1/2)(\pi/L_o)^2} \qquad \text{.... from 6.1}$$

The factor 1/2 appears in the denominator because we are not interested in those electrons which diffuse back to the same end of the hole from which they entered initially.
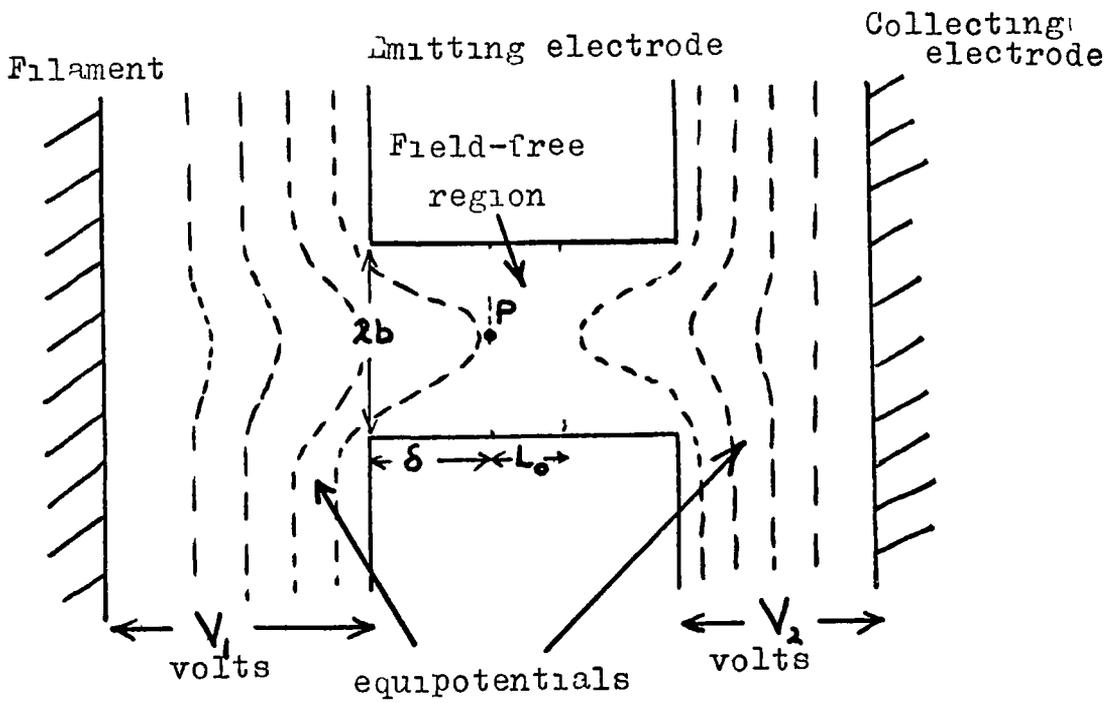
Fig 6.4. Field penetration into the emitting hole.
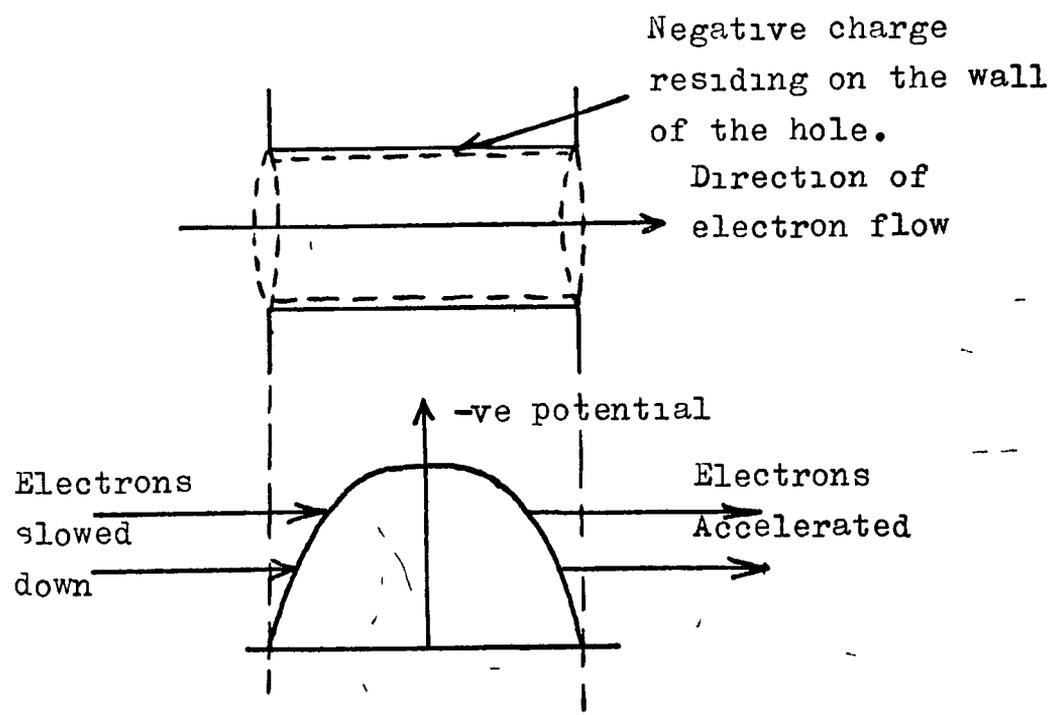
Fig 6.5. The effects of charging at the wall of
the emitting hole.

Then, $\sigma = 1.172 \ (L_0/b)^2$ 6.2

From this we may conclude that radial diffusion is negligible only for short holes where L_0 is negligible. But as soon as the hole dimensions become such that there is a field-free (or near field-free) region within the hole, (i.e. L_0 finite), diffusion losses to the walls of the hole can no longer be neglected, and may be expected to increase with the length of the hole.

L_0 is a function of L and b, and probably V_1 and E_{dc}, but, so far attempts to determine this function rigorously have not been successful. The following crude theory provides an approximate condition for there to be a field-free region inside the hole.

At a given point, P, on the axis inside the hole, the electric field due to field penetration is a function of the solid angle subtended at P by the mouth of the hole. (See Fig. 6.4). Assume that if the solid angle subtended is less than π, then the field at P is negligible.

The solid angle subtended at the mouth of the hole is

$$\phi = (\text{Area of mouth of hole})/x^2$$
$$= 2\pi b^2/(b^2 + \delta^2), \text{ where } \delta \text{ is the distance of P from}$$

the end of the hole, measured along the axis. For the field at P to be negligible

$$\pi > \phi$$
$$> 2\pi b^2/(b^2 + \delta^2)$$

Then, $\delta^2 > b^2$

Therefore for there to be a finite field-free region within the hole, and hence for electron losses inside the hole to be appreciable

$$L > 2\delta > 2b \qquad \qquad \dots\dots \ 6.3$$

(the factor 2 comes from considering the field penetration at both ends of the hole).

From this rough criterion, it is fairly clear that, with at least some of the hole configurations employed experimentally, electrons will be lost to the walls of the hole. But the experimental results (See fig. 6.3) do not confirm this view. Therefore we must consider the possibility that there is some other mechanism occurring which is helping to prevent electron losses inside the hole.

3.2 The effects of charging at the wall of the emitting hole on the current emerging into the gap

Ignoring the effects of field penetration, it is of interest to consider the effects of charging at the wall of the hole on the current emerging into the gap at the far end. Electrons flowing into the hole may, as has already been shown, reach the wall, and under the right surface conditions may become deposited there. Thus the walls may charge up to a potential high enough to produce electrostatic focussing of the electron stream within the hole. This becomes analogous to the operation of the Wehnelt cylinder, which is employed to concentrate the electron beam of a cathode ray tube as it leaves the filament[46]. To operate effectively, the wall of the hole must be raised to a negative potential higher than that of the electrons as they enter the hole. Fig. 6.5 shows approximately the expected potential distribution along the axis of a charged hollow cylinder (in this case the hole). The potential reaches its highest negative value at the centre, dropping to zero on

both sides. This distribution acts as a 'potential pass', having two effects. Firstly, the effect is to concentrate electrons towards the axis by electrostatic focussing, being strongest at the centre of the hole. Secondly, electrons arriving into the hole meet an unfavourable potential gradient which slows them down, more so the nearer to the centre of the hole that they get. Near the centre of the hole they are moving in near field-free space, and will reach thermal energies. This has the effect of decreasing the diffusion coefficient, assisting the prevention of electron loss by diffusion to the wall. But the field-free region is relatively short, and once the electrons have diffused across this, they find themselves in a favourable potential gradient, equal and opposite (in the absence of field penetration into the hole by the externally applied fields) to the gradient which caused them to slow down initially. The electrons now gain energy as they are driven down this potential gradient, and the net effect when they arrive in the gap is that their energy is about the same as it was when they entered the hole. Therefore the random velocity of electrons on entering the gap should be close to that corresponding to V_1.

These effects rely on the presence of an insulating layer over the walls of the hole, thus enabling the charging process to take place. Later experiments do point strongly to the presence of insulating layers on the electrode surfaces in the gap. Some of those measurements are also consistent with the suggestion that charging is occurring inside the emitting holes and acting so as to aid the injection of electrons into the gap. (See Chapter 9).

A THEORETICAL STUDY OF THE RELATIVE IMPORTANCES OF DRIFT AND DIFFUSION, AND OF THE ELECTRON DENSITY DISTRIBUTION IN THE GAP

The experimental amplification curves show that the dip in the curve at low values of E_u is controlled strongly by the value of the superimposed dc field. It appears that as E_{dc} is increased for a given gas at a given pressure, the dip is decreased in size by the growing effectiveness of electron drift. This chapter sets out to investigate theoretically the conditions under which drift takes over from diffusion as the predominant electron removal mechanism, and how this manifests itself in the experimental results for hydrogen. A comparison is made with the conditions under which the electron density distribution in the gap changes from the exponential to the sinusoidal form.

1. Drift and diffusion

Electrons moving in a gas in the absence of an electric field describe motions of random walk, moving in straight paths between successive collisions with gas molecules. There is a resultant net flow of electrons towards regions where the concentration of these particles is lower. (See Chapter 1). The rate of diffusion increases with the energy of the electrons.

In the presence of a uhf electric field, assuming that the distance moved by the electrons in one half cycle of the field is small compared

to the electrode spacing, the electrons gain energy as they oscillate to and fro in the field. The paths between collisions now become curved towards the direction of the electric force. (Townsend[5]). There is no net displacement of electrons preferentially to either electrode. The only electrons which can be lost by drift in the uhf field are those which are closer to the electrode than the distance they would move in the field in one half cycle.[31]

In the presence of a pure unidirectional field, the paths between collisions are again curved, but this time such that there is a net advance of electrons towards the anode.

In combined unidirectional and uhf fields, the electrons experience diffusion, drift in the uhf field and drift in the dc field. (In general throughout this thesis, the term 'drift', unless otherwise stated, refers to the unidirectional component). Drift and diffusion may be treated independently provided that the drift velocity is small compared to the random velocity. Then the system may be treated as one in which simple diffusion occurs, with the drift motion superimposed.

In the present experiment, the main removal processes for electrons are diffusion to the electrodes (particularly back diffusion to the emitting electrode), and drift to the collecting electrode in the dc field. Drift to the collecting electrode in the uhf field is another likely possibility, but at this stage it is neglected in comparison with the other two processes.

Two different approaches have been used in order to better under-

stand the relationship between drift and diffusion for different sets of conditions in the gap, and these are described below.

1.1 Pictorial representation of an electron swarm diffusing and drifting in combined dc and uhf fields.

To study the relative importances of drift and diffusion, a graphical approach has been devised to describe the fate of a swarm of electrons starting from a single point on the emitting electrode, and moving out into a parallel plate gap under the influence of combined dc and uhf electric fields. In all of the gases tested experimentally and in the range of E/p considered, the random electron velocity is at least one order of magnitude greater than the drift velocity, thus allowing diffusion and drift to be considered separately.

Under the action of diffusion alone, the average electron will move so that after a time, t, it will lie on the circumference of a sphere of radius $(12Dt/\pi)^{1/2}$. This sphere is frequently referred to in this thesis as the DIFFUSION SPHERE.

(Note:- It should be mentioned here that for electrons emitted from a single point source, diffusion is regarded as three-dimensional, hence the use of the above formula in the present context. But for electrons emitted into the gap through a slit, diffusion may now be regarded as essentially two-dimensional, and after a time, t, the average electron will be displaced a distance $(8Dt/\pi)^{1/2}$. This is now the radius of a 'diffusion cylinder'. Going a stage further, if electrons are emitted from a large finite area of the emitting electrode, or a dense distribution of point sources, diffusion may now be regarded as one-dimensional, and the average displacement of an electron after a time, t, will be $(4Dt/\pi)^{1/2}$. It may be argued that this should apply to the present experiments, where for most of the measurements there are a large number of emitting holes in the emitting electrode. However, it may be equally argued that the present distribution of holes is not dense enough for this to be the case, and that each point has independent emitting

-78-

$E_e/p = 10$ v/cm.torr
$E_{dc} = 5$ v/cm

20 v/cm.torr
5 v/cm

10 v/cm.torr
10 v/cm

10 v/cm.torr
10 v/cm

10 v/cm.torr
20 v/cm

20 v/cm.torr
10v/cm

20 v/cm.torr
20 v/cm
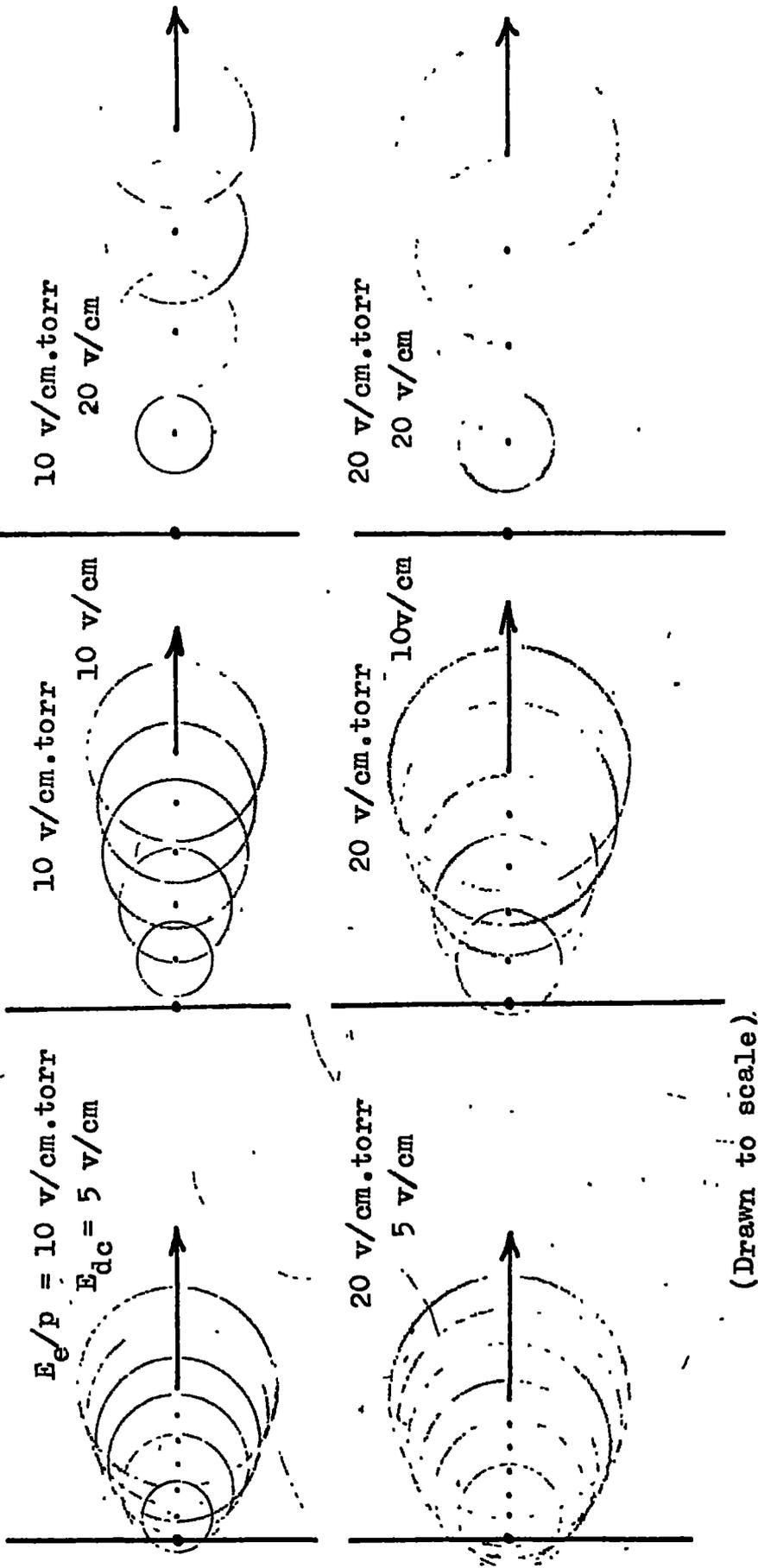
(Drawn to scale).

Fig 7.1. Graphical representation of an electron swarm
diffusing and drifting in combined dc and uhf
electric fields. (Successive microseconds).
HYDROGEN:p= 5 torr.

behaviour. Therefore such a system of discrete point sources may be expected to behave essentially in the same way as a single point source and the three-dimensional expression for diffusion of electrons leaving the emitting electrode should be the most applicable to the present case).

When a unidirectional field is applied, the centre of the diffusion sphere progresses in the field direction at the unidirectional drift velocity, v_d, so that after a time, t, it has moved a distance $v_d t$ into the gap. It is assumed for the present that the electrons attain this drift velocity immediately on entering the gap. In the next chapter of this thesis, the processes by which they reach this steady velocity during the first few instances of their lifetime in the gap are discussed in greater detail.

For a given set of conditions (E_u, E_{dc} and p) circles are drawn for successive suitable time intervals to represent graphically the diffusion sphere moving through the gap in hydrogen, and increasing in radius with time. (See Fig. 7.1).

The drift velocity is calculated from $v_d = \mu E_{dc}$ where μ is the electron mobility in the combined dc and uhf fields. (See Appendix 3).

The diffusion coefficient, D, is calculated from $D = 0.92 \lambda \bar{c}/3$, (Townsend[5]), where $\bar{c}$ is the electron random velocity, and λ is the mean-free-path between collisions of electrons with gas molecules in the combined fields. The quantities D and v_d are calculated using Townsend's data[5] for hydrogen. Since the aim here is to obtain only an approximate picture of the electron behaviour in the gap, these data, although obtained in slightly impure gas, are considered accurate enough for this purpose.

-79-

A boundary may be drawn at a distance x from the emitting electrode such that electrons which have crossed this can no longer return to the emitting electrode by back diffusion, but become influenced mainly be drift.

When the centre of the sphere reaches this boundary, the sphere just ceases to intersect the electrode surface. If this occurs at time $t = T$,

$$x = v_d T = \mu E_{dc} T \, . \qquad \ldots \ 7.1$$

and

$$x = (12DT/\pi)^{1/2} \qquad \ldots \ 7.2$$

From Eqs. 7.1 and 7.2, eliminating T,

$$x = 12D/(\pi \mu E_{dc}) \qquad \ldots \ 7.3$$

i.e. $x = 3.8 \, D/\mu E_{dc}$.

It is postulated that for drift to be the overall controlling electron loss process, x is very much less than the gap width, d.

Then, $\qquad d \gg 3.8 \, D/\mu E_{dc} \qquad \ldots \ 7.4$

This criterion holds provided that when the diffusion sphere has moved clear of the emitting electrode, an electron on its surface will no longer have a velocity in the direction that would return it to the emitting electrode. In other words, the velocity of the rear boundary of the sphere with respect to the centre must be at least balanced by the velocity with which the centre is advancing through the gap.

The velocity of the rear boundary of the sphere relative to the centre of the sphere is dr/dt, where

$$r = (12Dt/\pi)^{1/2}$$

Then, $dr/dt = (3D/\pi t)^{1/2}$

which decreases continuously as t is increased.

An electron on the boundary of the sphere finally ceases to move towards the emitting electrode when

$$v_d \geq dr/dt$$

$$\text{or, } \mu E_{dc} \geq (3D/\pi t)^{1/2}$$

$$\text{or, } t \geq 3D/\pi \mu^2 E_{dc}^2 \qquad \dots \quad 7.5$$

Therefore when the centre of the sphere has advanced into the gap further than the distance $3D/\pi\mu E_{dc}$, electrons on the boundary can no longer have a component of velocity towards the emitting electrode. This is smaller than the distance at which the sphere just ceases to intersect the electrode. Therefore the over-riding criterion for which electrons on the average can no longer be lost by back diffusion is given by Eq. 7.4.

1.2 Electron lifetimes in the gap as limited by drift and diffusion

It is of interest to discuss the relative importances of diffusion and drift in terms of the electron lifetime in the gap. The problem of the electron lifetime in a gap subjected to the combined dc and uhf fields has already been treated by Varnerin and Brown[13]. However in the present attempt to obtain a simple comparison between the two processes, we choose to consider drift and diffusion separately.

Let the time for an electron to be removed from the gap by pure diffusion be t_D.

Then, $$t_D = \Lambda^2/D \qquad \dots \quad 7.6$$
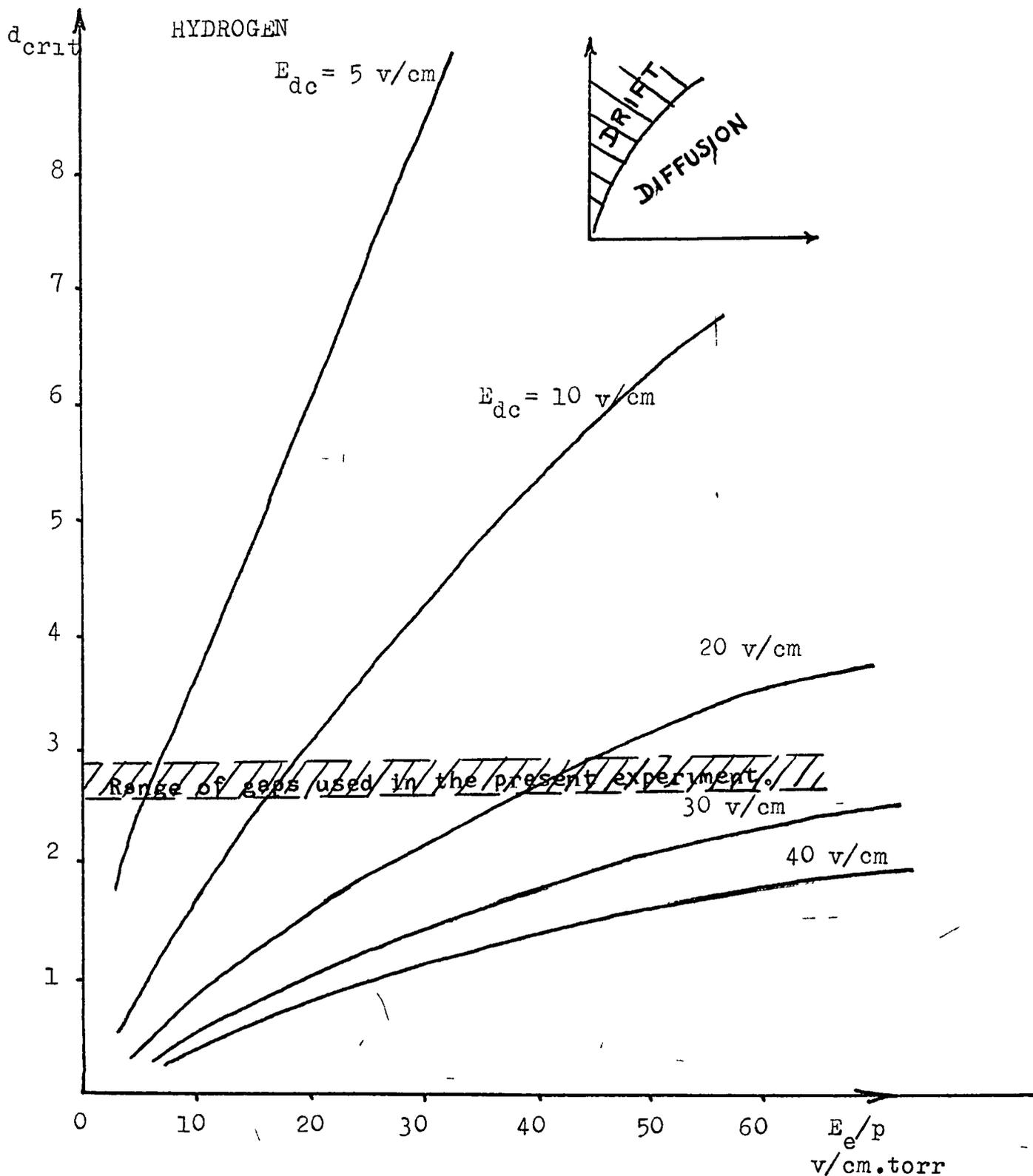
Fig 7.2. Gap width at which drift takes over from diffusion as the controlling electron loss process.

where $1/\Lambda^2 = (\pi/d)^2 + (2.405/a)^2$, from Herlin and Brown[10] and where $\underline{a}$ is the electrode radius.

Let the time for an electron to be removed from the gap by pure drift be t_T.

Then, $\qquad t_T = d/v_d,$ $\qquad$ where $v_d = \mu E_{dc}.$ $\qquad$ 7.7

When drift is the predominant removal mechanism, $t_D > t_T$.

When diffusion is the predominant removal mechanism, $t_T > t_D$.

In the critical case where drift and diffusion are equally important, $t_D = t_T.$

Then, from Esq. 7.6 and 7.7, $\quad \Lambda^2/D = d/\mu E_{dc}$

$\qquad$ or, $\quad d^2/D\oint = d/\mu E_{dc},$ where $\quad = \pi^2 + (2.405d/a)^2$

Therefore, $\qquad\qquad d_{crit} = \oint (D/\mu)(1/E_{dc}) \qquad\qquad$ 7.8

where d_{crit} is the critical gap width, for a given E_u, E_{dc} and gas pressure, at which drift takes over from diffusion as the controlling electron removal process, and vice-versa.

and $10.5 \leq \oint \leq 15.7$ for the range of gap widths $a/3 \leq d \leq a$.

Therefore for drift to be the controlling electron removal mechanism,

$$ d > \oint (D/\mu)(1/E_{dc}) \qquad\qquad .... 7.9 $$

Values of D/μ for hydrogen are obtained from the data of Varnerin and Brown[13].

d_{crit} is estimated as a function of E_e/p, where $E_e^2 = E_u^2 + E_{dc}^2$, and a family of curves is plotted for a range of E_{dc}. (See Fig. 7.2). Drift is expected to be the predominant electron removal mechanism within the

shaded area of the graph.

1.3 Summary of the conditions for which drift is the controlling electron removal mechanism in the gap

Summarising the findings of the previous two paragraphs, it is seen that drift is the controlling electron loss process when

a) $d \gg 3.8 \, (D/\mu)(1/E_{dc})$ from the diffusion spheres approach,

and, b) $d > \phi(D/\mu)(1/E_{dc})$, where $10.5 \leq \phi \leq 15.7$ for $a/3 \leq d \leq a$, from the electron lifetimes approach.

The assumptions in both cases are that

i) Diffusion and drift may be treated independently provided that the random velocity is considerably greater than the electron drift velocity,

ii) All electrons start out from a point on the surface of the emitting electrode,

iii) There is no ionization in the gas,

and iv) The electron ambit in a half cycle of the uhf field is small compared to the gap width.

The two expressions a) and b) are seen to be similar in form, and of the same order of magnitude within the limits of the initial assumptions. It must be emphasised that they are intended to give only a picture of the way in which the character of the electron flow changes with the various gap conditions, and are not expected to be more than approximate.

The expressions obtained may be related to actual experimental gap conditions. The curves relating d_{crit} with E_e/p for hydrogen (See Fig. 7.2) are used to decide, for a given set of d, E_{dc} and E_e/p, whether

$$\frac{t_D}{t_B} \neq \left(\frac{D}{u}\right)^2 \cdot \frac{u}{dE_d}$$

$$\frac{(volt)^2}{1} \quad \frac{1}{volts}$$

$$\frac{t_D}{t_B} \approx \frac{D}{u} \cdot \frac{1}{dE_d}$$

$$\text{cm sec}^{-1} \text{ volt}^{-1} \text{ cm}^{-1}$$

Take hydrogen $\quad \dfrac{E_a}{p} = 20.$

$\qquad\qquad\qquad\qquad E_d = 7.6$

$$\left(\frac{u}{D}\right)^2 = 20342_1$$

$$\frac{D}{u} = 1.71 \; ev$$

$$dE_d = 2.6 \times 7.6$$

$$\therefore \frac{t_D}{t_B} = \frac{\text{time of back diffusion}}{\text{drift time}}$$

$$\overline{z} = \frac{1.71}{2.6 \times 7.6} = .086 = \frac{1}{11.6}$$

During this time one new electron/electron must be produced. Thus if the ordinary (mixed field) avalanche has a multiplication of 11.6, the result is a self-maintaining discharge.

A

1

.8

.6

$E_{dc} = 3.78$ v/cm

18.9 v/cm   15.12 v/cm   11.34 v/cm

7.56 v/cm

HYDROGEN

d = 2.64 cm

p = 0.5 torr

—— Diffusion control
---- Drift control
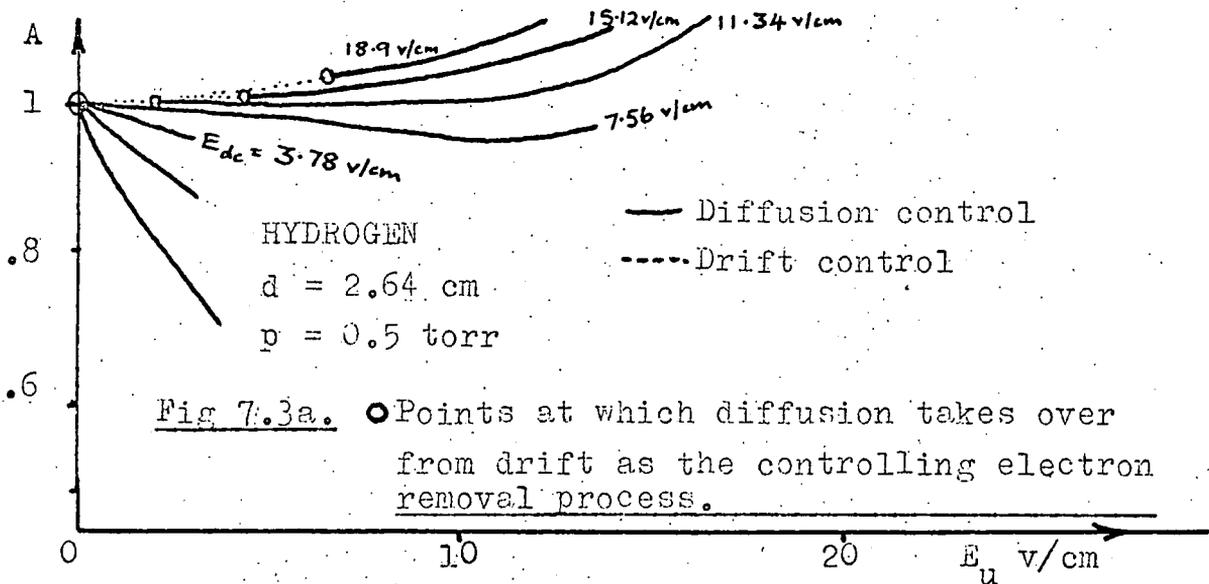
Fig 7.3a. ○ Points at which diffusion takes over
from drift as the controlling electron
removal process.

0   10   20 E_u v/cm

A
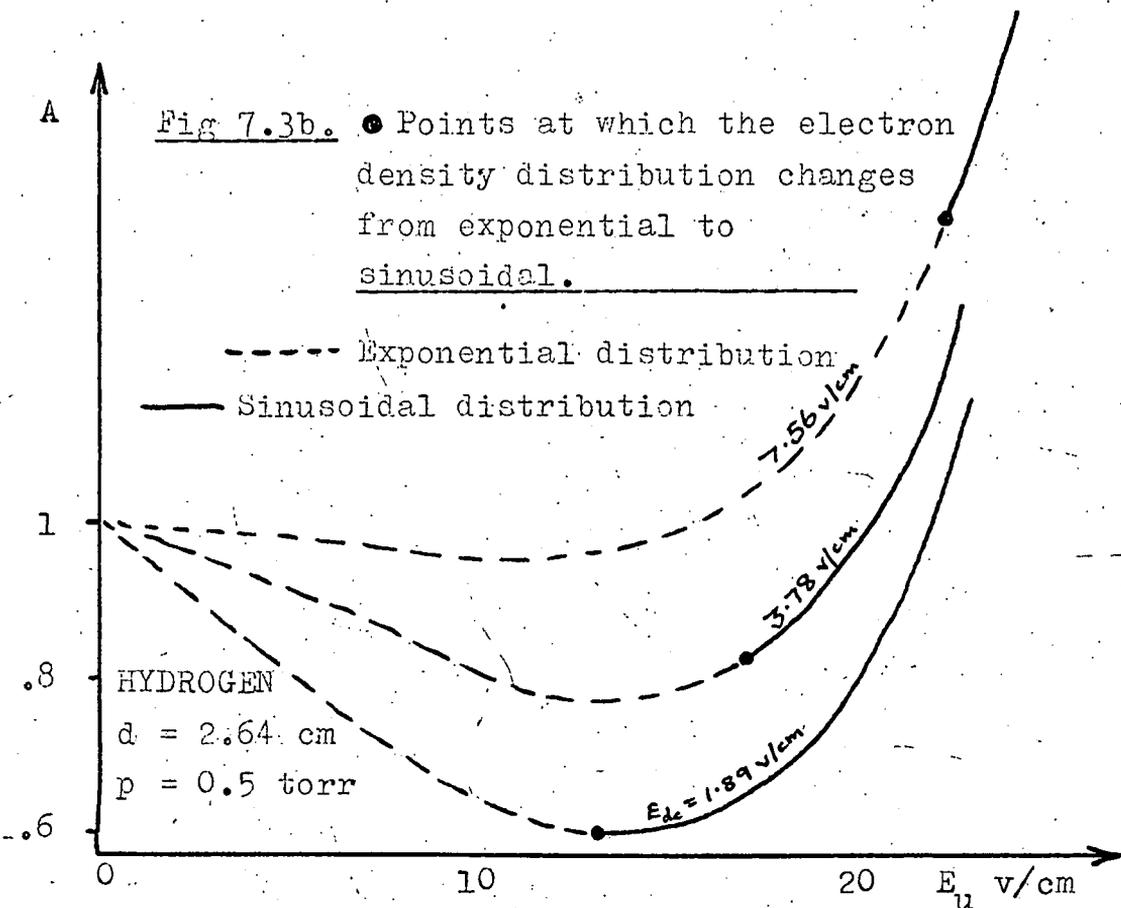
Fig 7.3b. ● Points at which the electron
density distribution changes
from exponential to
sinusoidal.

----- Exponential distribution
—— Sinusoidal distribution

7.56 v/cm

3.78 v/cm

$E_{dc} = 1.89$ v/cm

1

.8

HYDROGEN

d = 2.64 cm

p = 0.5 torr

.6

0   10   20 E_u v/cm

diffusion or drift should predominate.

Fig. (1); $d = 3$ cm, $E_{dc} = 20$ v/cm.

Drift predominates for $E_e/p < 45$ v/cm/torr.

Fig. (2); $d = 2$ cm, $E_{dc} = 20$ v/cm.

Drift predominates for $E_e/p < 25$ v/cm/torr.

Fig. (3); $d = 2$ cm, $E_{dc} = 5$ v/cm.

Drift predominates for $E_e/p < 3$ v/cm/torr.

1.4 Application of drift and diffusion theory to the experimental measurements

In the amplification curves described in Chapter 4, it is seen that drift should be the predominant electron loss process at low values of E_u and that diffusion should take over at higher values, depending on E_{dc}, the gap width, and the gas pressure. The change-over points are shown on some typical amplification curves in Fig. 7.3a. It is seen for very low values of E_{dc} that drift is not at any time predominant, even for zero E_u. This is sensible since there is a minimum value of E_{dc} below which even the thermal energy of the electrons is sufficient to make diffusion the controlling loss process. Eventually, however, at quite moderate values of E_{dc}, a drift controlled region in the curve does not appear. There appears to be no change in the shape of the curve near the change-over point between the two loss processes. For a given pressure, as E_{dc} is increased, the point at which diffusion takes over is pushed steadily nearer to breakdown. It is of interest to examine the conditions of diffusion and drift at breakdown.
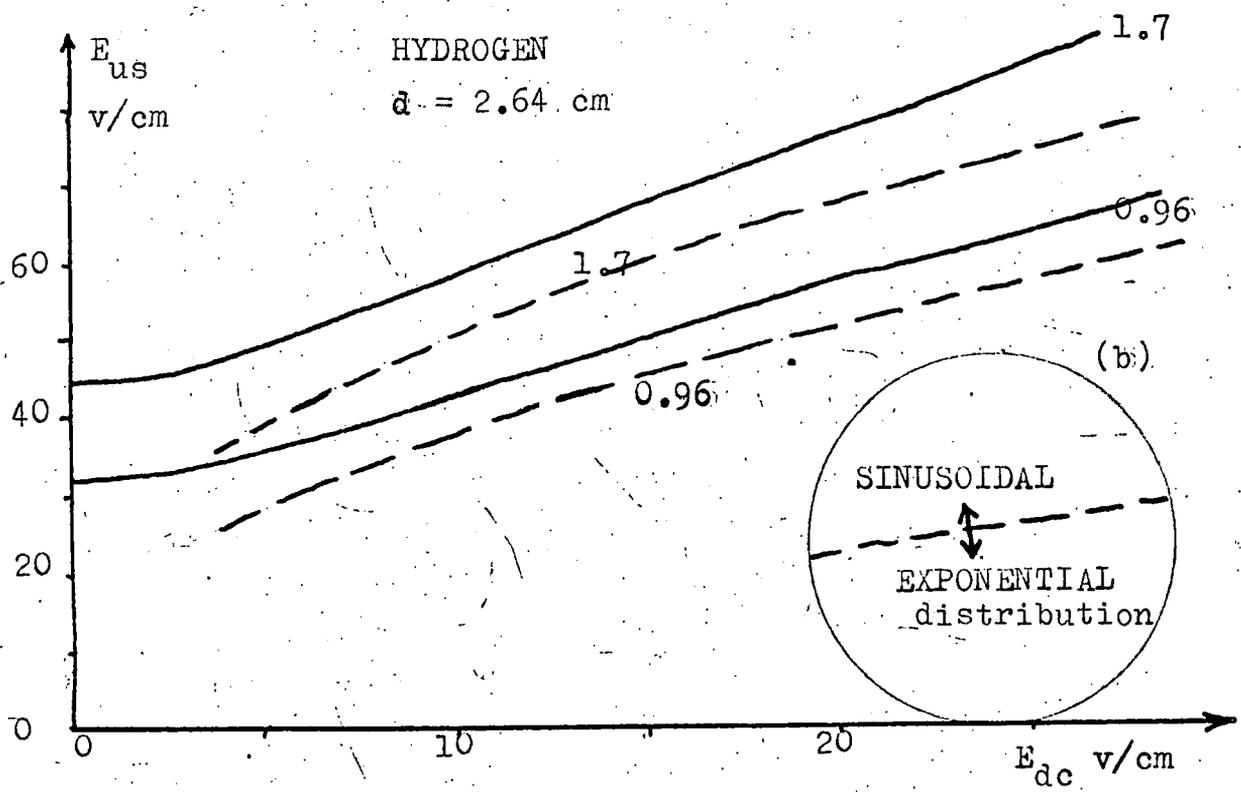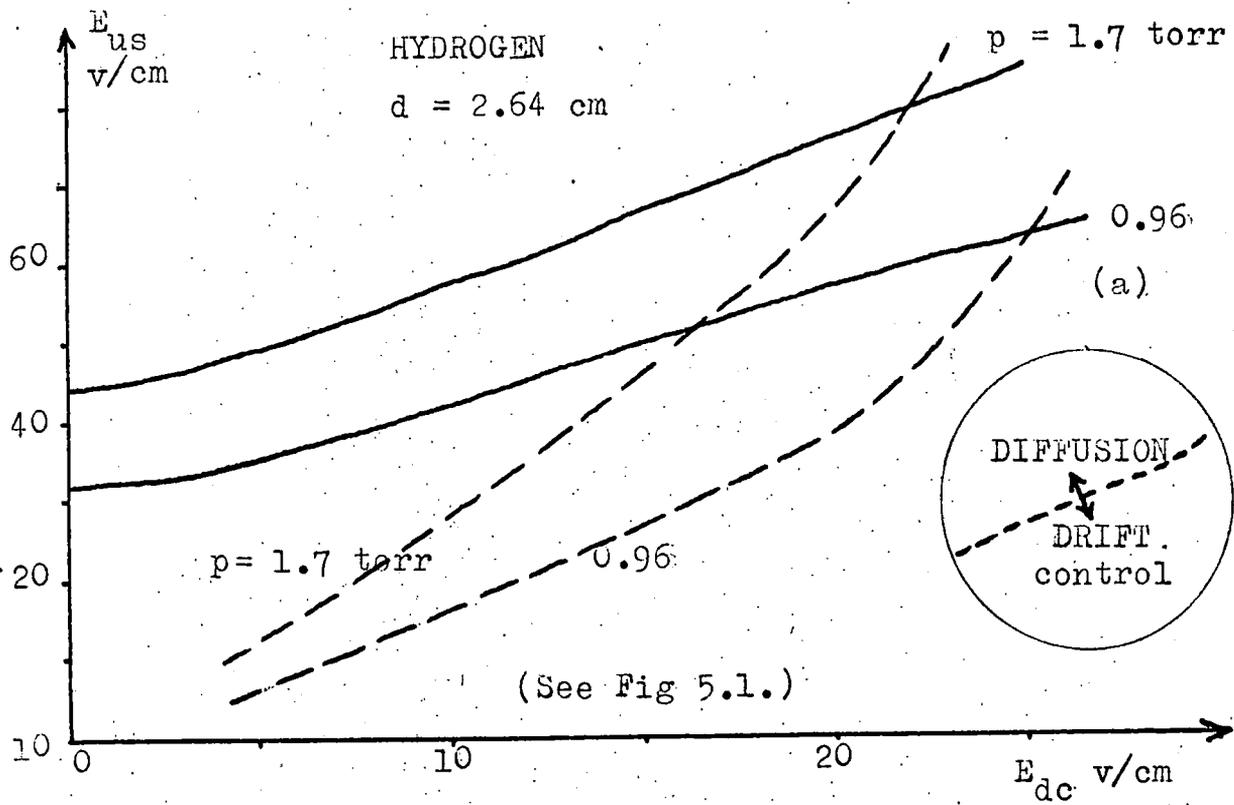
Fig 7.4. Investigation into the conditions at breakdown
in the combined dc and uhf fields.

Typical experimental curves are plotted showing the variation
of the uhf breakdown field as a function of E_{dc} in hydrogen. (From Fig.
5.1). On the same graph is plotted the uhf field at which diffusion
should take over from drift as the predominant electron removal mechanism,
also as a function of E_{dc}, for the same gap width and gas pressures.
(See Fig. 7.4a). It is seen that at low values of E_{dc}, diffusion is
the controlling loss process at breakdown. But, rather surprisingly,
(in view of the fact that the breakdown is controlled by the uhf field),
drift emerges as the controlling loss process at higher values of E_{dc}.
Despite the uncertainty involved in these particular experimental break-
down measurements (See Chapter 5, § 2) this trend is very clear.

It must be remembered that the condition for which drift and diffusion
are equally important is calculated only for electrons which start out
from the emitting electrode, and drift across the whole gap. But at
higher values of E_e/p, where multiplication is occurring in the electron
stream, many electrons which are lost by drift do not have to travel
the full gap width. In fact at low amplifications, from Townsend's
picture of the electron avalanche, most of the new electrons are created
in a region close to the collecting electrode. In this case, these
electrons are even more strongly influenced by drift than those which
start off initially. At very high values of amplification, where the
electron density distribution is almost sinusoidal in form, the centre
of the gap may now be regarded as the source. This being so, most of
the electrons which drift to the collecting electrode only need to travel
approximately half the gap width. The net effect of these considerations

is to increase the overall effect of drift to greater than that pre-
dicted by the simple theory given in §1.1, 1.2 and 1.3.   This effect
is indicated in Fig. 7.4a.   (See dotted curve).

2.   The electron density distribution in the gap

Closely related to what has gone before is the consideration of
the electron density distribution in the gap Long[2] has discussed
the conditions under which the electron density distribution in combined
dc and uhf fields changes from exponential at low ionization to sinusoidal
at higher ionization.   If electrons start off from a point on the emit-
ting electrode, and ionization in the gap is small, there is an exponen-
tial rise in electron density across the gap (from the simple picture of
the electron avalanche given by Townsend). This is the case provided
that the emitting electrode remains the main source of electrons.   But
at higher levels of ionization, when the rate of ionization in the gap
is considerably greater than the rate of supply from the emitting electrode,
the gap itself now becomes the predominant source of electrons.   The
density distribution now takes a sinusoidal form, deformed exponentially
as a result of drift.

For breakdown in a cylindrical gap and with no injected electrons,
Varnerin and Brown[13] showed that the electron density distribution is
given by
$$n = B. e^{\theta z}.\sin((\pi/d)z).\ J_0(k_1\rho) \qquad \dots \quad 7.10$$
where z is the axial and ρ the radial coordinate in space. k_1 is a
function of the electrode radius, J_0 is the zero order Bessel function

resulting from the consideration of radial diffusion, and $\theta = E_{dc}/2(D/\mu)$. Therefore in the present experiments where the rise to breakdown is controlled by the uhf field, it is concluded that the electron density distribution in the gap should become sinusoidal at breakdown. The conditions under which the distribution changes from exponential to sinusoidal are now discussed.

In the simple case, neglecting attachment, recombination and secondary electron generation effects, the scalar electron density is written as a function of drift, diffusion and ionization[2], thus:-

$$\nabla^2 n - 2\theta \cdot \partial n/\partial z + (\psi/D) \cdot n = 0 \qquad \qquad \dots \ 7.11$$

Drift, being controlled mainly be E_{dc}, is thus asymmetrical in space, being a function only of z. In order to transform this term into a symmetrical space function, the transform $n = U e^{\theta z}$ is applied. Thus Eq. 7.11 becomes

$$\nabla^2 U - \frac{\nu^2}{D} \cdot U = 0 \qquad \qquad \dots \ 7.12$$

where $\frac{\nu^2}{D} = \theta^2 - \psi/D$.

The solution of this equation gives the electron density in the gap in 'U-space', which essentially will be of the same form in real space. When $\nu^2/D > 0$, the electron density distribution in the gap in U-space, and also in real space, is exponential, becoming sinusoidal when $\nu^2/D < 0$. Thus, when $\nu^2/D = 0$, a critical condition is reached at which the electron density distribution changes from one form to the other.

Then, $$\theta^2 = \psi/D \qquad \qquad \dots \ 7.13$$

also we have, $$\psi = W\alpha \qquad \qquad \dots \ 7.14$$
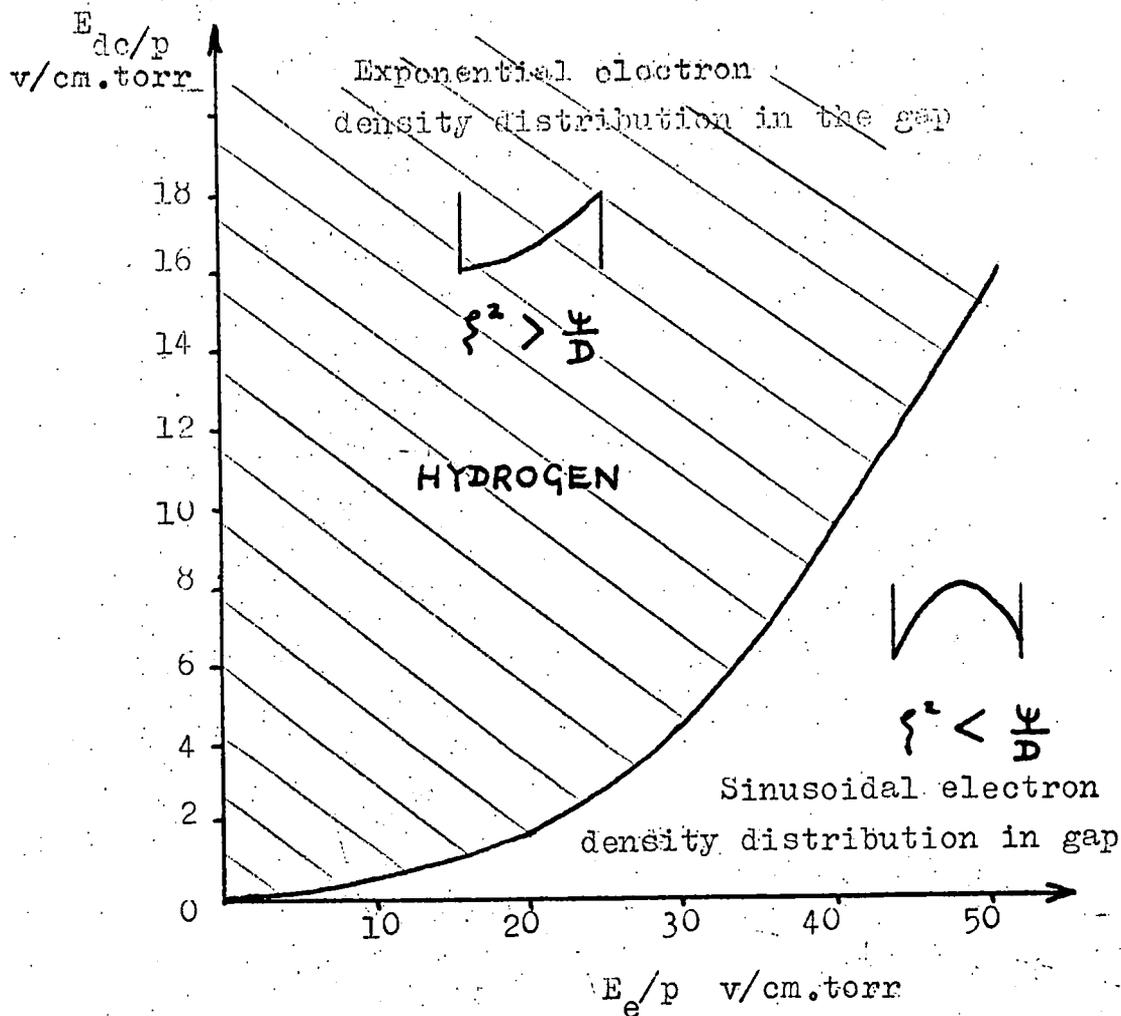
Fig 7.5. Conditions for which the electron density distribution in the gap changes from exponential to sinusoidal.

Values of D/μ from Varnerin and Brown[13].
Values of α/p from Chapter 5 of this thesis.

where ψ is the ionization rate, and W is the effective electron drift velocity in the combined fields.

Also, $\qquad W = \mu E_e \qquad\qquad$ 7.15

where μ is the electron mobility in the combined fields, and E_e is the effective field given by $E_e^2 = E_u^2 + E_{dc}^2$. (See Appendix 4).

Then, from Eqs. 7.13, 7.14 and 7.15,

$$\left(\frac{E_{dc}}{p}\right)^2 \cdot = \frac{\alpha}{p} \cdot \frac{D}{\mu} \cdot \frac{E_e}{p} \qquad\qquad \text{.... 7.16}$$

Therefore for a given value of E_e/p, the corresponding value of E_{dc}/p may be calculated at which the change-over in the form of the electron density distribution should occur. This is illustrated for hydrogen in Fig. 7.5. Values of D/μ are obtained from the data of Varnerin and Brown[13], and values of α/p from the data obtained from the breakdown measurements described in Chapter 5 of this thesis. The curve thus obtained relating E_{dc}/p and E_e/p divides the graph into two regions, one in which the electron density distribution is exponential (shaded portion), and the other in which it is sinusoidal.

2.1 Application of the electron density distribution considerations to the experimental measurements

As in the case of diffusion and drift, the amplification curve may be again divided into two regions, one in which the electron density distribution in the gap is exponential, and the other in which it is sinusoidal. The change-over points are marked on some typical experimental amplification curves in Fig. 7.3b. For all values of E_{dc}, the distribution is exponential at low E_u, becoming sinusoidal at higher

values. The change-over point moves steadily closer to breakdown as E_{dc} is increased. Once again it is of interest to examine the conditions at breakdown.

On the same graph as the typical curves relating the uhf breakdown field with E_{dc} (See Fig. 7.4b) is plotted the variation of the uhf field for which the distribution changes from exponential to sinusoidal. The indications are clear that although the change-over point moves closer and closer to breakdown as E_{dc} is increased, the distribution always becomes sinusoidal at or before breakdown. This confirms the view taken by Varnerin and Brown[13], (See Eq. 7.10) and does not fail within the range of E_{dc} examined.

3. **Comments**

There does not appear to be a direct simple relationship between the change-over from drift to diffusion controlled electron loss and the change-over from the exponential to the sinusoidal electron density distribution in the gap. A more rigorous mathematical treatment than has been performed here is required if such a relationship is to be found.

This study, although it has not gone very far towards helping to explain the shape of the amplification curves, has yielded some interesting general information about the behaviour of electron swarms subjected to the combined uhf and dc fields.

THEORETICAL PREDICTIONS FOR THE SHAPE OF THE AMPLIFICATION CURVE

1. Inspection of Long's expression for Amplification

Of the theories so far produced to explain the shape of the amplification curves[1,2,26,29], neither was tested sufficiently to enable any definite conclusions to be drawn as to their validity. The theory put forward by Long[2,29] based on the Huxley theory for lateral diffusion of carriers in a gas subjected to an electric field[19], is the more rigorous and agreement with the experimental results in the limited range of conditions that he examined was encouraging. As described in Chapter 4, experimental amplification curves have since been obtained for a comprehensive range of gap conditions and these form the basis of a thorough inspection of this theory.

Long's expression for amplification when ionization occurs in the gap is given by (See Chapter 2, Eqs. 2.15, 2.16 and 2.17)

$$A = \frac{(1 + \frac{d}{2b} e^{-\theta_1 b})}{(1 - \frac{d}{2}(\theta + \ell)(1 - e^{-(\theta - \ell)d}) + \frac{d}{2b} e^{-\ell b} e^{-(\theta - \ell)d})} \quad \dots \text{ 8.1}$$

where $\ell = (\theta^2 - \frac{\psi}{D})^{1/2}$, $2\theta = \frac{E_{dc}\mu}{D}$, d is the electrode spacing, and b is the radius of the emitting holes.

Clearly the calculation of a large number of theoretical amplification curves from this expression would be an extremely laborious process, and a computer programme was devised to enable the calculations to be more conveniently performed. Once the programme had been compiled, the

A

p=0.5 torr
E_{dc} = 1.89 v/cm
d = 2.64 cm
b = 0.0172 cm
HYDROGEN

0.5 torr
18.9 v/cm

0.97 torr
1.89 v/cm

0.97 torr
18.9 v/cm

1.5 torr
1.89 v/cm

1.5 torr
18.9 v/cm

4.5 torr
1.89 v/cm

4.5 torr
18.9 v/cm

E_u
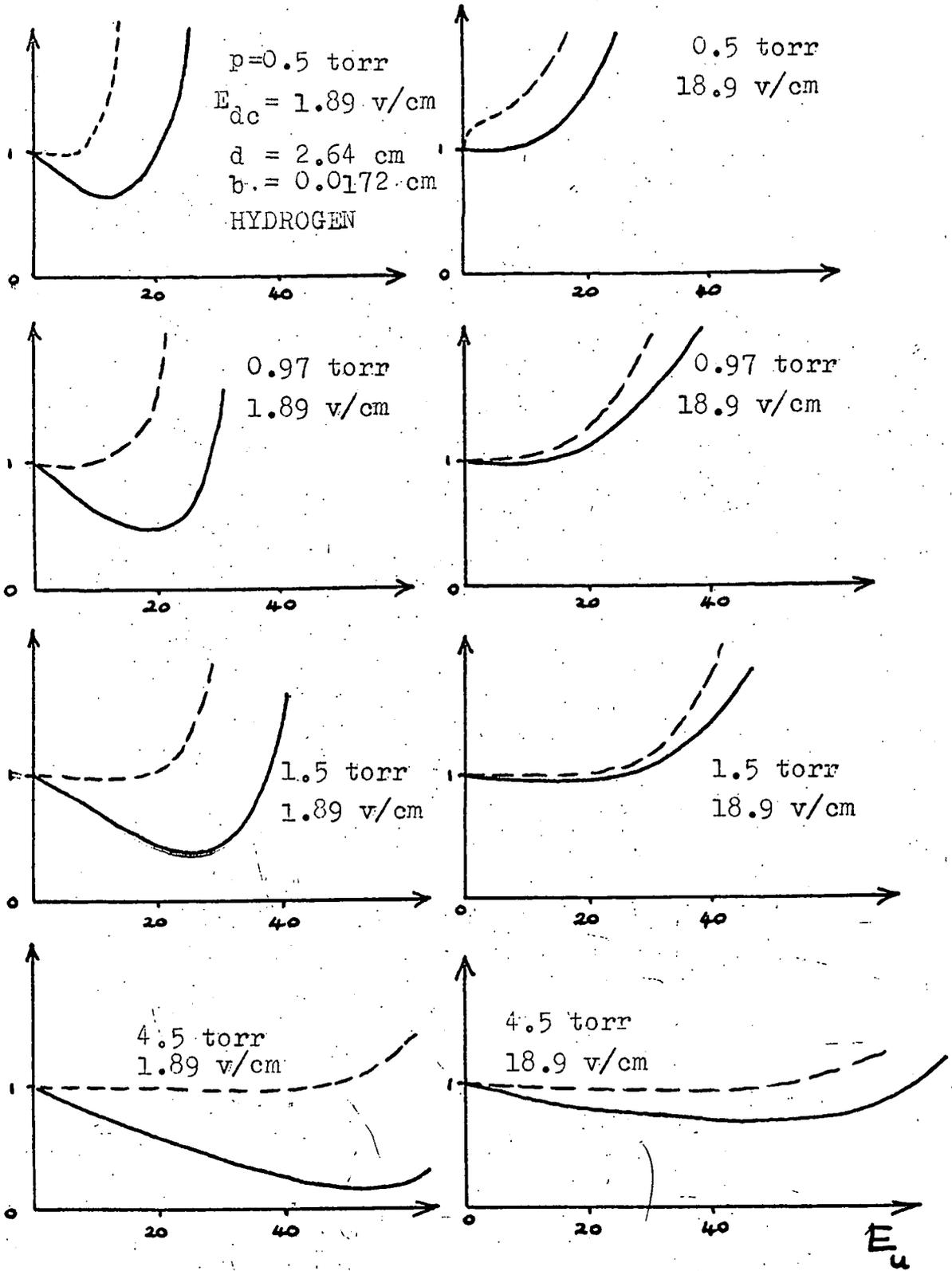
Fig 8.1. Comparison between calculated and experimental
amplification curves.
------ Calculated from Long's expression.(Eq 8.1)
——— Experimental (See Chapter 4)

operation was very quick, and fifty-four theoretical curves for hydrogen with over ten points on each curve were obtained within the space of one hour. Thus a comparison with the present experimental results over a wide range of conditions is possible (See Fig. 8.1). Values of D/μ were obtained from the data of Varnerin and Brown[13] and values of η from the data of Leiby[30].

The theory shows clearly the dip in the curve at low values of E_{dc}, and the eventual disappearance of the dip at higher values of E_{dc}. However the magnitude of the dip is not predicted accurately, the experimental dip being always considerably larger than the theoretical dip. The agreement is worst at low values of E_{dc}, improving slightly at higher values of E_{dc}. Also the rise to breakdown is less rapid in the experimental case.

It is therefore clear that the theory put forward by Long, although promising in many aspects, does not fully describe the processes occurring in the electron stream. It is therefore necessary to discuss the possible weaknesses in the theory. To do this, it suffices to consider Long's expression for amplification when no ionization occurs.

i.e. $$A = e^{-b(\theta_1 - \theta)} \qquad \dots\ 8.2$$

It can be seen from this that amplification contains a very strong dependence on the hole radius, b. It was this strong dependence that prompted the experiments in which amplification curves were obtained for different sets of hole dimensions. (See Chapter 6). These experiments show clearly that amplification is _not_ strongly dependent on the hole dimensions, and, in fact, show that there is no systematic variation in the shape of the curves with b. Therefore it appears that the presence

B cm

	E_c/P	P		E/P	P
	v/cm.torr	torr		v/cm.torr	torr
o	5	1	▲	10	3
+	"	2	▣	"	4
×	"	3	∅	12·5	1
△	"	4	θ	"	2
□	10	1	∝	"	3
●	"	2	β	"	4

HYDROGEN

d = 2.64 cm

E_{dc} v/cm.
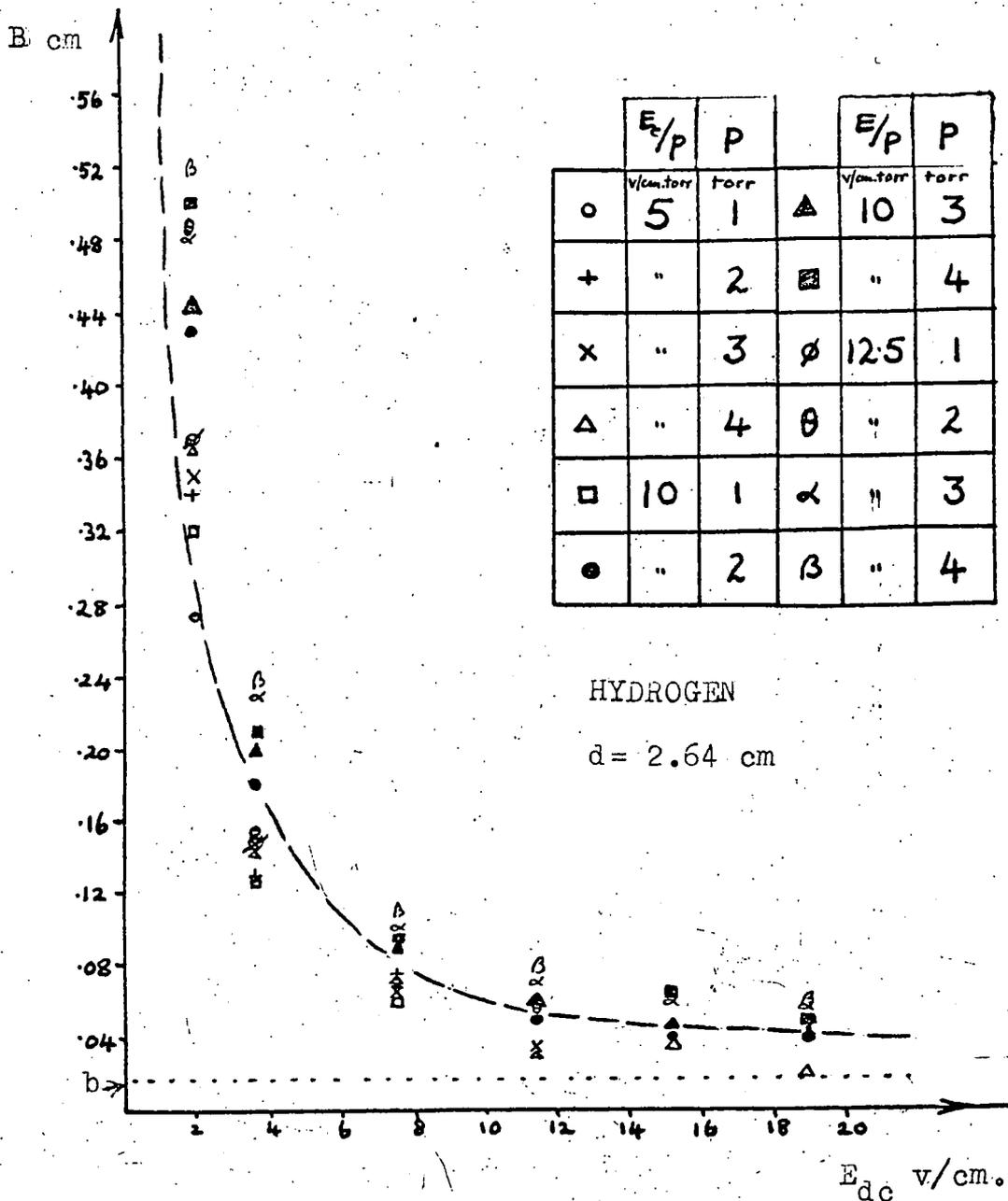
Fig 8.2. Values for the radius of the emitting
hole which would bring Long's expression
into agreement with experiment.
(No ionization).

of b in Long's expression for amplification is much overestimated.

It is of interest to examine the way in which b would need to vary in order to bring the theoretical and experimental amplification curves into agreement. The following test was performed for hydrogen. Using the present experimental results and values of D/μ obtained from Varnerin and Brown[13], the value of b required to make theory and experiment agree, say B, was calculated as a function of E_{dc} for various values of E_e/p below the onset of collision ionization. (See Fig. 8.2). The disagreement between the theoretical and the experimental results is clearly illustrated by these curves. At low values of E_{dc}, B is over an order of magnitude greater than the actual physical radius of the hole, decreasing steeply as E_{dc} is increased, tending to converge on the actual hole radius, b, at high values of E_{dc}. It is in this region that Long's expression gives the closest agreement with the experimental results. The calculations were performed for $E_e/p = 5$, 10 and 12.5 v/cm.torr, and for pressures, p = 1, 2, 3 and 4 torr, and it is seen that there is no systematic variation of B with E_e/p or p. Agreement between experiment and theory below the onset of ionization is therefore expected if we use the expression

$$A = e^{-B(\theta_1 - \theta)} \qquad \dots \quad 8.3$$

where B may be regarded as a 'virtual hole radius' which is a function of E_{dc}, but not of E_e/p or p.

This assumes that the rest of Long's argument is valid. However, attempts to derive a physical explanation for the quantity B have not been successful.

The hole radius is introduced into the expression for amplification (See Eq. 8.1) during the calculation of the current flowing back to the surface of the emitting electrode (See Chapter 2, p27). Huxley's original theory, on which Long's work was based, was derived partly to explain Townsend's measurements on the spread of a stream of electrons by the time they have reached the collecting electrode. At all times he considers conditions in which electrons are in equilibrium with the field in the gap, and that a steady state exists. This is a reasonable assumption close to the collecting electrode, provided that the gas pressure and gap width are large enough to enable electrons to suffer a sufficient number of collisions with gas molecules in the gap. This is _not_ so obviously true close to the emitting electrode, and Long's extension of Huxley's theory for the calculation of the current flowing back to the emitting electrode does not take into account the possibility that many of the electrons in the region close to the emitting electrode may not be in equilibrium with the field.

It would appear that there is no obvious simple modification that can be made to Long's expression for amplification in order to bring theory and experiment into agreement, and it might be advantageous to consider the possibility of another approach to find an explanation for the shape of the amplification curves.

2. A theoretical study of electron flow in the gap in the presence of diffusion, drift and ionization

Electrons entering the gap through the holes in the emitting electrode have a mean random energy which probably does not correspond to the

equilibrium value in the gap. These electrons come into equilibrium with the combined dc and uhf fields after suffering a number of collisions with gas molecules. By this time they will have advanced a certain finite distance into the gap under the influence of E_{dc}, while some, by virtue of their initial energy, may be 'reflected' (or 'back-scattered') back to the emitting electrode, and lost. Once the remaining electrons have come into equilibrium, they move and behave according to the steady state conditions in the gap. Some may still be lost by returning to the emitting electrode by diffusion in the steady state, but the rest will reach the collecting electrode (ignoring losses by radial diffusion) and so contribute to the unidirectional current flowing in the external gap circuit. If the effective field in the gap is high enough, collisions between electrons and gas molecules may produce ionization. Some of the new electrons generated near the emitting electrode may be lost by back diffusion, but the majority which are generated well out into the gap will flow to the collecting electrode, and so contribute to the unidirec-tional gap current, i_2.

So far we have considered a simple picture, in which the drift motion of the electrons is unidirectional, while the uhf field serves only to increase their random energy above that corresponding to just the pure dc field. However, electrons have superimposed on their random and dc drift motions a uhf component of drift. The main effect of this is to introduce into the loss processes at the emitting electrode a time dependence which periodically enhances and reduces these losses.
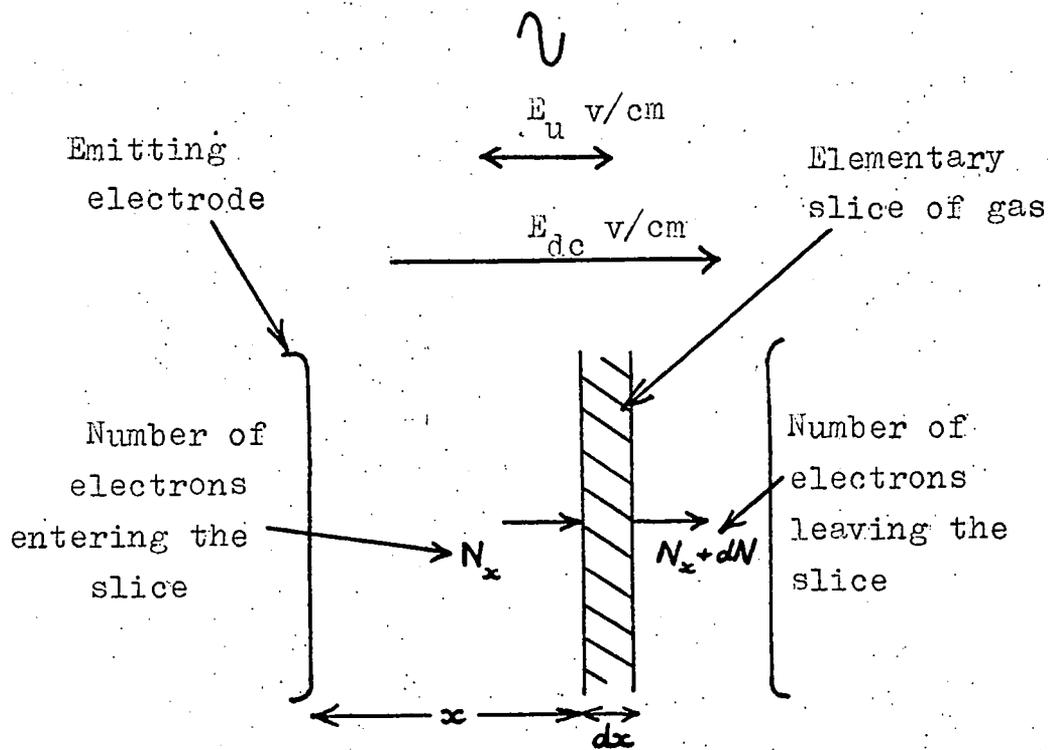
Fig 8.3. Diagram for the calculation of the number
of electrons lost and generated in an
elementary slice of gas in the gap.

$f(x,t)$

V_d

0

x

X

(a)

Surface area, a_b.

$(12Dt/\pi)^{1/2}$

Total surface area, a_t.

$p(t) = a_b/a_t$.

v_d

$\leftarrow v_d t \rightarrow$

Emitting electrode

DIFFUSION SPHERE

(b)

$p(t)$

.5

(c)

0

T

t secs
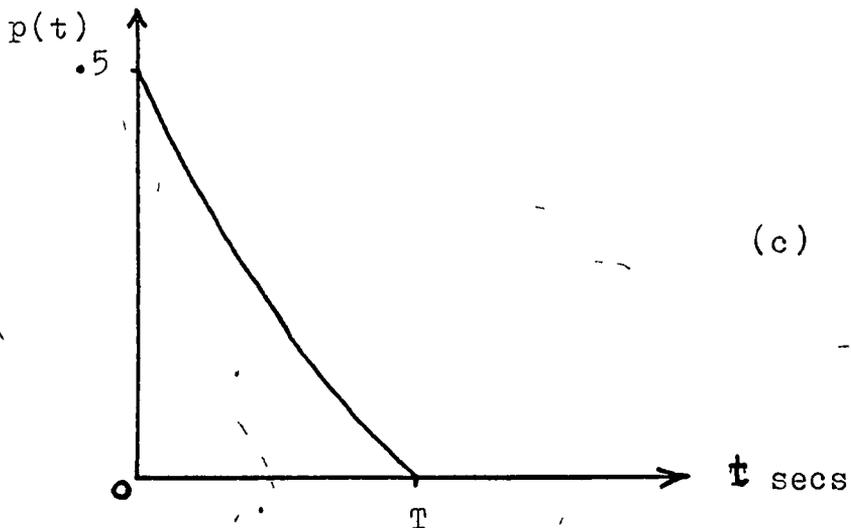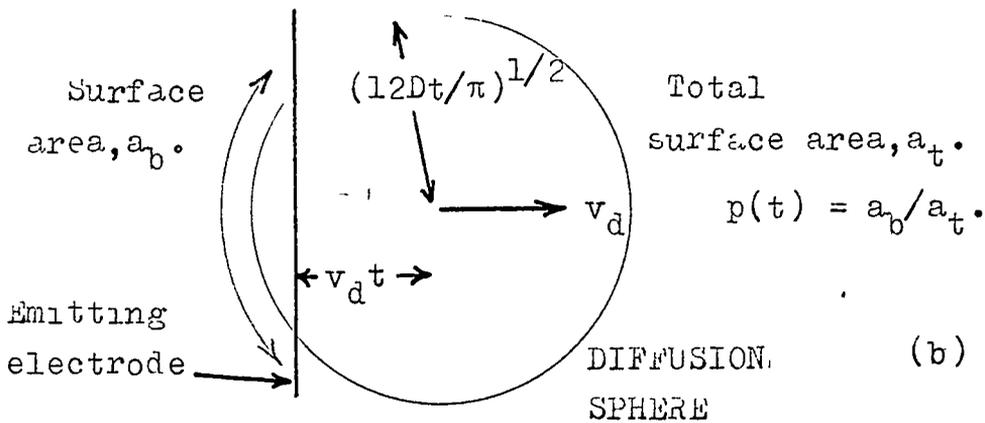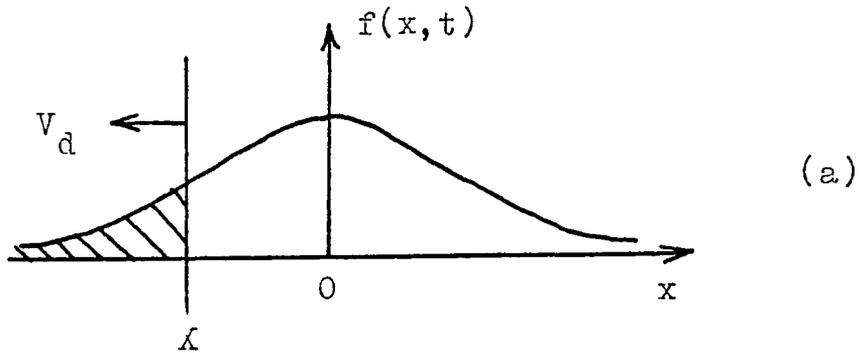
Fig 8.4. Diagrams for the calculation of losses of electrons by steady state back diffusion.

Consider the electron density distribution in coordinates of space and time. In one dimension this is given by the function f(x,t), where this is an error function of the type derived for diffusion by Einstein[15]. (See Fig. 8.4a).

The probability that an electron starting off at x = 0 at time t = 0 will have a position between x = X and x = -∞ at time, t, is given, provided that f(x,t) is continuous in x and t, by

$$\frac{\int_{-\infty}^{X} f(x,t)\ dx}{\int_{-\infty}^{+\infty} f(x,t)\ dx} \qquad \dots \quad 8.5$$

where the denominator of this expression serves to normalise the expression to unity. This means that if X = +∞, the electron will have unit probability of being within the region considered. The position x = X may be considered as a boundary such that all electrons which enter the range X to -∞ are lost to that boundary.

Then Eq. 8.5 expresses the instantaneous probability that an electron will be lost at time t.

Now let the position of the boundary x = X also be varying continuously with time and consider a small change in X, dX.

If the probability of an electron being in the region x = X to x = -∞ , given by Eq. 8.5 does not vary appreciably as X changes by dX, then the probability that an electron will be removed during the interval in which X is changing is given by

$$\frac{(\ \int_{-\infty}^{X} f(x,t)\ dx)\ dX}{\int_{-\infty}^{+\infty}(\ \int_{-\infty}^{+\infty} f(x,t)\ dx)\ dX} \qquad \dots \quad 8.6$$

where once again the denominator serves to normalise the expression to
unity, this time taking into account all possible positions of the
boundary $x = X$. Then the total probability that an electron will be re-
moved while X changes from 0 to $-\infty$ is given by

$$\frac{\int_0^{-\infty} \int_{-\infty}^{X} f(x,t) \, dx \, dX}{\int_{-\infty}^{+\infty} \int_{-\infty}^{+\infty} f(x,t) \, dx \, dX} \qquad \dots \quad 8.7$$

And if we substitute $X = v_d t$, assuming that the boundary is moving with
a velocity v_d in the direction of x negative, Eq. 8.7 becomes

$$\frac{\int_0^{+\infty} \int_{-\infty}^{v_d t} f(x,t) \, dx \, dt}{2 \int_0^{+\infty} \int_{-\infty}^{+\infty} f(x,t) \, dx \, dt} \qquad \dots \quad 8.8$$

This represents the probability in the one-dimensional case that an electron
starting off from a point $x = 0$ will be lost to the boundary which is
receding from $x = 0$ at a velocity v_d. In the present experimental case
we must consider the three-dimensional spacial distribution of electrons,
but using the above rigorous approach, this presents severe mathematical
problems. However, these may be simplified considerably by considering
the fate of the average electron. To do this we refer back to the spheres
of diffusion. (See Chapter 7). In form the approach is the same as that
just described, except that it is now more convenient to consider the
boundary as fixed, and the centre of the electron density distribution
function moving through the gas with a velocity v_d in the direction of x
positive.

The average electron after a time, t, will lie on the surface of a

sphere of radius $(12Dt/\pi)^{1/2}$, the centre of which is moving through the gas with a velocity v_d. It is seen that the sphere is continuously in contact with the electrode until a time T given by

$$T = 12D/\pi v_d^2 \qquad \qquad \text{.... 8.9}$$

after which it does not intersect with the emitting electrode again.

At a time, t, using analogy with the previous argument, the instantaneous probability that an electron will be removed by back diffusion is the ratio between the surface area of the sphere intersected by the emitting electrode to the total surface area of the sphere. (See Fig. 8.4b and 8.4c)

$$\text{i.e.} \quad p(t) = a_b/a_t$$

It may be shown that this is

$$p(t) = (r - x)/2r \qquad \qquad \text{.... 8.10}$$

where x is the distance now that the centre of the sphere has advanced through the gap after a time, t.

(Eq. 8.10 is directly analogous to Eq. 8.5).

More precisely, this should be written as $\dfrac{p(t)}{p(t) + q(t)}$ where the denominator normalises the expression to unity over all possible conditions, and q(t) is the instantaneous probability at time, t, that the electron will survive in the gap.

Trivially, $p(t) + q(t) = 1$

By analogy with Eq. 8.6, the probability that an electron will be removed by back diffusion in a time interval dt, provided that dt is small enough, is given by

$$\frac{p(t) \, dt}{\int_o^T (p(t) + q(t)) \, dt} \qquad \qquad \text{.... 8.11}$$

where T is the total time during which the sphere is in contact with the emitting electrode. It is noted that this finite time replaces the infinite time over which the integral must be performed in the more rigorous case, but this is a result of considering only the average electron. Once again, by analogy with the more rigorous case, the total overall probability that an electron will be removed from the gap by back diffusion is given by

$$P_r = \frac{\int_o^T p(t) \, dt}{\int_o^T (p(t) + q(t)) dt}$$

$$= \frac{\int_o^T p(t) \, dt}{T} \qquad \qquad \text{.... 8.12}$$

From Eq. 8.10, $p(t) = (r - x)/2r$

$$= \frac{1}{2} - \frac{1}{2} \, v_d (\pi/12D)^{1/2} \, t^{1/2}$$

Therefore, $P_r = \frac{1}{2} - \frac{1}{3} \, v_d (\pi/12D)^{1/2} \, T^{1/2}$

And substituting for T from Eq. 8.9,

$$P_r = \frac{1}{6} \qquad \qquad \text{.... 8.13}$$

In the absence of a dc field, the diffusion sphere does not advance through the gap, and all of the electrons in the swarm starting off from the emitting electrode will be lost the emitting electrode except for the few that might diffuse to the collecting electrode. This possibility does not appear in the above solution because when E_{dc} is zero, T becomes infinite, and the analysis is meaningless. Therefore the condition must be added that E_{dc} must take finite values.

The discovery that the probability of back diffusion loss is constant,

independent of the fields in the gap, is at first surprising, since, for a given E_{dc}, we might expect the loss to increase as the random energy of the electrons is increased. However it is fair to say that as the random energy, hence the diffusion coefficient, is increased, the increased chance of loss by back diffusion is balanced by the increased chance of escape, and the net result, given by Eq. 8.13, that back diffusion loss is independent of the electron energy is not outrageous.

Now referring back to the elementary slice of gas considered initially (See Fig. 8.3), for N_x electrons entering, the number lost by back diffusion is

$$dN_B \ = \ N_x \ p(t) \ dt \ / \ T \qquad \dots 8.14$$

Then from Eqs. 8.4 and 8.14, the net electron gain is

$$dN \ = \ dN_i \ - \ dN_B$$

$$= \ N_x \ (\ \psi \ dt \ - \ \frac{p(t) \ dt}{T}) \qquad \dots 8.15$$

The total gain over the whole gap is obtained by integrating the ionization term over the average lifetime of the electrons in the gap (τ) and the back diffusion term over the time during which the diffusion sphere is in contact with the emitting electrode (T).

Then, $$\int_{N_o}^{N} \frac{dN}{N_x} \ = \ \psi \int_0^\tau dt \ - \ \int_0^T \frac{p(t) \ dt}{T} \qquad \text{provided that}$$
$$\gg T$$

Whence, $$N = N_o \ e^{(\psi\tau \ - \ \frac{1}{6})} \qquad \dots 8.16$$

where N_o is the number of electrons which start off into the gap (in this case representing those which survive in the gap long enough to come into equilibrium) and N is the number arriving at the collecting electrode. This leads to, $$i = i_o e^{(\psi\tau \ -1/6)} \qquad \dots 8.17$$
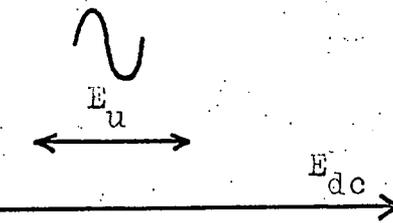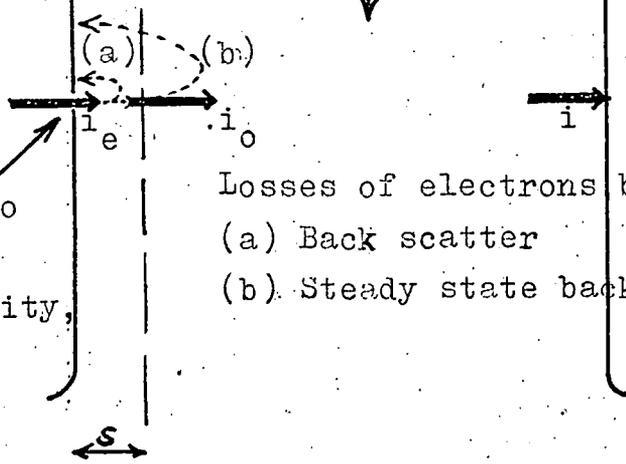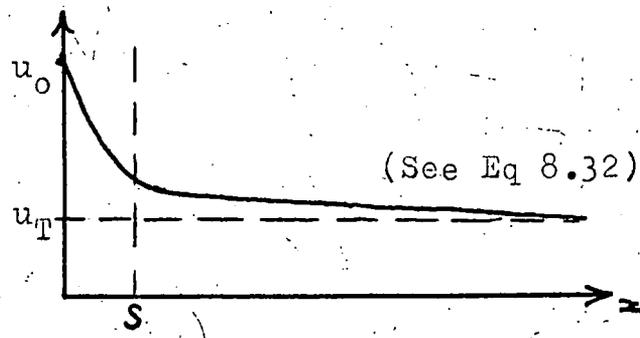
Fig 8.5. Factors influencing the current of electrons
that reaches the collecting electrode.

i includes the current due to electrons flowing to the collecting electrode and also that due to positive ions flowing to the emitting electrode. Diffusion of positive ions is neglected in comparison to electron diffusion. Provided that drift is the controlling electron removal mechanism (See Chapter 7)

$$\tau \gg T$$

and the electron lifetime may be most satisfactorily calculated from $\tau = d/v_d$, where d is the gap width.

2.2 Losses of electrons by back scatter to the emitting electrode before they have come into equilibrium with the field

It is now of interest to calculate i_o, the current due to electrons which survive in the gap long enough to reach the equilibrium energy. The following discussion is based on the theory of J.J. Thomson[17] for the back scatter of electrons to the emitting electrode by virtue of their initial random energy on emerging into the gap. (See Fig. 8.5, also see Chapter 1 §2.5).

The back scatter process occurs in a thin slice of gas close to the surface of the emitting electrode, and outside this slice electrons may be regarded as in equilibrium with the combined fields in the gap. Let n be the density of electrons at the point where they are just in equilibrium with the field. Then the current density at that point is given by

$$j_o = nev_d \qquad \qquad \dots \ 8.18$$

Consider a source of electrons on the surface of the emitting electrode, which emits electrons at a rate of n_o per second per cm^2. Then the current density of electrons starting out into the gap is given by

$$J = n_o e \qquad \qquad \dots \ 8.19$$
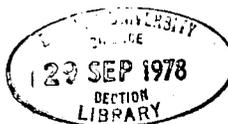
The current density of electrons returning to the emitting electrode by back scatter is calculated from kinetic theory as $n e \bar{v}_o / 4$, assuming that the electrons emerge into the gap with a distribution of energies which is approximately Maxwellian.

$\bar{v}_o$ is the random velocity with which the electrons emerge initially into the gap. Then the current density of escaping electrons is given by

$$j_o = J - n e \bar{v}_o / 4 = n e v_d \qquad \text{.... 8.20}$$

And eliminating n from Eq. 8.20

$$\frac{j_o}{J} = \frac{4 v_d}{(\bar{v}_o + 4 v_d)} \qquad \text{.... 8.21}$$

$$= \frac{i_o}{i_e} \text{ , assuming the absence of radial diffusion within}$$

the slice, where i_e is the total current leaving the emitting electrode.

Then,
$$i_o = \frac{4 \, i_e \, v_d}{(\bar{v}_o + 4 v_d)} \qquad \text{.... 8.22}$$

Therefore in Eq. 8.17, the current flowing to the collecting electrode is given by

$$i = \frac{4 \, i_e \, v_d}{(\bar{v}_o + 4 v_d)} \, e^{(\psi \tau - 1/6)} \qquad \text{.... 8.23}$$

2.3 Calculation of the finite distance travelled by the electrons before they come into equilibrium with the field

So far we have considered that electrons have been in equilibrium with the field during their whole lifetime in the gap. This, in fact, is not true since electrons entering the gap with energy which is not the equilibrium value in the gap must travel a finite distance before coming into equilibrium. Then the point in the gap beyond which we have so far considered steady state diffusion, drift and ionization to be applicable

must now be moved out into the gap a distance s, where s is the thickness of the slice of gas within which electrons come into equilibrium with the field (See Fig. 8.5). The effect of this on the ionization part of Eq. 8.16, assuming that there is no appreciable ionization within the slice itself, is to make it integrable not over the whole gap but over the distance d-s, which will not make much difference provided that d>>s.

If it is assumed that within the slice, the only loss process occurring is back scatter, and that there is no radial diffusion, the diffusion sphere referred to in §2.1 may be approximately regarded as starting from the point x = s at time t = 0.

Then, at time t, $x = v_d t + s$

and, $r = (12Dt/\pi)^{1/2}$.

And when the sphere just cuts the emitting electrode,

$$v_d^2 t^2 + (2vs - H)t + s^2 = 0 \qquad \qquad \text{.... 8.24}$$

where $H = 12D/\pi$

Clearly Eq. 8.24 has two roots, t_1 and t_2, one at which the sphere first cuts the emitting electrode, and the second at which it ceases to out it. In the simple case (See §2.1) where the sphere starts off with its centre at x = 0 at t = 0, let the distance moved by the centre of the sphere before the sphere has moved clear of the emitting electrode be Y.

Then if s << Y, it can be shown that $t_2 >> t_1$ and that $t_2 \sim T$. The probability that an electron will be lost by steady state back diffusion during its lifetime in the gap given by Eq. 8.10 must now be modified to include s.

Then, $P_r' = \dfrac{\displaystyle\int_{t_1}^{t_2} p'(t)\ dt}{\displaystyle\int_{t_1}^{t_2} (p'(t) + q'(t))\ dt}$ 8.25

where $p'(t) = (r - v_d t - s)/2r$ and $p'(t) + q'(t) = 1$

If $s \ll Y$, $P_r' = (\displaystyle\int_0^T p(t) - \int_0^T \dfrac{s}{2r}\ dt)/T$

$= \dfrac{1}{6} - \dfrac{s}{Y}$

$\sim \dfrac{1}{6} = P_r$, (See Eq. 8.13) 8.26

Therefore the finite thickness of the slice of gas within which the electrons come into equilibrium with the field does not appreciably affect the total probability of loss by back diffusion provided that $s \ll Y$.

It remains to perform an order of magnitude calculation of s, and to compare it with typical values of Y. Consider the simple case in which the effective field on the gap is unidirectional. Then the value thus obtained for the value of s will be an upper limit on the value that should be obtained when the effective field has an oscillating component. The rate of change of electron energy by elastic collisions in the gas is given by Compton[47] and Cravath[48] as

$$\frac{du}{dx} = E - \frac{a^2 u^2}{E} \qquad \qquad \text{.... 8.27}$$

assuming that the energy of the gas molecule is negligible in comparison to the electron energy u, where u is the electron energy after travelling a distance x from the electrode, E is the field on the gap, and $\underline{a}$ is given by

$$a^2 = 5.32 \frac{m}{M} \cdot \frac{1}{\lambda^2} \qquad \qquad \text{.... 8.28}$$

where the fractional electron energy lost per elastic collision is $2.66\ m/M$, and where λ is the electron mean-free-path, and m/M is the ratio of the

masses of the electrons and gas molecules. At equilibrium, $\frac{du}{dx} = 0$, and $E = a^2 u_T^2/E$, where u_T is the terminal electron energy at equilibrium.

Therefore,
$$u_T = E/a \qquad \qquad \dots \ 8.29$$

Therefore, in Eq. 8.27, $\frac{du}{dx} = \frac{a^2}{E}(u_T^2 - u^2) \qquad \qquad \dots \ 8.30$

Then integrating to obtain the distance the electrons must travel before reaching a certain energy u,

$$x = \frac{1}{2a} \quad \ln \left\{ \left(\frac{u + u_T}{u - u_T} \right) \left(\frac{u_o - u_T}{u_o + u_T} \right) \right\} \qquad \dots \ 8.31$$

where u_o is the energy with which the electrons start into the gap.

The results of Chapter 6 lead to the conclusion that u_o is probably greater than u_T.

Then, $u = \phi \, u_T$

and, $u_o = \beta \, u_T$, where ϕ and β are both greater than unity.

Therefore, $x = \frac{1}{2a} \quad \ln \ \left(\frac{\phi + 1}{\phi - 1} \right)\left(\frac{\beta - 1}{\beta + 1} \right) \qquad \qquad \dots \ 8.32$

Then, u is nearly equal to u_T, say $\phi = 1.1$, then electrons may be regarded as almost in equilibrium with the field.

Then, $x = s = \frac{1}{2a} \quad \ln \left(21 \left(\frac{\beta - 1}{\beta + 1} \right) \right)$

and $s < \frac{1}{2a} \quad \ln 21 \qquad \qquad \dots \ 8.33$

depending on the magnitude of β.

Putting in typical values for hydrogen at a pressure of 1 torr,

i.e. $m/M \sim 1/4000$, $\sim 10^{-2}$ cm.

$$s < 0.40 \ cm$$

So far we have only considered elastic collisions between electrons

and gas molecules, with the result that s is too large to ignore in comparison to d and Y.

However, electrons are emerging into the gap with energies corresponding to V_1, and at 1 torr, this corresponds to E/p of the order of 100 v/cm. torr. Electrons entering the gap are therefore certain to suffer inelastic collisions while coming into equilibrium. The value of $\underline{a}$ given by Eq. 8.28 is related to the fractional energy lost per collision, G, by

$$a^2 = 2 \, G/\lambda^2 \qquad \qquad \text{.... 8.34}$$

For inelastic collisions, at reduced fields approaching 100 v/cm. torr, G may be estimated from Townsend's data[3,5] to be of the order of 10^{-1} for hydrogen.

Then, $\qquad a \sim 44$

Now, we deduce that, $\qquad s < 0.030 \text{ cm}$

For the range of conditions examined experimentally, the distance, Y, moved by the centre of the sphere before the sphere ceases to cut the emitting electrode, ranges from about 0.30 to 7.60 cm. It is therefore reasonable to assume for hydrogen that $s \ll Y$, and that $s \ll d$, and that the finite width of the region in which the electrons come into equilibrium with the field does not seriously affect the arguments made previously based on the assumption that the electrons come into equilibrium within an infinitesimally thin slice of gas near the emitting electrode.

Similar conclusions hold for nitrogen, helium and neon.

2.4 The effects of uhf drift of electrons

So far a simplified picture has been presented, in which electrons drift steadily across the gap with a uniform drift velocity μE_{dc}, where
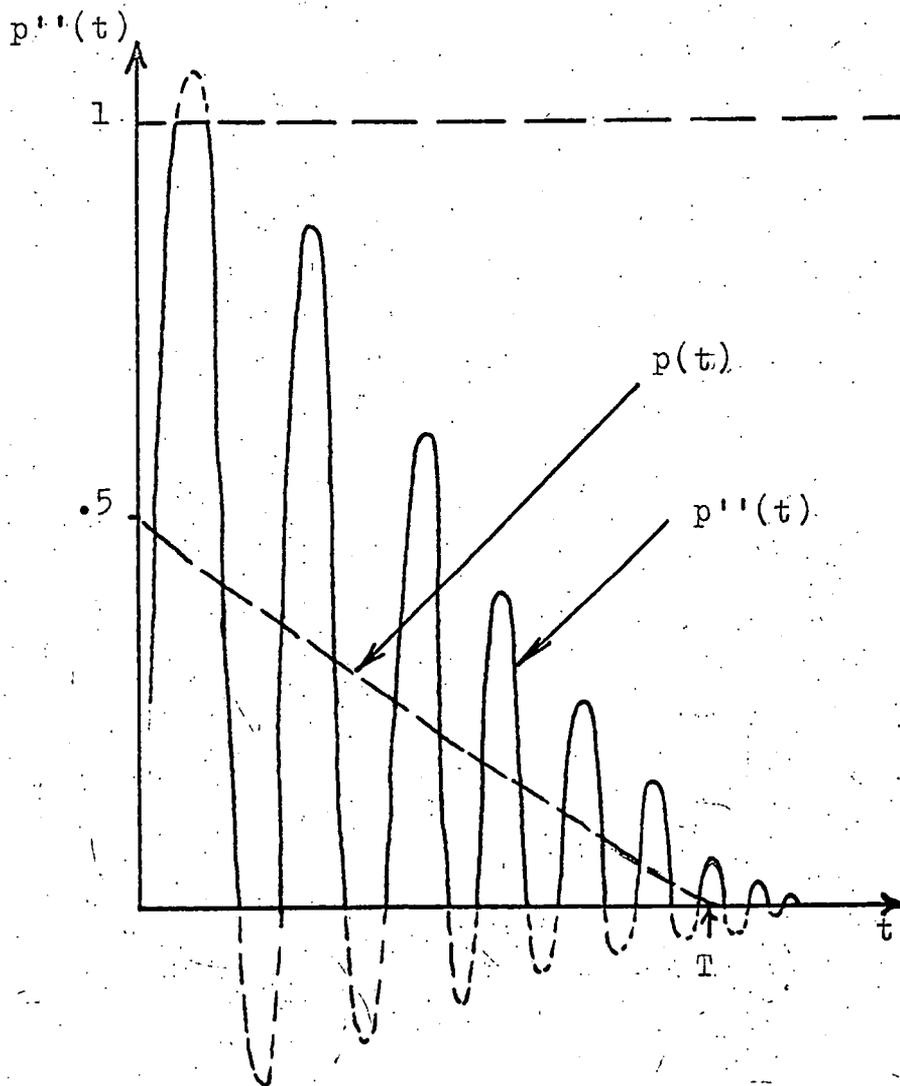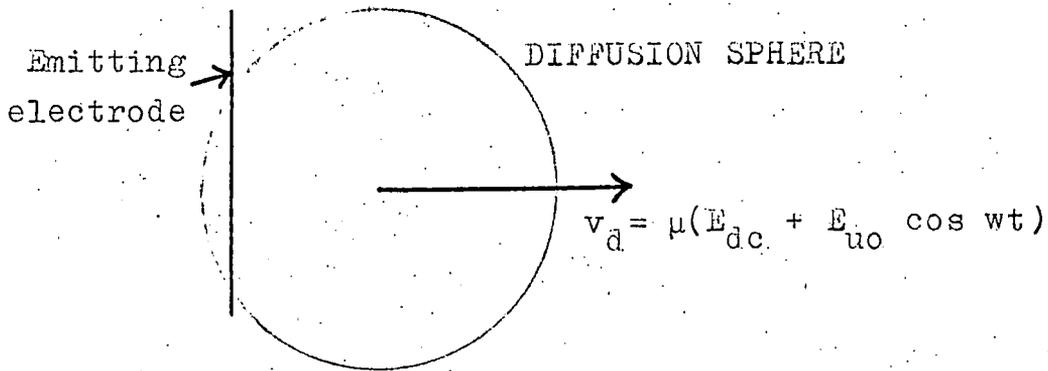
Fig 8.6. The effects of uhf drift of electrons.

μ is the electron mobility in the combined dc and uhf fields. The presence of the uhf field serves only to increase the random electron energy.

Now it is of interest to consider the effect of the uhf motion of electrons. Firstly consider the effects at points in the gap away from the surface of the emitting electrode where electrons are in equilibrium with the combined fields. The drift velocity of electrons in the gap in the combined fields should be written as

$$v_d = \mu (E_{dc} + E_{uo} \cos wt) \qquad \qquad \text{....} \ 8.35$$

where w is the angular frequency of the applied uhf field and E_{uo} is the peak value of this field. When the applied uhf is such that it tends to sweep electrons back to the emitting electrode, back diffusion is enhanced. Similarly in the opposite cycle of the field, back diffusion is reduced.

The instantaneous probability that an electron will be removed from the gap by back diffusion must again be modified from that given by Eq. 8.10 to give

$$p''(t) = \frac{1}{2} - \frac{\mu}{2} (E_{dc} + E_{uo} \cos wt) \ t^{1/2} (\pi/12D)^{1/2} \ \text{....} \ 8.36$$

$$= p(t) - \frac{\mu E_{uo}}{2} \ t^{1/2} \cos wt \ (\pi/12D)^{1/2}$$

(See Fig. 8.6)

Clearly $p''(t)$ should not take values greater than unity, although for certain values of t and E_{uo} the above expression _does_ take such values. At low values of t and high values of E_{uo}, for instance, it may be seen that for finite periods when the uhf field is sweeping electrons towards

the emitting electrode, the diffusion sphere lies completely within the boundary of the emitting electrode. Therefore it must be concluded that $p''(t)$ is not a continuous function of t, and therefore the analysis for the calculation of the total removal probability as used in §2.1 cannot be used again here, and some crude assumptions must be made. The curve of $p(t)$ is the envelope of $p''(t)$, and provided that the frequency of the applied field is high enough so that many cycles of the field occur before the diffusion sphere has moved out of range of the emitting electrode, we may deduce that

$$\int_0^T p(t)\ dt \sim \int_0^T p''(t)\ dt \qquad \qquad \text{.... } 8.37$$

and that the total probability that an electron starting out from the emitting electrode will be lost by back diffusion will still be very close to 1/6 as derived from the simple approach. Rough calculations of T indicate that over the range of experimental conditions examined in the present study, T, contains between about 10 and 600 oscillations of the uhf field.

Therefore Eq. 8.37 is a reasonable approximation.

Now consider the effects of uhf motion of electrons close to the surface of the emitting electrode before they have come into equilibrium with the field on the gap. Electrons are initially squirted out into the gap with energy which appears to be almost invariably greater than the equilibrium energy in the gap for the present range of conditions considered. Therefore the effect of the uhf field while the electrons still have this high energy (and the drift velocity away from the emitting electrode associated with it) is not likely to cause appreciable electron

-108-

loss back to the emitting electrode. The sweeping of electrons in the uhf field is only likely to become appreciable when the electrons have reached equilibrium with the field, and we have already deduced that this is not sufficient to greatly affect the electron loss back to the emitting electrode.

Attempts to derive a more rigorous solution for the effect of the uhf field have not been successful, but it appears to be a reasonable conclusion that such effects are negligible compared with the processes of back scatter and back diffusion already fully described.

2.5 Amplification

It has been shown above that the effects of the finite distance travelled by the electron before coming into equilibrium with the field, and the effects of the uhf motion of the electrons do not have an appreciable effect on the current flowing to the collecting electrode.
This current is therefore given by Eq. 8.23.
When there is no uhf field present, this current is

$$i \equiv i_{20} = \frac{4\,i_{e20}\,\mu_{20}\,E_{dc}}{((\bar{v}_o)_{20} + 4\mu_{20}E_{dc})}\; e^{(\psi_{20}\tau_{20} - 1/6)} \qquad \ldots\ 8.38$$

and similarly for the current flowing to the collecting electrode when there is a uhf field present, replacing the suffices $_{20}$ with $_2$.

Then, Amplification, $A = i_2/i_{20}$

$$= \frac{i_{e2}\mu_2((\bar{v}_o)_{20} + 4\mu_{20}E_{dc})}{i_{e20}\mu_{20}((\bar{v}_o)_2 + 4\mu_2 E_{dc})}\; e^{(\psi_2\tau_2 - \psi_{20}\tau_{20})}$$
$$\ldots\ 8.39$$

where i_e is the current of electrons emerging initially into the gap with
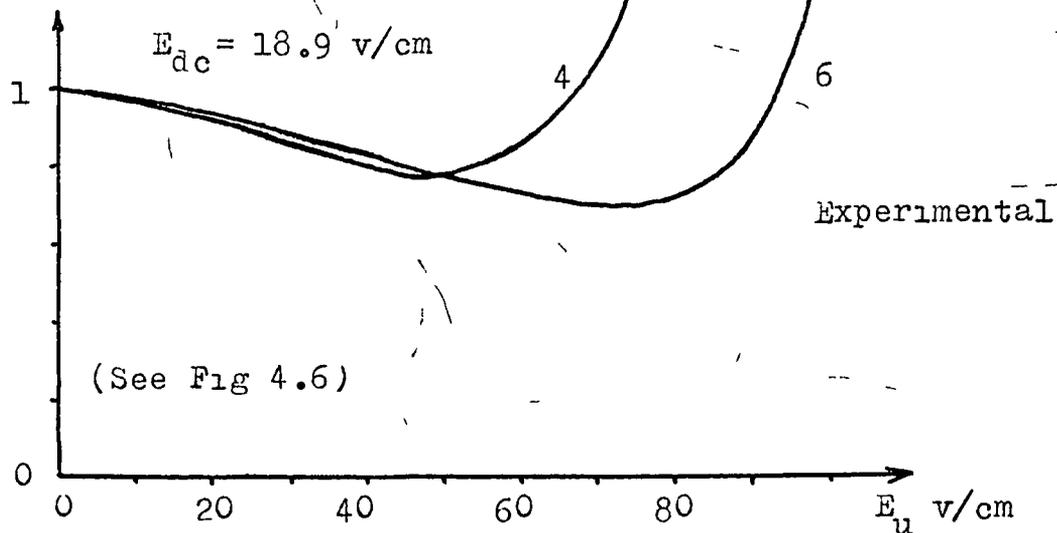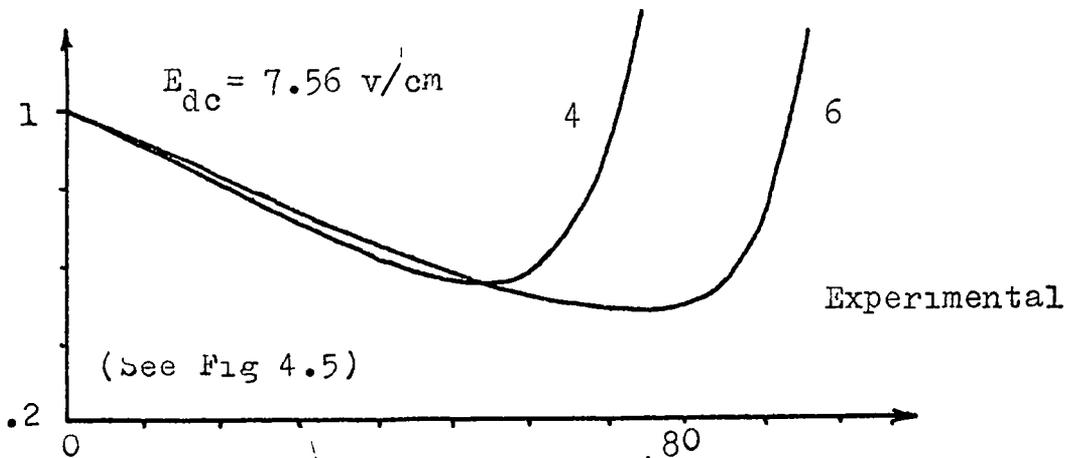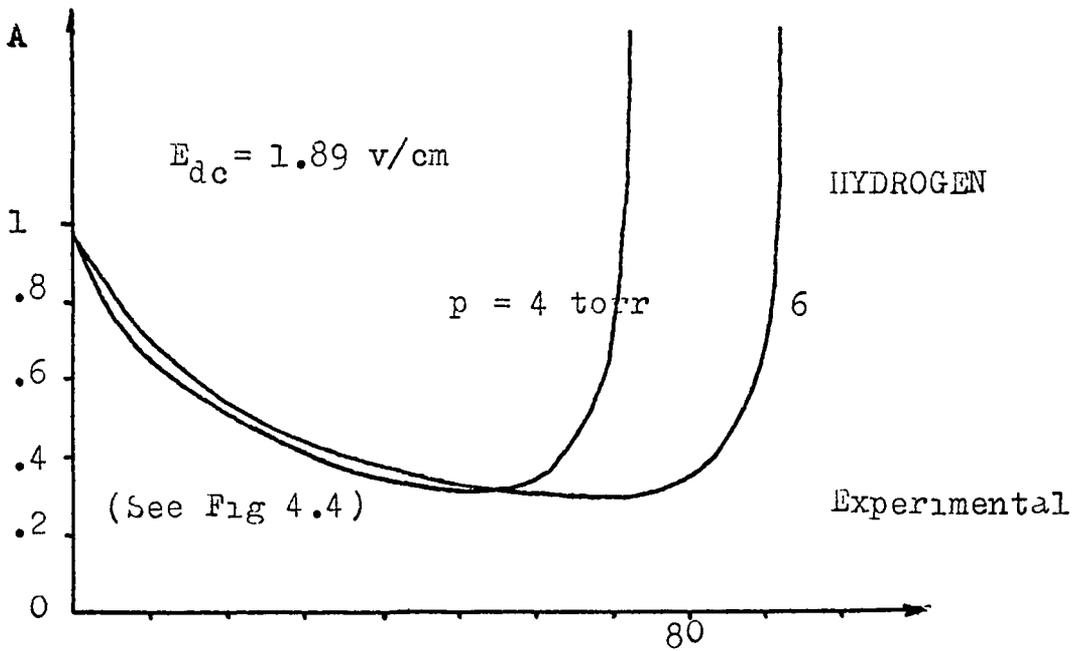
Fig 8.7. Calculated and experimental amplification
curves compared. HYDROGEN (d = 2.64 cm)

Ø 4 mm × 6 mm

4

6

Calculated
from
Eq. 8.44

$\frac{L}{0}$

4

6

$\frac{L}{0}$

4

6

$\frac{L}{0}$

NITROGEN
$E_{dc} = 6.89$ v/cm

Experimental

$p = 1.49$ torr

3.77

(See Fig 4.7)

E_u v/cm

$E_{dc} = 10.34$ v/cm

Experimental

$p = 1.14$ torr

3.18

(See Fig 4.8)

E_u v/cm
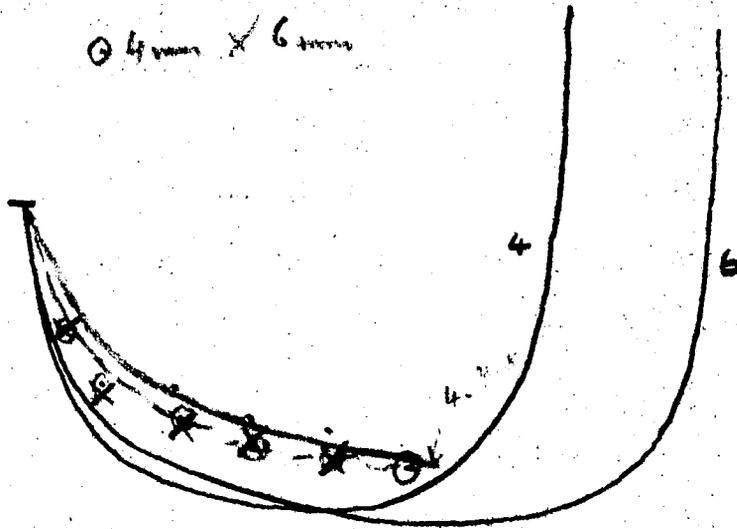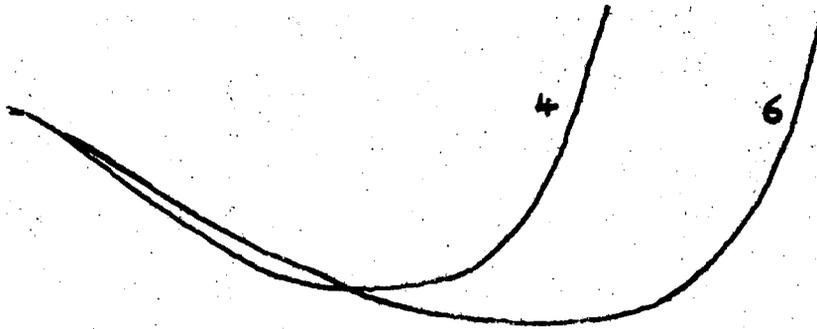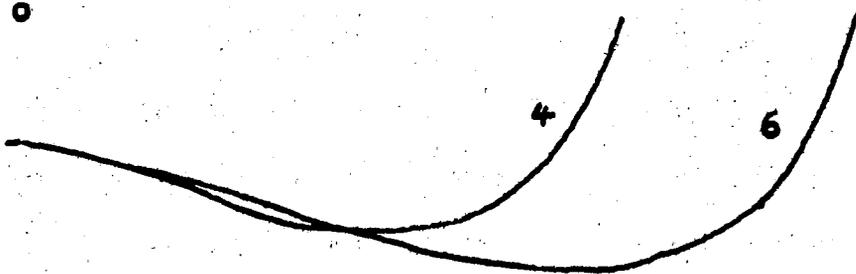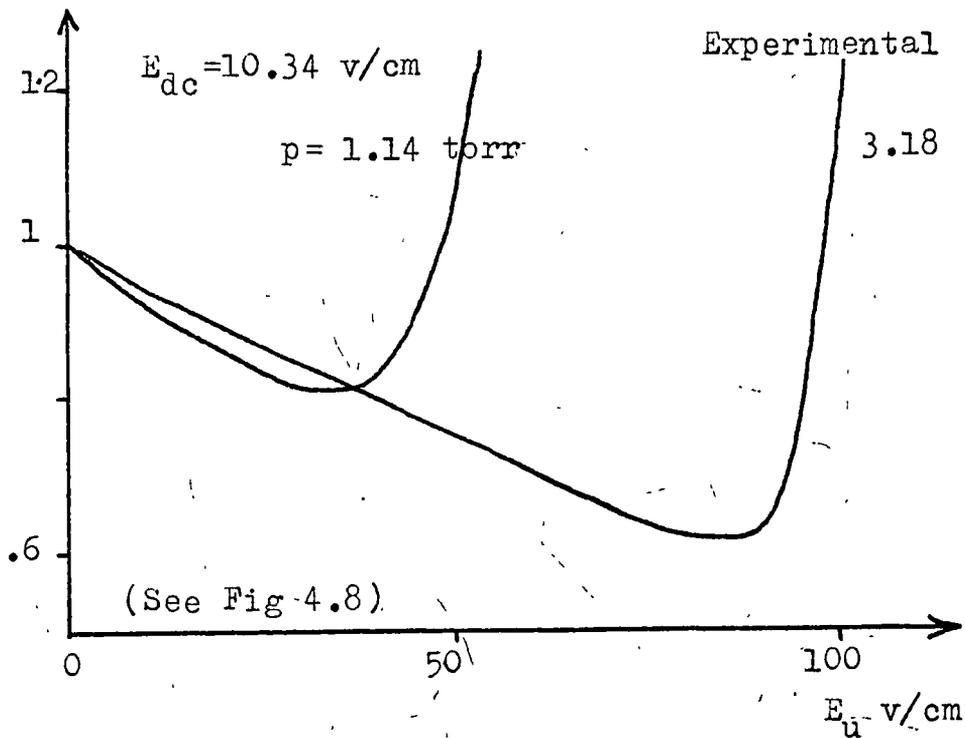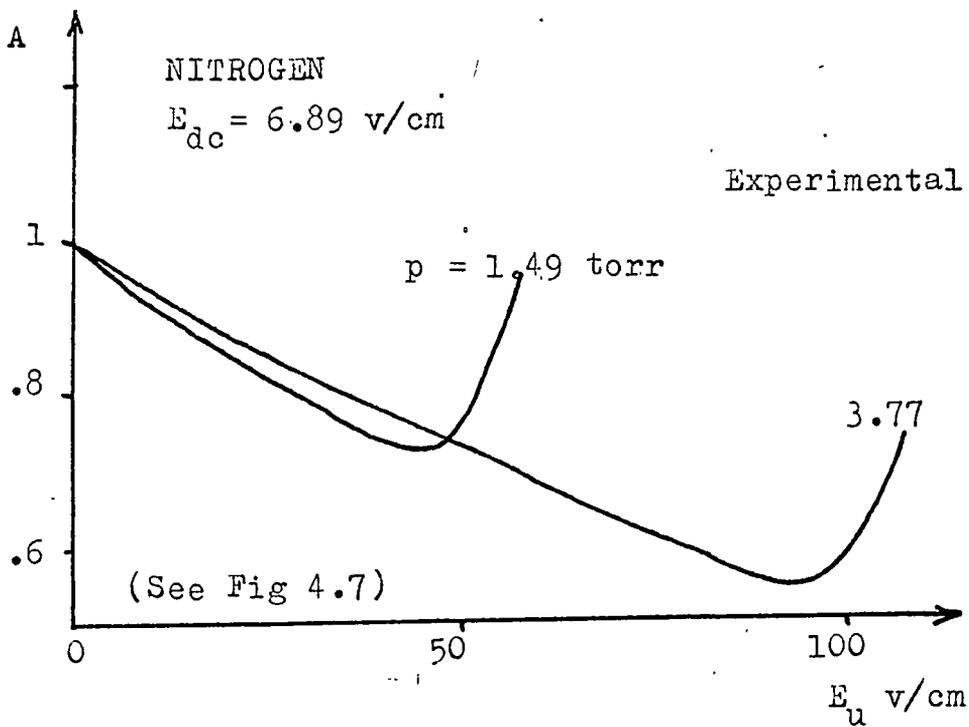
Fig 8.8. Calculated and experimental amplification
curves compared. NITROGEN (d = 2.9 cm).

@ 3.77 molar

1.49

Calculated
from
Eq. 8.44

3.77

L
O

1.14

3.18

L
O
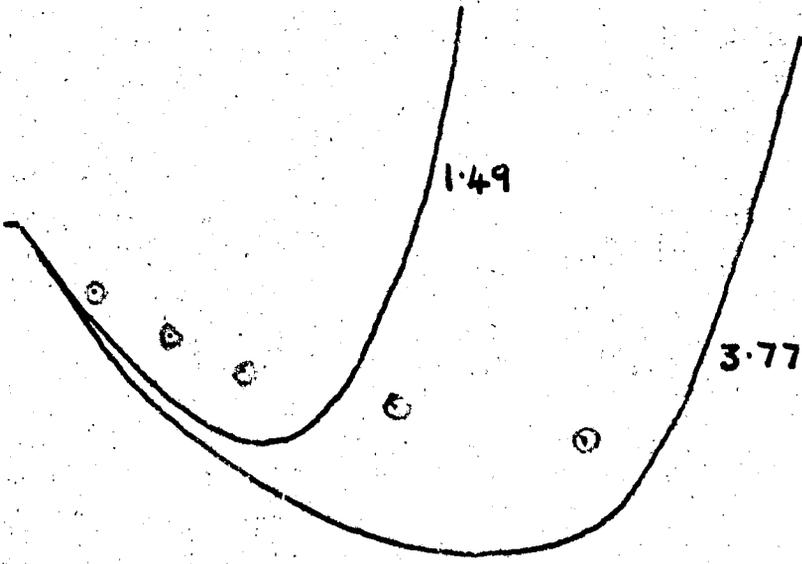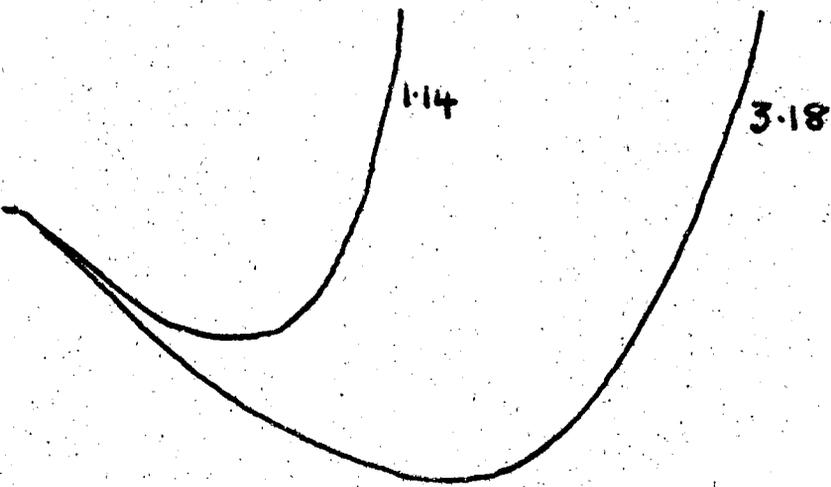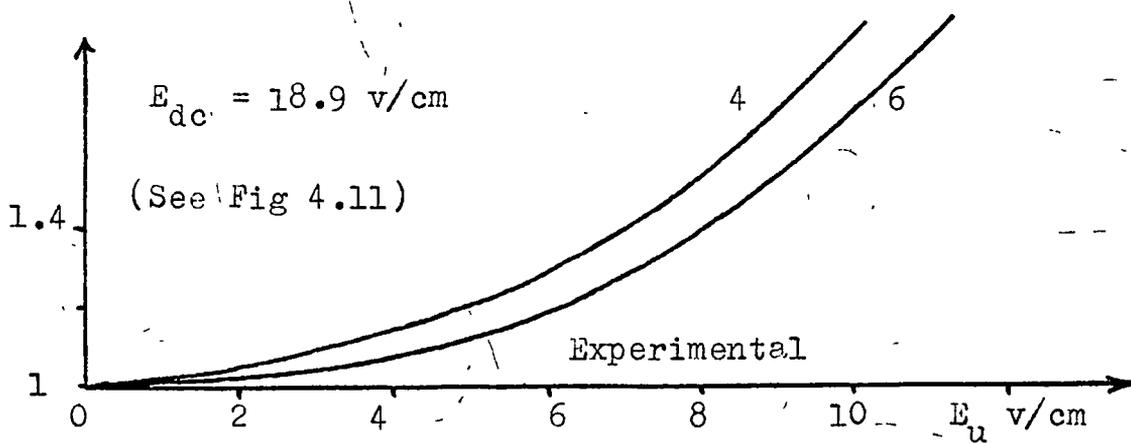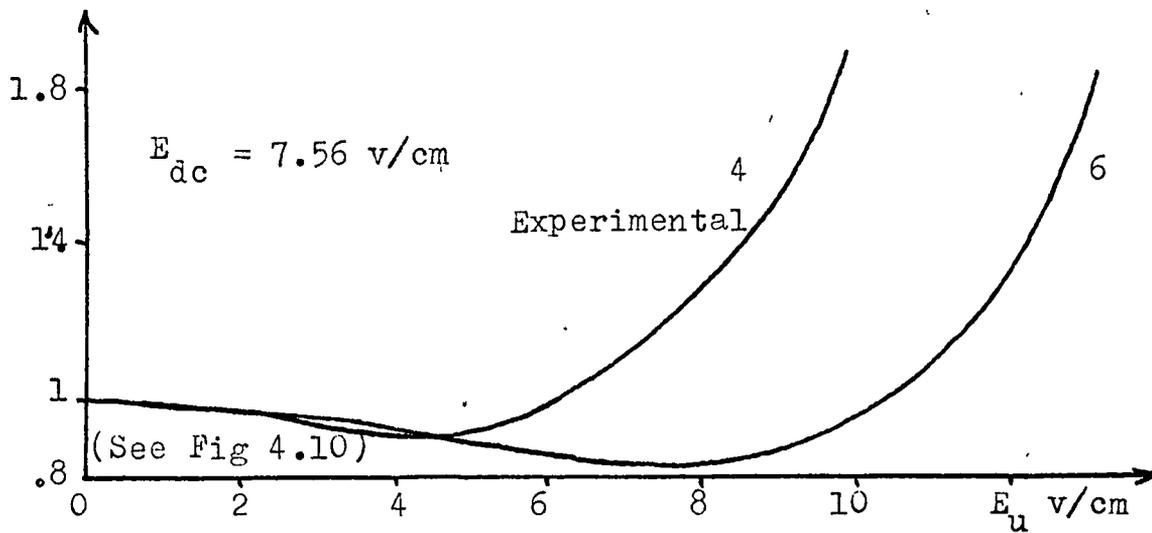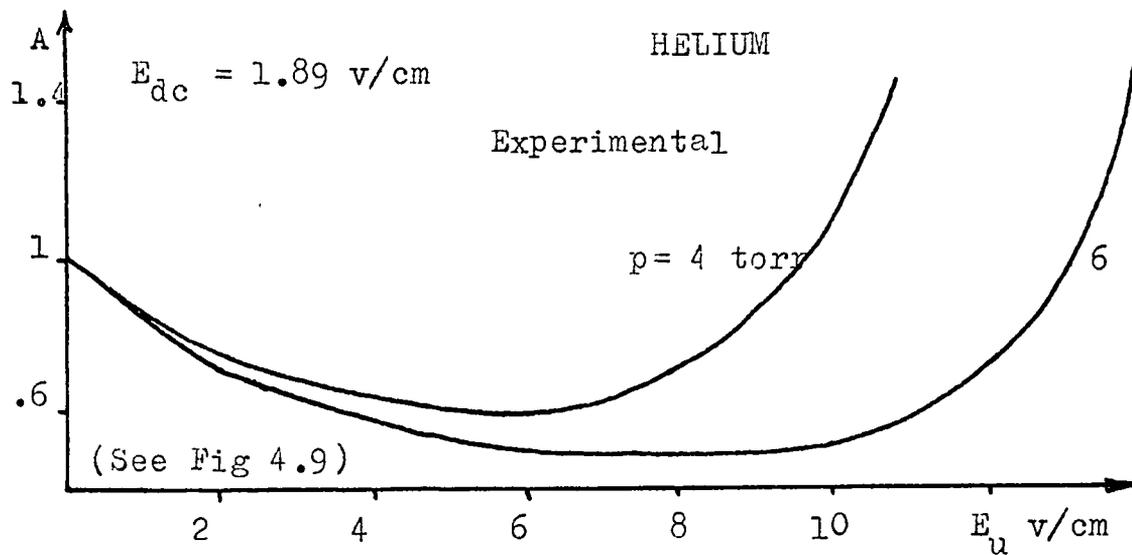
Fig 8.9. Calculated and experimental amplification curves compared. HELIUM (d = 2.64 cm).
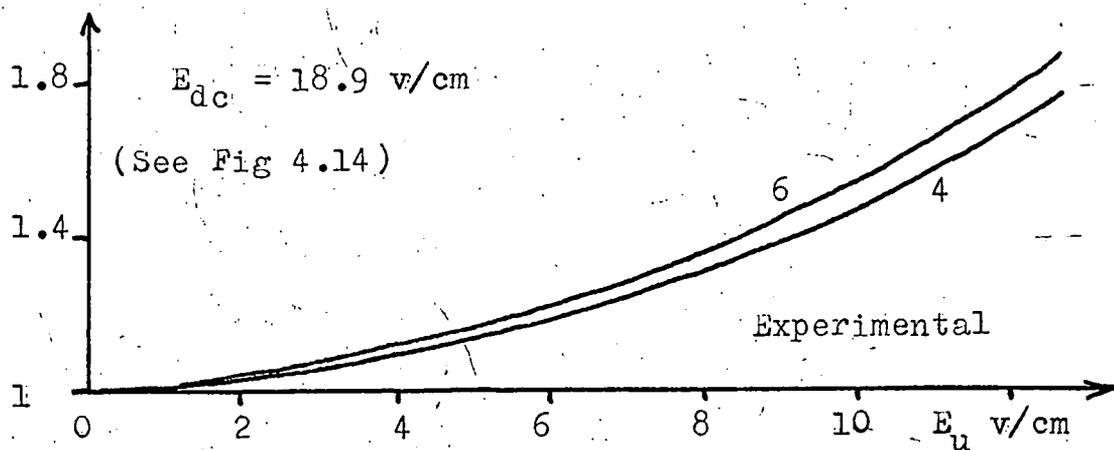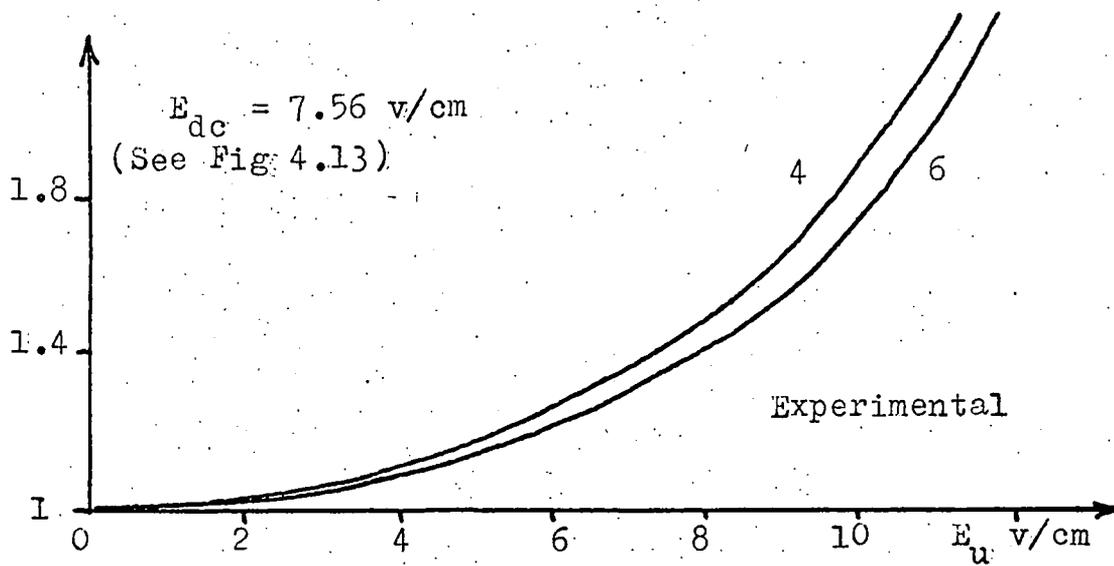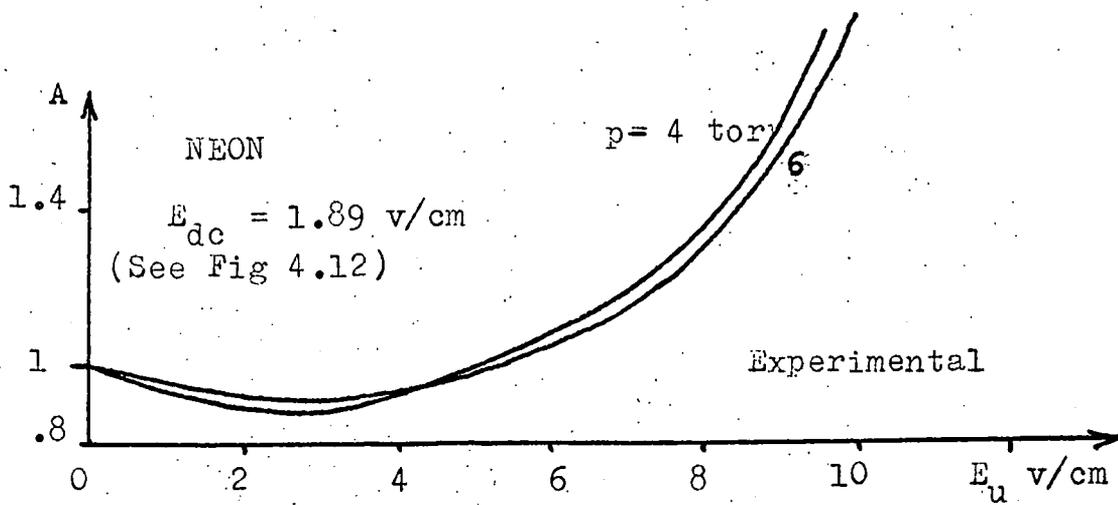
Fig 8.10. Calculated and experimental amplification curves compared. NEON (d = 2.64 cm).

© 6 mm, near

4

6

Calculated
from
Eq 8.44

6 4

4 6
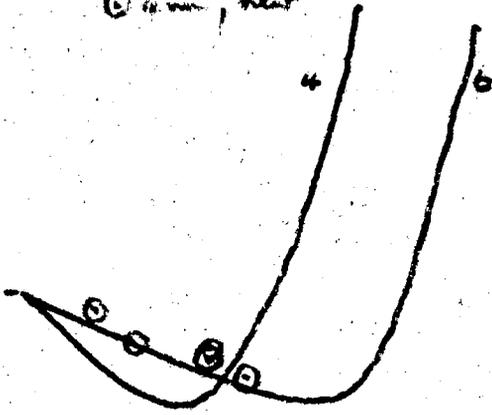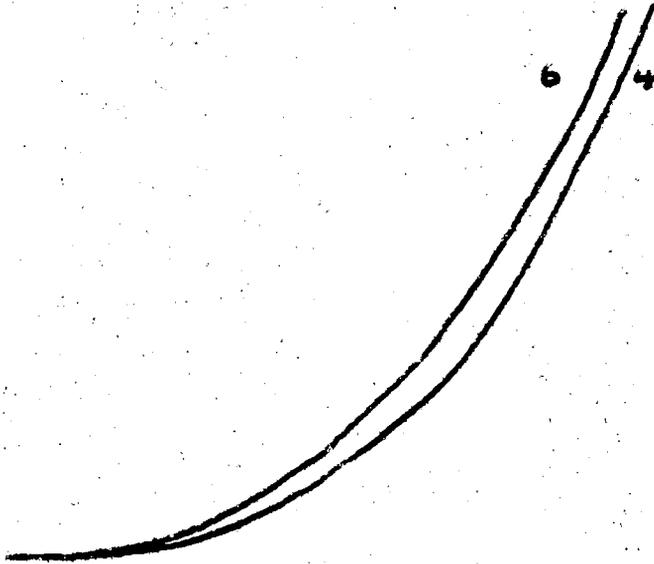
initial random velocity $\bar{v}_o$.

Assuming that the current emerging and the random velocity initially do not depend on the fields in the gap, and that the initial random velocity is large compared to the equilibrium electron drift velocity in the gap, Eq. 8.39 reduces to

$$A = \frac{\mu_2}{\mu_{20}} \cdot e^{(\psi_2 \tau_2 - \psi_{20} \tau_{20})} \qquad \dots \ 8.40$$

If drift is the controlling electron removal process, the electron lifetime in the gap may be given by

$$\tau = d/\mu E_{dc} \qquad \dots \ 8.41$$

Also, we may write, $\psi = \alpha \mu E_e$ $\qquad \dots \ 8.42$

Then, $\qquad \psi \tau = \alpha \dfrac{E_e}{E_{dc}} \cdot d$ $\qquad \dots \ 8.43$

Therefore Eq. 8.40 becomes

$$A = \frac{\mu_2}{\mu_{20}} e^{(\alpha_2 E_e / E_{dc} - \alpha_{20})d} \qquad \dots \ 8.44$$

(It is of interest to note that this expression in the absence of ionization is identical to that derived by Nicholls[1,26], although the two theories are quite different).

Theoretical amplification curves obtained from Eq. 8.44 are compared with typical experimental curves for hydrogen, nitrogen, helium and neon in Figs. 8.7, 8.8, 8.9 and 8.10. The electron mobilities are obtained from the drift velocity data of Bradbury and Neilsen[49,50,51], and the ionization coefficients from the measurements made using the present apparatus. (See Chapter 5). General comparisons between theory and

and experiment are made in Table 8.1.

The general agreement between theory and experiment is very encouraging, the theoretical curves exhibiting most of the trends observed experimentally. The poorest agreement is in neon where the predicted rise to breakdown is considerably faster than in the experimental case. The most likely source of error in all the gases is in the calculation of the lifetime of the electrons in the gap, where we have assumed that the electron flow across the gap is drift controlled.

When drift is the controlling loss process, the lifetime of electrons as controlled by drift, t_T, is less than that for electrons controlled by diffusion, t_D. (See Chapter 7).

Then, $\tau \sim t_T = d/v_d < t_D$

But in cases where diffusion is the more important electron removal process we should instead use the relation

$$\tau \sim t_D < d/v_d \qquad \qquad \text{.... 8.45}$$

Using the expression $\tau = d/v_d$ when diffusion is beginning to become important is likely therefore to give values of amplification which are too large. This may be one of the major sources of error at high E_u in cases where the predicted amplification is higher than the experimental values, particularly in neon where diffusion is more prominent than in the other gases examined.

Another source of error particularly below ionization may be in the calculation of the current, i_o, which escapes initial loss by Thomson-type back scatter. Thomson's theory[17] has been shown only to work well when

the random energy of the electrons on emerging is not much different from the equilibrium value in the gap. Other errors are likely to be introduced by assuming that the current emerging into the gap and the initial random velocity are independent of the field in the gap. Nevertheless, the experimental results give considerable support to the theory presented here.

TABLE 8.1

COMPARISON BETWEEN THEORETICAL AND EXPERIMENTAL AMPLIFICATION CURVES

	Low E_{do} Low E_u	Low E_{do} High E_u	High E_{do} Low E_u	High E_{do} High E_u
Hydrogen	Agreement Fair $\dfrac{A_T}{A_E} < 1$	Agreement Good $\dfrac{A_T}{A_E} \sim 1$	Agreement Good $\dfrac{A_T}{A_E} \sim 1$	Agreement Fair $\dfrac{A_T}{A_E} < 1$
Nitrogen	Agreement Fair $\dfrac{A_T}{A_E} < 1$	Agreement Fair $\dfrac{A_T}{A_E} > 1$	Agreement Fair $\dfrac{A_T}{A_E} < 1$	Agreement Fair $\dfrac{A_T}{A_E} > 1$
Helium	Agreement Fair $\dfrac{A_T}{A_E} > 1$	Agreement Fair $\dfrac{A_T}{A_E} > 1$	Agreement Good $\dfrac{A_T}{A_E} \sim 1$	Agreement Fair $\dfrac{A_T}{A_E} > 1$
Neon	Agreement Poor $\dfrac{A_T}{A_E} < 1$	Agreement Poor $\dfrac{A_T}{A_E} \gg 1$	Agreement Good $\dfrac{A_T}{A_E} \sim 1$	Agreement Fair $\dfrac{A_T}{A_E} > 1$

$$\frac{A_T}{A_E} = \frac{\text{Predicted Theoretical Amplification}}{\text{Experimental Amplification}}$$

See Figs. 8.7, 8.8, 8.9 and 8.10.

CHAPTER 9

THE STUDY OF LONG TIME CONSTANT PHENOMENA ASSOCIATED WITH ELECTRON FLOW

IN THE GAP

It was noticed during preliminary measurements of amplification that i_{20}, the current flowing to the collecting electrode in the absence of the uhf field, does not remain constant, despite the stabilization of the current to the back of the emitting electrode. The variations observed were not of the nature of random fluctuations, but appeared to be a function of time, long time constants being involved. Long[2], having observed similar effects, concluded that these variations resulted from the charging up of insulating layers present on the electrode surfaces. It was suggested that such insulating films could occur as the result of the decomposition of organic grease molecules under electron bombardment. This has been shown by Laurenson, Holland and Priestland[23], and by Christy[24] to be a possible mechanism. However in the present experiment, a great deal of trouble has been taken to avoid the presence of grease or oil vapours in the system, and yet the drifts in i_{20} persist. In a further attempt to remove these drifts, the aluminium electrode surfaces were gold-plated (by evaporation), and although there was a marked improvement, the situation was by no means remedied.

Further experiments have since been performed in order to investigate the causes of the present drifts in i_{20}, and are described in this chapter. (Constant reference is made to Fig. 2.1 throughout this chapter).

Fig 9.1. Variation of i_{20} with time.

i_{20}
(Deflection of G_2 in cm)

Backing pressure
d = 2 cm
E_{dc} = 5 v/cm

NEON, p=4 torr
d = 2 cm
E_{dc} = 5 v/cm

t mins

i_{20}

Equilibrium condition (a)

$i_B > i_{20}$ initially

Balance between i_{20}, i_B and V_g.

$i_B < i_{20}$ initially

Equilibrium condition (b)

t mins
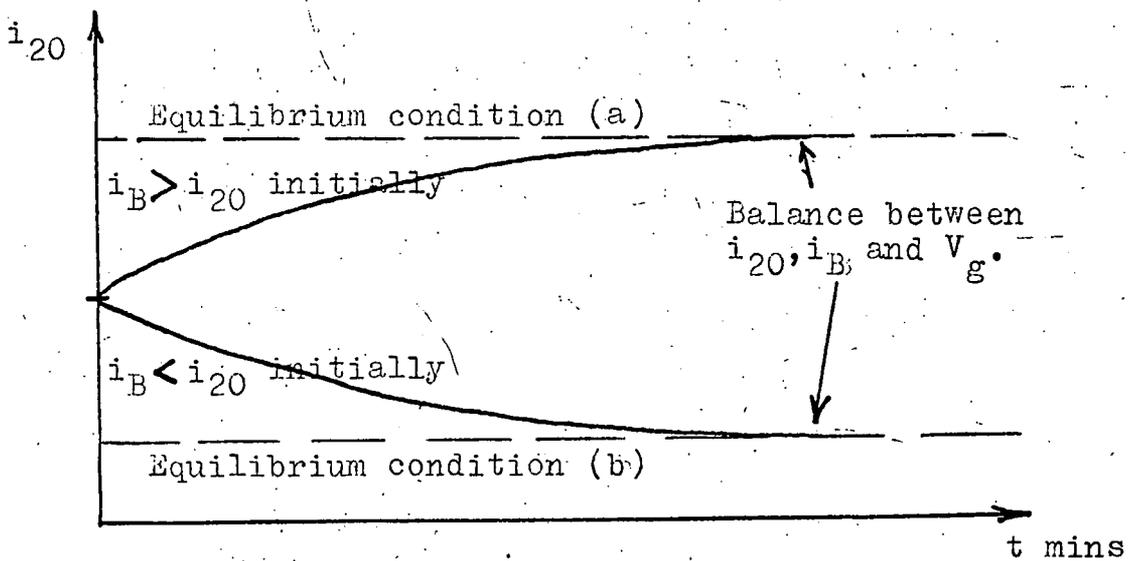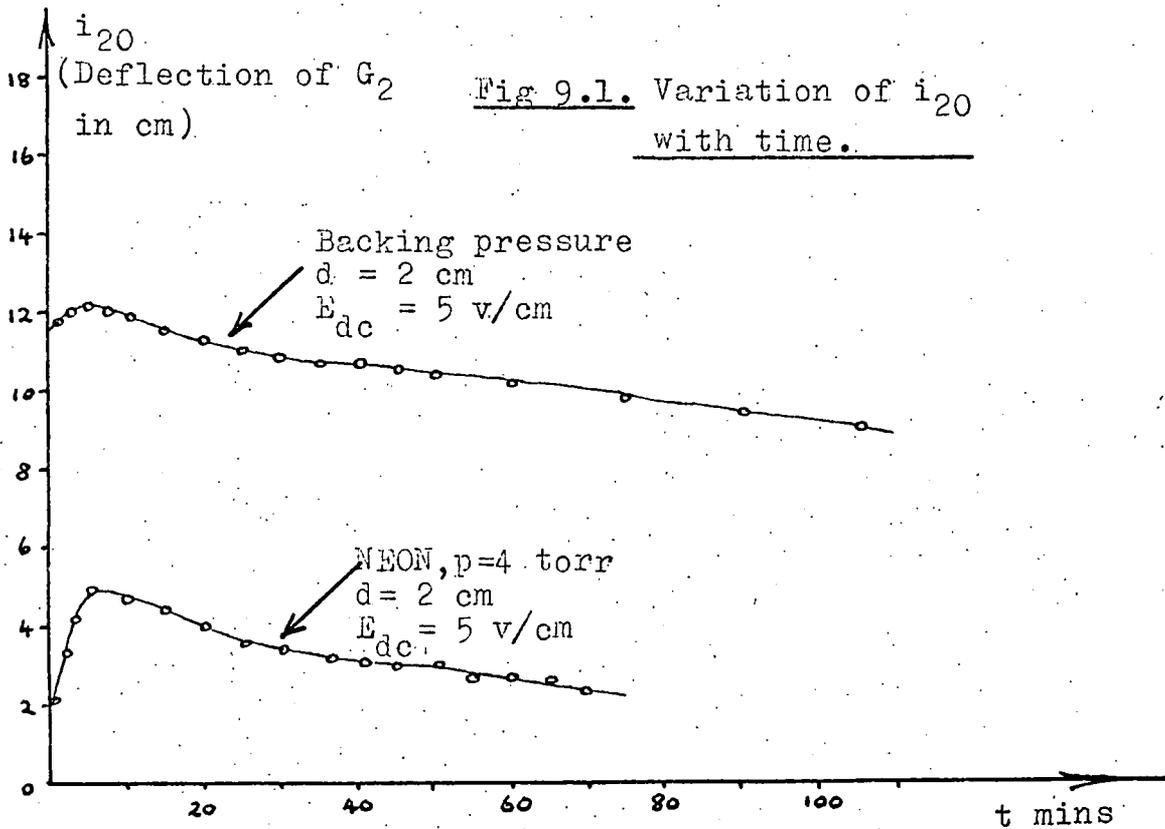
Fig 9.2. Predicted variation of i_{20} with time for
(a) $i_B > i_{20}$ and (b) $i_B < i_{20}$ initially.

1. <u>Variation of i_{20} with time, V_2 fixed</u>

The current flowing to the collecting electrode, i_{20} was measured as a function of time, with a unidirectional voltage, V_2, applied to the gap such that P_2 is positive with respect to P_1. This was done for various sets of conditions, and typical results are shown in Fig. 9.1. It is seen that the results do not differ greatly in form from those obtained by Long[2]. Time zero was taken when i_1 first became stabilized. The trends exhibited by the curves were fairly consistent from one curve to another.

As t increases from zero, i_{20} starts from a low value, rising quite sharply to a peak value (of the order of twice the magnitude of the initial current) after a time of about 5 to 10 minutes, after which it decreases steadily, showing no signs of levelling out, even after 2 hours.

Consider firstly the condition in which we assume that the stabilization of i_1 is a true indication that the current, i_e, emerging into the gap is constant. Of the current emerging, a fraction, i_B, will return to the emitting electrode, P_1, by back diffusion, and in the presence of an insulating film will form a negatively charged layer there. The remaining fraction, i_{20}, flows to the collecting electrode, P_2, and in the presence of an insulating film, will form a negatively charged layer there. It is assumed for the present that the charging rates for a given current are equal at both electrode surfaces.

If i_B is initially greater than i_{20}, P_1 may charge up more negatively than P_2. Then there is generated in the gap a net residual voltage in

required. In Chapter 6, it is related how it was discovered that the current flowing out of the hole in the emitting electrode does not depend on the length of the hole. A mechanism is suggested in which charging up of the wall of the hole by the current flowing into it brings about a situation in which the electron flow is concentrated electrostatically near the axis of the hole. This is analogous to the Wehnelt cylinder effect[46] as used to concentrate the electron beam as it leaves the filament in the cathode ray tube. Rough calculations (See Chapter 6) show that in the absence of such an effect, for hole dimensions as used in the above experiment, the current leaving the hole might be expected to be low compared to that entering the hole. Therefore at the time of stabilising i_1, (t=0), only a small fraction of the current entering the hole actually emerges into the gap. This fraction may be expected to rise as the walls of the hole become steadily charged negatively, and the concentrating effect begins to occur within the hole. The current emerging into the gap, i_e, will reach a maximum when the amount of charge residing on the walls of the hole has become high enough to totally prevent losses to the walls.

As i_e rises during the charging up period, i_{20} should also rise provided that i_B does not increase as quickly as i_e. Once conditions inside the hole have reached the steady state condition, the time dependence of i_{20} now depends on conditions in the gap. And provided that i_e at this stage is greater than i_B, it should decrease under the mechanism described earlier in this section until the final steady state

condition has been achieved.

This argument accounts for the shape of the curves, which support the assumption that initially i_{20} is greater than i_B in all the experiments performed. This may not always be the case, and will depend on the voltages V_1 and V_2. For instance if electrons are injected into the gap with a high random energy, a larger proportion may expect to return to the emitting electrode by Thomson-type back scatter[17], than for electrons injected with a small random energy.

There follows a very approximate calculation of the expected relative orders of magnitudes of the time constants for the two effects just mentioned. (See Fig. 9.3).

The second part of the curve of i_{20} against time has a time constant T_2, say. The higher the current density flowing to P_2, the greater the rate of charging, and so the steady state situation is achieved more quickly.

Then, $$T_2 \sim F A_1/(i_{20} - i_B) \qquad \dots \ 9.1$$

taking into account charging at both electrodes, where A_1 is the area of the electrode surfaces, and F is a constant depending on the nature of the electrode surfaces, assuming that it is the same for both electrodes.

Now consider electrons entering the hole from the back of the emitting electrode. Then the current entering the hole is $i_1 \pi b^2/A_2$, where A_2 is the area of the back of the electrode on which i_1 impinges and b the hole radius. Therefore from this, the current density flowing to the

walls of the hole, assuming that all electrons entering the hole reach the wall, is of the order of $i_1 \pi b^2 / A_2 2\pi b L$, where L is the length of the hole. The flow of electrons out of the hole into the gap is controlled by the amount of charge residing on the wall of the hole. Then if the time constant of the increase of the current coming into the gap is T_1, then

$$T_1 \sim FA_2 2\pi b L / i_1 \pi b^2 \qquad \dots \text{ 9.2}$$

where F is a constant depending on the nature of the inside surface of the hole, assuming that this is the same as for the electrode surfaces in the gap.

Then, $$T_1/T_2 \sim \frac{2A_2 L(i_{20} - i_B)}{A_1 b\, i_1} \qquad \dots \text{ 9.3}$$

Putting figures into this rough expression, we are required to estimate A_1, A_2 and $(i_{20} - i_B)$.

Typically, try $A_1 = 25$ cm^2, $A_2 = 5$ cm^2, $(i_{20} - i_B) = 10^{-8}$ amps. Also $i_1 = 6.10^{-7}$ amps; b = 0.02, L = 0.04 cm.

Giving, $T_1/T_2 \sim 1/75$. The values of T_1/T_2 estimated from the experimental i_{20}, t curves indicate reasonable agreement with this value, affording support to the theory.

2. <u>Variation of i_{20} with applied gap voltage, V_2</u>

It was hoped that measurements on the variation of i_{20} with the applied unidirectional voltage, V_2, would enable the residual voltage generated in the gap to be estimated with a reasonable degree of accuracy. The experiments were performed at low pressure, with the system continuously pumped, thus reducing the effects of back diffusion which are
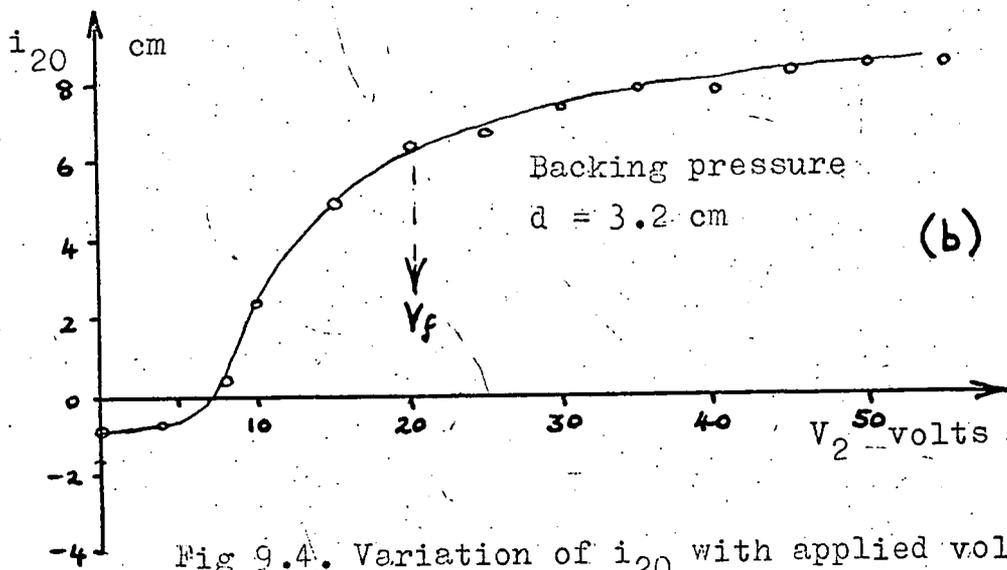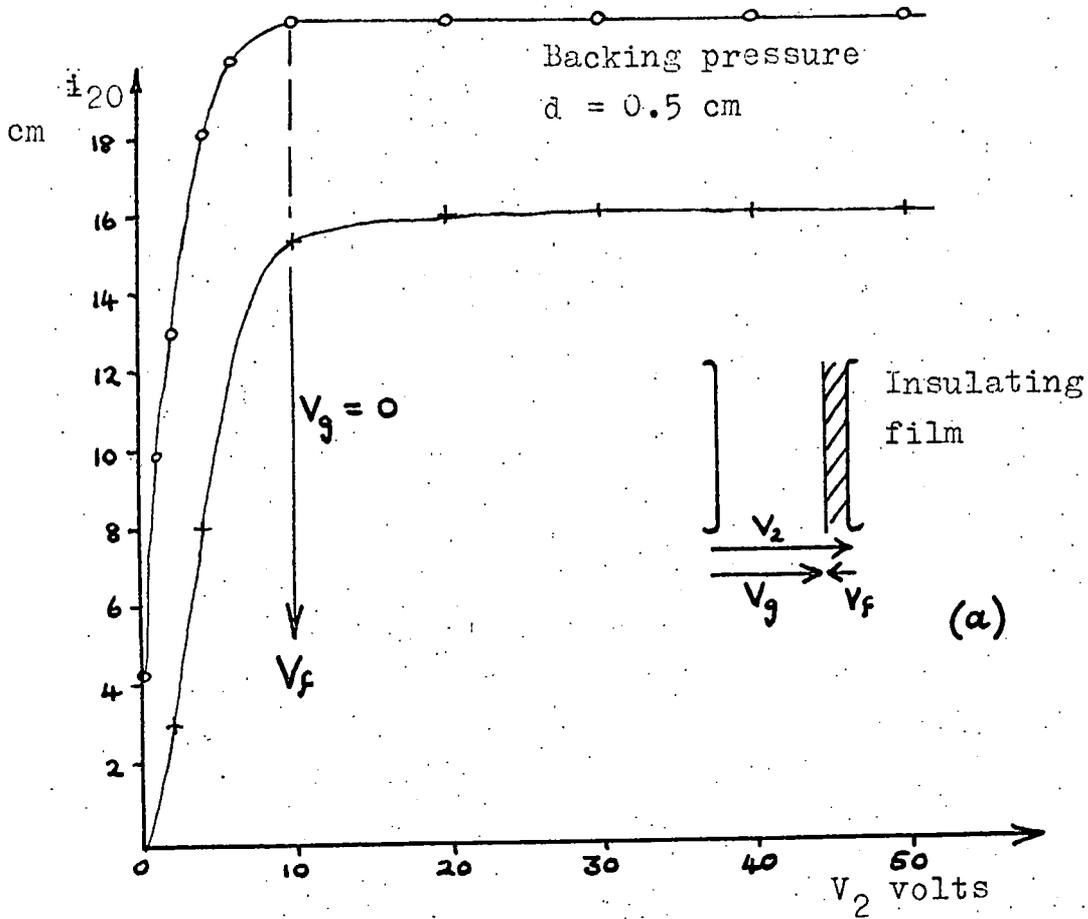
Fig 9.4. Variation of i_{20} with applied voltage, V_2.

not of interest in this particular study. Curves showing the variation of i_{20} with V_2 are given in Fig. 9.4. It was shown experimentally that the values of i_{20} for which V_2 was taken increasing stepwise from zero agreed quite well with those in which V_2 was started from a higher value, and was decreased in steps, thus tracing back down the curve. This is a satisfactory check on the reproducability of the results. Results were obtained at low pressures (backing pressure around 10^{-2} to 10^{-3}torr) and for gap widths of 0.5 and 3.2 cm.

At high V_2 all the electrons emitted are swept to the collecting electrode, neglecting the few which, at this low pressure, return to the emitting electrode by Thomson-type back scatter.[17] Neglecting collisions with gas molecules, provided that the field is tending to sweep electrons towards P_2, i_{20} should be constant independent of V_2. As V_2 is reduced, a point is eventually reached where the field in the gap, given by $V_g = V_2 - V_f$ is zero. (Experiments described in the previous paragraph show that the electrodes charge up with the passage of i_{20} such that the residual voltage V_f is opposite to V_2). Now there is no field tending to sweep the electrons to the collecting electrode, so the only transport mechanisms to that electrode are diffusion, and the drift velocity with which the electrons are injected into the gap. The electrons are emitted into the gap with a distribution of energies, so when V_2 is just less than V_f, some of the lower energy electrons will be returned to the emitting electrode in the now unfavourable field, and a reduction in i_{20} will result. As V_2 is reduced further, some of the higher energy electrons will be returned to P_1, causing a further reduction in i_{20}.

Eventually, if V_f is high enough, V_2 may be reduced to the point where all the emitted electrons are returned to P_1. These returning electrons are not registered in the current measuring circuit, since they are cancelled out by emerging electrons. The applied voltage should equal the residual voltage when electrons <u>start</u> to be returned to P_1 by the field. That is at the point where i_{20} starts to drop appreciably from the steady value observed at higher values of V_2.

In the experiments at the shorter gap width of 0.5 cm, (Fig. 9.4a), the curve <u>does</u> follow this pattern, exhibiting a steady value of i_{20} above a certain value of V_2, and dropping off near the critical point in quite a marked fashion. From these results, bearing in mind what has gone before, it is possible to estimate with some degree of confidence the magnitude of V_f. The values of V_f obtained from the curves range from 8 to 18 volts. Great reproducability is not expected in these results, since so much depends on the previous history of the system.

In the experiments using the longer gap widths, the curves are not so satisfying. The value of i_{20} does not reach a steady value at higher V_2, but continues a slight upward trend as V_2 is increased. As before the curve drops off quite sharply as V_2 is decreased below the value of V_f, but owing to the upward trend of i_{20} at higher V_2, it is difficult to estimate the exact point at which electrons start to be swept back to the emitting electrode. Attempts to do so give values of V_f in the range 16 to 24 volts, but we cannot expect accuracy to be as good as in the case of the shorter gap width. The variation in i_{20} at higher values

of V_2 may be explained in terms of collisions which are now more likely to occur between electrons and gas molecules at this longer gap. In fact the probability of collision is increased 6-fold. There is the change now of some ionizing collisions and of back diffusion. Whichever of these is the case, increasing V_2 will cause an increase in i_{20}.

At the longer gap width, and low V_2, the curve drops such that i_{20} takes negative values. This is not the case at the short gap width, so it is fairly clear that this effect also is the result of collisions between electrons and gas molecules. This effect is discussed in greater detail in a later paragraph. (See §3.3).

This method of estimating the residual polarizing voltage in the gap after the electrode surfaces have been changed up is open to the following criticisms.

a) During a given run it is not possible to account for the variation in V_f caused by the continual passage of a current across the gap. It would be more satisfactory to devise a method of measuring these voltages in which no current is passed in the gap.

b) It is difficult to estimate the exact point at which the effective field in the gap should be zero, (i.e. $V_2 = V_f$), owing to the finite energy distribution of electrons coming into the gap, and to the effects of collisions in the gap between electrons and gas molecules, particularly at longer gap widths.

The results are therefore only approximate, and need verification by another method. One such method is described in the next chapter of this thesis.

3. Variation of i_{20} with time, with zero applied voltage

When the applied voltage is zero, the only voltage remaining in the gap is the residual voltage on the electrode surfaces, V_f. Measurements of the current to the collecting electrode, i_{20}, were performed as a function of time in hydrogen for contrasting sets of conditions in the gap. Typical results are shown in Fig. 9.5. Zero time was taken at the moment that i_1 became stabilised.

3.1 The results

a) Plates charged initially with a pure uhf discharge

The plates are charged by the uhf discharge such that there is no net residual voltage generated in the gap. i.e. $V_f = 0$. At a pressure of 0.37 torr, and for a small value of i_1, i_{20} takes a positive value, increasing initially with time as the walls of the emitting holes become negatively charged, and the holes become more efficient emitters of electrons. When the holes reach their peak transmission efficiency, i_{20} levels off, and begins to decrease, indicating that i_{20} is charging up the film on P_2 more rapidly than i_B is charging up the film on P_1. The curve levels out as the steady state condition is approached. At the same pressure, but with a higher i_1, the holes reach their peak efficiency more rapidly owing to the increased rate of charging within the holes. At low pressures, there is no initial rise in i_{20}, indicating that the holes reach their highest transmission efficiency almost immediately. This suggests that at this low pressure, there is virtually no electron loss within the holes even without the Wehnelt cylinder effect, which is reasonable in view of the low probability of collisions between electrons

-122-

and gas molecules within the holes.

b) <u>Plates charged with a dc voltage superimposed on the uhf discharge such that P_1 becomes charged negatively with respect to P_2</u>

The plates are now charged up so that there is a residual voltage in the gap tending to sweep electrons to the collecting electrode, P_2. The results have the same form as those just described, except that i_{20} now takes higher values.

c) <u>Plates charged with a dc voltage superimposed on the uhf discharge such that P_2 becomes charged negatively with respect to P_1</u>

The plates are now charged up so that there is a residual voltage in the gap tending to sweep the electrons back to the emitting electrode.

For a pressure of 0.37 torr, and a low value of i_1, i_{20} takes initially a small negative value, dropping to a larger negative value as the holes in the emitting electrode become more efficient transmitters of electrons. Then i_{20} increases, tending to level out to a smaller negative value after about 20 minutes. For a higher value of i_1, the holes reach their maximum transmitting efficiency more quickly. i_{20}, starting off negatively, increases steadily, becoming positive after about 6 minutes, and tending to level off at a small, positive value after about 20 minutes. At lower pressures, i_{20} initially takes a high negative value but rises to a smaller steady negative value after about 20 minutes.

The implications of these negative values of i_{20} are discussed in detail later in this section. (See §3.3).

3.2 To compare the charging rates at the two electrode surfaces

When a pure uhf discharge is run in the gap (See §3.1a) there should be no net residual voltage in the gap afterwards. When the current is then switched on, those electrons which get to the collecting electrode can only get there by diffusion. A considerably larger proportion should be lost by diffusion back to the emitting electrode, particularly at the long gaps discussed in this experiment. This certainly applies to the higher pressure examined, and would be expected to apply in the lower pressure cases, provided the mean free path is short enough for electrons to make a number of collisions during their lifetime in the gap.

But the results (See §3.1a) show that the system behaves as though P_2 is charging up under the influence of i_{20} more rapidly than P_1 is charging up under the influence of i_B (See §1) despite the fact that i_B must surely be greater than i_{20} in this case. We must consider therefore the possibility that the surfaces at P_1 and P_2 charge up at different rates for the same current reaching them. It is convenient to define the quantity 'efficiency of charging.' Let the efficiency of charging at P_1 be ϵ_1, and the efficiency of charging at P_2 by ϵ_2, such that the charging rate at P_1 under the influence of i_B is given by $i_B\epsilon_1$, and that at P_2 under the influence of i_{20} is $i_{20}\epsilon_2$.

In all the experiments, except those in which P_1 was initially charged up positively with respect to P_2 (where electrons which get back to P_1 get there by drift), the experimental evidence shows that P_2 charges up more rapidly than P_1. (From §1).

Then, $$i_{20}\epsilon_2 > i_B\epsilon_1 \qquad\qquad \dots\ 9.4$$

and, when equilibrium is eventually reached,

$$i_{20}\epsilon_2 = i_B\epsilon_1 \qquad\qquad \dots\ 9.5$$

In the case where $\epsilon_1 = \epsilon_2$, $i_{20} = i_B$, at equilibrium (as assumed in §1 earlier). Before equilibrium is reached, $i_B < i_{20}\epsilon_2/\epsilon_1$. The fraction of the electrons which reach P_2 is given by,

$$i_{20}/i_e = i_{20}/(i_{20} + i_B) > \epsilon_1/(\epsilon_1 + \epsilon_2) \qquad\qquad \dots\ 9.6$$

from Eq. 9.4.

Thomson's expression[17] for the fraction of the electrons leaving the cathode which arrive at the anode gives

$$i_{20}/i_e = 4\,v_d/(\bar{v}_0 + 4v_d) \qquad\qquad \dots\ 9.7$$

where v_d is the drift velocity of electrons in the gap, under the influence of V_f, and $\bar{v}_0$ is the random velocity of the electrons as they emerge into the gap.

Then from Eqs. 9.6 and 9.7, ignoring ionization occurring as a result of the initial electron random energy.

$$4v_d/(\bar{v}_0 + 4v_d) > \epsilon_1/(\epsilon_1 + \epsilon_2)$$

Whence, $\bar{v}_0 < 4v_d\epsilon_2/\epsilon_1 \qquad\qquad \dots\ 9.8$

And at equilibrium, $\bar{v}_0 = 4v_d\epsilon_2/\epsilon_1 \qquad\qquad \dots\ 9.9$

If it were possible to estimate ϵ_1 and ϵ_2, and the equilibrium value of V_f, it would be possible to calculate the velocity with which the electrons emerge into the gap. So far insufficient information about the nature of

the surface films involved has been obtained to enable such a calculation to be performed. It has, however, already been suggested that the random energy with which electrons emerge into the gap is approximately that corresponding to V_1. (See Chapter 6). V_1 is of the order of 75 volts, resulting in a field inside the emitting electrode of about 100 v/cm, so at the sort of pressures used in these experiments, it can be seen that the random velocity of emerging electrons is high. In comparison, rough measurements of V_f indicate that it is of the order of 10 volts, resulting in a field in the gap of about 3 v/cm. The drift velocity corresponding to this is clearly very small in comparison with $\bar{v}_o$. Therefore we may crudely deduce from Eq. 9.9 that

$$\epsilon_2 \ggg \epsilon_1.$$

3.3 Investigation of the variation of i_{20} when P_1 is initially charged up positively with respect to P_2

When the initial charging up operation is performed such that P_1 is made positive with respect to P_2 (See §3.1c) electrons which emerge into the gap enter a residual field which tends to sweep them back to the emitting electrode. Under these conditions, very few electrons are expected to reach P_2. Electrons which enter the gap with very low energies are almost immediately controlled by drift, returning them quickly to P_1. Those entering with higher energies may reach P_2 if the pressure is so low that there are very few collisions with gas molecules, and the adverse V_f is small. But in general, particularly at the pressures the present experiments have been concerned with, increased initial energy increases the efficiency of the back scatter process, according to the

Thomson theory[17] and thus reinforces the electron flow back to P_1.
Therefore we conclude that electrons have very little chance of reaching
the collecting electrode.

Electrons returning to P_1 do not contribute to the net current
flowing in the gap since their current vectors are cancelled out.
It has been shown that electrons probably emerge into the gap with high
random energy, so some ionization in the region close to the emitting
hole is likely, and new electrons thus generated are swept back to P_1 do
contribute to a negative current $(-i_{20})$ in the external gap circuit. As
P_1 thus becomes steadily charged up under the influence of this ioniza-
tion current, V_f is reduced, and hence so is the current flowing back to
P_1. Eventually, V_f is reduced to the point where electrons start to
reach P_2 by diffusion. Positive values of i_{20} are registered in the
external gap circuit when the current flowing to P_2 becomes greater than
that due to the electrons generated in the gap by ionization which flow
back to P_1. The charging process continues until P_2 becomes negative
enough with respect to P_1 to satisfy the equilibrium condition, $i_B \epsilon_1 =$
$i_{20} \epsilon_2$.

The rate of rise of i_{20} when it is still negative is controlled by
the charging efficiency at P_1, ϵ_1. Once electrons start to reach P_2, this
rate of rise now depends on ϵ_1 and ϵ_2. As shown in the previous para-
graph, ϵ_1 is almost certainly a lot smaller than ϵ_2, but when i_{20} is
negative, so few electrons get to P_2 that charging at P_1 is not having
to compete with the charging at P_2, so the change in V_f, and hence i_{20}
might be quite rapid, as is shown to be the case experimentally.

3.4 Comparison of the results

It is expected from the above arguments that the steady state condition for the gap should be the same for a given gas and pressure, regardless of the initial electrical state of the electrodes, and that all the curves should eventually converge on the condition, $i_B \epsilon_1 = i_{20} \epsilon_2$. The rates at which the curves converge will not be expected to be the same, since in the different experiments, equilibrium is not necessarily brought about the charging at the same electrode. For instance, the curves referred to in §3.1a and 3.1b are controlled by charging mainly at the surface of P_2. But in the curves referred to in §3.1c and in §3.1.3, the early part of the curve is controlled by charging at the surface of P_1.

Only when there is a fairly high current flowing in the gap do the experimental results support the theory that the curves should approach a common equilibrium condition, regardless of the state of charging in the gap initially. At the lower currents, the charging processes are slower, so the curves would be expected to converge on the equilibrium condition more slowly, which may account for the fact that the equilibrium is not reached in the duration of these particular runs. It may be concluded that the experimental results afford reasonable support to the qualitative arguments forwarded.

4. Conclusions to Chapter 9

All of these results confirm the view that charging occurs at the surfaces of the electrodes during the passage of a current in the gap,

suggesting that insulating films are present. In the present experiments, the formation of films due to the presence of grease is eliminated by the use of a grease-free vacuum system, and the effects of oxidation at the electrode surfaces are eliminated by the use of gold-plated electrodes. The most likely remaining possibility to produce the effects observed is the formation of layers of gas at the surfaces of the electrodes. The experimental evidence suggests that the charging rate is not the same at the two electrodes, and that the collecting electrode charges up more efficiently than the emitting electrode. One reason that the surfaces of the two electrodes are not electrically similar is that during the running of the filament, the emitting electrode, P_1, is at a higher temperature than the collecting electrode, P_2. (On occasions when the emitting electrode was removed from the test cell in order to replace the filament, it was observed that if the filament had been running just previously, the electrode was quite warm). Thus we expect the efficiency of outgassing at the emitting electrode to be greater than that at the collecting electrode, and hence the adsorbed gas layer at the emitting electrode surface to be thinner, resulting in a smaller degree of insulation. Therefore the effect of heat at the emitting electrode will result in a smaller charging efficiency there compared to the collecting electrode, which, in general, is not subjected to such effects.

Measurements of the residual gap voltage by plotting the variation of i_{20} with the externally applied voltage, V_2, are not very accurate. During a particular run, V_f is likely to change under the influence of

i_{20} which is passing continuously. The next chapter describes a method of measuring the residual voltage in the gap without needing to pass a current in the gap.

In all of the arguments put forward in this chapter, we have been concerned only with the variation of V_f when there is a current flowing in the gap and have not considered the possibility that the voltage across the surface film might decay by the passage of a current through the film itself. Later measurements however, (See Chapter 10) indicate that in the absence of a current flowing in the gap itself, there is little variation in the residual voltage in the gap. This suggests that the voltages generated across the films decay with time constants which are large compared to the other time constants discussed in this chapter.

If more were known about the nature of the films on the electrode surfaces, and V_f at equilibrium could be measured accurately, it has been shown that it might be possible to calculate the random velocity with which the electrons emerge into the gap, making use of the equilibrium condition between i_{20} and i_B (See Eq. 9.9). This could be done, for instance, if the films at the two electrodes were known to be electrically similar i.e. $\epsilon_1 = \epsilon_2$.

Then at equilibrium, $\bar{v}_o = 4 v_d$, v_d being calculable from V_f and the gas pressure.

As seen from the Chapter 8, the measurement of $\bar{v}_o$ would assist greatly the understanding of back diffusion processes and of electron flow through holes.

CHAPTER 10

THE DEVELOPMENT OF THE ELLIPSOID VOLTMETER FOR THE MEASUREMENT OF SMALL RESIDUAL VOLTAGES IN THE GAP

1. Introduction

(See Chapter 3, §5.1). The ellipsoid voltmeter, originally developed by Thornton and Thompson[25] for the absolute measurement of high voltages between parallel plate electrodes, is not sensitive enough in its original form for the measurement of small voltages. It has not been possible during the present work to develop a system which will accurately measure fields less than about 20 v/cm, using the instrument in the orthodox fashion.

This chapter describes attempts that were made to extend the range of the working of the instrument to the measurement of the small residual voltages generated in the gap.

2. Adaption of the ellipsoid voltmeter for the measurement of small residual gap voltages

Consider the presence of a small residual voltage on the gap, V_f, too small to measure with the ellipsoid voltmeter used in the orthodox fashion. Also consider a unidirectional voltage, V_E, applied externally to the gap. Initially let the two voltages reinforce one another.

Then, $(V_E + V_f)^2 = K(n_1^2 - n_0^2)$ 10.1

where n_1 is the frequency of oscillation of the ellipsoid in the two fields and n_0 is the frequency in the absence of a field.

Now V_E is reversed so that it is in the opposite direction to V_f.

Then,
$$(V_E - V_f)^2 = K(n_2^2 - n_0^2) \qquad \dots 10.2$$

Eliminating n_0 between Eqs. 10.1 and 10.2 gives

$$4 V_E V_f = K(n_1^2 - n_2^2)$$

Therefore,
$$V_f = \frac{K}{4V_E} (n_1^2 - n_2^2) \qquad \dots 10.3$$

Then, V_f is proportional to $(n_1^2 - n_2^2)$ for a given K and V_E. V_E^2 is plotted as a function of n^2 (assuming that V_f is made zero by running a pure uhf discharge in the gap) and K is obtained from the slope of the straight line thus obtained. The fact that the curve turns out to be a straight line is confirmation that V_f is in fact zero. If required, n_0 may be obtained from the intercept on the n^2 axis.

It is seen from the above expression that for a given residual voltage on the gap, the greater the value of V_E, the greater the difference in the ellipsoid frequency when V_E is reversed. Therefore, high sensitivity in the measurement of V_f is obtained when a high value of V_E is used.

3. Experimental considerations

The basic experimental system for the ellipsoid voltmeter, and the method of measuring the frequency of the torsional oscillations are described in Chapter 3.

Hydrogen was admitted into the system at a pressure of about 5 torr, and the electrodes were charged up by running a discharge in the gap. The external voltage, V_E, was applied to the gap, and the time for 10 swings was measured. Using a Leybod clock, and carefully observing

-132-

the oscillations as the ellipsoid passed through its equilibrium

position, the time for 10 swings could be measured to better than 1/5th

second. The external voltage was then reversed, and the reading repeated.

Thus n_1 and n_2, hence $(n_1^2 - n_2^2)$ were found, and hence V_f from Eq. 10.3.

It takes about three minutes to obtain a single value of V_f. Thus it is

possible to plot V_f as a function of time.

It is expected that the error in V_f for a single reading is quite

large. So much depends on the accuracy with which the time for the

10 swings can be measured, errors being introduced at the starting and

the stopping of the clock. However if many values of V_f are obtained over

a period of time, much of this error can be accounted for.

Certain modifications were made to the original ellipsoid voltmeter

system, in an attempt to reduce some of the sources of systematic error.

The magnet supporting the ellipsoid assembly exerts a force on the

small piece of iron wire placed on the fibre between the ellipsoid and the

support (See page 45) constraining the motion of the wire, and hence of

the ellipsoid. This does not seriously affect the calibration of the uhf

indicating meters (See Chapter 3), since, provided that the position of

the magnet does not alter between the dc and the uhf parts of the cali-

bration, any such effects cancel. However, when the instrument is used

for absolute voltage measurements, as in the present case, this perturba-

tion may well affect the readings obtained. A non-magnetic form of

support was therefore built, similar to that used by Long[2]. This

introduced the use of greased connections into the vacuum system in

order to provide for the raising and lowering of the ellipsoid into and

out of the gap. However, by this time, the main measurements of amplification and breakdown voltages had been completed, so the introduction of grease into the system was not considered to be a serious objection at this stage in the work.

The possibility was not ruled out that the motion of the small piece of iron wire placed on the fibre could perturb the motion of the ellipsoid by the double pendulum effect, but it was assumed that such an effect would be negligible provided that the moment of inertia of the ellipsoid is large compared to that of the piece of wire. Later measurements of V_f with the iron wire placed actually on the ellipsoid itself (thus eliminating the double pendulum effect) showed no improvement confirming that the above assumption is a reasonable one.

4. The results

Measurements of V_f were made as a function of time after the plates had previously been charged up by

a) A pure uhf discharge such that the plates should charge up equally, with the gap electrically neutral,

b) A uhf discharge with a dc field superimposed to sweep electrons to P_2, thus charging P_2 up negatively with respect to P_1,

and c) A uhf discharge with a dc field superimposed to sweep electrons to P_1, thus charging P_1 up negatively with respect to P_2.

Zero time was taken at the moment that the charging discharge was switched off.

Graphs showing the variation of V_f with time for these three cases

(a) Plates charged with a pure uhf discharge.

(b) Plates charged with uhf discharge with a dc field sweeping electrons to P_2.

(c) Plates charged with uhf discharge with a dc field sweeping electrons to P_1.
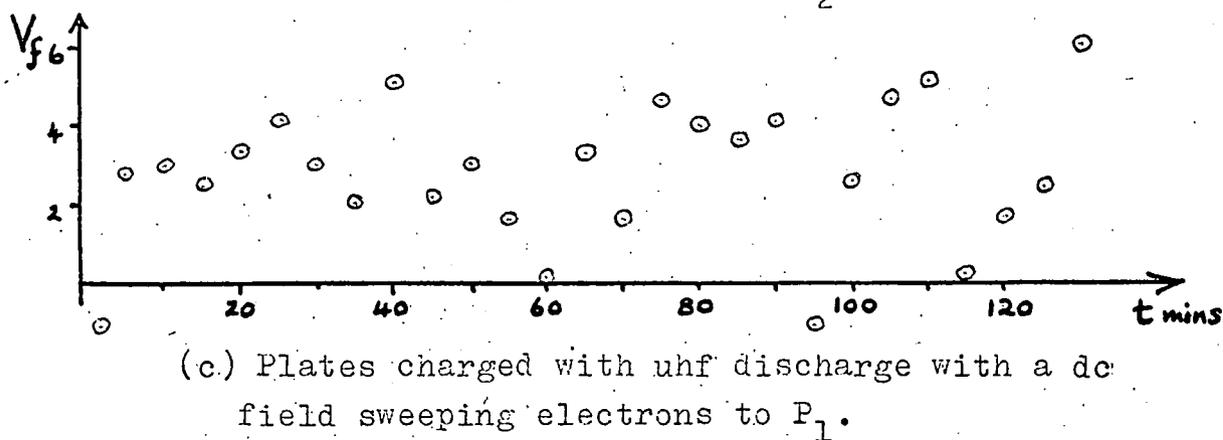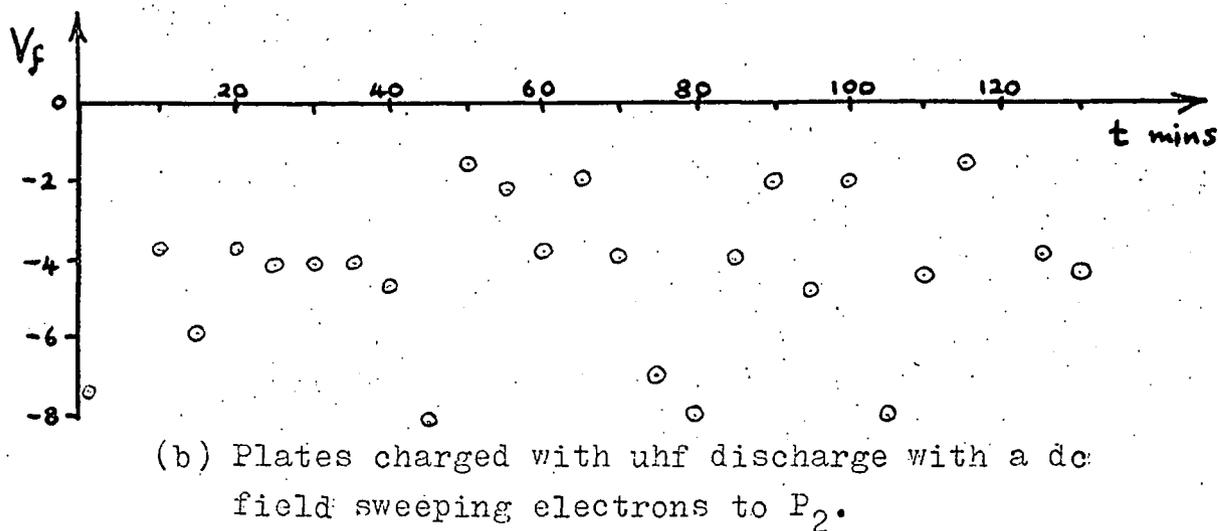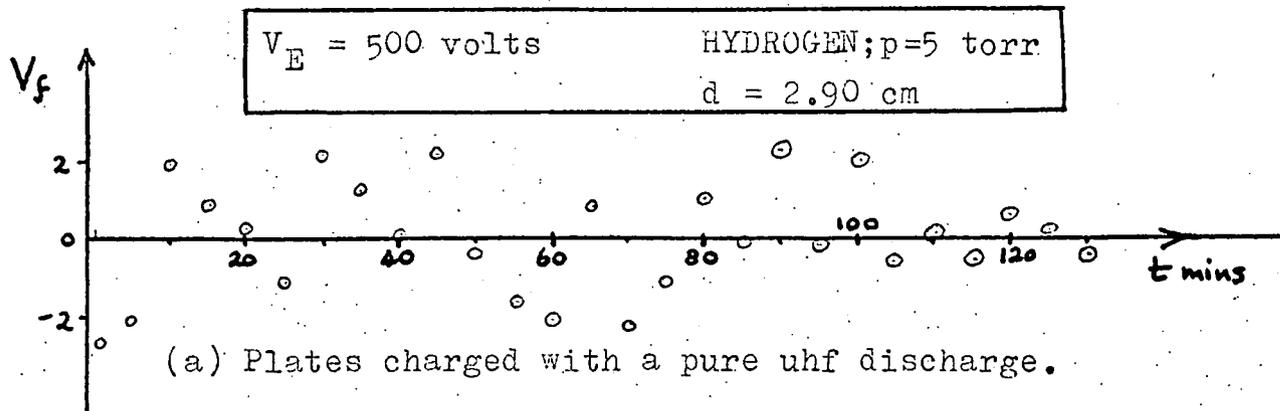
Fig 10.1. Values of the residual voltage in the gap measured using the ellipsoid voltmeter.

are given in Fig. 10.1. V_f is taken to be positive when P_2 is positive with respect to P_1.

The values of V_f do not lie on a smooth curve owing to the unavoidable error involved in individual readings, but it is possible to take a general view of the behaviour of V_f. It is clear from the results that the plates charge up as expected for the three types of charging process. It is also confirmed that the pure uhf discharge produces no net residual voltage in the gap.

The actual values of V_f obtained are smaller than obtained from the earlier experiments (See Chapter 9), ranging from about +6 volts when P_1 is charged up negatively with respect to P_2, to about -6 volts when P_2 is charged up negatively with respect to P_1.

Typical example of calculation of V_f:-

Time for 10 swings, $t_1 = 49.36$ secs, $t_2 = 50.16$ secs.

$$n_1 = .2026 \text{ sec}^{-1}, n_2 = .1994 \text{ sec}^{-1}.$$

Then, $(n_1^2 - n_2^2) = .00129$

$V_E = 500$ volts, and $k = 7.75.10^6$ volts^2.sec^2.

Then, $V_f = 5$ volts.

Despite the spread in the points on the graph, it is clear from these results that V_f does not vary appreciably with time when there is no current flowing in the gap. From this it is concluded that the time constants for the decay of the voltages across the surface films are long compared to the duration of the experiments. If it is therefore assumed that V_f does not alter during a course of measurments, the many

readings taken during that time may be averaged to obtain a more accurate value for V_f. The accuracy of the measurement of V_f does not depend so greatly now on the accuracy of a single reading.

Thus, the following values for V_f were obtained for the three sets of conditions examined.

a) Plates charged with uhf discharge

1) V_f = -0.26 $\pm$ 1.69 volts.

2) V_f = +0.17 $\pm$ 1.07 volts.

b) Plates charged with uhf discharge with dc field sweeping electrons to P_2

1) V_f = -4.54 $\pm$ 2.01 volts.

2) V_f = -3.96 $\pm$ 1.64 volts.

c) Plates charged with uhf discharge with dc field sweeping electrons to P_1

1) V_f = +2.38 $\pm$ 1.49 volts.

2) V_f = +2.93 $\pm$ 1.69 volts.

These voltages refer to the net residual voltage in the gap after the plates have been charged up with a discharge. So far it has not been possible to measure the voltage across the films at the individual electrode surfaces, but these results indicate that P_2 charges up more efficiently under electron bombardment than P_1, thus supporting the conclusions drawn from the experiments described in the previous chapter.

5. Discussion

Here is a method of measuring quite small residual voltages in a

parallel plate gap, in which the electrodes, covered with insulating films, have become charged up by the passage of a current in the gap. The polarity of the residual voltage is given, and the magnitude has been obtained to within ± 2 volts. Greater accuracy may be obtained with the introduction of more sophisticated methods of timing the swings of the ellipsoid in the gap. Throughout this study, the basic assumption is made that the presence of the external voltage, V_g, does not itself disturb the value of V_f.

These measurements show that even after a heavy current has been passed in the gap the residual voltage generated is quite small in relation to most values of the applied unidirectional gap voltages used during the amplification experiments. (See Chapter 4). Thus it may be concluded that when high currents are avoided in the gap the residual voltage generated may be neglected in comparison to E_{dc}.

The preliminary measurements of V_f using this method are quite promising, and it is hoped that the method might have useful applications elsewhere.

CHAPTER 11

SUMMARY OF PROGRESS AND SUGGESTIONS FOR FUTURE WORK

The main body of the work described in this thesis is aimed at
furthering the understanding of the movement and behaviour of electrons
in gases under the influence of combined unidirectional and ultra-high-
frequency electric fields. From considerations of drift, diffusion and
ionization, an expression has been derived for the amplification of a
stream of electrons crossing the gap which gives very encouraging agree-
ment with the experimental results in all of the gases tested. (See
Chapter 8). The picture presented considers the possibility of two types
of back diffusion. Firstly back scatter under the influence of the initial
random energy with which the electrons emerge into the gap, and secondly
steady state back diffusion, and assumes that these two processes may be
treated independently. The size of the hole in the emitting electrode
does not appear at any stage in the discussion. The theoretical pre-
dictions for the shape of the amplification curves make use of the values
for the ionization coefficient obtained from the breakdown measurements
made with the present apparatus, using the same gas samples as used for
the experimental amplification curves. The values obtained for hydrogen
and nitrogen give reasonable agreement with the results of other workers.
The values for helium and neon are less satisfactory, being over an order
of magnitude greater than the data published by other workers for pure gas

samples. However, since these values were obtained in the present apparatus it is reasonable to apply them in making theoretical predictions for the shape of the amplification curves. An interesting feature of the breakdown measurements made in helium and neon is the apparent departure from the diffusion theory of breakdown suggested by Prowse and Clark[12], but more extensive measurements are required before this is established.

One of the major difficulties encountered in the interpretation of the amplification curves has been the uncertain nature of electron flow through the holes in the emitting electrode. Although much has been learned about this (See Chapter 6), assumptions that the current emerging into the gap and the initial electron random energy are not dependent on the field in the gap were necessary in order to arrive at a final expression for amplification from which theoretical values of amplification can be obtained. (See Eq. 8.44). Experimental amplification curves were obtained for a wide range of E_{dc} and gas pressure in hydrogen, nitrogen, helium and neon, but only a narrow range of gap widths were employed. More measurements are required to extend this range and so make the picture more complete. It would also be interesting to perform experiments where electrons are released into the gap by a method other than the one used at present, for example photoelectric emission from the surface of the emitting electrode. This has two advantages. Firstly the emitting holes, and the associated problems (See Chapter 6), are eliminated, and electrons are now introduced into the gap with a random

energy which can be calculated from the wavelength of the impinging light and from the work function of the metal from which they are released. Secondly, the system does not now contain the impurities associated with the oxide coated cathode as at present.

The theoretical treatment given in this thesis looks very promising. However, considerable improvement between theory and experiment would be expected if the electron lifetime in the gap, at present calculated from $\tau = d/v_d$, can be determined with greater certainty. Nicholls[1] has suggested a method for measuring the transit time of a swarm of electrons crossing the gap in combined dc and uhf fields, based on the method used by Bradbury and Neilsen[49,50,51] for the measurement of electron drift velocities, and this might be employed to advantage for the determination of τ in the present case.

Investigation into the drifts in i_{20} (See Chapter 9) have established that residual voltages are generated in the gap by the passage of a uni-directional current, assisted by the presence of insulating films on the electrode surfaces. A method has been suggested for the measurement of such voltages (See Chapter 10) making use of the ellipsoid voltmeter. Measurements with this instrument enabled the conclusion to be drawn that if high currents are avoided in the gap, the residual field generated is small in comparison to the values of E_{dc} used in the amplification curves. Therefore the presence of residual voltages in the gap experienced during the present experiments may be neglected.

Finally, it is of interest to suggest a mechanical model which might be constructed and used to assist the understanding of electron

SIDE VIEW

'E_u'(Amplitude(rms) of oscillation)

Point at which
'electron'(ball)
is fired onto
table.

θ

'E_{dc}'
(Slope of
table in
mean position)

Pins ,or
'Gas molecules'.

Movement
to and fro
of the point
of firing

PLAN
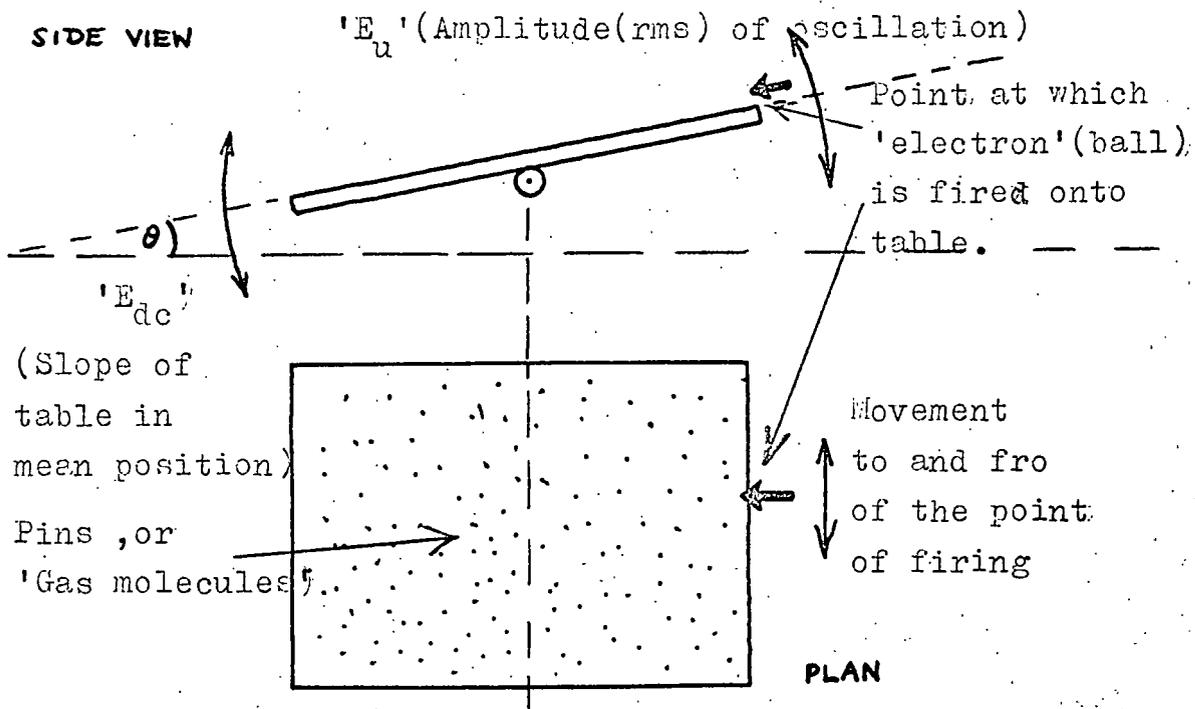
<u>Fig 11.1.</u> Pin-table analogue of diffusion and
drift processes.

It may be possible to automate the machine so that
each time an 'electron' is lost,it is counted at the
point at which it leaves the table,then returned to
the start and fired again.The point of firing in
the plane of the emitting end of the table should
be made random,in order to simulate,partly at
least,the random movement of the gas molecules.
(Clearly in this case it is not possible for the
'gas molecules'(i.e.,pins) to move independently
of the 'field' themselves.)

motion close to the emitting electrode. (See Fig. 11.1). Ball bearings, representing electrons, are shot horizontally onto a table consisting of a 'frictionless' surface on which are situated a large number of pins, representing gas molecules, with which the balls make 'elastic' collisions. It should be possible to measure the initial velocity with which the balls are shot onto the table. The table may be tilted such that the balls experience a force corresponding to E_{dc}, and the table may be made to oscillate about this position with a certain amplitude and frequency corresponding to E_u. The necessary conditions are that the frequency of oscillation of the table should be small compared to the frequency of collisions between balls and pins, and high enough so that the balls do not drift to the far end of the table in one half cycle.

A ball starting off at the origin will collide with pins and may as a result of these collisions eventually reach a terminal 'drift' velocity towards the far end of the table, or, alternatively, may return to the starting end. By counting the proportion of those starting which return to the starting end of the table, as a function of 'E_u', 'E_{dc}' and '$\bar{v}_o$', it may be possible to obtain results similar to the theoretical back diffusion relations described in Chapter 8.

TO SHOW THAT THE BELLOWS SENSITIVITY IS INDEPENDENT OF THE INITIAL TENSION ON THE BELLOWS IN THE ZERO POSITION, AND ALSO THAT THE PRESSURE AS MEASURED WITH THIS GAUGE IS A LINEAR FUNCTION OF BELLOWS DISPLACEMENT ONLY

The differential bellows gauge effectively measures the difference in pressures between two gas systems. (See Fig. 3.4). The zero position occurs when both systems are at the same pressure. When the pressure on one side becomes greater than on the other, the resultant displacement of a pointer fixed between the two bellows is a function of the pressure difference.

The bellows system may be compared with two springs in tension against one another. The pressure change may be related to a change in tension on one side of the system. Let T_1 and T_2 be the initial tensions on the springs, and the extensions x_1 and x_2 from their natural lengths. Initially let the pressures in the two systems be equal, and so let the forces on each side be A_1p and A_2p, where A_1 and A_2 are constants depending on the bellows dimensions. Initial the pointer fixed between the two bellows is at zero. In the initial position, resolving forces,
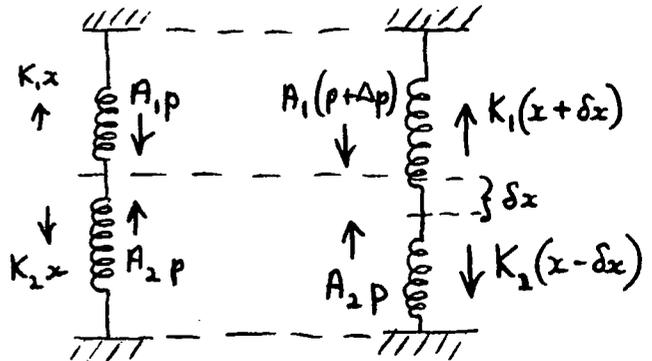
$$T_1 - A_1 p = T_2 - A_2 p$$

or, $\quad K_1 x_1 - A_1 p = K_2 x_2 - A_2 p \qquad \qquad \dots. \text{ I}$

(From Hooke's law where K_1 and K_2 are the elastic constants of the two springs).

When the pressure on one side changes by Δp, the pointer moves to a new equilibrium position, a displacement δx from the zero position.

Resolving forces again

$$K_1 (x + \delta x) - A_1 (p + \Delta p) = K_2 (x - \delta x) - A_2 p \qquad \dots. \text{ II}$$

And from I and II

$$\delta x = \frac{A_1}{K_1 + K_2} \cdot \Delta p \qquad \qquad \dots. \text{ III}$$

Then it is seen that δx is a linear function of pressure change and does not depend on the initial tension on the system.

APPENDIX 2

IMPURITY CONTENT OF THE GAS SAMPLES USED

HYDROGEN   99.995% Pure

Impurities	N_2	5 parts per million
	O_2	1 "
	CO_2	0.5 "
	CO	0.5 "

NITROGEN   99.999% Pure

Impurities	A	5 parts per million
	O	1 "
	H	1 "
	He	1 "
	Ne	1 "

NEON   99.95% Pure

Impurities	He	500 parts per million
	N_2	1 "
	O_2	1 "
	Hg	0.5 "

HELIUM   99.995% Pure

Impurities	Ne	3 parts per million
	N_2	1 "
	O_2	1 "
	A	1 "
	H	1 "
	CO_2	0.5 "

Gas samples supplied in 1 litre flasks from:

> The Rare Gas Department,
> British Oxygen Company.

ELECTRON MOBILITY IN THE COMBINED DC AND UHF FIELDS

v_d is the velocity with which the electron swarm travels across the gap in the dc field direction.

W_d = Electron drift velocity in the pure dc field, E_{dc}.

V_d = Electron drift velocity in the effective field, E_e, corresponding to the combined dc and uhf fields.

V_e = Electron random velocity in the effective field.

The unidirectional swarm velocity, $v_d = \dfrac{W_d \cdot V_d}{V_e}$ I

The drift velocity in the pure dc field,

$$W_d = 0.92 \frac{e}{m} \frac{1}{V_d} \frac{L_d E_{dc}}{p}$$ II

where L_d is the electron mean free-path. (Townsend[5])

The drift velocity in the effective field,

$$W_e = 0.92 \frac{e}{m} \frac{1}{V_e} \frac{L_e E_e}{p}$$ III

Dividing II and III,

$$\frac{W_d V_d E_e}{W_e V_e E_{dc}} = \frac{L_d}{L_e}$$ IV

Approximately, for a given pressure, $L_d = L_e$.

Then, $$\frac{W_d V_d}{V_e} = \frac{W_e E_{dc}}{E_e}$$ V

Then from I and V, $$v_d = \frac{W_e E_{dc}}{E_e}$$

The electron mobility in the combined fields, $\mu_e = W_e / E_e$.

And so,

$$v_d = \mu_e E_{dc}$$

APPENDIX 4

THE EFFECTIVE FIELD IN COMBINED DC AND UHF FIELDS

The effective field in combined unidirectional and oscillatory fields is given by Varnerin and Brown[13] as

$$E_e = \left(E_{dc}^2 + \frac{\gamma_c^2}{\gamma_c^2 + w^2} E_u^2 \right)^{1/2}$$

where γ_c is the frequency of collisions between electrons and gas molecules.

In the present experiment, $w \sim 10^7$ radians per second.

The collision frequency is given by

$$\gamma_c \sim P_c p V$$

where P_c is the collision probability and V the electron random velocity. From Townsend's data[5] on random velocities and from Brode's data[39] on collision probabilities, it is clear that for the gases examined in the present experiment, $\gamma^2 \gg w^2$.

Therefore, $\qquad E_e = (E_{dc}^2 + E_u^2)^{1/2}$

REFERENCES

1. Nicholls, M.J. 'Measurements on the growth of gaseous ionization at uhf'; Ph.D. Thesis, Durham University, 1960.

2. Long, R.E. 'An experimental study of the development of gaseous ionization at uhf'; Ph.D. Thesis, Durham University, 1962.

3. Townsend, J.S.E. 'Motion of electrons in gases'; Oxford, 1925.

4. 'Electricity in gases'; Oxford, 1915.

5. 'Electrons in gases'; Oxford, 1947.

6. Nature, Lond., 62, 340, 1900.

7. Phil. Mag., 6, 358, 1903.

8. Gill, E.W.B. and Donaldson, R.H., Phil. Mag., 12, 719, 1931.

9. Gutton, C. and Gutton, H., Comptes Rendu, 186, 303, 1928.

10. Herlin, M.A. and Brown, S.C., Phys. Rev., 74, 291, 1948.

11. Phys. Rev., 74, 902, 1948.

12. Prowse, W.A. and Clark, J.L., Proc. Phys. Soc., 72, 625, 1958.

13. Varnerin, L.J. and Brown, S.C., Phys. Rev., 79, 946, 1950.

14. Lucas, J., J. Electronics and Control, 17, 43, 1964.

15. Einstein, A., Ann. d. Physik, 17, 549, 1905.

16. Loeb, L., 'Basic Processes of Gaseous Electronics'; California, 1955.

17. Thomson, J.J., 'Conduction of Electricity through Gases', Third edition, Cambridge, p466ff.

18. Theobald, J.K., J. App. Phys., 24, 123, 1953.

19. Huxley, L.G.H., Phil. Mag., 30, 396, 1940.

20. Thomson, J.J., Phil. Mag. (5th series), 44, 293, 1897.

21. Llewellyn-Jones, F. and Davies, D.E., Proc. Phys. Soc. B, 64, 397, 519, 1951.

22. Llewellyn-Jones, F. and Morgan, G.D., Proc. Phys. Soc. B, _64_, 560, 1951.

23. Holland, Laurenson and Priestland, Rev. Sci. Inst., _34_, 377, 1963.

24. Christy, R.W., J. App. Phys., _31_, 1680, 1960.

25. Thornton, W.M. and Thompson, W.G., J. Inst. El. Eng., _71_, 1,

26. Prowse, W.A. and Nicholls, M.J., Proc. Phys. Soc., _84_, 545, 1964.

27. Crompton, R.W., and Sutton, D.J., Proc. Roy. Soc. A., _215_, 467, 1952.

28. Brown, S.C., MIT Tech. Report 283, June 1958.

29. Prowse, W.A. and Long, R.E., E.R.A. Report, April 1964.

30. Leiby, C.C. Jnr., S.B. Thesis, MIT. (Reproduced in Brown, S.C., 'Basic Data of Plasma Physics', Wiley, 1950, p136).

31. Schneider, F., Z. Phys., _6_, 456, 1954.

32. Jones, D.V., E.R.A. Tech. Report, L/T334, 1956.

33. Boyer, M., Ph.D. Thesis, Durham University, 1965.

34. Prowse, W.A., J.B.I.R.E., _10_, 333, 1950.

35. Wolfendale, E., Electronic Eng., _29_, 83, 1957.

36. Brown, S.C., Handbuch der Physik, XXII, 559, 1956.

37. Clark, J.L., 'The electrical breakdown of gases at uhf', Ph.D. Thesis, Durham University, 1956.

38. Thomson, J., Phil. Mag., _23_, 1, 1937.

39. Brode, R.B., Revs. Mod. Phys., _5_, 257, 1933.

40. Deas, H.D. and Emeleus, K.G., Phil. Mag., _40_, 460, 1949.

41. Harrison, M.A., Phys. Rev., _105_, 366, 1957.

42. Reder, F.H. and Brown, S.C., Phys. Rev., _95_, 885, 1954.

43. Mierdel, G., Wiss. Veroff. Siemens-Konz, _17_, 515, 1938. (Reproduced in Von Engel's 'Ionized Gases'; Oxford, p248).

44. Druyvestyn, M.J. and Penning, F.M., Rev. Mod. Phys., _12_, 87, 1940.

45. Dutton, J., Haydon, S.C., Llewellyn-Jones, F., Proc. Roy. Soc., A, 213, 203, 1953.

46. Czech, J., 'The cathode ray oscilloscope', Philips Tech.Lib., 1956, p6.

47. Compton, K.T., Phys. Rev., 22, 333, 432, 1923.

48. Cravath, A.M., Phys. Rev., 36, 248, 1930.

49. Bradbury, N.E., and Neilsen, R.A., Phys. Rev., 49, 338, 1936.

50.   Phys. Rev., 51, 69, 1937.

51. Neilsen, R.A., Phys. Rev., 50, 590, 1936.